Epigenetic profiling of the developing zebrafish embryo, and technical developments towards cloning zebrafish and isolating pluripotent stem cells

Sanjay Thakrar

Centre for Cardiovascular Science

The University of Edinburgh

Thesis presented for the Degree of Doctor of Philosophy

2009

Declaration

I declare that this thesis was composed by myself and that the research presented is my own, except where otherwise stated. None of the work presented in this thesis has been submitted for any other degree or professional qualification.

Sanjay Thakrar

September 2009

Acknowledgements

There are a lot of people who have helped me over the course of my PhD, without whom I would have not been able to have got this far. Firstly I would like to thank my supervisor Dr Sari Pennings for her invaluable advice, support and encouragement throughout the entirety of my project. I am also extremely grateful to Professor John Mullins for supporting my work in his lab and the Zebrafish facility. Thanks also go to Dr Carl Tucker, Patricia Smart and Chiu-Ju Huang for their help in the fish room. Thanks as well to all the members of the lab both past and present for welcoming me and showing me the ropes, especially Dr Tom Van Agtmael, Dr Walid Maalouf and Busabun Wongtawan. In particular, Madina Kara was a great help with the stem cell work during her summer project. Additionally, the rest of the CVS was always there for help and advice. I must also mention Professor Ian Wilmut and the rest of his laboratory for all their invaluable assistance and useful feedback. I would also like to thank the rest of the CRM for their support, in particular Dr Ian Chambers and Douglas Colby for their initial help with the stem cell characterisation. Dr Richard Meehan and his laboratory were also an invaluable source of feedback during the entirety of my PhD, with numerous meetings helping me to refine my work. Many others also assisted me during the course of my project, in particular Dr Andy Cronshaw of the University of Edinburgh helped with the mass spectrometer, the Reugels/Campos-Ortega Lab at the University of Cologne provided a valuable fish line, and Dr Claire Allen from the University of Sheffield taught me how to strip. I would also like to thank my other EdZeb and NZN colleagues for their assistance and useful feedback. This work was supported by the British Heart Foundation.

Finally, my thanks go to my friends both in and out of the institute for making Edinburgh such an interesting place to live! And lastly, my family for always being there for me.

Abstract

In normal embryonic development, cells generated from a fertilised oocyte lose their pluripotent status and become restricted to a particular differentiation pathway. This production of functionally distinct cell lineages is thought to be mediated by epigenetic processes that help control gene expression both temporally and spatially without any changes to the DNA sequence. These epigenetic changes consist of post-translational modifications of the N-terminal tails of histones and differential DNA methylation. Together these act by altering local chromatin structure, which in turn directs gene transcription by regulating the accessibility of the underlying DNA. To examine the potential developmental roles of these modifications, we determined the global cellular patterns of DNA methylation, as well as histone H3 lysine 9 (H3K9) and histone H4 lysine 20 (H4K20) methylation in the developing zebrafish embryo. These modifications are seen as hallmarks of heterochromatin, which consists of DNA that is tightly packaged, gene-poor and transcriptionally silent. Thus using immunostaining techniques, we confirmed the occurrence of genome-wide DNA methylation changes during zebrafish embryogenesis, as well as observing the unique localisation of this mark around the nuclear periphery in conjunction with pericentric heterochromatin. For mono-, di- and tri-methylated H3K9, it was observed by both immunostaining and immunoblotting that these marks became apparent after the onset of zygotic transcription. Ultimately their levels increased as development progressed, in a fashion similar to that of DNA methylation, consistent with a link between these epigenetic marks. Using the same methodology, the three methylation states of H4K20 were seen to vary differentially during zebrafish development, where in particular the levels of H4K20me1 decreased in concert with a potentially sumoylated form. In contrast, the levels of H4K20me2 increased progressively during embryogenesis, while those of H4K20me3 decreased rapidly after the mid-blastula transition. Together, these findings demonstrate that both DNA and histone lysine methylation take place in a highly dynamic manner, further supporting their roles in augmenting chromatin structure and directing cellular differentiation, while also providing a valuable comparison to the developmental

epigenetics of other model organisms characterised to date. Preparatory work for somatic cell nuclear transfer in zebrafish was also undertaken. In future studies, the dynamics of these marks could be compared with those of cloned embryos, so that the specific epigenetic profiles necessary for development can be elucidated. Epigenetically, a homologous process occurs within pluripotent embryonic stem cells (ESCs), which can differentiate into any cell type or undergo indefinite self-renewal. Advantageously, we were able to derive zebrafish ESC-like clusters which were morphologically similar to those derived from mice. These clusters were alkaline phosphatase-positive and expressed key ESC markers as detected by RT-PCR and immunofluorescence. In pilot studies, GFP-expressing ESC-like clusters have so far also contributed to ectodermal tissues when transplanted into wild type zebrafish embryos. Subsequently, these ESC-like clusters were epigenetically profiled using immunofluorescence, which showed that they had a similar complement of modifications to ESCs derived from mice. The derivation and initial characterisation of these ESC-like clusters from zebrafish, in addition to the development of somatic cell nuclear transfer in this species, will help pave the way for future studies involving tissue repair and regeneration, as well as opening up the potential of targeted genetic manipulation in this valuable model organism.

Contents Page

List of Figures and Tables

List of Abbreviations

ABC	Ammonium bicarbonate
ACN	Acetonitrile
ADP	Adenosine diphosphate
AP	Alkaline phosphatase
APS	Ammonium persulphate
AU	Arbitrary units
bFGF	Basic fibroblast growth factor
BMP4	Bone morphogenetic protein 4
bp	Base pairs
BSA	Bovine serum albumin
C-	Carboxy
ChIP	Chromatin immunoprecipitation
cm	Centimetre
CO_2	Carbon dioxide
DAPI	4,6-diamino-2-phenylindole
ddH_20	Double-distilled water
DEPC	Diethyl pyrocarbonate
DNA	Deoxyribonucleic acid
DNase	Deoxyribonuclease
DNMT	DNA methyltransferase
dNTP	Deoxyribonucleoside triphosphate
dpf	Days post-fertilisation
DTT	Dithiothreitol
EC	Embryonic carcinoma
EDTA	Ethylenediaminetetraacetic acid

EG	Embryonic germ
ENU	N-ethyl-N-nitrosourea
EpiSC	Epiblast stem cell
ES	Embryonic stem
ESC	Embryonic stem cell
FBS / FCS	Foetal bovine serum / Foetal calf serum
FGF	Fibroblast growth factor
g	Relative centrifugal force
GFP	Green fluorescent protein
GSK3	Glycogen synthase kinase 3
h	Hour
HAT	Histone acetyltransferase
HCl	Hydrochloric acid
HDAC	Histone deacetylase
HEPES	4-(2-hydroxyethyl)-1-piperazineethanesulphonic acid
HP1	Heterochromatin protein 1
hpf	Hours post-fertilistaion
HRP	Horse radish peroxidise
ICM	Inner cell mass
iPS	Induced pluripotent stem
JAK	Janus kinase
K	Lysine
kb	Kilobase
kDa	Kilodalton
KDM	Histone lysine demethylase
KMT	Histone lysine methyltransferase
l	Litre
LDS	Lithium dodecyl sulphate

LIF	Leukaemia inhibitory factor
LINE	Long interspersed nucleotide element
M	Molar
mA	Milliamp
MALDI-TOF	Matrix-assisted laser desorption/ionisation- time of flight
MBD	Methyl CpG binding domain
MBT	Mid-blastula transition
me1	Mono-methylation
me2	Di-methylation
me3	Tri-methylation
MEF	Mouse embryonic fibroblasts
mg	Milligram
min	Minute
ml	Millilitre
mM	Millimolar
mRNA	Messenger ribonucleic acid
N-	Amino
NaCl	Sodium chloride
ng	Nanogram
nm	Nanometre
NT	Nuclear transfer
pADPr	Poly-ADP-ribose
PAGE	Polyacrylamide gel electrophoresis
PBS	Phosphate buffered saline
PBST	PBS tween
PcG	Polycomb group
PCR	Polymerase chain reaction
PEV	Position effect variegation

PFA	Paraformaldehye
PGC	Primordial germ cell
pH	-log10[H+]
pl	Picolitre
PVDF	Polyvinylidene fluoride
rbbFGF	Recombinant basic bovine fibroblast growth factor
RNA	Ribonucleic acid
RNAi	RNA interference
RNase	Ribonuclease
rpm	Revolutions per minute
RT-PCR	Reverse transcription-polymerase chain reaction
SAM	S-adenosyl-L-methionine
SCNT	Somatic cell nuclear transfer
SET	Su(var)3-9, Enhancer of zeste and Trithorax
SINE	Short interspersed nucleotide element
siRNA	Small interfering RNA
ssDNA	Single-stranded DNA
STAT	Signal transducers and activator of transcription
SUMO	Small ubiquitin-related modifier
TBE	Tris / Borate / EDTA
TBS	Tris-buffered saline
TBST	TBS tween
TEMED	Tetramethylethylenediamine
TGF	Transforming growth factor
T_m	Melting temperature
Tris	Tris(hydroxymethyl)aminomethane
UV	Ultra-violet
V	Volts

XIC	X inactivation centre
µg	Microgram
µl	Microlitre
µm	Micrometre
°C	Centigrade
5MeC	5-methylcytosine

Chapter One

1 Introduction

1.1 Epigenetics

During the development of a multicellular organism, a single fertilised oocyte gives rise to a myriad of different specialised cell types. These cells all contain the same genetic information, but clearly differ in how it is expressed. It was in the 1950's when Conrad Waddington first introduced the "epigenetic landscape" model to help explain the interplay between genetics and developmental transitions during embryo development (Waddington 1957). More recently, epigenetics has been defined as "the study of mitotically and/or meiotically heritable changes in gene function that cannot be explained by changes in DNA sequence" (Russo, Riggs et al. 1996). This definition has been revised to state that epigenetics involves "the structural adaptation of chromosomal regions so as to register, signal or perpetuate altered activity states" (Bird 2007). This latter definition highlights that the study of both heritable and non-heritable epigenetic modifications is very much concerned with changes to the structure of chromatin, a filamentous nucleoprotein complex contained within the nuclei of eukaryotes that allows DNA to be packaged compactly yet accessed when required.

1.2 Chromatin

It is this chromatin structure which allows approximately two metres of DNA in a human cell to be packaged into a nucleus that has an average diameter of 10 μm (Mohd-Sarip and Verrijzer 2004). The nucleosome, which is the fundamental unit of chromatin, contains 146 bp of DNA wrapped around an octamer composed of two copies of each of the four core histone proteins, known as H2A, H2B, H3 and H4 (Luger, Mader et al. 1997). These nucleosomes form the "beads" of the 11 nm "beads-on-a-string" array observed by electron microscopy (Woodcock 2006). These arrays are packaged into yet tighter higher-order chromatin structures with the help

of linker histone H1 (Woodcock, Skoultchi et al. 2006) (Fig. 1.1). The precise positioning of nucleosomes is related to DNA sequence and can be altered by a process termed chromatin remodelling (Segal, Fondufe-Mittendorf et al. 2006; Rando and Ahmad 2007). This process alters the structure of chromatin so that the underlying DNA can be made more or less accessible (Workman and Kingston 1998). Accordingly, the chromatin within a eukaryotic nucleus is not uniformly organised, and can be broadly categorised into two main classes, euchromatin and heterochromatin, both of which can impact strongly on nuclear processes such as transcription, recombination and DNA repair (Kosak and Groudine 2004).

1.2.1 Characteristics of heterochromatin

Early cytological studies first distinguished these two types of chromatin. Heterochromatin was seen to be condensed and heteropycnotic at interphase, while euchromatin was more dispersed (Passarge 1979). Subsequent work identified that heterochromatic regions, such as those near the telomeres and centromeres of chromosomes, not only had a low gene density, but were also particularly rich in repetitive sequences (Richards and Elgin 2002; Grewal and Jia 2007). Structurally, heterochromatin also appeared to be less accessible to nucleases than euchromatin, and had nucleosomes that were regularly spaced over large arrays (Henikoff 2000). Large segments of the genome are packaged in a permanently inactive form, which is known as constitutive heterochromatin. Facultative heterochromatin, on the other hand, refers to genomic regions which are found in a heterochromatic state only in a subset of cells or for only one homolog, and the inactive X chromosome in female mammals is an excellent example of this (Chadwick and Willard 2004).

There is a strong correlation between heterochromatin and transcriptional repression (Grewal and Moazed 2003). This is aptly demonstrated by genes that are normally active in euchromatin becoming silenced when placed next to or within a heterochromatic region. This repression is thought to reflect the heterochromatinisation of the formerly euchromatic region, but is often unstable,

leading to gene expression in some clonal cells, a phenomenon referred to as position effect variegation (PEV) (Reuter and Spierer 1992). However, some genes actually require a heterochromatic environment for their expression, and the reasons for this are still not entirely clear (Weiler and Wakimoto 1995; Lu, Emtage et al. 2000; Yasuhara and Wakimoto 2006).

Recently, a great deal has been learnt about the biochemistry of heterochromatin, and in the process it has become clear that some of the biochemical modifications which are important for the packaging of heterochromatin are also important for the regulation of gene expression. In particular, the post-translational modifications of the N-terminal tails of histones have a marked impact on numerous nuclear processes, such as transcription and DNA repair, in addition to heterochromatin formation (Kouzarides 2007). The modifications include acetylation, methylation, phosphorylation, and ubiquitination, among others, and they exert their effects by providing a specialised docking site for numerous factors which can modulate chromatin structure, as well as changing the physical characteristics of chromatin directly (Kouzarides 2007).

1.2.2 Histone acetylation

Histone acetylation was one of the first post-translational histone modifications identified and was first associated with transcriptional activation more than 40 years ago (Allfrey, Faulkner et al. 1964; Pogo, Allfrey et al. 1966). Since then, roles in DNA repair and DNA replication have also been observed (Kouzarides 2007). Acetylation occurs at specific lysine residues on all four core histone proteins (Fig. 1.2), and is thought to promote gene transcription by recruiting factors and altering DNA-histone interactions, helping to create a more open chromatin structure (Shahbazian and Grunstein 2007). This modification is catalysed by histone acetyltransferases (HATs) which transfer an acetyl moiety from acetyl-coenzyme A to the epsilon-amine of target lysine residues. These HATs are frequently found as components of large transcriptional activatory complexes, such as Gcn5/PCAF,

CBP/p300 and SRC-1 (Bhaumik, Smith et al. 2007). In general, these enzymes can modify more than one lysine residue, but a degree of specificity has been detected for some enzymes (Kouzarides 2007).

The reverse process is carried out by a family of proteins known as histone deacetylases (HDACs). Consequently, the levels of histone acetylation within a cell are dynamically controlled by the combined activities of both HATs and HDACs. HDACs form parts of large transcriptional complexes which repress gene expression, such as mSin3a, NCoR/SMRT and NURD/Mi-2 (Denslow and Wade 2007; Shahbazian and Grunstein 2007). Histone deacetylation also plays an important role in the maintenance of heterochromatin, as one of its characteristics in various organisms is that it is hypoacetylated (Richards and Elgin 2002). A direct involvement for this process has been observed in budding yeast, where the formation of heterochromatin at telomeres involves the initial recruitment of the Sir silencing complex, and its spread requires the active deacetylation of H4 (Shahbazian and Grunstein 2007).

1.2.3 Histone methylation

As well as being unmodified, histones can also be mono- or di-methylated at specific arginine residues (Fig. 1.2), in either a symmetric or asymmetric configuration. This modification can be both activatory and repressive for gene expression (Kouzarides 2007), and is mediated by specific enzymes which are recruited to promoters by transcription factors (Lee, Teyssier et al. 2005). However, to date, there are no known proteins that can specifically bind to methylated arginine residues on histones, and no known enzymes that can reverse this modification (Kouzarides 2007). Nonetheless, arginine residues can be deiminated to a citrulline by the PADI4 enzyme, which is thought to prevent arginine methylation and antagonise its effects (Cuthbert, Daujat et al. 2004; Wang, Wysocka et al. 2004). Di-methylation of arginine residues prevents deimination by the PADI4 enzyme, however, mono-

methylated arginine residues can still be deiminated (Cuthbert, Daujat et al. 2004; Wang, Wysocka et al. 2004).

Lysine residues on the other hand can be mono-, di- or even tri-methylated, as well as unmodified. These marks in their various conformations can either activate or repress transcription, which is aptly demonstrated by specific sets of methyl-lysine residues on histone H3 (Kouzarides 2007) (Fig. 1.2). For instance, H3K4 and H3K36 methylation are associated with actively transcribed genes (Shilatifard 2006). At the other end of the spectrum, methylation of H3K9, H3K27 and H4K20 are all associated with transcriptional repression (Kouzarides 2007). H3K9 methylation provides a binding surface for a factor known as Heterochromatin Protein 1 (HP1) which leads to the propagation and stabilisation of heterochromatin and transcriptional silencing (Grewal and Jia 2007). Specific marks appear to have specific roles, for example, H3K9me2 appears to be associated with the inactive X chromosome (Rougeulle, Chaumeil et al. 2004), while H3K9me3 is intimately associated with the formation of pericentric heterochromatin (Lehnertz, Ueda et al. 2003). However, recently it has been observed in mammalian cells that H3K9me3 and HP1γ are enriched in the coding regions of active genes (Vakoc, Mandat et al. 2005). H3K9me1 has also been observed to associate with active promoters in human T cells (Barski, Cuddapah et al. 2007). These discrepancies underline the fact that methyl marks can have multiple functions in cells which are undoubtedly context-dependent. Nevertheless, H3K27 methylation is involved in the silencing of HOX gene expression, as well as the silencing of the inactive X chromosome (Shilatifard 2006). In contrast, very little is known about the function of H3K79 methylation. This mark is particularly unusual as it takes place within the globular domain of histone H3 (Ng, Feng et al. 2002). Nevertheless, it is thought to play a role in limiting the spread of heterochromatin (Kouzarides 2007), as well as mediating gene activation in budding yeast (Pokholok, Harbison et al. 2005).

However, on histone H4, lysine 20 is the only lysine residue that has been observed to be methylated (Fig. 1.2). This epigenetic mark is particularly interesting as each degree of methylation on this residue appears to be distinctly involved in the regulation of a diverse range of cellular processes (Yang and Mizzen 2009). H4K20me1 is also observed as a mark of the inactive X chromosome in mammals (Sims, Houston et al. 2006; Shen, Matsuno et al. 2008). However, evidence of a more direct role for this mark in gene repression comes from studies involving the L3MBTL1 protein in human cells (Kalakonda, Fischle et al. 2008; Sims and Rice 2008), a protein that is thought to bind H4K20me1 and mediate its repressive effects via nucleosome compaction (Trojer, Li et al. 2007). Nevertheless, numerous other studies have linked this mark with active gene expression in both murine and human cells (Talasz, Lindner et al. 2005; Vakoc, Sachdeva et al. 2006; Barski, Cuddapah et al. 2007). H4K20me3 on the other hand appears to be preferentially associated with constitutive heterochromatin (Wang and Jia 2009).

The enzymes that catalyse the addition of these methyl groups are known as histone lysine methyltransferases (KMTs), and unlike HATs whose action can be quite promiscuous in terms of their substrate specificity, KMTs are selective for the methylation of specific lysine residues within the tails of both histones H3 and H4. Nearly all KMTs characterised to date contain a SET domain (named after *Drosophila melanogaster* Su(var)3-9, Enhancer of zeste and trithorax), and in mammals, many of these enzymes are observed to methylate H3K9 (Bhaumik, Smith et al. 2007). For example, ESET methylates H3K9 (Yang, Xia et al. 2002), as does G9a in euchromatic regions (Tachibana, Ueda et al. 2005), while Suv39h1/h2 appears to specifically methylate H3K9 in pericentric heterochromatin (Lehnertz, Ueda et al. 2003). Ezh2 on the other hand has been observed to catalyse H3K27 methylation (Cao, Wang et al. 2002), while PR-Set7 and Suv4-20h1/2 catalyse the methylation of H4K20 (Yang and Mizzen 2009). Set1 and Set2 have been shown to methylate H3K4 and H3K36 respectively (Shilatifard 2006), and in marked contrast to all these enzymes, the KMT Dot1, which is necessary for H3K79 methylation,

lacks a SET domain and cannot modify free histones, requiring a nucleosomal substrate instead (Feng, Wang et al. 2002).

Initially, the process of histone lysine methylation was not known to be reversible (Bannister, Schneider et al. 2002), however the recent discovery of two distinct families of histone lysine demethylases (KDMs) has resolved this issue (Nottke, Colaiacovo et al. 2009). Amine oxidases, such as LSD1, and the hydroxylases of the JmjC family have been observed to demethylate specific lysine residues. LSD1 can only demethylate mono- and di-methyl substrates, as it requires a protonatable methyl ammonium group, and appears to demethylate H3K9 and H3K4 depending on its associated proteins (Klose and Zhang 2007; Shi 2007). In contrast, many JmjC family members have a unique substrate specificity, with specific demethylases identified for H3K4, H3K9, H3K27 and H3K36. These enzymes are also capable of demethylating tri-methylated lysines (Klose and Zhang 2007; Shi 2007). Together these KDMs play a key role in numerous developmental processes, such as gametogenesis and differentiation (Nottke, Colaiacovo et al. 2009).

1.2.4 Histone phosphorylation

Post-translational phosphorylation occurs on all four histones at specific serine and threonine residues (Fig. 1.2), and is mediated by several distinct kinases (Bhaumik, Smith et al. 2007). Histone phosphorylation appears to play a key role in numerous biological processes, such as cell division and DNA repair. Some reports also suggest a relationship between this mark and gene transcription (Kouzarides 2007). For example, in mouse cells, histone H3 phosphorylation has been observed to be critical for NFKB-regulated gene expression (Anest, Hanson et al. 2003; Yamamoto, Verma et al. 2003), as well as for the induction of immediate early genes, such as *c-fos* and *c-jun* (Mahadevan, Willis et al. 1991). A global ChIP on CHIP analysis of kinases in *Saccharomyces cerevisiae* also recently showed that many were present on the chromatin of specific genes (Pokholok, Zeitlinger et al. 2006), suggesting that the direct phosphorylation of chromatin may play a key role in regulating gene

expression. Recent data has demonstrated that one of the mechanisms by which H3 phosphorylation may function is via the displacement of HP1 from methylated H3K9, suggesting that this mark may antagonise the formation of heterochromatin (Fischle, Tseng et al. 2005).

1.2.5 Histone ubiquitination

Ubiquitin is a 8 kDa, highly-conserved regulatory protein that is ubiquitously expressed in eukaryotes, hence its name. Histone ubiquitination is catalysed by the formation of an isopeptide bond between the C-terminal glycine of ubiquitin and the epsilon-amine of a lysine residue on the target histone. The ubiquitination cascade is started by the E1-activating enzyme, followed by the sequential catalytic activities of the E2-conjugating enzymes and E3-ligases (Zhang 2003). The same E1-activating enzyme is involved in the ubiquitination of all target proteins, while different E2-conjugating enzymes are required for the ubiquitination of different substrates, with E3-ligases providing protein target specificity (Zhang 2003).

Ubiquitination has been reported to occur on H2A and H2B (Fig. 1.2) as a means of transcriptional regulation (Zhang 2003). Recently the ubiquitination of H3 and H4 has also been reported during DNA repair (Wang, Zhai et al. 2006). Nevertheless, several studies show that histone ubiquitination is associated with active gene expression. For example, ubiquitinated H2A and H2B are seen to be more associated with transcriptionally active sequences than those which are transcriptionally silent in *Tetrahymena thermophila* macronuclei, chicken erythrocytes and bovine thymus (Zhang 2003). Ubiquitination in yeast and human H2B have also been observed to be activatory for transcription (Kao, Hillyer et al. 2004; Zhu, Zheng et al. 2005). However, the links between histone ubiquitination and gene regulation also appear to be context dependent, as histone H2A ubiquitinylation, which is not found in yeast, has been seen to be associated with *Hox* gene silencing in humans (Wang, Wang et al. 2004; Cao, Tsukada et al. 2005). The transcriptionally inactive micronuclei of *T.*

thermophila and the spermatid sex body of mice also carry ubiquitinated histones (Zhang 2003).

The fact that both the presence and absence of ubiquitin is important for the stimulation of transcription is highlighted by enzymes which also deubiquitinate histones. A H2B deubiquitinylase has been seen to be involved with transcriptional silencing at heterochromatic sites in budding yeast (Emre, Ingvarsdottir et al. 2005; Gardner, Nelson et al. 2005). However, another enzyme that can deubiquitinylate H2B in *Saccharomyces cerevisiae* has also been implicated in gene activation (Wyce, Xiao et al. 2007). Consequently, the way in which ubiquitinylation controls gene transcription is relatively unclear, but it is likely that it recruits numerous factors to chromatin, in addition to altering the local structure of chromatin with its large size (Kouzarides 2007).

1.2.6 Sumoylation, ADP-ribosylation and proline isomerisation

Another family of evolutionary conserved polypeptides that can be reversibly conjugated to proteins are the small ubiquitin-related modifiers (SUMOs) (Geiss-Friedlander and Melchior 2007). In this family, there are three paralogs that are observed to be widely expressed in mammals, called SUMO1-3, where SUMO 2 and 3 are 96 % identical, and SUMO 1 and 2 are 45 % identical (Ouyang, Shi et al. 2009). As their names suggest, these proteins resemble ubiquitin in terms of their size and tertiary structure, even though they share less than 20% amino-acid sequence identity. The SUMO conjugation process is also similar to that of ubiquitin, although no enzymes are shared between these two modification systems (Geiss-Friedlander and Melchior 2007). Sumoylation was first associated with transcriptional repression in mammalian cells on histone H4 (Shiio and Eisenman 2003). In budding yeast, it has also been observed to be a repressive modification that is found on all four core histones, with specific sites of sumoylation identified on histones H2A, H2B and H4 (Nathan, Ingvarsdottir et al. 2006). Sumoylation appears to recruit factors, such as HDACs and HP1 (Shiio and Eisenman 2003), which

mediates heterochromatin formation, but it also appears to promote gene repression by antagonising histone acetylation by competing for lysine residues (Nathan, Ingvarsdottir et al. 2006).

ADP ribosylation of histones can occur in mono- and poly-ADP-ribose forms, and is catalysed by mono-ADP-ribosyltransferases and poly-ADP-ribose polymerases, respectively (Kouzarides 2007). This modification has also been implicated in a number of nuclear functions, such as DNA repair, DNA replication and recombination (D'Amours, Desnoyers et al. 1999). Moreover, it is a well established histone modification in mammalian cells (Adamietz and Rudolph 1984; Thraves, Kasid et al. 1985). However, it is still unclear what role this mark plays during gene transcription, independent of its other functions. For instance, a role for poly-ADP-ribose polymerase activity in transcription was recently identified in human cells, but only under conditions where DNA repair was induced (Ju, Lunyak et al. 2006).

Proline is an α-amino acid that can exist in either a *cis* or *trans* conformation. Recently an enzyme has been identified that can isomerise prolines in the N-terminal tail of histone H3 in *Saccharomyces cerevisiae* (Nelson, Santos-Rosa et al. 2006) (Fig. 1.2). This isomerisation is thought to severely distort the polypeptide backbone of histone H3, enabling its identification by other chromatin modifying enzymes (Nelson, Santos-Rosa et al. 2006). These results identify proline isomerisation as a novel non-covalent histone modification that also regulates transcription.

1.3 Histone modifications during development

By virtue of their roles within a diverse range of cellular processes, histone modifications play an integral part during the process of embryonic development. In particular, these epigenetic marks have an influence over differentiation by dint of their regulation of gene expression. Indeed, knock-out studies of various chromatin-modifying enzymes demonstrate that histone methylation, acetylation and

phosphorylation are all essential for embryonic development (Margueron, Trojer et al. 2005; Lin and Dent 2006; Torres-Padilla, Parfitt et al. 2007). In fact, various enzymes even appear to have specific functions within particular tissues during development (Lin and Dent 2006).

During the early stages of mouse development, the paternal pro-nucleus is negative for H3K9me2 and me3, while the maternal pro-nucleus is positive for these residues. This epigenetic asymmetry is maintained up until the two-cell stage, and a large increase in the levels H3K9 methylation is then observed at the four-cell stage, which is maintained right up to the blastocyst (Lepikhov and Walter 2004; Liu, Kim et al. 2004; Santos, Peters et al. 2005; Yeo, Lee et al. 2005). In non-mammalian vertebrates such as *Xenopus*, a comparable situation to the mouse appears to be occurring, where H3K9 methylation levels increase as development and differentiation progress (Dunican, Ruzov et al. 2008; Nicklay, Shechter et al. 2009; Shechter, Nicklay et al. 2009). At the midgestation stage of mouse development, H3K9me3 and H4K20me3 are enriched at pericentric heterochromatin. Additionally H4K20me3 is found in differentiating neurons, and H3K9me3 and H4K20me1 are present in proliferating cells (Biron, McManus et al. 2004). In comparison, detailed analysis in *Drosophila* showed that H4K20me1 and me3 were present throughout embryogenesis, while H4K20me2 appeared later on during development (Karachentsev, Druzhinina et al. 2007). Preliminary analysis in *Xenopus* also showed that H4K20 methylation became apparent as development and differentiation progressed (Dunican, Ruzov et al. 2008; Shechter, Nicklay et al. 2009). These increases, in what are considered to be marks of gene repression, could reflect a role in the silencing of genes that are no longer necessary for the maintenance and function of various differentiated cell types. On the other hand, histone methylation of arginine residues appears to mark pluripotent cells in the mouse blastocyst (Torres-Padilla, Parfitt et al. 2007). Additionally, Trx, a KMT for H3K4 was seen to positively regulate *Hox* gene expression in *Drosophila* (Ringrose and Paro 2004). However, the PcG protein E(z), which catalyses H3K27 methylation, was seen to silence *Hox* gene expression, and it is though that these two proteins antagonistically

regulate this particular system to help control body axis patterning (Ringrose and Paro 2004).

1.4 DNA methylation

The most common form of DNA modification in vertebrates is the addition of a methyl group at the 5' position of cytosine residues within CpG dinucleotides (Rein, DePamphilis et al. 1998) (Fig. 1.3). This epigenetic modification occurs post-replicatively in approximately 70 - 80 % of the cytosine residues present within the genome (Meehan 2003), however, many unmethylated CpGs are grouped in clusters called "CpG islands" that are present in the 5' regulatory regions of many genes (Bird 2002). DNA methylation is established and maintained by *de novo* and maintenance DNA methyltransferases (DNMTs), and is generally associated with transcriptional repression. The essential role of DNA methylation in normal development is exemplified by its involvement in genomic imprinting and X chromosome inactivation, as well as its role in genome stability (Bird 2002). Gene knock-out studies further highlight its importance, where removing DNMT activity in mice leads to embryonic lethality (Li, Bestor et al. 1992; Okano, Bell et al. 1999). Interestingly, not all organisms use DNA methylation as a regulatory mechanism; the yeast *Saccharomyces cerevisiae* and the nematode worm *Caenorhabditis elegans* have no discernable *Dnmt*-like genes and appear to be devoid of this epigenetic mark (Suzuki and Bird 2008).

1.4.1 DNA methyltransferases

DNMTs are the enzymes that are responsible for transferring methyl groups to DNA (Fig. 1.3) in both prokaryotes and eukaryotes (Kumar, Cheng et al. 1994; Stephens, Reisenauer et al. 1996). To date, three families of DNMTs have been identified based on sequence homology, namely DNMT1, DNMT2 and DNMT3 (Goll and Bestor 2005). The first DNMT to be identified, DNMT1, is generally regarded as a "maintenance" methyltransferase, as it methylates hemimethylated CpG dinucleotides far more efficiently than those that are unmethylated (Gruenbaum,

Cedar et al. 1982; Bestor and Ingram 1983). Accordingly, it is thought that these enzymes are responsible for maintaining the patterns of parental cytosine methylation in DNA strands that are newly synthesised (Leonhardt, Page et al. 1992). Gene knock-out studies in mice further highlight its importance, as targeted mutation of the *Dnmt1* gene results in embryonic lethality (Li, Bestor et al. 1992).

In contrast, the functional significance of DNMT2 has remained elusive, as there are no discernable phenotypes observed when DNMT2 is lost in higher eukaryotes (Goll, Kirpekar et al. 2006). In fact, DNMT2 was seen to methylate a small tRNA in mice, *Arabidopsis* and *Drosophila* (Goll, Kirpekar et al. 2006), and work in zebrafish has shown that this process may potentially mediate organ differentiation (Rai, Chidester et al. 2007). However, recent work has demonstrated that DNMT2-mediated DNA methylation also appears to play a role in maintaining retrotransposon silencing and telomere integrity in *Drosophila* (Phalke, Nickel et al. 2009).

The observation that the deletion of DNMT1 in mouse embryonic stem cells (ESCs) did not impair *de novo* DNA methylation (Lei, Oh et al. 1996), led to the conclusion that other DNMTs existed that were capable of this particular action. Searches eventually yielded two enzymes capable of *de novo* DNA methylation, and these were termed DNMT3a and DNMT3b (Okano, Xie et al. 1998; Hsieh 1999; Aoki, Suetake et al. 2001). Both are essential proteins, and their knock-out phenotypes in mice indicate that they are necessary for the establishment of genomic DNA methylation patterns during embryogenesis (Okano, Bell et al. 1999). These enzymes are also required for the maintenance of certain methylation patterns in mammals (Kim, Ni et al. 2002; Liang, Chan et al. 2002; Chen, Ueda et al. 2003).

1.4.2 DNA methylation and transcriptional repression

The idea that DNA methylation is strongly correlated with transcriptional repression was established over three decades ago by Razin and Cedar (1977), with later studies

consolidating this view. For example, methylated DNA transfected into mammalian cells was observed to be transcriptionally silent (Eden, Hashimshony et al. 1998). More recently, the silencing of several germ-cell specific genes in non-germ cells was also seen to depend on DNA methylation of the CpG islands associated with these genes (Maatouk, Kellam et al. 2006). Further work has elucidated the mechanisms by which DNA methylation interferes with gene expression, and it is observed to be both direct and indirect.

Firstly, DNA methylation is thought to physically affect the binding of transcription factors to their recognition sequences. For example, CpG methylation inhibits proenkephalin gene expression by directly interfering with the binding of AP-2, a positively acting transcription factor (Comb and Goodman 1990). More recently, activation of the gene encoding glial fibriallary acidic protein was seen to involve the demethylation of DNA within its promoter, which allows the STAT3 transcription factor to bind (Takizawa, Nakashima et al. 2001).

Secondly, DNA methylation can attract methylated DNA binding domain (MBD) proteins, such as MeCP2, which recruit chromatin-modifiers to silence gene expression (Nan, Cross et al. 1998; Nan, Ng et al. 1998). This latter repressive mechanism highlights the fact that DNA methylation works in concert with histone modifications to control gene expression, and suggests that DNA methylation may be the primary signal for gene inactivation. However, several studies have shown that DNMTs also take their cues from histone modifications, demonstrating that there is a significant degree of cross-talk between these epigenetic modifications (D'Alessio and Szyf 2006).

1.4.3 Epigenetic cross-talk and heterochromatin formation

Histone deacetylation, histone methylation and DNA methylation all play a major role in transcriptional repression, and several mechanistic links have been identified

between them that go some way in explaining how gene silencing and heterochromatin formation are established and maintained. MeCP2, a MBD-containing protein, is seen to associate with both HDACs and Suv39h1, which leads to histone deacetylation and H3K9 methylation respectively (Pazin and Kadonaga 1997; Jones, Veenstra et al. 1998; Nan, Cross et al. 1998; Fuks, Hurd et al. 2003). The H3K9 methyltransferase SETDB1 also appears to associate with a methyl-DNA-binding protein (MBD1) at sites of DNA replication, and it is suggested that this could be a mechanism by which H3K9 methylation is heritably maintained at sites of DNA methylation during chromatin assembly (Sarraf and Stancheva 2004).

However, several studies have shown that histone modifications can also help direct DNA methylation (Vaissiere, Sawan et al. 2008). This was implicated by work which demonstrated that H3K9 methylation and H3 deacetylation preceded *de novo* DNA methylation during the progressive silencing of the RASSF1A promoter in human mammary epithelial cells (Strunnikova, Schagdarsurengin et al. 2005). Further work also showed that following the integration of a transgene into chicken erythroid cells, histone hypoacetylation and H3K4 demethylation were earlier events than H3K9 methylation and DNA methylation during transcriptional silencing (Mutskov and Felsenfeld 2004). These findings are consistent with evidence from *Neurospora crassa* and *Arabidopsis* that show that DNA methylation is directed by H3K9 methylation in these organisms (Tamaru and Selker 2001; Jackson, Lindroth et al. 2002). A similar process can be seen in mammals during heterochromatin formation, where HP1 can interact with a variety of DNMTs to direct DNA methylation at sites of H3K9 tri-methylation (Lehnertz, Ueda et al. 2003; Fuks 2005). Specific HDACs and H3K9 KMTs can themselves also interact with DNMTs, further highlighting the cross-talk between these modifications (Rountree, Bachman et al. 2000; Fuks 2005; Esteve, Chin et al. 2006; Smallwood, Esteve et al. 2007; Epsztejn-Litman, Feldman et al. 2008).

1.5 DNA methylation during development

Levels of DNA methylation have been observed to dynamically change during the course of embryonic development, and this modification is also involved in several other important processes, such as imprinting, X chromosome inactivation and retroviral transposon silencing (Bird 2002). Once again, the importance of this epigenetic mark during development is underscored by the fact that a loss of DNMT activity in mice leads to embryonic lethality (Li, Bestor et al. 1992; Okano, Bell et al. 1999).

1.5.1 Genomic imprinting

In diploid organisms, cells have two homologous copies of each chromosome, usually one from the mother and one from the father. Each autosomal gene is therefore represented by two copies, or alleles, and for the vast majority of genes, expression occurs from both of these alleles simultaneously. In mammals however, a small proportion (< 1%) are imprinted, meaning that some genes are only expressed from one allele in a manner which is dependent upon its parental origin (Bartolomei 2009). This developmental asymmetry between the parental genomes explains why uni-parental embryos are inviable (McGrath and Solter 1984; Surani, Barton et al. 1984), and why uni-parental disomy is associated with such severe developmental abnormalities (Reik 1989). Currently, there are approximately 100 imprinted genes identified in the mouse genome (see http://www.har.mrc.ac.uk/research/genomic_imprinting for a full list), and many of these appear to have roles in the development of specific lineages and pre-natal growth (Bartolomei and Tilghman 1997; Reik and Walter 2001). There are many theories regarding the evolutionary origins of genomic imprinting, and a widely accepted hypothesis is that it stems from a genetic conflict over maternal resources during pregnancy (Moore and Haig 1991).

DNA methylation plays a crucial role in the transcriptional regulation of imprinted genes (Li, Beard et al. 1993; Ferguson-Smith and Surani 2001). These genes are

frequently clustered together and often share regulatory elements, known as imprinting control regions (ICRs). The process of imprinting frequently involves the mono-allelic methylation of these ICRs, and even though they may be located many kilobases away from the genes that they regulate, this methylation can still control their expression (Paulsen and Ferguson-Smith 2001; Reik and Walter 2001). A well documented example involves the regulation of the *H19*/*Igf2* locus in mice (Barlow, Stoger et al. 1991; Bartolomei, Zemel et al. 1991; DeChiara, Robertson et al. 1991). Here *H19* encodes a non-coding RNA, while *Igf2* codes for a protein that has clear effects on pre-natal growth (Zemel, Bartolomei et al. 1992). The methylation of the paternal allele prevents the binding of an insulating factor, called CTCF, which allows the expression of *Igf2*. While on the maternal allele, this region is unmethylated, enabling CTCF to bind, allowing *H19* to be expressed instead (Bartolomei 2009).

1.5.2 X chromosome inactivation

X chromosome inactivation is a process by which one of the two copies of the X chromosome present in female mammals is inactivated. This process takes place in order to achieve dosage compensation of X-linked genes (Lyon 1961; Riggs and Pfeifer 1992; Migeon 1994). In mice, this process takes place around the late blastocyst stage (McMahon and Monk 1983) and the choice between the two X chromosomes is made at random (Gardner and Lyon 1971). However, in extraembryonic lineages, this process is non-random, and it is the paternally inherited X chromosome that is selectively silenced (West, Frels et al. 1977; Takagi, Wake et al. 1978). In marsupials, the inactivation process is also non-random and it applies exclusively to the paternally derived X chromosome in all lineages (VandeBerg, Johnston et al. 1983).

X chromosome inactivation is mediated by a large non-coding RNA, called X-inactive specific transcript (Xist), which is transcribed from the X inactivation centre (XIC) (Borsani, Tonlorenzi et al. 1991; Brockdorff, Ashworth et al. 1991; Brown,

Ballabio et al. 1991; Brockdorff, Ashworth et al. 1992; Brown, Hendrich et al. 1992). Xist functions by progressively coating the chromosome, and is thought to induce inactivation by recruiting numerous different silencing factors (Wutz and Gribnau 2007). Following this process, the entire inactive X chromosome is packaged into a heterochromatic state, and can be visualised as a Barr body at the nuclear periphery during interphase (Barr and Bertram 1949). In addition to DNA methylation (Mohandas, Sparkes et al. 1981; Pfeifer, Tanguay et al. 1990) and the presence of the histone variant macroH2A (Costanzi and Pehrson 1998; Costanzi and Pehrson 2001), the inactive X chromosome is also characterised by hypoacetylated H3 and H4 (Csankovszki, Nagy et al. 2001), H3K9me2 (Heard, Rougeulle et al. 2001; Boggs, Cheung et al. 2002), H3K27me3 (Plath, Fang et al. 2003; Silva, Mak et al. 2003), and a lack of H3K4me2 and me3 (Boggs, Cheung et al. 2002; Chaumeil, Okamoto et al. 2002; Chadwick and Willard 2003; O'Neill, Randall et al. 2003). In many cases, the appearance of these modifications occurs soon after Xist coats the chromosome (Chaumeil, Okamoto et al. 2002; O'Neill, Randall et al. 2003; Plath, Fang et al. 2003; Silva, Mak et al. 2003).

1.5.3 Protection of genome stability

Approximately 96% of the total DNA in the mouse and human genomes is non-coding (Lander, Linton et al. 2001; Waterston, Lindblad-Toh et al. 2002). Of this "junk" DNA, 30-50% is composed of various transposable elements, such as DNA transposons, retrotransposons, long interspersed nucleotide elements (LINEs) and short interspersed nucleotide elements (SINEs) (Lander, Linton et al. 2001; Waterston, Lindblad-Toh et al. 2002). These mobile elements have the potential to be deleterious, as they can induce mutations by inserting near or within a functional gene, or they can even facilitate recombination between non-homologous loci, which could lead to chromosomal deletions or translocations (Kazazian 2004). Most of these mobile elements are very old, and are inactive due to their accumulated mutations. However, many are still active, and these mobile elements are transcriptionally silenced using mechanisms involving small interfering RNAs (siRNAs) and DNA methylation (Kazazian 2004) .

Retrotransposons tend to be heavily methylated (Jahner, Stuhlmann et al. 1982; Yoder, Walsh et al. 1997) and this is seen to repress their transcription (Harbers, Schnieke et al. 1981; Schmid 1996). In particular, transcription of the mouse retrotransposon intracisternal A particle (IAP) is constrained by DNA methylation (Walsh, Chaillet et al. 1998). The importance of this process is highlighted by experiments which show that a reduction in the levels of DNMT1 in mouse embryos leads to DNA demethylation and transcriptional activation of the IAP elements, which persists throughout adult life and increases the chance of retrotransposition and insertional mutagenesis (Walsh, Chaillet et al. 1998).

1.5.4 DNA methylation during embryonic development

Gene knock out studies have demonstrated that DNA methylation is essential for embryonic development in mice (Li, Bestor et al. 1992; Okano, Bell et al. 1999). However, periods of genome-wide DNA methylation changes do take place naturally during various stages of mouse development. During gametogenesis in mice, primordial germ cells become demethylated by embryonic day 14 in both male and female germ lines, with remethylation taking place for each gamete at different time points several days later (Reik, Dean et al. 2001). This reprogramming process ensures that the primordial germ cells have their original biparental DNA methylation patterns erased, so that sex-specific marks can be imposed at imprinted genes (Chaillet, Vogt et al. 1991; Stoger, Kubicka et al. 1993; Tremblay, Saam et al. 1995; Morgan, Santos et al. 2005).

Dynamic reprogramming of DNA methylation during early mouse embryogenesis is also seen to occur (Monk, Boubelik et al. 1987; Santos, Hendrich et al. 2002). Soon after fertilisation, the paternal genome is rapidly demethylated, possibly due to an active mechanism. However, direct evidence for this active mechanism is still lacking (Mayer, Niveleau et al. 2000; Oswald, Engemann et al. 2000). Meanwhile, the maternal genome undergoes a passive demethylation process, and only reaches

equivalency with the paternal genome at the morula stage of development (Howlett and Reik 1991; Santos, Hendrich et al. 2002). The levels of DNA methylation in both parental genomes then continues to fall passively, as DNMT1 is excluded from the nucleus (Howlett and Reik 1991; Monk, Adams et al. 1991; Carlson, Page et al. 1992; Rougier, Bourc'his et al. 1998). However, certain sequences are protected from this demethylation process, such as imprinted genes, IAP retrotransposons and centromeric DNA, which may function to ensure chromosomal stability and genomic imprinting during the reprogramming process (Olek and Walter 1997; Rougier, Bourc'his et al. 1998; Lane, Dean et al. 2003). During implantation, DNMT3a and 3b-dependent *de novo* methylation takes place (Okano, Bell et al. 1999), and by the blastocyst stage, the DNA of the inner cell mass is remethylated to levels similar to that seen in somatic cells (Monk, Boubelik et al. 1987; Reik, Dean et al. 2001; Santos, Hendrich et al. 2002). Such remethylation is not observed in the cells of the trophoectoderm, possibly due to the fact that these cells appear to lack *de novo* methyltransferase activity (Watanabe, Suetake et al. 2002). This overall pattern of reprogramming in mice appears to be conserved in cows, however the developmental timing of such events does seem to differ between these species (Fig. 1.4) (Dean, Santos et al. 2001). In sheep however, no demethylation of the male pro-nucleus was observed during the first cell cycle (Young and Beaujean 2004). Additionally, only limited demethylation of the sheep embryonic genome was observed between the two- and eight-cell stages, with no evidence of any remethylation by the blastocyst stage (Young and Beaujean 2004). This demethylation process also appears to be lacking in rabbit and pig zygotes (Shi, Dirim et al. 2004; Jeong, Yeo et al. 2007), indicating that these organisms may represent another model for early embryonic development in mammals.

1.6 Pluripotent cells

A pluripotent cell is one which can give rise to all the tissues that reside within an embryo. These cells exist naturally for short time periods during the course of embryonic development, both in the inner cell mass (ICM) of the blastocyst embryo, as well as in the foetal gonads, as primordial germ cells (PGCs). These transient cells

can be maintained as established cell lines in culture, and in the past few decades several such cell lines from both mice and humans have been characterised. Cells derived from the ICM of blastocyst embryos are known as embryonic stem cells (ESCs) (Evans and Kaufman 1981; Martin 1981; Thomson, Itskovitz-Eldor et al. 1998), while those derived from PGCs are called embryonic germ (EG) cells (Evans and Kaufman 1981; Martin 1981; Matsui, Zsebo et al. 1992; Resnick, Bixler et al. 1992; Shamblott, Axelman et al. 1998). In addition to these lines, pluripotent cells have also been derived from tumourigenic derivatives of germinal tissues from both mice and humans, which are known as embryonic carcinoma (EC) cells (Kleinsmith and Pierce 1964; Andrews, Damjanov et al. 1984), and recently cells have also been derived from the epiblast of early post-implantation rodent embryos, and these are called epiblast stem cells (EpiSCs) (Brons, Smithers et al. 2007; Tesar, Chenoweth et al. 2007).

Although these cell lines share some characteristics, such as immortality, their different origins are reflected in their various developmental potentials. For example, EC cells appear to be more restricted in their differentiation potential, and cannot be transmitted through the germline in chimeric animals (Brinster 1974), possibly due to their karyotypic abnormalities. On the other hand, EpiSCs are karyotypically normal, but appear to lack the ability to contribute to the blastocyst to form chimeras, and are only able to differentiate into various cell types *in vitro* (Tesar, Chenoweth et al. 2007; Guo, Yang et al. 2009). In contrast to both these cell lines, EG and ES cells are able to give rise to all the cell lineages of a developing mouse, including the germline (McLaren and Durcova-Hills 2001; Smith 2001).

1.6.1 Embryonic stem cells

Mouse ESCs in particular are very well characterised, and they represent the *in vitro* counterpart of the epiblast cells that go on to form the entirety of the foetus (Gardner and Beddington 1988; Nichols and Smith 2009). These cells, in appropriate conditions, display the dual properties of unlimited self-renewal and pluripotency,

which in real terms means that they can be cultured indefinitely *in vitro*, yet still retain the ability to contribute to all tissues of an embryo (Smith 2001). A great deal of work has been conducted to see what factors and signalling pathways regulate this pluripotent state, since this information could ultimately lead to the development of a wide range of patient-specific therapies involving tissue repair and regeneration.

1.6.2 ESC regulation by extrinsic factors

Initially, the successful derivation of ESCs involved their co-culture with mouse embryonic fibroblasts (MEFs) and foetal bovine serum (FBS). The significance of the MEF's is now known to involve their production of the cytokine Leukaemia Inhibitory Factor (LIF) (Nichols, Evans et al. 1990), while the active ingredient within the serum was identified as the growth factor Bone Morphogenetic Protein 4 (BMP4) (Ying, Nichols et al. 2003). LIF is a member of the IL6 family of cytokines, and it functions by binding the cell surface LIF receptor, which induces heterodimerisation with the glycoprotein 130 (Gearing, Thut et al. 1991; Davis, Aldrich et al. 1993). This leads to JAK-kinase mediated recruitment of the STAT3 transcription factor, which ultimately inhibits ESC differentiation and promotes self-renewal (Niwa, Burdon et al. 1998).

BMP4 acts by binding BMPR1, a specific serine/threonine kinase receptor. This leads to the activation of the SMAD1/5 transcription factors, which in turn induces the expression of the inhibitor of differentiation (*Id*) genes. The products of these genes sequester neurogenic basic helix-loop-helix transcription factors, which inhibits neural induction in mouse ESCs (Ying, Nichols et al. 2003).

However, recent work has shown that these factors act primarily downstream of the mitogen activated kinase (Erk) signalling pathway, which is mediated by Fibroblast Growth Factor 4 (FGF4), as well as other stimuli (Ying, Wray et al. 2008). Activating this pathway triggers the differentiation of pluripotent ESCs into neural

and mesodermal tissues (Kunath, Saba-El-Leil et al. 2007; Stavridis, Lunn et al. 2007). Consequently, studies demonstrated that the suppression of FGF signalling and glycogen synthase kinase-3 (GSK3) with a cocktail of specific small-molecule inhibitors could in fact permit the maintenance of pluripotent mouse ESCs in conditions free of LIF and BMP4 (Ying, Wray et al. 2008). Recently, these inhibitors have also been applied to the culture of rat cells, and ESCs capable of chimera production and germline transmission in this organism have also been derived (Buehr, Meek et al. 2008).

In contrast, human ESCs seem to require FGF2, in addition to TGFβ/Activin/Nodal factors to maintain self-renewal and pluripotency (James, Levine et al. 2005; Vallier, Alexander et al. 2005; Levenstein, Ludwig et al. 2006). They also do not depend on the LIF/STAT3 signalling pathway for their maintenance (Humphrey, Beattie et al. 2004), and BMP signalling appears to induce differentiation (Pera, Andrade et al. 2004; James, Levine et al. 2005).

1.6.3 ESC regulation by intrinsic factors

A number of factors have been discovered which are critical for the maintenance of pluripotency in ESCs both *in vivo* and *in vitro*. Among them are the transcription factors Oct4, Sox2 and Nanog, which when depleted cause ESCs to differentiate. Consequently, they have been proposed to act cooperatively as the master regulators of a transcriptional network that controls pluripotency in both mouse and human ESCs (Boyer, Lee et al. 2005; Loh, Wu et al. 2006).

1.6.3.1 Oct4

Oct4 (octamer-binding transcription factor 4) is encoded by *Pou5f1*, and is a member of the POU (Pit-Oct-Unc) family of homeodomain proteins. It is a DNA-binding transcription factor that binds to the classical octamer sequence ATGCAAAT. It is expressed throughout oogenesis and during early embryonic development. However,

after blastocyst formation, it is gradually downregulated in the trophoblast and becomes restricted to the epiblast (Palmieri, Peter et al. 1994). This expression pattern persists until gastrulation, but as the epiblast begins to differentiate, Oct4 is lost from all somatic cell lineages and only remains in the developing germ cells (Pesce and Scholer 2001). Oct4 deficient embryos only develop to the blastocyst stage due to the abnormal differentiation of the ICM into trophoblast cells (Nichols, Zevnik et al. 1998). RNAi knockdown of Oct4 *in vitro* also induces differentiation in ESCs, reemphasising the crucial role of Oct4 in maintaining pluripotency in these cells (Hay, Sutherland et al. 2004). However, differing levels of this protein are crucial for specifying ES cell fate, as overexpression of Oct4 also leads to differentiation, this time to primitive endoderm and mesoderm (Niwa, Miyazaki et al. 2000).

1.6.3.2 Sox2

Sox2 belongs to the Sox (SRY-related HMG box) family of transcription factors, and like Oct4 is essential for normal pluripotent cell development (Avilion, Nicolis et al. 2003). It is expressed in both the ICM and early primitive ectoderm (Wood and Episkopou 1999; Avilion, Nicolis et al. 2003), and embryos devoid of this protein appear to arrest at a similar time to those that lack Oct4 (Avilion, Nicolis et al. 2003). Sox2 forms heterodimers with Oct4 and regulates the expression of numerous genes, such as *Rex1*, *Utf1*, *Fbx15*, as well as *Pou5f1*, *Sox2* and *Nanog* themselves (Ben-Shushan, Thompson et al. 1998; Botquin, Hess et al. 1998; Nishimoto, Fukushima et al. 1999; Tomioka, Nishimoto et al. 2002; Tokuzawa, Kaiho et al. 2003; Catena, Tiveron et al. 2004; Chew, Loh et al. 2005; Okumura-Nakanishi, Saito et al. 2005; Rodda, Chew et al. 2005). In fact, recent work has shown that one of the essential functions of Sox2 is to stabilise ESCs in a pluripotent state by maintaining the requisite levels of Oct4 expression (Masui, Nakatake et al. 2007).

1.6.3.3 Nanog

The homeodomain containing protein Nanog is also essential for early embryonic development in mice (Mitsui, Tokuzawa et al. 2003). This protein is expressed in the ICM, but in contrast to Oct4, it becomes transcriptionally downregulated at implantation (Chambers, Colby et al. 2003). However, it is re-expressed again in the egg cylinder epiblast (Hart, Hartley et al. 2004); this second wave of Nanog expression is thought to protect the egg cylinder from early differentiation during gastrulation (Chambers, Silva et al. 2007). However, as the epiblast differentiates, this factor disappears from all somatic cell lineages (Chambers, Colby et al. 2003; Mitsui, Tokuzawa et al. 2003) and only remains within the primordial germ cells (Yamaguchi, Kimura et al. 2005). Nanog overexpressing human and mouse ESCs were able to self-renew without feeders or supplemented medium, while still retaining their pluripotency (Chambers, Colby et al. 2003; Mitsui, Tokuzawa et al. 2003; Darr, Mayshar et al. 2006). Gene deletion studies (Chambers, Silva et al. 2007) and work which demonstrated that it cooperates with Sox2 to upregulate other pluripotency markers, such as Rex1 (Shi, Wang et al. 2006), also showed its importance. However, even though they have a tendency for differentiation, it has been seen that Nanog null cells can still self-renew and retain pluripotency (Chambers, Silva et al. 2007), and it has been suggested that Nanog is in fact involved in the generation of pluripotency, rather than its maintenance (Silva, Nichols et al. 2009).

1.6.4 Epigenetic regulation of ESCs

In addition to these transcription factors, chromatin organisation and epigenetic modifications are also key elements for controlling gene expression during ES cell self-renewal and differentiation. Polycomb group (PcG) proteins, which are associated with H3K27 methylation, are seen to be particularly important (Boyer, Plath et al. 2006; Lee, Jenner et al. 2006). Using genome-wide location analysis, it was found that PcG proteins repress a large number of developmental regulators in ESCs, which if expressed would lead to their differentiation (Boyer, Plath et al. 2006). In fact, H3K27 methylation was also observed to be part of a mechanism that

kept ESCs “poised” for differentiation. Here, the promoters of a large cohort of developmentally important tissue-specific genes were marked with both activatory H3K4me3 and repressive H3K27me3 (Azuara, Perry et al. 2006; Bernstein, Mikkelsen et al. 2006). Upon differentiation, these “bivalent domains” resolved to a monovalent state in a variety of promoters, whereby H3K4me3 marked genes that were expressed and H3K27me3 marked those that were repressed (Mikkelsen, Ku et al. 2007). Importantly however, this bivalent pattern was not found at the promoters of a number of other genes (Azuara, Perry et al. 2006; Bernstein, Mikkelsen et al. 2006; Williams, Azuara et al. 2006), indicating that another regulatory system must be at play. Subsequent work demonstrated that many of these genes tend to be marked by DNA methylation (Fouse, Shen et al. 2008). In fact, comparisons between pluripotent tissues and primary MEFs reveal that a number of pluripotency related genes were hypomethylated in stem cells and hypermethylated in differentiated cells (Farthing, Ficz et al. 2008). Another study also showed that DNA methylation underwent extensive changes in the regulatory regions of genes during cellular differentiation (Meissner, Mikkelsen et al. 2008), and together these results suggest that DNA methylation represents another level of regulation that ensures appropriate gene expression in ESCs.

Epigenetic factors also interact with Oct4, Sox2 and Nanog to regulate pluripotency. For example, numerous genes which are bound by both Polycomb Repressive Complex 1 and 2 components are also bound by Oct4, Sox2 and Nanog in human ESCs (Boyer, Plath et al. 2006). Additionally, other epigenetic marks play a role in maintaining pluripotency in ESCs. The H3K9 KDMs *jmjd1a* and *jmjd2c* have been shown to positively regulate a variety of pluripotency-associated genes in ESCs. In particular, these KDMs have been observed to reverse the repressive H3K9me3 marks at the Nanog locus, and depleting these enzymes leads to a loss of self-renewal and ESC differentiation (Loh, Zhang et al. 2007). Thus it is suggested that a form of combinatorial control between all these factors helps regulate the pluripotent state within ESCs.

When ESCs are induced to differentiate their global epigenetic state also drastically alters, which ultimately reflects a change in their chromatin structure. For example, ESC chromatin contains more marks of transcriptionally active or permissive euchromatin, such as acetylated histones, than the chromatin of more differentiated cells (Francastel, Schubeler et al. 2000; Arney and Fisher 2004). Chd1, a chromatin remodelling factor, was also recently observed to be required for open chromatin and ESC pluripotency in mice, suggesting that this chromatin state may indeed be necessary for ESC potential (Gaspar-Maia, Alajem et al. 2009). In line with these findings, several types of stem cells in organisms ranging from planarians to mammals have been seen to have nuclei largely devoid of heterochromatin (Spangrude, Heimfeld et al. 1988; Terstappen, Huang et al. 1991; Reddien and Sanchez Alvarado 2004). Further studies in mice also demonstrated that various structural chromatin proteins were loosely associated with the chromatin of ESCs, and that these cells appeared to accumulate regions of more rigid heterochromatin after differentiation (Meshorer, Yellajoshula et al. 2006). Transmission electron microscopy even revealed a transition from chromatin that appeared homogenous and decondensed in undifferentiated mouse ESCs, to chromatin that had distinct heterochromatic domains present upon differentiation into neural progenitor cells (Efroni, Duttagupta et al. 2008). This apparent predisposition for open chromatin in ESCs may also represent another mechanism by which they are "poised" for differentiation.

1.6.5 Epiblast stem cells

Recently, two groups independently reported the isolation of a new type of pluripotent cell in rodents (Brons, Smithers et al. 2007; Tesar, Chenoweth et al. 2007). These cells were derived from the post-implantation epiblast and were therefore called epiblast stem cells (EpiSCs). These EpiSCs were cultured in conditions free of LIF, but included FGF2 and Activin, much like human ESCs (Brons, Smithers et al. 2007; Tesar, Chenoweth et al. 2007). Furthermore, they had a similar morphology to human ESCs, where their cells formed large, flat colonies which grew in a monolayer. These EpiSCs expressed the core pluripotency-

associated transcription factors of Oct4, Sox2 and Nanog, but differed from mouse ESCs in their expression of several other transcripts. In fact, they had a similar pattern of gene expression to their human counterparts (Brons, Smithers et al. 2007; Tesar, Chenoweth et al. 2007). The pluripotency of these cells was confirmed *in vitro* through embryoid body formation. However, they appeared to lack the ability to contribute to the blastocyst to form chimeras (Tesar, Chenoweth et al. 2007; Guo, Yang et al. 2009). The discovery of these EpiSCs is significant as they may represent an intermediate stage of development between mouse ESCs and committed cells. Additionally, they provide a valuable experimental system for determining whether the differences between mouse and human ESCs reflect a difference in the species or a difference in their temporal origins.

1.6.6 Induced pluripotent stem cells

Recently, in addition to the specific proteins discussed, numerous other factors have been identified which appear to play a role in the establishment and maintenance of pluripotency. For example, both c-Myc and Klf4, in combination with Oct4 and Sox2, have recently been seen to reprogramme adult mouse fibroblasts to pluripotency when expressed retrovirally (Takahashi and Yamanaka 2006). These first generation induced pluripotent stem (iPS) cells were identified based on drug selection for the expression of the ES cell-specific, but non-essential, *Fbx15* gene (Takahashi and Yamanaka 2006). Based on transcriptional and epigenetic patterns, they appeared similar, but not identical to ESCs. However, subsequent studies demonstrated that the identification of iPS cells based on drug selection using *Oct4* or *Nanog* expression gave rise to cells that were more similar to ESCs (Maherali, Sridharan et al. 2007; Okita, Ichisaka et al. 2007; Wernig, Meissner et al. 2007). At the molecular level, these completely reprogrammed iPS cells showed transcriptional and epigenetic patterns that were virtually indistinguishable from those in ESCs derived from the blastocyst (Maherali, Sridharan et al. 2007; Okita, Ichisaka et al. 2007; Wernig, Meissner et al. 2007; Mikkelsen, Hanna et al. 2008). Additionally, at the functional level, these iPS cells could also contribute to the germline of chimeric mice, and were even seen to support the development of embryos that were wholly

derived from these cells via tetraploid complementation (Boland, Hazen et al. 2009; Kang, Wang et al. 2009; Zhao, Li et al. 2009). Since 2006, iPS cells have also been generated from the cells of multiple tissues, and moreover, have been specifically generated from human fibroblasts and keratinocytes (Hochedlinger and Plath 2009).

The roles of Oct4 and Sox2 in the establishment and maintenance of pluripotency have been discussed previously, but what are the functions of the other two factors? The DNA-binding transcription factor *c-Myc* has been seen to be involved in numerous biological processes, such as cell proliferation and apoptosis (Adhikary and Eilers 2005). However, during reprogramming it is thought that c-Myc could act by inducing global histone acetylation through its recruitment of HATs (McMahon, Wood et al. 2000; Fernandez, Frank et al. 2003), which could promote the binding of Oct4 and Sox2 to their target genes. On the other hand, the kruppel-like transcription factor, Klf4, has already been observed to promote self-renewal and reduce differentiation in ESCs (Li, McClintick et al. 2005). Additionally, Klf4 has been seen to cooperate with Oct4 and Sox2 to activate the stem cell specific gene *Lefty1* (Nakatake, Fukui et al. 2006), and during reprogramming it could function to promote the expression of other genes in iPS cells.

1.7 Somatic cell nuclear transfer

During embryonic development, pluripotent cells derived from a fertilised oocyte lose the capacity to form all the tissues of an embryo when they become committed to a specific differentiation pathway. The activated and repressed states of gene expression, as mediated by DNA methylation and histone modifications, are epigenetically maintained and are not normally reversed or redirected (Meehan, Dunican et al. 2005). Such changes can however be induced in somatic cell nuclear transfer (SCNT) experiments, in which a differentiated somatic cell nucleus is inserted into the cytoplasm of an enucleated oocyte. As with iPS cells, this reversal of the differentiated mature cell state to one that is characteristic of the undifferentiated embryonic state is defined as reprogramming. Using SCNT, it was

established that adult cells were genetically equivalent to embryonic cells, and that their gene expression and epigenetic profiles could be reprogrammed to direct development to term. The first successful cloning of a live mammal from an adult somatic cell in 1996 (Wilmut, Schnieke et al. 1997) followed earlier seminal cloning experiments using embryonic cells from frogs (Gurdon and Byrne 2004).

There are two basic strategies by which cloning by SCNT can be achieved; both of these require the removal of the maternal pro-nuclear DNA from the oocyte, but differ in the way in which the donor cell nucleus is introduced. To begin with, enucleation of the metaphase II oocyte is achieved most commonly by suction of the maternal pro-nuclear material into a glass pipette using a micromanipulator. Following on from this, the introduction of the donor cell nucleus from tissue culture can be achieved either by injection of the donor cell or its isolated nucleus into the oocyte cytoplasm, or by fusion of the donor cell with the enucleated oocyte through appropriately timed electrical pulses (Fig. 1.5). The cell cycle state of the donor cells is also of great importance, and full-term cloned animals have been obtained most consistently from donor cells in a quiescent state (G_0 or G_1). This can be induced in cultured cells by serum starvation, or acquired by using cells that are naturally quiescent in the donor organism. The advantage of quiescent cells is thought to be attributable to their reduced transcriptional activity and chromatin modifications that enhance their epigenetic plasticity (Gardner, Lane et al. 2004).

Despite the success of cloning animals of many species, SCNT is still an extremely inefficient process. The majority of cloned animals (irrespective of species) do not survive to birth, and those that do succumb to a variety of abnormalities that greatly reduces their life expectancy (Hill, Burghardt et al. 2000; Amano, Kato et al. 2001; Sakai, Tamashiro et al. 2005). This failure of development to term has been attributed to a number of factors, such as technical limitations in embryo construction, the use of incompetent or low quality oocytes, or the lack of cell-cycle synchrony between the donor and recipient cells. However, increasing experimental

evidence indicates that the occurrence of many of these defects is due to insufficient epigenetic reprogramming of the donor somatic cell nucleus, including the inability to correctly reprogramme the major mammalian epigenetic phenomena of imprinting and X chromosome inactivation. All combined this is thought to lead towards the failure of the carefully orchestrated gene expression programme required for embryonic development (Shi, Zakhartchenko et al. 2003; Tian 2004).

The efficiency of reprogramming by the oocyte cytoplasm during SCNT varies considerably depending on the type of donor cell used. There is now growing evidence suggesting that using embryonic stem cells (ESCs) as donors gives rise to viable offspring at a considerably higher rate than with many somatic cell types (Rideout, Wakayama et al. 2000; Saito, Liu et al. 2004). ESCs are pluripotent cells that have the ability to give rise to all the cells of an embryo and adult, and it may be for this reason that they seem to be more amenable to or require less reprogramming than the nucleus of a differentiated somatic cell. It is likely that epigenetic differences are the fundamental reason underlying this variability (Mullins, Wilmut et al. 2004).

1.8 Zebrafish

Zebrafish (*Danio rerio*) is a tropical freshwater fish which is native to the south-eastern Himalayan region of Asia. As well as being a popular aquarium species, this organism is also an important research model used in the study of vertebrate development and gene function (Spence *et al.*, 2008). At present, studies involving mammals have provided a wealth of information about the epigenetic mechanisms that control development in vertebrates. However, zebrafish may represent an ideal system for the study of epigenetics, as this particular model organism benefits from easy maintenance at high densities in the laboratory, a short generation time, the large numbers of eggs produced year-round by each mating, and the fact that its externally fertilised eggs can develop rapidly as transparent embryos (Fig. 1.6) (Grunwald and Eisen 2002). The latter is especially appealing as it permits the live

and direct observation of vertebrate development, which mammalian model organisms cannot provide.

In particular, it can be seen that there are seven broad periods of zebrafish embryogenesis, namely the zygote, cleavage, blastula, gastrula, segmentation, pharyngula and hatching stages (Kimmel *et al.*, 1995). The newly fertilised egg is in the zygote period until the first cleavage occurs, approximately 40 minutes after fertilisation. Then follows the cleavage period, where the cells of the embryo divide rapidly and synchronously from the 2-cell stage to the 64-cell stage at approximately 15 minute intervals (Fig. 1.6). During the blastula period (between 2.25 and 5.25 hpf), these cell cycles give way to lengthened asynchronous ones at the mid-blastula transition at 3 hpf (Kane and Kimmel 1993). Epiboly, which involves the thinning and spreading of the embryonic cells over the yolk, then begins in the late blastula, and its progress is measured by the percentage of yolk that is covered by the cells (Fig. 1.6). During the gastrula period (between 5.25 and 10 hpf), epiboly continues, and the morphogenetic movements of involution, convergence and extension occur, which produce the primary germ layers and the embryonic axis (Kimmel *et al.*, 1995). After the completion of epiboly, the segmentation period begins and continues until 24 hpf. Here, the somites develop, the developing organs and tail become visible, and the first body movements become apparent (Fig. 1.6). The pharyngula period then takes place between 24 and 48 hpf, during which the embryo has progressed to the phyolotypic stage of development, where it possesses all the attributes of the classic vertebrate bodyplan. At this stage, pigmentation becomes evident, the fins grow, and the circulation begins to function (Kimmel *et al.*, 1995). Finally, around 3 dpf, the embryos are well developed and sporadic hatching begins to occur (Fig. 1.6).

Furthermore, in contrast to mammalian systems, parental imprinting and X chromosome inactivation appear to be absent in zebrafish, as androgenetic and gynogenetic fish are viable (Westerfield 1995; Corley-Smith, Lim et al. 1996) and no

specific sex chromosomes appear to be present (von Hofsten and Olsson 2005). Combined with the availability of genetic and molecular tools permitting detailed molecular study (Skromne and Prince 2008), all these factors point towards the zebrafish being a simpler model system with which to investigate the potential roles of various epigenetic modifications during vertebrate development.

Taking this into account, numerous epigenetic studies have been conducted in the zebrafish to date. For example, embryos treated with 5-azacytidine, a nucleotide analog known to induce cellular differentiation and DNA hypomethylation in mammalian cells, also induces DNA hypomethylation and developmental defects in zebrafish (Martin, Laforest et al. 1999). Morpholino knock-down studies of DNMT1 in zebrafish also reiterate the fact that DNA methylation is essential for vertebrate development (Rai, Nadauld et al. 2006). Furthermore, as discussed previously, DNA methylation studies in mice demonstrated that a global reprogramming event occurred soon after fertilisation (Monk, Boubelik et al. 1987; Santos, Hendrich et al. 2002). However, in the zebrafish, the presence of any genome-wide DNA methylation changes is still subject to some debate. Previous studies reported that there were indeed variations in global DNA methylation levels during zebrafish development (Martin, Laforest et al. 1999; Mhanni and McGowan 2004; MacKay, Mhanni et al. 2007), while others concluded that such genome-wide changes did not occur (Macleod, Clark et al. 1999).

The significance of histone modifications within zebrafish has also been investigated. Numerous SET domain-containing genes are conserved within its genome (Sun, Xu et al. 2008). As discussed, SET domain-containing proteins represent an evolutionary conserved family of epigenetic regulators which are responsible for histone lysine methylation. Some of these genes show specific patterns of expression in certain tissues at certain stages, suggesting their involvement during the development of these systems (Sun, Xu et al. 2008). For example, homologues for SYMD2 and SYMD3, which catalyse the methylation of H3K36 and H3K4 respectively, appear to

be involved in somite formation. However, the vast majority of the SET domain-containing genes detected so far have an unknown function (Sun, Xu et al. 2008). Additionally, in another study, the zebrafish homologue of Suv39h1, which catalyses the tri-methylation of H3K9, was found to be essential for maintaining the levels of this mark, as well as for the terminal differentiation of several specific tissues (Rai, Nadauld et al. 2006).

Embryonic stem cells have also been derived from the zebrafish (Ma, Fan et al. 2001; Fan, Crodian et al. 2004; Fan and Collodi 2006). These cells were cultivated on a rainbow trout spleen cell feeder layer, and after transplantation were shown to contribute to the germ-line (Ma, Fan et al. 2001), even after several culture passages (Fan, Crodian et al. 2004; Fan and Collodi 2006). The medium utilised contained both FBS and trout serum, in addition to trout embryo extract, bovine insulin, human FGF and human epidermal growth factor (Fan, Crodian et al. 2004; Fan and Collodi 2006). However, it was seen that the frequency of germ-line chimera formation was very low (approximately 2-4%; Ma, Fan et al. 2001; Fan, Crodian et al. 2004; Fan and Collodi, 2006).

Zebrafish may also represent an ideal genetic system for the study of reprogramming, as nuclear transfer is also possible in this species (Lee, Huang et al. 2002). In this study, fertile transgenic zebrafish were obtained by nuclear transfer using long-term-cultured embryonic fibroblasts which were modified by GFP-expressing retroviral insertions (Lee, Huang et al. 2002). Donor nuclei were transplanted into manually enucleated eggs, with approximately 2% of the total oocytes operated on reaching adulthood. These nuclear transplants expressed GFP and produced fertile, diploid F1/F2 offspring that continued to express GFP in a manner identical to that of the founder fish (Lee, Huang et al. 2002).

1.9 Project aims

Thus, one of the main goals of this project was to examine the epigenetic dynamics that underlie pluripotency and differentiation within the zebrafish embryo. In particular, the roles of DNA methylation, and H3K9 and H4K20 methylation were investigated. These marks are of particular interest as they are tightly associated with the formation of heterochromatin. Specifically, in Chapter 3 we sought to clarify whether DNA methylation reprogramming took place during the development of the zebrafish. In Chapters 4 and 5 we went about profiling the levels of mono-, di- and tri-methylated H3K9 and H4K20 at several distinct stages of development. In Chapter 6 we developed techniques for somatic cell nuclear transfer in zebrafish, and in Chapter 7 we derived and characterised ESC-like clusters from the zebrafish in order to define their pluripotent state.

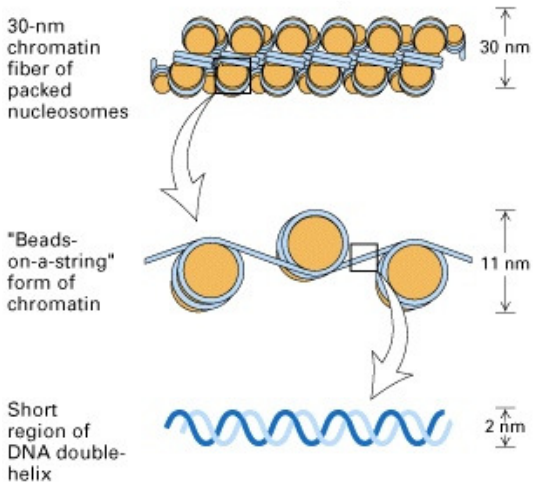

Fig. 1.1: Hierarchical folding of chromatin. 146 bp of DNA is wrapped around a nucleosome, which forms the "beads" of the "beads-on-a-string" array. These arrays can then be packaged into yet tighter higher-order chromatin structures with the help of linker histone H1. Adapted from Lodish *et al.* (2000).

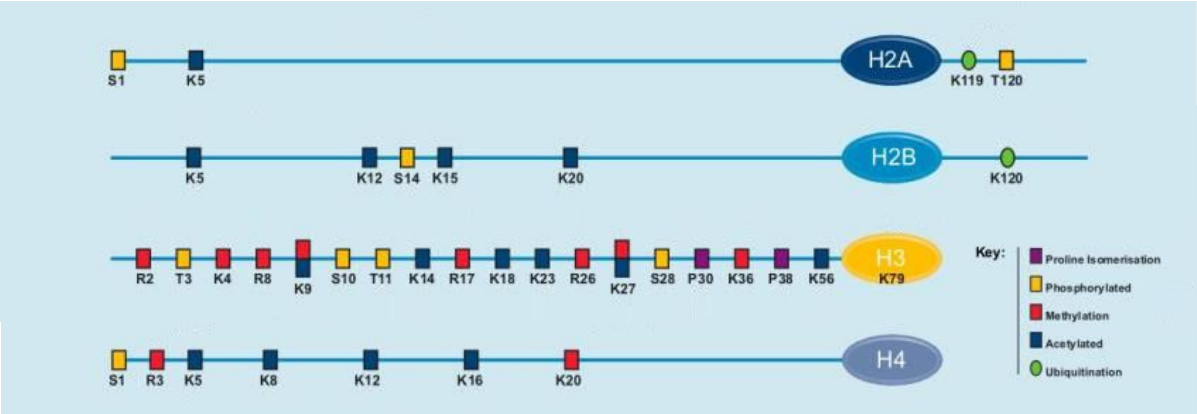

Fig. 1.2: Post-translational modifications of nucleosomal histones. Most modifications occur on the N-terminal tails of histones, however there are some exceptions, including modifications on the C-terminal tails of H2A and H2B, as well as modifications in the globular domain of H3. The globular domains of each core histone are represented as coloured ovals. Adapted from www.abcam.com.

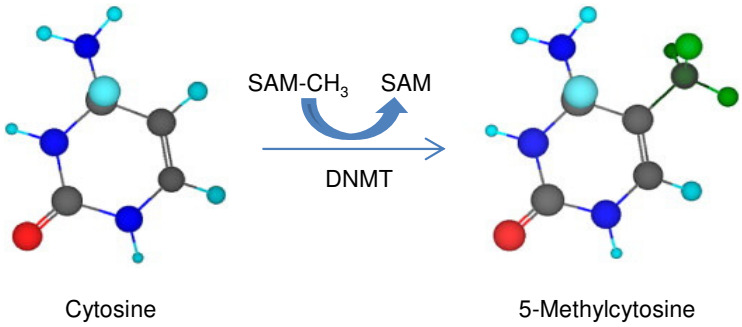

Fig. 1.3: DNA cytosine methylation. A DNA methyltransferase (DNMT) catalyses the transfer of a methyl group (CH_3) from S-adenosylmethionine (SAM) to the 5-carbon position of cytosine to produce 5-methylcytosine. Adapted from Prokhortchouk and Defossez (2008).

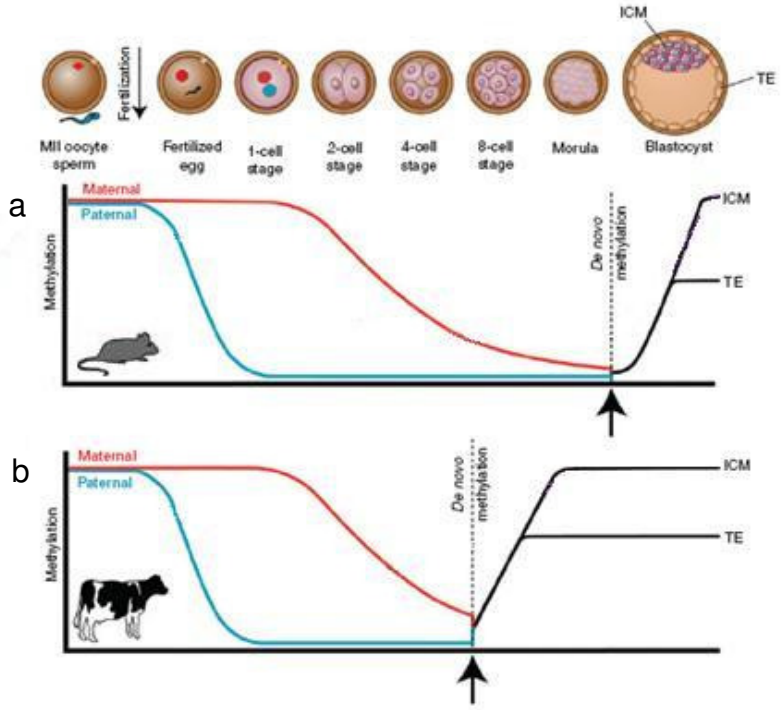

Fig. 1.4: Methylation dynamics during early embryonic development. **(a)** In mice, the paternal genome (blue) is demethylated soon after fertilisation by what appears to be an active mechanism. The maternal genome (red) is demethylated by a passive mechanism that depends on DNA replication. *De novo* methylation occurs at the blastocyst stage, and differential methylation states are observed between the inner cell mass (ICM) and the trophectoderm (TE). **(b)** In cattle, a similar reprogramming process appears to take place. However, *de novo* methylation occurs at the 8- to 16-cell stage. Adapted from Yang *et al.* (2007).

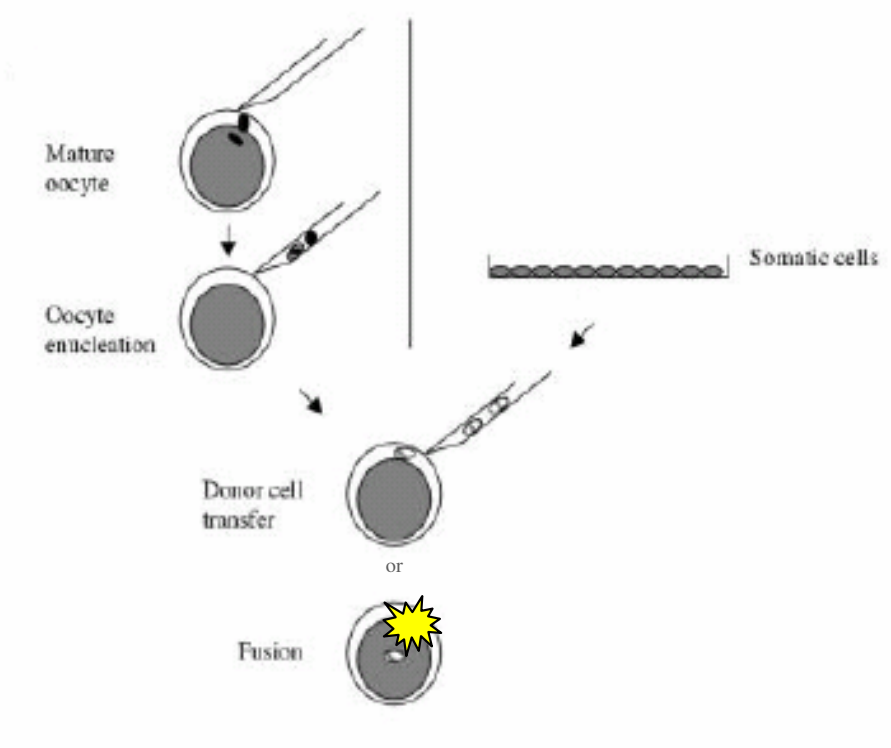

Fig. 1.5: Somatic cell nuclear transfer techniques. A mature oocyte is first enucleated by a glass pipette, and then a somatic cell nucleus is either transferred or fused to it by appropriately timed electrical pulses. Adapted from Hodges & Stice (2003).

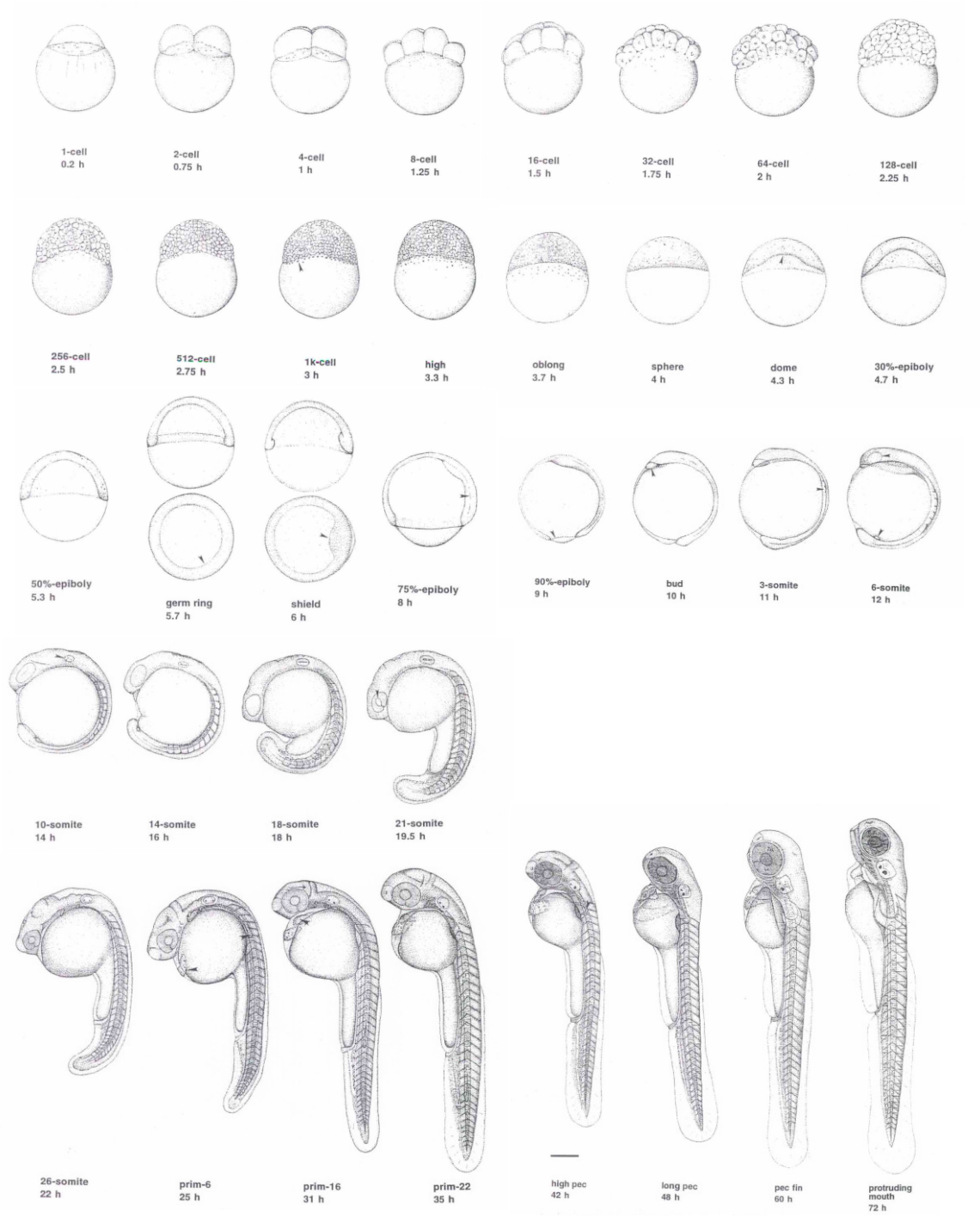

Fig. 1.6: Camera lucida sketches of the zebrafish embryo at selected stages. Adapted from Kimmel *et al*. (1995), with development stages proceeding from left to right. Note that the embryonic cleavage stages take place on top of a yolk sac, which is enveloped during the gastrulation movements of epiboly. Scale bar, 250 µm.

Chapter Two

2 Materials and Methods

2.1 Chemicals and solutions

Acids, alcohols, solvents and analytical grade chemicals were supplied by Sigma (Sigma-Aldrich Company Ltd., Poole, UK) and BDH (BDH Laboratory Supplies, Poole, UK). All solutions were made using Milli-Q water (Millipore, Molsheim, France) and were autoclaved before use where appropriate. For RNA work, solutions were treated with 0.01% diethyl pyrocarbonate (DEPC) (Sigma) or prepared using DEPC-treated water. Compositions and uses of standard solutions are outlined in Table 2.1:

Reagent	Details	Notes
PBS	140 mM NaCl, 3 mM KCl, 2 mM KH_2PO_4, 10 mM Na_2HPO_4	Buffer solution
TBS	50 mM tris, 150 mM NaCl, pH 7.5	Buffer solution
TBE	45 mM tris, 45 mM boric acid, 1 mM EDTA, pH 8.0	For agarose gel electrophoresis

Table 2.1 Standard solutions

2.2 Zebrafish

2.2.1 Strains and maintenance

Wild-type WIK strain zebrafish (*Danio rerio*) were maintained and embryos collected using standard methods (Westerfield 1995) in a Z-plex stand-alone aquarium system (Aquatic Habitats, Florida, USA) in the zebrafish facility at the Queen's Medical Research Institute, University of Edinburgh. A transgenic line of zebrafish that expresses a fusion of a histone variant (H2A.F/Z) to green fluorescent protein (GFP) (Pauls, Geldmacher-Voss et al. 2001) was also used as a source of

embryos for a sub-set of experiments, and was kindly provided by the Reugels/Campos-Ortega Lab, Institut für Entwicklungsbiologie, Universität zu Köln. Fish were kept in a 14 h-light/10 h-dark cycle, and all embryos produced were maintained at 28.5 ºC and staged according to Kimmel *et al*. (1995) by time in hours post fertilisation (hpf) and morphology (Fig. 1.6).

2.2.2 Unfertilised oocyte retrieval

The day before unfertilised eggs were required, individual mating pairs of fertile fish were placed in nesting tanks, with a divider separating the male from the female. After initiation of the light cycle the following morning, the female was removed from the nesting tank and squeezed to obtain unfertilised eggs as described previously (Westerfield, 1995). Immature eggs appeared whitish and withered, however, eggs of a good quality were slightly granular and yellowish in colour, and appeared intact and smooth on the surface.

2.2.3 Sperm collection and mounting

Sperm was squeezed from anaesthetised male zebrafish as described previously (Westerfield, 1995). The resulting sperm was resuspended in aquarium system water and cytospun in a Shandon SP3 centrifuge (Shandon, Massachusetts, USA) at 300 rpm for 3 mins on polysine microscope slides (BDH Laboratory Supplies). The mounted sperm sample was then encircled with wax using a PAP pen (Sigma) to facilitate further processing.

2.3 Protein techniques

2.3.1 Immunofluorescence

2.3.1.1 Fixation, de-chorionation and de-yolking

Unfertilised oocytes, mounted sperm samples and whole embryos of various selected stages (0.75 / 1.5 / 3 / 5 / 12 / 18 / 24 hours post fertilisation (hpf)) were fixed

overnight at 4 ºC in 4 % (wt/vol) paraformaldehyde (PFA) in phosphate-buffered saline (PBS), pH 7.4. Fixed oocytes and embryos of various stages then had their chorions and yolks removed using fine forceps (Dumont No. 5, Basel, Switzerland).

2.3.1.2 Permeabilisation

Zebrafish samples were then washed in PBS for 10 mins three times, and permeabilised in 0.2 % Triton X-100 for 2hrs at room temperature. After being washed twice with 0.05 % Tween 20 in PBS (PBST) for 15 mins they were ready for blocking or additional treatment outlined below.

2.3.1.3 Acid treatment for detection of methylated DNA

After permeabilisation, samples being probed for methylated DNA (unfertilised oocytes, mounted sperm samples and 0.75 / 1.5 / 3 / 5 / 12 / 18 / 24 hpf embryos) were treated for 10 mins with 2 M HCl in ddH2O at 37 °C, in order to denature the DNA. These samples were then washed twice with PBST for 15 mins ready for blocking.

2.3.1.4 Blocking, antibody incubation and washing

Fixed and permeabilised 3 / 5 / 12 / 18 / 24 hpf embryos for the histone modification studies and the denatured samples from above were blocked in 2 % bovine serum albumin (BSA) in PBS for a minimum of 1 hr at room temperature. These samples were then probed with primary antibody at a 1:200 dilution in fresh 2 % blocking solution (1:400 for the single stranded DNA (ssDNA) control antibody utilised in the DNA methylation study). Section 2.6 lists the antibodies used in this study. For the unfertilised oocytes and whole embryos, 25 µl micro-drops of the primary antibody solution were prepared in a Petri dish (Corning Inc., New York, USA) and covered with mineral oil, where the zebrafish samples could be placed into the drop with a fixed volume microdispenser (Drummond Scientific Company, Pennsylvania, USA) and incubated overnight at 4 °C. After three 15 mins wash steps in PBST, samples

were then incubated with 1:200 secondary antibody (diluted in blocking solution) for 1 hr at room temperature in the dark, in mineral oil-covered micro-drops. The samples were then washed a further three times in PBST for 15 mins.

2.3.1.5 Sample mounting

Unfertilised oocytes and whole zebrafish embryo samples were placed on ethanol-washed multi-well diagnostic slides (Menzel-Gläser, Braunschweig, Germany). All samples were mounted with a small drop of room temperature Prolong Gold (containing 4,6-diamino-2-phenylindole (DAPI) for the histone modification studies) (Invitrogen, Paisley, UK). Slides were then gently covered with an ethanol-washed cover slip, and the mounting medium allowed to cure overnight at room temperature in the dark. Nail polish was then used to seal the edges of the cover slip, and the slides stored at 4 °C in the dark until observation.

2.3.1.6 Microscopic imaging

The presence of fluorescing nuclei was determined with a sequentially scanned z-stack through the entire embryo (with slices of $\leq$ 5µm) using a Leica TCS SP5 inverted confocal laser scanning microscope, with primary and secondary-only controls undertaken (to assess autofluorescence and signal specificity) and settings within each experiment kept constant to allow sample comparison. Composite images were produced, where appropriate, using the LAS AF confocal microscope software (Leica, Milton Keynes, UK), and fluorescent profiles mapped using ImageJ software (National Institutes of Health, Maryland, USA). All experiments were repeated at least twice as a whole, each time with more than 5 embryos.

2.3.2 Sodium dodecyl sulphate polyacrylamide gel electrophoresis (SDS-PAGE) and western blotting

2.3.2.1 Acid extraction of histones from zebrafish embryos

Whole zebrafish eggs containing embryos from specific stages of development (3 / 5 / 12 / 18 / 24 / 48 hpf) were collected into separate 2 ml microcentrifuge tubes. These eggs were briefly washed in aquarium system water treated with methylene blue (Interpet Aquatic, Surrey, UK), and frozen with as little water as possible at -80 °C. Once each selected stage of development was collected, the samples were resuspended in 1 ml fresh, ice-cold lysis buffer (10 mM HEPES pH 7.9, 1.5 mM $MgCl_2$, 10 mM KCl, 0.5 mM dithiothreitol (DTT) and 1x Complete Mini Protease Inhibitor Cocktail stock solution (Roche Applied Science)). These eggs were then homogenised with ice-cold metal beads in a Retsch MM 301 mixer mill (Retsch UK Ltd., Leeds, UK) for 1 min at 4 °C. Ice-cold HCl was added to a final concentration of 0.2 M, and the samples incubated on ice for 30 mins. The tubes were then centrifuged at 11,000 x g for 10 mins at 4 °C to pellet the acid-insoluble debris. The supernatant was retained and the acid-soluble proteins within, such as histones, were precipitated overnight at -20 °C in eight volumes of acetone. The precipitate was recovered by centrifugation at 2000 x g for 10 mins at 4 °C. The pellets were washed and centrifuged a further two times with ten pellet volumes of freshly prepared 100 mM HCl / acetone solution at 2000 x g for 10 mins at room temperature. Finally the histone-containing pellet was washed three times with at least 10 pellet volumes of dry acetone at room temperature to remove residual acid, centrifuging as above, and then dried under vacuum at room temperature. The acid-extracted histone-containing pellet was then stored at -20 °C until sample preparation.

2.3.2.2 Polyacrylamide gel preparation

Polyacrylamide gel electrophoresis (PAGE) for separation of proteins employed 15 % resolving gels (0.375 M Tris pH 8.8, 0.1 % SDS, 0.1 % APS, 0.04 % TEMED and 15 % acrylamide) set using Atto gel casting equipment (Atto Corporation, Tokyo, Japan), with a 5 % stacking gel (0.125 M Tris pH 6.8, 0.1 % SDS, 0.1 % APS, 0.1 % TEMED and 5 % acrylamide) cast above it with a comb. Freshly prepared gels were

then assembled into a mini-slab gel electrophoresis tank (Atto Corporation) which was then filled with 1 x running buffer (0.025 M Tris, 0.19 M glycine and 0.1 % SDS).

2.3.2.3 Sample preparation for gel electrophoresis

1 x LDS sample buffer (Invitrogen) was used to dissolve the histone-containing extracts from various stages of zebrafish development. After brief centrifugation to pellet any insoluble material, clarified samples were transferred into fresh tubes and stored at -20 °C. Prior to running a gel, tubes were thawed on ice and 100 mM DTT added to aliquots of each sample. These mixtures were then boiled at 95 °C for 10 mins, and after spinning briefly, were loaded on to 15 % polyacrylamide gels along with a pre-stained protein marker (PageRuler, Fermentas, York, UK). Once all the samples were loaded, the gel was run at 125 V for 2 hrs, or until the loading dye had reached the bottom of the gel. Gels were then either stained with coomassie brilliant blue staining solution (Bio-Rad, Hemel Hempstead, UK) for 45 mins with multiple washes of ddH_2O after, or processed for western blot.

2.3.2.4 Semi-dry transfer on to polyvinylidene fluoride (PVDF)

Proteins were transferred on to Hybond-P PVDF membranes (Amersham Biosciences, Amersham, UK) for antibody detection using a semi-dry blotter (Bio-Rad). Firstly, a gel-sized piece of PVDF membrane was briefly wet in methanol, and then soaked in transfer buffer (39 mM Glycine, 48 mM Tris, 0.0375% (w/v) SDS and 20% Methanol) for 5 mins with two sheets of equally-sized extra thick blot paper (Bio-Rad). In the meantime, the gel-casting plates were disassembled and the stacking gel removed using a clean spatula. The semi-dry blotter was then loaded up with a 'sandwich' composed of the extra thick blot paper, the PVDF membrane, the 15 % resolving gel and the last remaining piece of extra thick blot paper one after another. Air bubbles were removed by gently rolling a pipette over the surface, and the cathode plate and lid of the blotter finally put in place. A current of 2 mA / cm^2

was applied for 45 mins, and the efficiency of the transfer was assessed visually by how well the pre-stained protein marker had transferred on to the membrane.

2.3.2.5 Blocking, antibody incubations and washing

Membranes were blocked for 1 hr at room temperature with 5 % non-fat dried milk with 1 % BSA in 0.1 % Tween 20 / tris-buffered saline (TBST) with constant agitation. Blocked membranes were then probed with primary antibody diluted in fresh blocking solution, the conditions and timing of which were specified in the relevant certificate of analysis (with the antibodies used outlined in section 2.6). These membranes were washed with TBST 4 x 5 mins, and then probed with a 1:10,000 dilution (in blocking solution) of the anti-rabbit horse radish peroxidise (HRP)-conjugated secondary antibody (GE Healthcare UK Ltd., Amersham, UK) for 1 hr at room temperature with constant agitation. Subsequently, the PVDF membranes were washed again with TBST 4 x 5 mins ready for chemiluminescent detection. Once again, all experiments were repeated independently at least twice for each antibody tested.

2.3.2.6 Chemiluminescent signal detection

The membranes were briefly washed in ddH_2O, and the Immobilon Western HRP Substrate (Millipore) prepared according to the instructions provided by the supplier. After 5 mins incubation with the chemiluminescent substrate, the membranes were drained and placed in a suitable detection pocket in an X-ray film cassette. A sheet of Kodak Biomax Light Film (Sigma) was placed on top of the PVDF membrane and exposed for 5 secs to 15 mins depending on the strength of the signal. The exposed films were developed using an autoradiograph developer (Konica Minolta, New Jersey, USA).

2.3.2.7 Multiple infrared signal detection

Gels were run as above with at least two independent repeats, but blotted on to Immobilon-FL PVDF (Millipore). Membranes were blocked for 1 hr at room temperature with constant agitation in Odyssey blocking buffer (Licor Biosciences UK Ltd., Cambridge, UK). Blocked membranes were then probed with two different primary antibodies (one from rabbit, the other from mouse, as outlined in section 2.6) and washed as usual, substituting the milk-based block with the Odyssey blocking buffer, and the TBST with 0.1 % PBST. However, at the relevant stage these membranes were probed with a 1:10,000 dilution of anti-rabbit and anti-mouse differentially-labelled fluorescent secondary antibodies (Licor Biosciences) for 1 hr at room temperature with constant agitation in the dark. Section 2.6 lists the antibodies used. Subsequently, the PVDF membranes were rinsed with PBS ready to scan with the Odyssey Infrared Imaging System (Licor Biosciences), according to the directions of the manufacturer. This system was also used with single primary antibodies as an alternative to chemiluminescent detection.

2.3.2.8 Membrane stripping and re-probing

Where appropriate, membranes were stripped of primary antibody by being incubated in pre-heated stripping buffer (2 % SDS, 62.5 mM Tris-HCl pH 6.8 and 100 mM β-Mercaptoethanol) for 45 mins at 50 °C with constant agitation within a sealed container in a fume hood. The membranes were then rinsed under a running deionised water tap for 1 – 2 hrs. After a 1 min methanol rehydration step, they were washed with TBST 3 x 5 mins, ready for the blocking stage and the rest of the immunodetection protocol.

2.3.3 Protein fingerprinting using matrix assisted laser desorption / ionization- time of flight (MALDI-TOF) mass spectrometry

2.3.3.1 Sample preparation

A gel was run and blotted on to a PVDF membrane as above. Clean gloves were worn to ensure that there was no contamination from keratins in the skin. The regions

of interest in the unblocked PVDF membrane were cut with clean scissors and processed individually. To begin with, the PVDF fragments were briefly washed with 300 µl 200 mM ammonium bicarbonate (ABC) in 50 % acetonitrile (ACN). They were then incubated in 300 µl 20 mM DTT / 200 mM ABC / 50 % ACN for 1 hr to reduce the disulfide bonds in the proteins. The fragments were briefly washed again in 300 µl 200 mM ABC in 50 % ACN three times, and then incubated with 100 µl 50 mM iodoacetamide / 200mM ABC / 50% ACN at room temperature for 20 mins in the dark to alkylate the cysteines present in the samples. The membranes were briefly washed with 20mM ABC in 50% ACN three times, and then allowed to dry. A stock solution of trypsin was prepared by adding 50 µl 50mM ABC to a new 20 µg vial of sequencing grade modified trypsin (Promega, Southampton, UK) at 4 °C. The dried membranes were wet with 3 µl ACN, and then incubated overnight at 32 °C with 30 µl 50mM ABC in 30% ACN containing 1 µl of the trypsin stock. The next day the supernatants were transferred into individual 0.5 ml Eppendorf tubes. Peptides were further extracted by sonicating the PVDF fragments with 30 µl 80% ACN for 15min in a sonicating water bath (IKA Labortechnik, Staufen, Germany). The respective supernatants were then ready for spotting on to a MALDI plate.

2.3.3.2 Mass spectrometric analysis

MALDI-TOF separation of the tryptic peptides prepared from the protein samples was performed with a Voyager DE-STR instrument (Applied Biosystems, Warrington, UK) located within the Swann Building, University of Edinburgh. Operation of the mass spectrometer, as well as subsequent streamlining and calibration of the spectra obtained was conducted under the supervision of Dr. Andy Cronshaw (Proteomics Facility Manager, Swann Building, University of Edinburgh). In order to identify the origins of the peptide masses detected, the experimental mass spectra obtained were compared *in silico* against a library of predicted tryptic mass spectra composed of zebrafish histones, using the software FA-Index in conjunction with the internet-based programme MS-Fit (University of California, San Francisco, USA). Sequence alignments were produced using ClustalW (European Bioinformatics Institute, Cambridge, UK).

2.4 Tissue culture

To establish long-term cultured cells and to obtain ESC-like clusters, 16 – 20 hpf embryos were prepared for cell culture using a protocol adapted from Westerfield (1995), as described below.

2.4.1 Preparation of zebrafish embryos for cell culture

Firstly, approximately 100 embryos were placed in a sterile cell strainer (BD Biosciences, Oxford, UK) and disinfected in 0.5 % fresh bleach in ddH_2O for 2 minutes (using 10 -13 % sodium hypochlorite from Sigma). The embryos were then rinsed in 10 % Hank's balanced salt solution (Sigma) for 2 mins and de-chorionated in 3 mg/ml pronase (Sigma) in PBS for 45 mins under sterile conditions.

2.4.2 Protease dissociation and plating of cells

De-chorionated embryos were subsequently washed in sterile filtered calcium-free Ringer's solution (116 mM NaCl, 2.9 mM KCl, 5 mM HEPES pH 7.2) for 15 minutes and then incubated with 1x trypsin / EDTA (Lonza BioWhittaker, Maryland, USA) for 1 – 2 hrs at 28.5 °C with occasional agitation until completely dissociated. 1 mM $CaCl_2$ and 10 % fetal calf serum (FCS) (Sigma) were added to stop the reaction, and the cells collected by centrifugation at 150 x g for 3 mins. The supernatant was discarded and the cells resuspended in Leibowitz's L-15 medium (Invitrogen) supplemented with 0.3 mg/ml glutamine, 50 U/ml penicillin, 0.05 mg/ml streptomycin and 0.8 mM $CaCl_2$. The centrifugation step was repeated and the resulting pellet resuspended in supplemented L-15 medium (as above) with 10 % zebrafish embryo extract (Westerfield, 1995), 3 % FCS and 50 ng/ml recombinant bovine basic fibroblast growth factor (rbbFGF) (R & D Systems, Abingdon, UK) to make a final concentration of 50 embryos/ml. Cell suspensions were finally plated into 4-well Nunclon culture plates (Fisher Scientific UK, Loughborough, UK) or 4-well LabTek II chamber slides (Fisher Scientific UK), and left to grow overnight at 28.5 °C without additional atmospheric CO_2. Cells were gently washed with sterile

PBS the following day to remove cellular debris, and were maintained in fresh medium thereafter (with the media being replaced approximately every 2 days from then on).

2.4.3 Passaging of cells

Once almost confluent, cells were washed twice with PBS, and then enough pre-warmed trypsin added to cover the base of the well. Culture dishes were then incubated at 28.5 °C for a maximum of 2 mins, and the reaction neutralised by the addition of 5 x the volume of fully supplemented medium. Cell suspensions were spun down at 150 x g for 3 mins, and the supernatant discarded. The pellet was then resuspended in 1 ml fully supplemented L-15 medium, and the cells split 1 : 2 in new plates.

2.5 Somatic cell nuclear transfer set-up

2.5.1 Zebrafish strains

For donor cells, a transgenic line of zebrafish expressing a H2A.F/Z:GFP fusion protein was utilised (Pauls, Geldmacher-Voss et al. 2001), while recipient eggs were obtained from wild-type Tupfel long fin zebrafish.

2.5.2 Preparation of recipient eggs

Recipient eggs were obtained by first anaesthetising and then squeezing female fish, as is described previously by Westerfield (1995). To delay activation, these eggs were placed directly into Hank's saline solution supplemented with 0.5% BSA (Nusslein-Volhard and Dahm 2002). Immature eggs appeared whitish and withered, however, eggs of a good quality were slightly granular and yellowish in colour, and appeared intact and smooth on the surface.

2.5.3 Visualisation of cell nuclei from embryos

Fertilised embryos of various stages were first dechorionated with 3 mg/ml pronase (Sigma) as described by Westerfield (1995). Samples were then sequentially fixed and stained with 4% (wt/vol) paraformaldehyde and 1 μg/ml Hoechst 33342 (Sigma) in phosphate buffered saline (PBS) following Huang *et al.* (2003).

2.5.4 Visualisation of the polar body and maternal pro-nucleus of oocytes

To visualise the nuclei from unfertilised and recently fertilised eggs, a 50:50 fixative/stain mix was injected into the oocyte cytoplasm under a Leica MZFLIII dissecting stereomicroscope, using a micromanipulator (Leica, Milton Keynes, UK) and a Narashige programmable IM-300 microinjector (Tokyo, Japan). Glass capillary tubes (Harvard Apparatus Ltd., Kent, UK) were pulled on a Narashige PC-10 pipette puller (Tokyo, Japan), and the ends of these pipettes were removed using fine forceps (Dumont No. 5, Basel, Switzerland) to give an opening of between 5-10 μm in diameter, with approximately 125-250 pl of the fixative/stain mix being administered per injection. The samples were then visualised under UV light using the same microscope, as were the polar bodies but under phase contrast.

2.5.5 Preparation of donor cells

Primary cells were collected from 5-15 somite embryos as described in Huang *et al.* (2003). To establish long-term cultured cells, 16-20 somite embryos from H2A.F/Z:GFP zebrafish were prepared for cell culture using the tissue culture protocol from section 2.4. Cells were plated in L-15 growth medium (Invitrogen), containing 10% embryo extract, 3% fetal calf serum and 50 ng/ml recombinant basic bovine fibroblast growth factor (rbbFGF), and left to grow at 28.5 ºC without any additional CO_2. They were maintained in fresh medium and passaged when confluent.

2.5.6 Microinjection set-up

The holding pipette and microinjection pipettes were a kind gift from Dr. Walid Maalouf (Molecular Physiology, QMRI, University of Edinburgh). Recipient eggs were manipulated with their chorions left intact in a Petri dish containing 0.5% BSA / Hank's saline solution, using a Leica MZFLIII dissecting stereomicroscope and micromanipulator (Leica, Milton Keynes, UK).

2.6 Embryonic stem-like cell characterisation

2.6.1 Alkaline phosphatase staining

Cell cultures were evaluated for alkaline phosphatase (AP) activity using an AP detection kit (Sigma) in accordance with the manufacturer's instructions. Briefly, the cells were washed with PBS once, fixed with a citrate / acetone / formaldehyde solution for 1 minute, and then stained with an AP staining solution for 15 minutes in the dark. AP-positive cells stained red, and the experiment repeated at least twice.

2.6.2 Reverse transcription - polymerase chain reaction (RT-PCR)

2.6.2.1 RNA extraction

To prevent contamination from RNases, clean gloves were worn at all times, RNase-free plasticware and solutions were used throughout, and surfaces were treated with RNase Away (VWR International, Lutterworth, UK). Following these precautions, RNA was isolated from cell cultures using TRIzol reagent (Invitrogen) according to the manufacturer's instructions. The isolated RNA was resuspended in 50 µl DEPC-treated ddH_2O and stored at -80 ºC. The concentration and quality of the extracted material was quantified by spectrophotometry.

2.6.2.2 Reverse transcription

Maintaining an RNase-free environment, cDNA synthesis from 5 µg total RNA was carried out using Superscript II reverse transcriptase (Invitrogen) with either oligo dT or random primers following the manufacturer's protocol.

2.6.2.3 PCR amplification of cDNA

PCR was performed in a Peltier Thermal Cycler (Bio-Rad) using primers outlined in Table 2.3. 10 µl PCR reactions were set up that contained 1 x PCR buffer, 1.5 mM $MgCl_2$, 0.2 mM of each dNTP, 0.2 µM of each primer, 0.4 U of *Taq* polymerase (Qiagen, Crawley, UK) and 0.4 µl of the cDNA reaction mixture. With controls conducted using no cDNA, as well as samples from a reverse transcription reaction where no reverse transcriptase was added, in order to check for contaminating DNA. An example of a typical PCR cycle is shown below, with annealing temperatures based upon the calculated melting temperature (T_m) of each primer pair:

Step	Temperature	Time	Purpose	
1	94ºC	2 min	*Taq* polymerase added for hot start	
2	94ºC	30 secs	Denaturation	x30
3	T_m	1 min	Annealing	
4	72ºC	45 secs	Extension required for *Taq* polymerase	
5	72ºC	5 mins	Final extension	
6	4ºC	Hold	End	

2.6.2.4 Agarose gel electrophoresis

PCR reactions were loaded with 6 x Blue / Orange Loading Dye (Promega), and were separated according to their size on 1% agarose gels prepared using SeaKem LE agarose (BioWhittaker Molecular Applications, Wokingham, UK), 0.5 x Tris / Borate / Ethylenediaminetetraacetic acid (EDTA) TBE buffer and 0.5 µg/ml

ethidium bromide (Sigma). Samples were run with a 1 kb DNA ladder (Promega) at 6 V/cm, and gel images captured using a Kodak EDAS 290 digital camera system and Kodak 1D 3.5.3-USB Scientific Imaging System software (Eastman Kodak Company, New York, USA). With the whole experiment independently repeated at least twice.

2.6.3 Microinjection of zebrafish embryos

2.6.3.1 Micropipette preparation

Glass capillary tubes (Harvard Apparatus Ltd., Kent, UK) were pulled on a Narashige PC-10 pipette puller (Tokyo, Japan), and the ends of these pipettes were removed using fine forceps (Dumont No. 5) to give an opening of between 5-10 µm in diameter.

2.6.3.2 H2A.F/Z:GFP cell preparation

Cell cultures derived from H2A.F/Z:GFP zebrafish embryos were treated with enough pre-warmed trypsin to cover the base of the well. Culture dishes were then incubated at 28.5 °C for a maximum of 2 mins, and the reaction neutralised by the addition of 1 mM $CaCl_2$ and 10 % FCS. Cell suspensions were spun down in 0.5 ml eppendorfs at 150 x g for 3 mins, and the supernatant discarded. The pellet was resuspended in 10 µl cell transplantation solution (100 mM NaCl, 5 mM KCl, 5 mM HEPES, pH 7.1) ready for microinjection.

2.6.3.3 Microinjection and imaging

Micropipettes were loaded with cell solution, and wild-type embryos were injected at 3 hpf under a Leica MZFLIII dissecting stereomicroscope using a micromanipulator (Leica) and a programmable IM-300 microinjector (Narashige). Cells aspirated directly from H2A.F/Z:GFP 3 hpf embryos were also injected into wild-type blastulas as a control, and a group of non-injected wild-type embryos was also kept aside in order to assess the viability of the acceptor embryos in general. The

developing microinjected embryos were placed in filtered system water and incubated at 28.5 °C. They were regularly monitored for fluorescence for up to 5 days post fertilisation (dpf), after which they were disposed of in accordance with the Animals (Scientific Procedures) Act 1986. Images were taken with the GFP-2 fluorescence filter (Leica) and under white light using a DFC300 FX Digital Camera System (Leica), and the whole experiment repeated independently at least twice.

2.6.4 Cell immunofluorescence

Cells within LabTek II chamber slides (Fisher Scientific UK) were fixed overnight at 4 ºC in 4 % PFA / PBS, pH 7.4. Fixed cells were then washed in PBS for 5 mins two times, and permeabilised in 0.4 % Triton X-100 / PBS for 20 mins at room temperature. After being washed twice in PBS for 10 mins they were blocked in 2 % BSA in PBS for a minimum of 1 hr at room temperature. These samples were then probed with primary antibody at a 1:200 dilution in fresh 2 % blocking solution overnight in a humidified chamber. After three 15 mins wash steps in PBST, samples were then incubated with 1:200 secondary antibody (diluted in blocking solution) for 1 hr at room temperature in the dark. The samples were then washed a further three times in PBST for 15 mins. The chambers were then removed from the slides and all samples mounted with a small drop of room temperature Prolong Gold containing DAPI (Invitrogen). Slides were then gently covered with an ethanol-washed cover slip, and the mounting medium allowed to cure overnight at room temperature in the dark. Nail polish was then used to seal the edges of the cover slip, and the slides stored at 4 °C in the dark until observation. The presence of fluorescing nuclei was determined with a sequentially scanned z-stack (with slices of $\leq 5\mu m$) using a Leica TCS SP5 inverted confocal microscope, with primary and secondary-only controls undertaken prior to investigation. Composite images were produced, where appropriate, using the LAS AF confocal microscope software (Leica), with each experiment repeated at least twice for each antibody tested.

2.7 Antibodies

2.7.1 Primary

Name	Type	Supplier	Cat. No.
Anti-5-Methylcytidine	Mouse monoclonal IgG	Eurogentec	BI-MECY-0100
Anti-single stranded DNA	Rabbit polyclonal IgG	Demeditec Diagnostics	18731
Anti-centromere, CREST antibodies	Human antiserum	Immunovision	HCT-0100
Anti-Histone H3, CT, pan	Rabbit antiserum	Millipore	07-690
Anti-monomethyl-Histone H3 (Lys9)	Rabbit polyclonal IgG	Millipore	07-450
Anti-dimethyl-Histone H3 (Lys9)	Rabbit polyclonal IgG	Millipore	07-441
Anti-trimethyl-Histone H3 (Lys9)	Rabbit polyclonal IgG	Millipore	07-442
Anti-monomethyl-Histone H4 (Lys20)	Rabbit immunoaffinity purified IgG	Millipore	07-440
Anti-dimethyl-Histone H4 (Lys20)	Rabbit antiserum	Millipore	07-367
Anti-trimethyl-Histone H4 (Lys20)	Rabbit antiserum	Millipore	07-463
Anti-poly (ADP-ribose)	Rabbit polyclonal Ig	BD Biosciences	551813
Anti-Ubiquitin, clone P4D1-A11	Mouse monoclonal IgG	Millipore	05-944
SUMO-2/3 (FL-103)	Rabbit polyclonal IgG	Gift from Irina Stancheva	
Anti-trimethyl-Histone H3 (Lys4)	Rabbit antiserum	Millipore	07-473

Anti-trimethyl-Histone H3 (Lys27)	Rabbit polyclonal IgG	Millipore	07-449
SSEA1 antibody [MC480]	Mouse monoclonal IgG	Gift from Ian Chambers	
SOX2 antibody - Embryonic Stem Cell Marker	Rabbit polyclonal IgG	Abcam	ab15830
Oct-3/4 (C-10)	Mouse monoclonal IgG	Gift from Ian Wilmut	

Table 2.2 Primary antibodies

2.7.2 Secondary

Name	Type	Supplier	Cat. No.
Amersham ECL anti-rabbit IgG HRP-linked species-specific whole antibody	Donkey antiserum	GE Healthcare	NA934
IRDye 680 anti-rabbit IgG (H+L) antibody	Donkey antiserum	Gift from Licor	
IRDye 800CW anti-rabbit IgG (H+L) antibody	Donkey antiserum	Gift from Licor	
IRDye 800CW anti-mouse IgG (H+L) antibody	Donkey antiserum	Gift from Licor	
Alexa Fluor 488 anti-mouse IgG (H+L) antibody	Donkey antiserum	Invitrogen	A21202
Alexa Fluor 488 anti-rabbit IgG (H+L) antibody	Donkey antiserum	Invitrogen	A21206
Alexa Fluor 555 anti-rabbit IgG (H+L) antibody	Donkey antiserum	Invitrogen	A31572
Alexa Fluor 647 anti-human IgG (H+L) antibody	Goat antiserum	Invitrogen	A21445

Table 2.3 Secondary antibodies

2.7.3 Primers

Marker	Forward primer 5'-3'	Reverse primer 5'-3'	T_M	Reference
vasa	TGTGGACGTGAGTGGCAGCAATC	CTAGATAGCGCACTTTACTCAGG	64 °C	Ma *et al*., 2001
pou2	CCACCATGGAGACTCTGACTACTGAAGATT	ATCAATACTGTGCTTCAACACACTCGTCAT	62 °C	Takeda *et al.*, 1994
sox2	CGCTCCAGTACAACTCCATGACC	TTACATATGCGATAAGGGAATCGTGC	55 °C	Okuda *et al*., 2006
gsc	AAGAGAACAACTGGCACGAA	GGTACATCTTATCACGACAA	58 °C	Sagerstrom *et al*., 1996
MyoD	CACGTCCACCAACCCGAACCA	TCCAAACTCGACACCACTGA	58 °C	Sagerstrom *et al*., 1996
eng3	CTGTTGCAGGCTCCTGGAAA	CTGTCCTCCGTGTTAATCAC	55 °C	Sagerstrom *et al*., 1996
wnt-1	TGTGTCCTCCTGGTGTCCTCT	ATTCGCCCTGCCTCATTGTTG	55 °C	Sagerstrom *et al*., 1996
β-actin	CTGGGTATGGAATCTTGCGGTATC	CGAGAGTTTAGGTTGGTCGTTCG	55 °C	Okuda *et al*., 2006

Table 2.4 RT-PCR primer sequences

Part I: Epigenetic profiling of the developing zebrafish embryo

Chapter Three

3 Global nuclear DNA methylation changes in the developing zebrafish embryo

3.1 Introduction

As discussed in sections 1.4 and 1.5, DNA methylation is established and maintained by *de* novo and maintenance DNA methyltransferases, and forms the basis of numerous regulatory mechanisms involved in the repression of gene expression by various protein complexes. The important function of DNA methylation in normal development is underscored by its involvement in genomic imprinting and X chromosome inactivation, as well as its role in retroviral transposon silencing involved in "genome defence" (Bird 2002). CpG methylation is also one of the hallmarks of chromatin that is found in condensed heterochromatin. Gene knock-out studies further highlight its essential role, as removing DNA methyltransferase activity in mice leads to major dysfunctions in embryonic development and eventual mortality (Li, Bestor et al. 1992; Okano, Bell et al. 1999).

Changes in genome-wide DNA methylation levels nevertheless occur naturally during various stages of mouse development, such as during early embryogenesis (Monk, Boubelik et al. 1987). Further studies confirmed that the maternal and paternal contributions to the genome are demethylated after fertilisation, and that the embryonic genome is subsequently remethylated by the blastocyst stage of development (Santos, Hendrich et al. 2002). This pattern of reprogramming appears to be largely conserved in eutherian mammals, although the extent of demethylation and developmental timing of these events do seem to differ between various species (Fig. 1.4) (Dean, Santos et al. 2001). However, the concept of a global demethylation process being an essential feature of early mammalian development is still controversial, and work stating that this process is lacking in rabbit, sheep and pig

zygotes definitely challenges this point of view (Beaujean, Hartshorne et al. 2004; Shi, Dirim et al. 2004; Jeong, Yeo et al. 2007).

The functional significance of this reprogramming event during embryogenesis (as observed in the mouse, but not every species studied to date) is at present unclear. It could have a role in imprinting (Reik and Walter 2001) or reflect a general removal of gametic methylation patterns, ensuring totipotentcy in preparation for subsequent somatic development (Monk, Boubelik et al. 1987). Another reciprocal possibility could be that remethylation of the zygotic genome may play a part in defining cell fate decisions during embryogenesis (Reik, Santos et al. 2003).

Taking this into consideration, knock-down studies in non-mammalian vertebrates, such as *Xenopus* and zebrafish, reiterate the fact that DNA methylation is essential for development (Martin, Laforest et al. 1999; Stancheva, Hensey et al. 2001; Rai, Nadauld et al. 2006). Studies in *Xenopus*, however, have observed no global active reprogramming events after fertilisation (Stancheva, El-Maarri et al. 2002). In zebrafish, on the other hand, the presence of any genome-wide DNA methylation changes is still under some discussion. Previous studies reported that there were indeed variations in global DNA methylation levels during early zebrafish development (Martin, Laforest et al. 1999; Mhanni and McGowan 2004; MacKay, Mhanni et al. 2007), while others concluded that such genome-wide changes did not occur (Macleod, Clark et al. 1999). A similar result to Macleod *et al.* was also observed in medaka (*Oryzias latipes*), a teleost related to zebrafish, where no alterations in the levels of DNA methylation were seen during its development (Walter, Li et al. 2002).

Thus, in this chapter I set out to resolve whether genome-wide DNA methylation changes do indeed take place during zebrafish embryogenesis. The objective was to use an anti-5-methylcytosine antibody in a set of novel whole-embryo

immunofluorescence experiments, which take advantage of the transparency of the zebrafish embryo. Global nuclear levels of CpG methylation were visualised with a fluorescent secondary antibody and recorded by laser confocal microscopy, an imaging approach not employed before with this species. These studies demonstrated that the DNA of both parental gametes was initially methylated, and that reprogramming of the DNA methylation mark did in fact occur during zebrafish development. This observation was demonstrated by a decrease in the genomic DNA methylation signal during early embryogenesis, followed by an increase by the blastula stage. This CpG methylation signal was localised around the nuclear periphery, and was seen to persist in all subsequent stages examined.

3.2 Results

3.2.1 DNA methylation dynamics during development

To assess the presence of genome-wide DNA methylation changes in the developing zebrafish embryo, immunofluorescence experiments were conducted using a well-characterised mouse anti-5-methylcytosine antibody. Zebrafish embryos from a range of successive developmental stages were collected and fixed, and samples were processed simultaneously and subject to identical conditions throughout each procedure to allow direct comparison between the stages. Immunocytochemical detection of DNA 5-methylcytosine on slide-mounted zebrafish samples was supported by counterstaining for single stranded DNA (ssDNA). This additional antibody control provided a reference signal for the amount of DNA in the nuclei of these rapidly replicating cells, as the anti-5-methylcytosine antibody required prior denaturation of nuclear DNA for epitope recognition. The sperm samples were directly cyto-spun on to slides, and all other stages were mounted on the slides without the obscuring yolk sac and with some flattening by the coverglass to allow for better presentation of cells in the focal plane.

Fig. 3.1 shows the immunocytochemical detection of DNA 5-methylcytosine for a range of zebrafish developmental stages. Methylation reprogramming is evident

when comparing the top half of each panel to the simultaneous immunocytochemical detection of the ssDNA control in the bottom half. In Fig. 3.1a the methylated state of zebrafish sperm is shown, next to a representative brightfield image (adapted from Kurita et al., 2004). Fig. 3.1b demonstrates that the DNA within an unfertilised oocyte is also methylated in the maternal pronucleus (asterisk) and polar body (arrow), with a representative brightfield image alongside. However, DNA methylation is undetectable at the 2-cell stage at ≈ 0.75 hpf (Fig. 3.1c), and remains undetectable at the 16-cell stage at ≈ 1.5 hpf (Fig. 3.1d). Subsequently, the 512-cell early blastula stage embryo at ≈ 2.75 hpf shows nuclei with varying degrees of DNA methylation around the nuclear periphery (Fig. 3.1e). The early gastrula stage embryo during 50%-epiboly at ≈ 5.3 hpf presents comparatively more nuclei with detectable DNA methylation around the nuclear perimeter (Fig. 3.1f). As development proceeds, peripherally-localised methylated DNA is also evident within the cell nuclei of the 3-somite embryo at ≈ 11 hpf (Fig. 3.1g), the 18-somite embryo at ≈ 18 hpf (Fig. 3.1h), as well as the ≈ 24 hpf embryo (Fig. 3.1i). For clarity, all zygotic stages are accompanied with their corresponding camera lucida sketches from Kimmel et al. (1995).

In summary, these experiments showed that mature sperm were indeed strongly methylated (Fig. 3.1a), and that the maternal pro-nucleus and polar body within the unfertilised oocyte were also methylated (Fig. 3.1b). In contrast, DNA methylation in the early cleavage stages (from 2 to 16-cells) was reduced to undetectable levels (Fig. 3.1c-d). The positive ssDNA signal in these samples indicated that there were indeed antibody stainable nuclei present at these stages of development. At the 512-cell stage or approximately 2.75 hpf, just as zygotic transcription begins at the mid-blastula transition (MBT) (Kane and Kimmel 1993), DNA methylation becomes detectable around the nuclear periphery asynchronously throughout the embryo (Fig. 3.1e). At this stage only some cell nuclei stain for CpG methylation, while others do not. From 50%-epiboly, almost all cell nuclei appeared positive for this antibody, with the nuclear peripheral staining pattern persisting throughout gastrulation and through all subsequent stages examined (up until 24 hpf) (Fig. 3.1f-i).

3.2.2 Peripheral localisation of DNA methylation and pericentric heterochromatin

Closer inspection of the localisation of DNA methylation in the 512-cell embryo indicated that it was indeed situated around the nuclear periphery (Fig. 3.2a-b). Using the immunocytochemical patterns of DNA 5-methylcytosine (green) and ssDNA (red) from Fig. 3.2a, the immunofluorescence profile of a single nucleus (Fig. 3.2a, white bar) was graphically represented in Fig. 3.2b. This demonstrated the peripheral localisation of DNA methylation (green) in the 512-cell early blastula stage embryo (≈ 2.75 hpf) in marked contrast to the ssDNA control (red).

This striking peripheral localisation of DNA methylation was investigated further by determining the location of pericentric heterochromatin within the nuclei. Using antibodies from patients with CREST syndrome, it could be seen that centromeres, which are flanked by pericentric heterochromatin, also localised around the edges of nuclei around this stage of development. Fig. 3.2c shows centromeres localised around the edges of four individual nuclei as detected by CREST antibodies (red), with DNA stained by DAPI (blue). In the mouse and other organisms, centromeres are the primary site for constitutive heterochromatin formation, and this co-localisation supports a perinuclear organisation of heterochromatin in the cell nuclei of the developing zebrafish embryo.

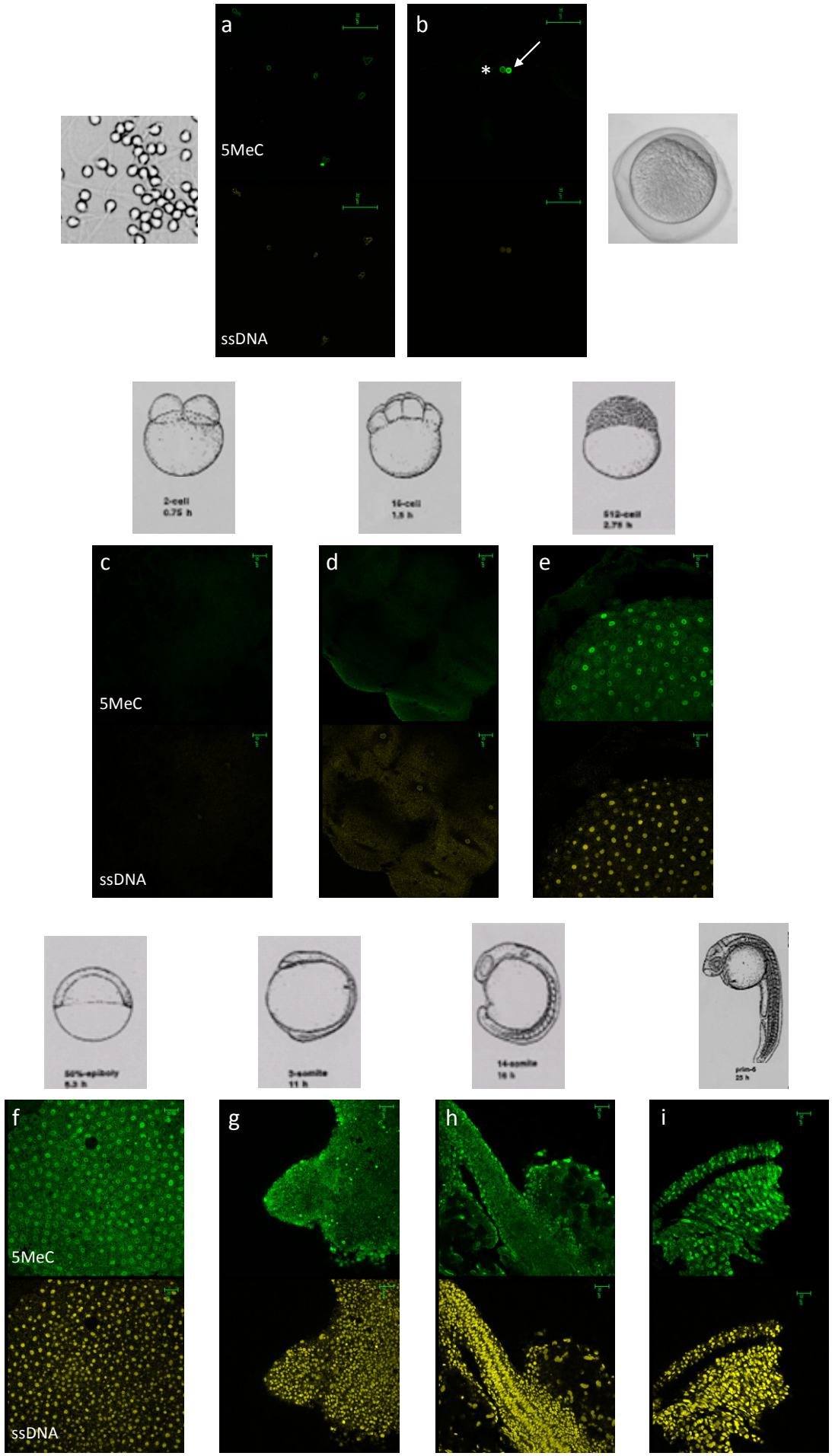

Fig. 3.1: Legend overleaf.

Fig. 3.1: Immunocytochemical detection of DNA 5-methyl cytosine (5MeC) at various developmental stages (green), as analysed by confocal microscopy and illustrated by single sections. **(a)** Zebrafish sperm. **(b**) An unfertilised oocyte with the maternal pronucleus (asterisk) and polar body (arrow) present. **(c)** The 2-cell stage at ≈0.75 hpf. **(d)** The 16-cell stage at ≈1.5 hpf. **(e)** The 512-cell stage at ≈2.75 hpf. **(f)** The 50%-epiboly stage at ≈5.3 hpf. **(g)** The 3-somite stage at ≈11 hpf. **(h)** The 18-somite stage at ≈18 hpf. **(i)** ≈24 hpf. All stages are accompanied with their corresponding single stranded DNA (ssDNA) control images (yellow). The representative zebrafish sperm image is adapted from Kurita *et al.* (2004), and all zygotic stages are partnered with their camera lucida sketches from Kimmel *et al.* (1995). Scale bar, 30 μm.

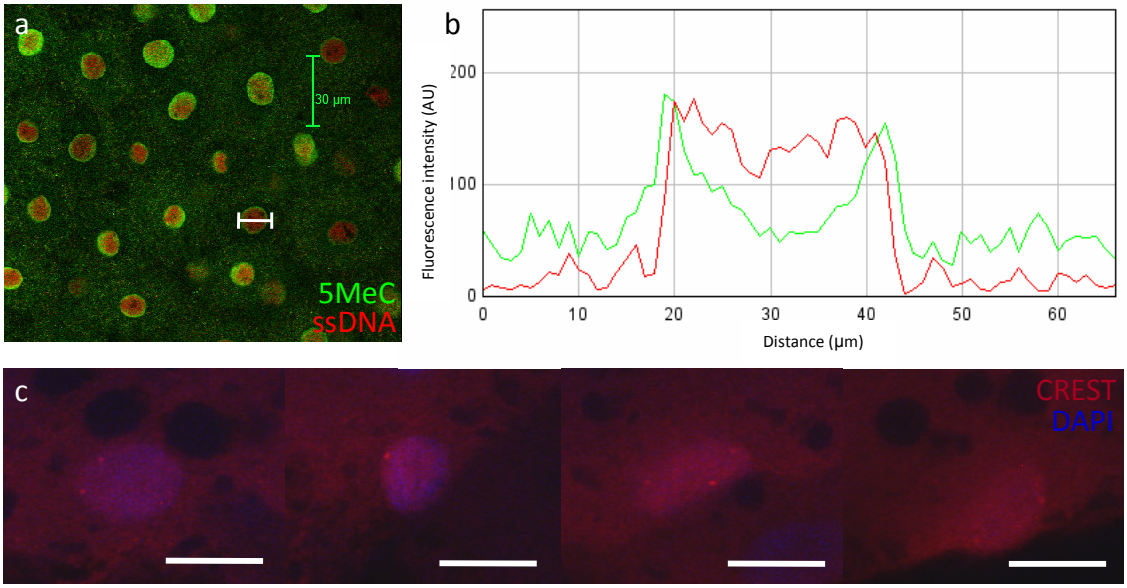

Fig. 3.2: Peripheral localisation of DNA methylation and pericentric heterochromatin within the nuclei of 512-cell early blastula stage embryos (≈2.75 hpf), as analysed by confocal microscopy with single sections shown. **(a)** Immunocytochemical detection of DNA 5-methyl cytosine at the periphery of a number of nuclei (green), as opposed to ssDNA (red). Scale bar, 30 μm. **(b)** Immunofluorescence profile of a nucleus in Fig. 3.2a (white bar) graphically representing the peripheral localisation of DNA methylation (green) in marked contrast to the ssDNA control (red). **(c)** Centromeres localised around the edges of four individual nuclei as detected by CREST antibodies (red), with DNA stained by DAPI (blue). Scale bar, 15 μm.

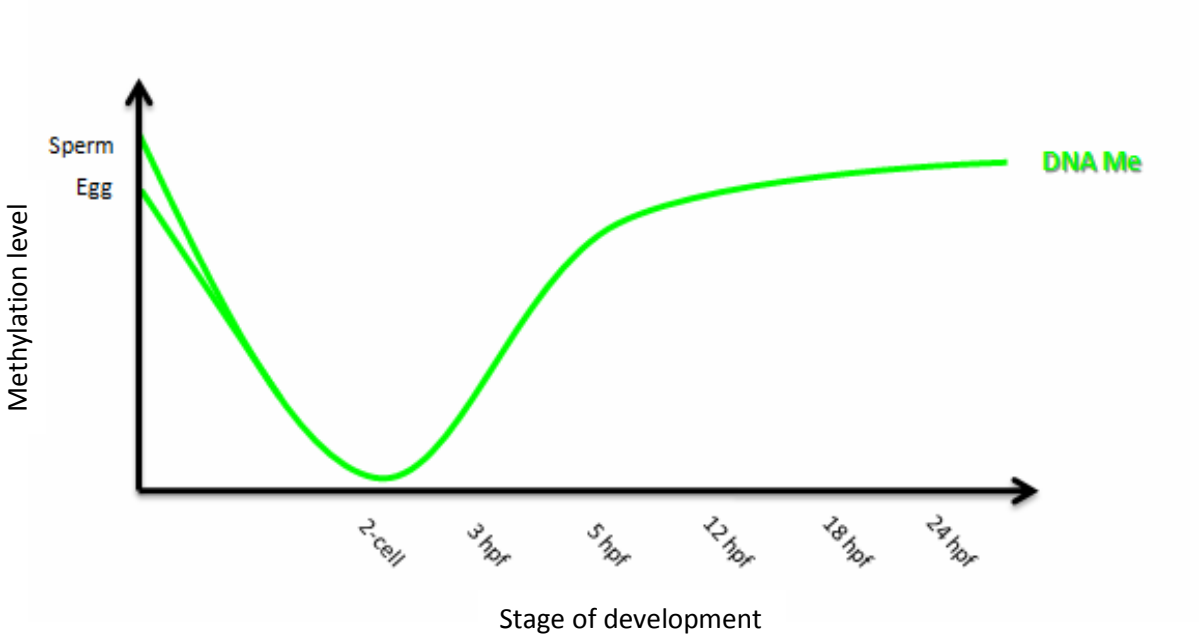

Fig. 3.3: Methylation dynamics during normal embryonic development in zebrafish. This schematic graph was constructed based on data from Fig. 3.1.

3.3 Discussion

The data presented here can be summarised into a schematic graph (Fig. 3.3) which illustrates the dynamic nature of the genome-wide DNA methylation changes taking place during the development of the zebrafish embryo. It can be seen that both the maternal and paternal contributions to the genome undergo a rapid reprogramming event after fertilisation, where in the early cleavage stages of development, the genomic DNA is substantially demethylated. This is followed by a remethylation process, whereby the zygotic DNA becomes remethylated by the early blastula stage and remains so as development proceeds. Interestingly, nuclei appear to acquire signal one by one, rather than to increase levels as a cohort. The lack of a methylation signal in the early cleavage stages of development does not indicate that the entire genome has been completely demethylated at the local gene level, but that there is a substantial reduction in global methylation levels in comparison to the later stages of development. This result correlates well with those obtained in the previous studies of Martin et al. 1999, Mhanni and McGowan 2004, and MacKay et al. 2007, in which similar changes in global DNA methylation levels have been observed during the development of the zebrafish embryo using methylation-sensitive restriction enzyme analysis and immunohistochemistry. However, the mature zebrafish sperm data in our study did not indicate a hypermethylated state, as was suggested in these earlier studies, and this is most likely due to insufficient antibody penetration, as spermatozoa are extremely difficult to permeabilise due to the very condensed state of their nuclei (Hazzouri, Rousseaux et al. 2000).

In the first study on this topic, no differences in DNA methylation levels were observed using methylation-sensitive restriction enzyme analysis from the blastula stage to 5 dpf (Macleod, Clark et al. 1999), however, the sensitivity of the assay may have masked the small variations present during this developmental timeframe. Macleod *et al.* (1999) also examined three randomly selected genes (*whn*, *rag-1* and *fgf3*) using bisulphite sequencing and saw no developmental differences in their DNA methylation status, however only two were examined at the important cleavage stage of development. It is during this period where the dynamic nature of genomic

DNA methylation is at its most contentious, and it is possible that these two genes are immune from the broad reduction in DNA methylation levels seen at this stage of development. A similar phenomenon has been reported in the mouse for methylated IAP retrotransposons and imprinted genes, which appear to be unaffected during periods of DNA methylation reprogramming (Santos and Dean 2004). Notably, in our study and that of Mhanni *et al.* (2007), protocols were established for the immunological detection of 5-methlycytosine within the zebrafish embryo. This is a sensitive technique that has been recently utilised to establish that variations in genomic DNA methylation do in fact occur during the development of *Drosophila melanogastor* (Kunert, Marhold et al. 2003) and *Dictyostelium discoideum* (Katoh, Curk et al. 2006), where even the presence of DNA methylation was once in doubt.

Immunological techniques were also used to confirm the temporal variations of DNA methylation during mammalian development (Santos, Hendrich et al. 2002; Santos and Dean 2004), and the patterns observed in this present study show similarities (Fig. 3.3 compared to Fig. 1.4). However, in the mouse, only the paternal pronucleus is rapidly demethylated, with maternal levels decreasing with each cell division. Whether the apparent absence of DNA methylation in our results presents a more complete demethylation than in the mouse will warrant further investigation. However, imaging of the pronuclear stages in the one-cell zebrafish embryo is particularly difficult due to the fragility of the eggs and the short developmental timescales involved (Fig. 1.6). Consequently, the levels of DNA methylation in the maternal and paternal pronuclei immediately after fertilisation were not directly assessed in this body of work. Nevertheless, the rapid loss of this mark in the early cleavage stages of development (Fig. 3.1c-d) suggests that the demethylation process may have an active component, as is observed in many (but not all) mammalian species (Lepikhov, Zakhartchenko et al. 2008). This is supported by data in which a methylated DNA construct is rapidly demethylated in a replication-independent manner once injected into a newly fertilised zebrafish embryo (Collas 1998). Recent evidence of an active mechanism for DNA demethylation in zebrafish embryos also lends weight to a conserved role for DNA methylation reprogramming during

vertebrate development, although it remains to be determined whether this particular system is directly involved in this process (Rai, Huggins et al. 2008). The discovery of zebrafish orthologs of mammalian DNA methyltransferases (Mhanni, Yoder et al. 2001; Shimoda, Yamakoshi et al. 2005; Smith, Dueck et al. 2005) also hints at conservation of the overall mechanism, and even though no global active demethylation was observed during the early embryogenesis of *Xenopus* (Stancheva, El-Maarri et al. 2002) or medaka (Walter, Li et al. 2002), a more subtle gene- (Stancheva, El-Maarri et al. 2002; Simonsson and Gurdon 2004) or cell-specific (Stancheva and Meehan 2000) reprogramming event could be occurring during the development of these organisms. Nevertheless, further work involving bisulphite sequencing will be necessary to document the methylation status of various candidate promoter regions in order to fully confirm the active nature of the demethylation process during the development of the zebrafish embryo.

The functional significance of a loss of methylation during vertebrate development is still at present unclear. A role for reprogramming paternal germline imprints was suggested by Reik and Walter (2001), and there is some evidence that genomic imprinting exists in zebrafish (McGowan and Martin 1997). However, the survival of gynogenetic (Westerfield 1995) and androgenetic (Corley-Smith, Lim et al. 1996) zebrafish strongly suggests that it does not. Nonetheless, the timing of remethylation in zebrafish also coincides with other important events during its development, such as the activation of zygotic transcription at MBT and the initiation of cellular differentiation. Although it is not entirely known whether these processes are related to the reestablishment of DNA methylation, it was suggested for Xenopus that this mark - or at least DNMT1 - does indeed regulate the timing of zygotic transcription at MBT (Stancheva, El-Maarri et al. 2002). DNA methylation is also postulated to have a role in determining cell fate (Reik, Santos et al. 2003) and seems to be necessary for differentiation in mouse ES cell cultures (Jackson, Krassowska et al. 2004). Accordingly, the differing levels of DNA methylation seen in this study, beginning at the 512-cell stage of development (Fig. 3.1e), could be indicative of

early differentiation events taking place in the zebrafish embryo as zygotic transcription initiates at MBT.

Cytosine methylation is also a hallmark of heterochromatin, which consists of DNA that is tightly packaged, gene-poor and transcriptionally silent (Richards and Elgin 2002). Although the previous study into the dynamics of DNA methylation during zebrafish development also used immunological techniques (MacKay, Mhanni et al. 2007), the experiments discussed in this chapter uniquely kept most of the structures within the developing embryo intact allowing us to visualise the nuclear CpG methylation patterns *in situ*. This enabled us to localise the methylated DNA towards the nuclear periphery (Figs. 3.1e-i and 3.2a-b). Whether this epigenetic mark co-localised with other typically heterochromatic regions, such as those around the centromeres of chromosomes, was of particular interest. Thus, experiments were undertaken to resolve this issue, and revealed that these regions also localised around the nuclear periphery at the developmental stage examined (Fig. 3.2c). This information supports recent data in mammalian cells which revealed a novel interaction between a fundamental component of the centromere and a DNA methyltransferase, illustrating a new mechanism by which DNA methylation can be targeted to discrete regions of the genome (Gopalakrishnan, Sullivan et al. 2009). However, the striking nuclear peripheral location of centromeric heterochromatin is not observed in the mouse, where constitutive heterochromatin is typically concentrated in chromocentre foci, or in less prominent speckles in other mammals.

Therefore, the findings presented in this chapter add to the debate of whether the spatial organisation of the genome within the nucleus can help regulate gene expression. Conventionally, transcriptionally active genes tend to reside towards the interior of the nucleus, while those that are inactive localise closer to the nuclear periphery (Zink, Amaral et al. 2004; Williams, Azuara et al. 2006). Though there are exceptions to this convention, it is thought that mammalian cells do indeed modulate the expression of certain genes through the relocalisation of genomic regions relative

to the nuclear periphery (Finlan, Sproul et al. 2008). Although the position of centromeres is dependent on a number of different factors ranging from the cell cycle to development (Goncalves Dos Santos Silva, Sarkar et al. 2008), the periphery of the nucleus does appear to be the preferred region occupied by these structures when cells differentiate (Kim, McQueen et al. 2004; Wiblin, Cui et al. 2005). A similar situation could be occurring within the developing zebrafish embryo, where genes silenced during the course of differentiation by DNA methylation could be specifically sequestered at the nuclear periphery. Further work will be needed to confirm this novel link, as the way in which epigenetics and nuclear architecture interact adds yet another complex layer of control over gene expression (Shaklai, Amariglio et al. 2007).

Chapter Four

4 Gradual development of nuclear H3K9 methylation patterns during zebrafish embryogenesis

4.1 Introduction

In all eukaryotes, genetic information is stored as chromatin, which consists of genomic DNA packaged with a wide variety of proteins, of which the histones are the most prominent. The nucleosome, which is the fundamental unit of chromatin, contains 146 bp of DNA wrapped around an octamer composed of two copies of each of the four core histone proteins, known as H2A, H2B, H3 and H4 (Luger, Mader et al. 1997). The N-terminal tails of these globular histone proteins protrude out from this nucleosomal complex and can be post-translationally modified by acetylation, methylation, phosphorylation, and ubiquitination, among others. These modified residues can form a platform that can recruit numerous factors, which in turn can regulate gene expression by modulating the accessibility of the genome via conformational changes in chromatin structure (Kouzarides 2007).

As stated earlier in section 1.2.3, histones can be methylated on lysine and arginine residues (Fig. 1.2), with arginines being either mono- or di-methylated in a symmetric or asymmetric configuration. Lysine residues on the other hand can be either mono-, di- or even tri-methylated. Both these sets of epigenetic marks can either activate or repress gene expression depending on the specific modification state, and this aptly demonstrated by specific sets of methyl-lysine residues on histone H3 (Kouzarides 2007). For instance, H3K4 tri-methylation is associated with actively transcribed genes in numerous organisms from yeast to higher eukaryotes (Shilatifard 2006). At the other end of the spectrum, H3K9 tri-methylation is associated with condensed heterochromatin, where it provides a binding surface for HP1, which leads to the propagation and stabilisation of heterochromatin and transcriptional silencing (Grewal and Jia 2007). However, the H3K9 methylation

marks appear to have a range of cellular functions which are very likely to be context-dependent.

The enzymes that catalyse the addition of these modifications are known as histone lysine methyltransferases (KMTs), and the mammalian H3K9 KMTs identified so far include Suv39h1, Suv39h2, G9A and ESET, among others (Bhaumik, Smith et al. 2007). From a developmental perspective, histone lysine methylation plays a central role, given that severe defects in embryogenesis are observed upon targeted loss of these KMTs (Peters, O'Carroll et al. 2001; Tachibana, Sugimoto et al. 2002; Dodge, Kang et al. 2004). Initially, it was unclear whether the process of histone lysine methylation was reversible (Bannister, Schneider et al. 2002), however the recent discovery of two distinct families of histone lysine demethylases (KDMs) has laid this issue to rest (Nottke, Colaiacovo et al. 2009). Amine oxidases and distinct hydroxylases have been observed to demethylate specific lysine residues. In particular, LSD1, JHDM2A and JHDM3A are observed to reverse H3K9 methylation, which has been shown to play a activatory role in gene expression (Metzger, Wissmann et al. 2005; Klose, Yamane et al. 2006; Whetstine, Nottke et al. 2006; Yamane, Toumazou et al. 2006).

The discovery of specific H3K9 KMTs and KDMs suggests that H3K9 methylation is a dynamically regulated epigenetic mark, which is indeed observed during gametogenesis and embryogenesis in mice (Lepikhov and Walter 2004; Liu, Kim et al. 2004; Santos, Peters et al. 2005; Yeo, Lee et al. 2005; Tachibana, Nozaki et al. 2007). Similar H3K9 methylation dynamics are also observed during the embryonic development of rabbits, cows and sheep (Hou, Liu et al. 2008; Lepikhov, Zakhartchenko et al. 2008), but not in pigs, where no pro-nuclear asymmetry is detected (Jeong, Yeo et al. 2007).

In non-mammalian vertebrates such as *Xenopus*, a comparable situation to the mouse appears to be occurring, where H3K9 methylation levels increase as development and differentiation progress (Dunican, Ruzov et al. 2008; Shechter, Nicklay et al. 2009). In zebrafish, numerous SET domain-containing genes are conserved within its genome (Sun, Xu et al. 2008), and Suv39h1, a specific KMT for H3K9me3, was found to be essential for its normal embryonic development (Rai, Nadauld et al. 2006). However, the dynamics of H3K9 methylation during zebrafish development have not been studied prior to this investigation.

Consequently, in this chapter I report how H3K9 mono-, di- and tri-methylation levels vary during the course of zebrafish development. These marks were investigated using well-characterised rabbit polyclonal antibodies for H3K9me1, me2 and me3 in a series of whole-embryo immunofluorescence experiments visualised by secondary anti-rabbit IgG with Alexa Fluor 488/555. Concomitant western blots were visualised using secondary anti-rabbit IgG horseradish peroxidise. These complementary approaches reinforced one another and demonstrated that H3K9 methylation appears after MBT and persists in all subsequent stages examined, ultimately increasing as development proceeds.

4.2 Results

4.2.1 Dynamic regulation of H3K9me1 during zebrafish development

The dynamics of H3K9 methylation in zebrafish have not been studied prior to this investigation, thus the levels of H3K9me1 during zebrafish embryogenesis were analysed using a combination of immunofluorescent and western blot analysis. To allow direct comparison between the stages, samples were processed simultaneously and subject to identical conditions throughout each procedure. Figure 4.1 shows the immunocytochemical detection of H3K9me1 (depicted in yellow) at specific developmental stages by confocal laser scanning microscopy. Fig. 4.1a shows the 512-cell early blastula stage at ≈ 2.75 hpf; Fig. 4.1b the early gastrula stage during 50%-epiboly at ≈ 5.3 hpf; Fig. 4.1c the 3-somite stage at ≈ 11 hpf; Fig. 4.1d the 18-

somite stage at ≈ 18 hpf; and Fig. 4.1e the ≈ 24 hpf embryo. Corresponding DAPI stained images (blue) served as a reference for the location of the nuclei. Western analysis of the corresponding stages and the 48 hpf embryo are shown in Fig. 4.1f, with the C-terminal histone H3 loading control in Fig. 4.1g. Western blots were also quantified, and the results are summarised in Appendix I.

Initially, it was seen that there was very little to no specific H3K9me1 signal detected in the nuclei of the 512-cell embryo by immunofluorescence (Fig. 4.1a). A background of non-specific staining was visible relative to the positive DAPI signal in this sample indicating where the nuclei were at this stage of development. This result was recapitulated in the immunoblottting, where extremely low levels of H3K9me1 were also observed at this stage (Fig. 4.1f). After MBT, at 50%-epiboly, nuclear staining of H3K9me1 became apparent (Fig. 4.1b), and remained present until at least 24 hpf (Figs. 4.1c-e). However, by western blot there appeared to be a slight dip of H3K9-Me1 levels at 11 hpf, which gradually increased in all subsequent stages examined (up until 48 hpf) (Fig. 4.1f). Loading was controlled using an H3 modification-insensitive antibody (Fig. 4.1g), and the 48 hpf sample was not examined by immunostaining due to insufficient permeabilisation of the embryo, leading to inadequate antibody penetration (data not shown).

4.2.2 Gradual development of H3K9me2 and me3 during zebrafish embryogenesis

Methylation of H3K9me2 and me3 is synonymous with the creation and maintenance of heterochromatic environments within the genome (Lachner, O'Sullivan et al. 2003). H3K9me3 is a hallmark of constitutive heterochromatin, while H3K9me2 is associated with facultative chromatin (Rougeulle, Chaumeil et al. 2004; Lehnertz, Ueda et al. 2003). Consequently, the dynamics of these marks were also assessed during zebrafish development using both immunostaining and immunoblotting techniques. Fig. 4.2 and 4.3 respectively show the immunocytochemical detection by confocal microscopy of H3K9me2 and me3 alongside western blot analysis. The

stages examined were: the 512-cell early blastula stage (a); the early gastrula stage during 50%-epiboly (b); the 3-somite stage (c); the 18-somite stage (d); and the 24 hpf embryo (e). Corresponding DAPI staining of DNA indicates the nuclei (in blue, lower half of panels). Western blot analysis of the corresponding stages and the 48 hpf embryo are shown in (f), with the C-terminal histone H3 loading control (g). Western blots were also quantified, and the results are summarised in Appendix I.

During embryogenesis, it was seen by immunofluorescence that there was initially very little to no specific H3K9me2 (green) or me3 signal (yellow) detected in the DAPI-positive nuclei (blue) of the early pre-MBT blastula (Figs. 4.2a and 4.3a). This finding was reiterated by western analysis, where extremely low levels of H3K9me2 and me3 were observed at this stage of development (Figs. 4.2f and 4.3f). At gastrula, nuclear staining of H3K9me2 and me3 became apparent (Figs. 4.2b and 4.3b), and remained present until 24 hpf (Figs. 4.2c-e and 4.3c-e). However, with the H3K9me3 result in Figs. 4.3b-c, more DAPI-staining nuclei (blue) appeared to be present than H3K9me3 nuclei (yellow). Nevertheless, in the immunoblots, a gradual increase in the levels of H3K9me2 and me3 was seen as development progressed up to 48 hpf (Figs. 4.2f and 4.3f). Once again, the loading was monitored using a modification-insensitive antibody of histone H3 (Figs. 4.2g and 4.3g), and the 48 hpf sample was not examined by immunostaining due to insufficient antibody penetration (data not shown).

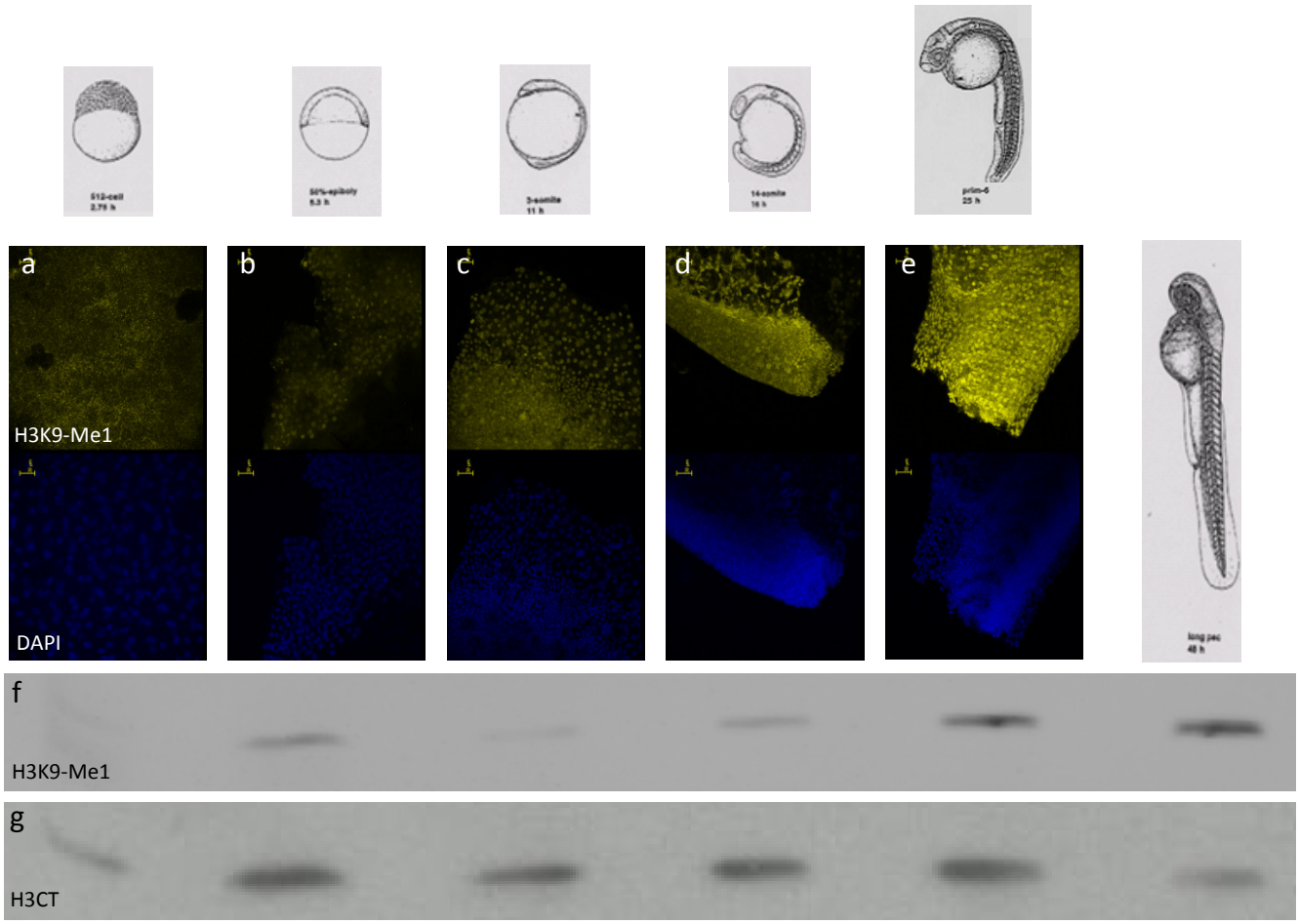

Fig. 4.1: Immunocytochemical detection of mono-methylated lysine 9 of histone H3 (H3K9-Me1) at specific developmental stages (yellow) using confocal microscopy. Shown are full projections of Z-series sections taken every ≤ 5 µm. **(a)** The 512-cell early blastula stage at ≈2.75 hpf. **(b)** The early gastrula stage during 50%-epiboly at ≈5.3 hpf. **(c)** The 3-somite stage at ≈11 hpf. **(d)** The 18-somite stage at ≈18 hpf. **(e)** ≈24 hpf. All stages are accompanied with their corresponding DNA DAPI stain images (blue) and camera lucida sketches from Kimmel *et al*. (1995). Western analysis of the corresponding stages and the 48 hpf embryo are shown below **(f)**, with the C-terminal histone H3 loading control **(g)**. Scale bar, 30 µm.

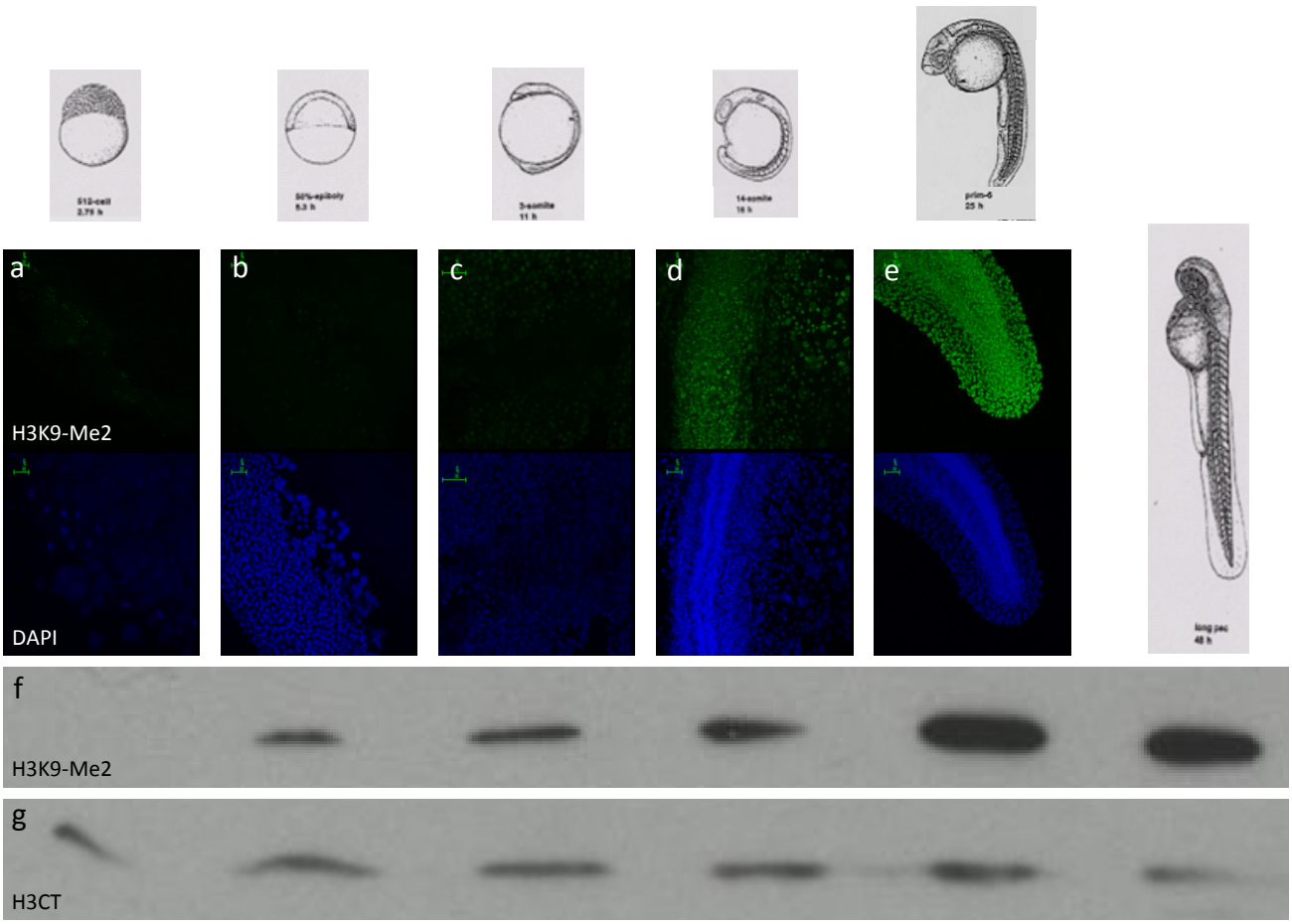

Fig. 4.2: Immunocytochemical detection of di-methylated lysine 9 of histone H3 (H3K9-Me2) at specific developmental stages (green) using confocal microscopy. Shown are full projections of Z-series sections taken every $\leq$ 5 µm. **(a)** The 512-cell early blastula stage at ≈2.75 hpf. **(b)** The early gastrula stage during 50%-epiboly at ≈5.3 hpf. **(c)** The 3-somite stage at ≈11 hpf. **(d)** The 18-somite stage at ≈18 hpf. **(e)** ≈24 hpf. All stages are accompanied with their corresponding DNA DAPI stain images (blue) and camera lucida sketches from Kimmel *et al*. (1995). Western analysis of the corresponding stages and the 48 hpf embryo are shown below **(f)**, with the C-terminal histone H3 loading control **(g)**. Scale bar, 30 µm.

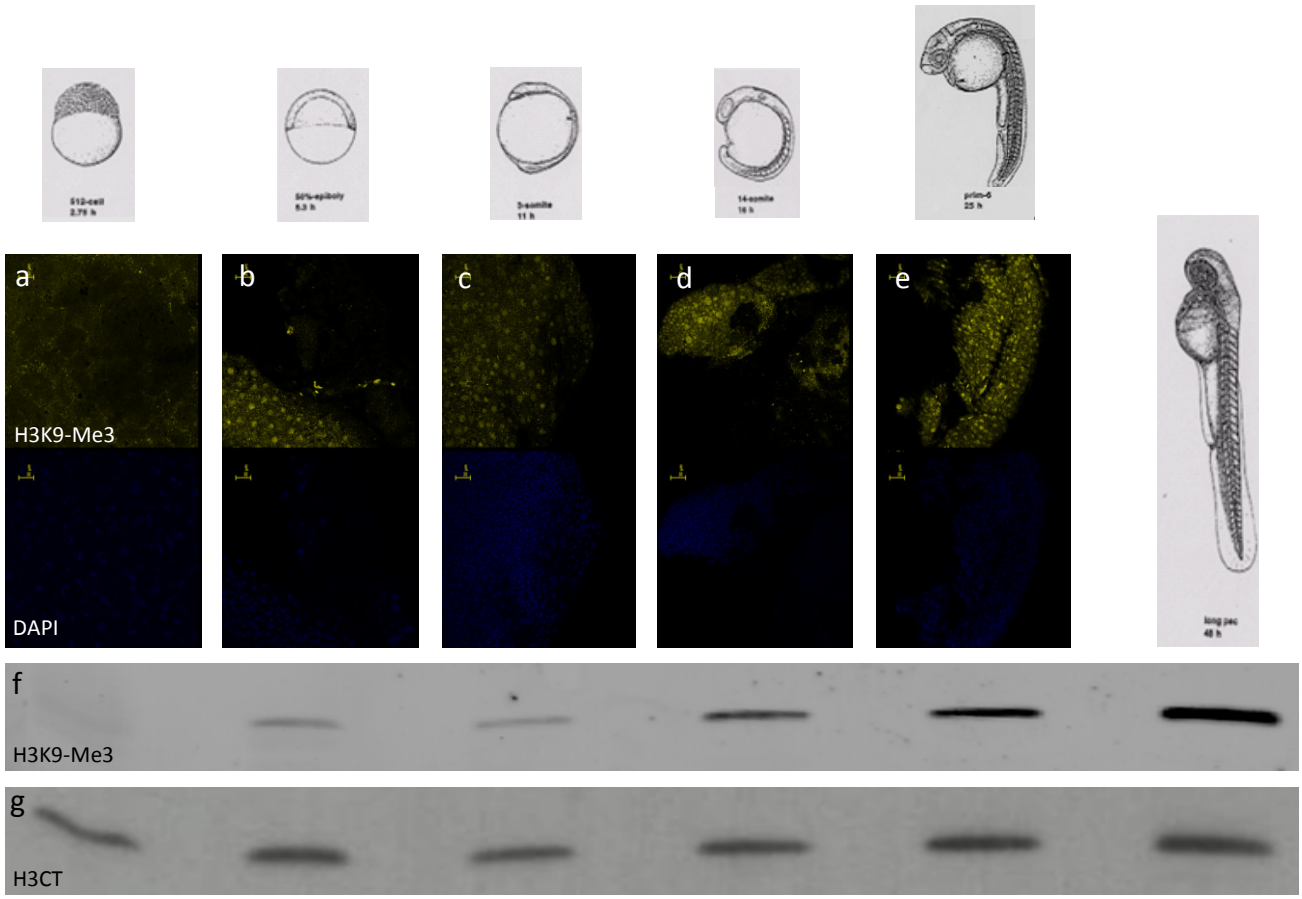

Fig. 4.3: Immunocytochemical detection of tri-methylated lysine 9 of histone H3 (H3K9-Me3) at specific developmental stages (yellow), as analysed by confocal microscopy and illustrated by single sections. **(a)** The 512-cell early blastula stage at ≈2.75 hpf. **(b)** The early gastrula stage during 50%-epiboly at ≈5.3 hpf. **(c)** The 3-somite stage at ≈11 hpf. **(d)** The 18-somite stage at ≈18 hpf. **(e)** ≈24 hpf. All stages are accompanied with their corresponding DNA DAPI stain images (blue) and camera lucida sketches from Kimmel *et al*. (1995). Western analysis of the corresponding stages and the 48 hpf embryo are shown below **(f)**, with the C-terminal histone H3 loading control **(g)**. Scale bar, 30 μm.

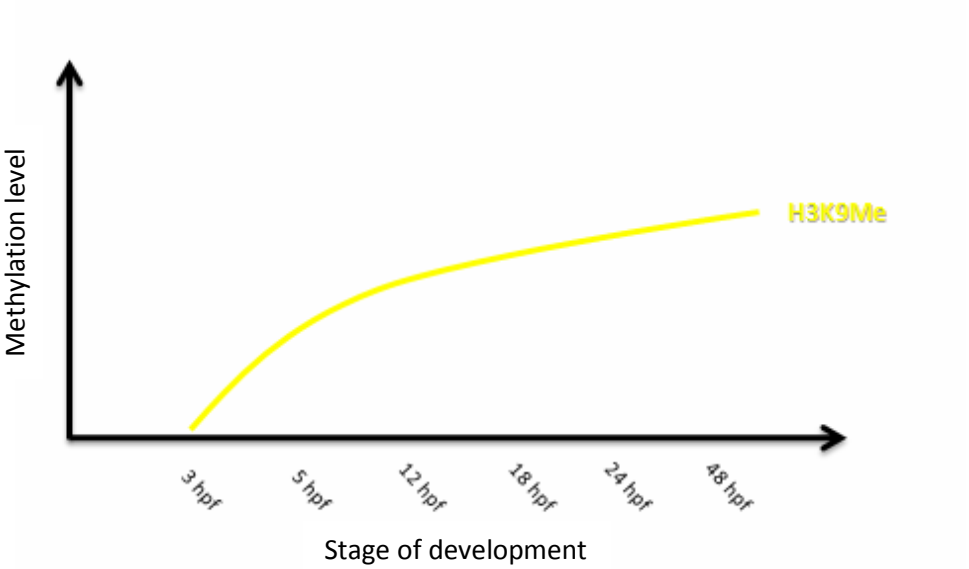

Fig. 4.4: H3K9 methylation dynamics during normal embryonic development in zebrafish. This generalised schematic graph is based on the patterns observed in Figs. 4.1 to 4.3, and the data in Appendix I.

4.3 Discussion

The data presented in this chapter and quantified in Appendix I can be summarised as a generalised schematic graph (Fig. 4.4), which shows that H3K9 methylation in the zebrafish embryo appears after MBT, and that its levels ultimately increase as development proceeds. The mono, di, and trimethylated states of H3K9 follow a similar trend in this regard. This trend is in concordance with results obtained from the mouse, where H3K9 methylation levels increase during preimplantation development (Lepikhov and Walter 2004; Liu, Kim et al. 2004; Santos, Peters et al. 2005; Yeo, Lee et al. 2005). Other mammalian systems show a similar pattern of H3K9 methylation, even during pro-nuclear stages, where paternal genomes are also devoid of H3K9me3 (Hou, Liu et al. 2008; Lepikhov, Zakhartchenko et al. 2008). However, pig zygotes lack this pro-nuclear asymmetry, and may represent an additional model of early embryonic development in mammals. The levels of H3K9 methylation in the maternal and paternal pronuclei of zebrafish were not directly assessed in this study due to the extremely short developmental timescales involved (Fig. 1.6), adding to the problems of imaging the pronuclei in the 1-cell embryo. However, it would be of particular interest to observe whether pronuclear asymmetry of epigenetic markers in embryonic development is conserved in this vertebrate.

During zebrafish development, zygotic transcription at MBT starts around 3 hpf (Kane and Kimmel 1993), and it is after this stage that H3K9 methylation begins to emerge (Figs. 4.1 to 4.3). This process can also be observed in mice and *Xenopus*, where zygotic gene activation at the two and 4000-cell stage respectively (Newport and Kirschner 1982; Nothias, Majumder et al. 1995) is soon followed by an increase in H3K9 methylation in the later stages of development (Lepikhov and Walter 2004; Liu, Kim et al. 2004; Santos, Peters et al. 2005; Yeo, Lee et al. 2005; Dunican, Ruzov et al. 2008). This phenomenon could readily be due to specific H3K9 KMTs being expressed and starting to function at this time. The timing of H3K9 methylation in zebrafish also coincides with the initiation of cellular differentiation. The H3K9me2/3 epigenetic marks are key features of heterochromatin (Grewal and Jia 2007), and their presence during development may reflect a role in stably

silencing genes that are no longer necessary for the maintenance and function of various differentiated cell types. In particular, nuclear staining of H3K9me3 was observed to be present in only a subset of cells at 50% epiboly and 11 hpf (Figs. 4.3b-c), and the differing levels of this modification at these stages could be indicative of early differentiation events taking place in the zebrafish embryo after MBT. The relationship between H3K9 methylation and differentiation is further supported by data in *Xenopus* that shows an increase in all three methylation states of H3K9 in a number of differentiated cells (Shechter, Nicklay et al. 2009). For a deeper analysis of heterochromatin during development, the action of HP1 in its maintenance and spread should be addressed in zebrafish, as should the recent discovery that RNAi plays a major role in its initiation (Grewal and Jia 2007).

The recent observation that H3K9me3 and HP1γ are enriched in the coding regions of active genes (Vakoc, Mandat et al. 2005), should not detract from the fact that this epigenetic mark is primarily associated with pericentric heterochromatin in mammalian cells (Peters, Kubicek et al. 2003; Rice, Briggs et al. 2003; Biron, McManus et al. 2004). Its link with H3K9me2, a mark of silent euchromatin (Rice, Briggs et al. 2003), can be seen by its co-precipitation in native chromatin immunoprecipitation experiments (Kimura, Hayashi-Takanaka et al. 2008), as well as by the identification of a specific KMT (ESET/SETDB1) that can catalyse the production of H3K9me3 from its dimethyl substrate (Fischle, Wang et al. 2003). The similarity of the results obtained in this zebrafish study also adds to this connection (Figs. 4.2 and 4.3). However, H3K9me1 has also been associated with active gene expression (Barski, Cuddapah et al. 2007), and its dynamics during zebrafish development did not precisely match the other two methylation marks described in this study (Fig. 4.1). This may be due to experimental error, however, the role of H3K9me1 during vertebrate development as a whole is still unclear, and more work will be needed in order to fully understand this variation during the development of the zebrafish embryo. Nonetheless, H3K9me1 also appears to characterise silent euchromatin (Rice, Briggs et al. 2003), and is thought to mark newly formed histones for subsequent trimethylation in pericentric regions (Loyola, Tagami et al. 2009).

This conclusion is supported by experiments that demonstrated an increase in H3K9me1 levels upon removal of the KMT responsible for H3K9me3 (Peters, Kubicek et al. 2003). All these findings together consolidate the observations that H3K9 methylation plays an essential role in defining specific types of chromatin and their associated transcriptional states.

Chapter Five

5 Variation of H4K20 methylation levels during early zebrafish development

5.1 Introduction

As mentioned previously in section 1.2.3, histones can be unmodified, or mono-, di- or tri-methylated on lysine residues. These marks in their various configurations can either activate or repress transcription, which is particularly evident with HOX gene regulation by H3K4 and H3K27 methylation respectively (Shilatifard 2006). Histone H3 can also be methylated at lysine 9, 36 and 79 (Fig. 1.2), with new sites of modification still being elucidated (Daujat, Weiss et al. 2009). However, on histone H4, lysine 20 is the only lysine residue that has been observed to be methylated. This mark is particularly interesting as each degree of methylation on this residue can specifically contribute to the regulation of a diverse range of cellular processes (Yang and Mizzen 2009).

For example, in addition to a role in cell cycle progression, H4K20me1 is also implicated in the regulation of chromosome condensation and gene expression (Wang and Jia 2009). Consistent with studies showing that this mark is preferentially associated with condensed mitotic chromatin in a variety of organisms (Karachentsev, Druzhinina et al. 2007; Houston, McManus et al. 2008), H4K20me1 is also observed as a mark of X chromosome inactivation in mammals (Sims, Houston et al. 2006; Shen, Matsuno et al. 2008). However, as discussed in detail in section 5.3, evidence of a more direct role for this mark in gene repression comes from studies involving the L3MBTL1 protein in human cells (Kalakonda, Fischle et al. 2008; Sims and Rice 2008), which is thought to mediate its effects through nucleosome compaction (Trojer, Li et al. 2007). The association of this protein with chromatin correlates with H4K20me1 levels *in vivo*, and its transcriptional repression is enhanced by the H4K20 monomethyltransferase (Kalakonda, Fischle et al. 2008).

Within nuclei, this mark is also absent from transcriptionally active regions in mouse embryonic fibroblasts (Sims, Houston et al. 2006), however numerous other studies have linked it with active gene expression in both murine and human cells (Talasz, Lindner et al. 2005; Vakoc, Sachdeva et al. 2006; Barski, Cuddapah et al. 2007), so the role of this modification in gene expression awaits further clarification.

In comparison, the function of H4K20me2 in DNA damage checkpoint control is relatively well defined (Yang and Mizzen 2009). Nevertheless, in mammalian ChIP and immunostaining experiments, this mark also appears to be associated with transcriptionally silent chromatin (Miao and Natarajan 2005; Sims, Houston et al. 2006). However, it has been observed that H4K20me2 is the most abundant form of H4K20 methylation present in a variety of cells (Pesavento, Bullock et al. 2008; Pesavento, Yang et al. 2008; Phanstiel, Brumbaugh et al. 2008; Yang, Pesavento et al. 2008), which argues against the possibility that this mark is selectively localised for transcriptional regulation.

H4K20me3 on the other hand appears to be preferentially associated with constitutive heterochromatin (Biron, McManus et al. 2004; Kourmouli, Jeppesen et al. 2004; Schotta, Lachner et al. 2004; Sims, Houston et al. 2006). This enrichment suggests a role in transcriptional silencing, which is observed in *Drosophila* HOX gene regulation, where H4K20me3 is only seen in the promoter and 5' coding region of the ultrabithorax gene when it is inactive (Papp and Muller 2006). H4K20me3 is also observed to be present in the promoters of silent imprinted genes in mouse embryonic fibroblasts (Regha, Sloane et al. 2007). However, a genome-wide ChIP-sequencing study in human T-cells failed to detect any direct relationship between H4K20me3 and promoter activity, but did observe an association between this mark and various large repeat domains, such as those near centromeric regions (Barski, Cuddapah et al. 2007). Similar results were observed in mouse embryonic stem cells, where H4K20me3 also localised to various repeat sequences within the genome (Martens, O'Sullivan et al. 2005; Mikkelsen, Ku et al. 2007). These studies imply

that the main role of H4K20me3 may involve the packaging of repetitive DNA into heterochromatin, the importance of which is demonstrated by work which shows that a loss in this function is a common hallmark of human cancers (Fraga, Ballestar et al. 2005).

As with most KMTs, H4K20 methyltransferases also contain an evolutionarily conserved SET domain, and two groups of these enzymes have been observed to catalyse H4K20 methylation in higher eukaryotes. The first set, which includes mammalian PR-Set7/Set8 and *Drosophila* PR-Set7, was seen to be responsible for H4K20me1 (Fang, Feng et al. 2002; Nishioka, Rice et al. 2002; Couture, Collazo et al. 2005; Xiao, Jing et al. 2005; Yin, Liu et al. 2005). Structural analysis showed that a tyrosine residue in the active site of this enzyme was responsible for preventing further addition of methyl-groups to H4K20, resulting in its strict H4K20me1 product specificity (Collins, Tachibana et al. 2005; Couture, Collazo et al. 2005; Xiao, Jing et al. 2005; Yin, Liu et al. 2005). Removal of this protein from mice or *Drosophila* resulted in defects in cell cycle progression and chromatin condensation (Karachentsev, Sarma et al. 2005; Sakaguchi and Steward 2007; Oda, Okamoto et al. 2009), consistent with the roles of H4K20me1 described earlier. These defects also resulted in lethality, underscoring the necessity of this epigenetic mark during development. The second group of H4K20 methyltransferases includes the mammalian Suv4-20h enzymes and *Drosophila* Suv4-20 which are responsible for both H4K20me2 and me3 (Schotta, Lachner et al. 2004; Schotta, Sengupta et al. 2008; Yang, Pesavento et al. 2008). It is thought that these enzymes use H4K20me1 as a substrate, as loss of the H4K20 monomethyltransferase results in the diminished levels of H4K20me2 and me3 (Karachentsev, Sarma et al. 2005; Oda, Okamoto et al. 2009), while loss of the Suv4-20h enzymes in mice and Suv4-20 in *Drosophila* results in the accumulation of H4K20me1 (as well as the absence of H4K20me2 and me3) (Sakaguchi, Karachentsev et al. 2008; Schotta, Sengupta et al. 2008). The sequential action of these two sets of H4K20 KMTs is further demonstrated in experiments which show that newly synthesised histones are progressively methylated to higher degrees during the cell cycle (Pesavento, Yang et al. 2008).

Nevertheless, the importance of this second set of H4K20 KMTs during development is highlighted by the fact that mice deficient for the Suv4-20h enzymes are embryonic lethal (Schotta, Sengupta et al. 2008).

Despite intense research into the identification and characterisation of various KDMs (Nottke, Colaiacovo et al. 2009), a demethylase specific for H4K20 methylation has not yet been identified. However, *in vitro* studies demonstrate that the Tudor domain of the KDM Jmjd2A interacts with H4K20me2 and me3, but the functional significance of this interaction is not yet understood (Kim, Daniel et al. 2006; Wang, Reddy et al. 2009). Equally, little is known about the dynamics of H4K20 methylation during the embryonic development of vertebrate organisms. In *Drosophila*, detailed analysis showed that H4K20me1 and me3 were present throughout embryogenesis, while H4K20me2 appeared later on during development (Karachentsev, Druzhinina et al. 2007). In non-mammalian vertebrates such as *Xenopus*, preliminary analysis also showed that H4K20 methylation became apparent as development and differentiation progressed (Dunican, Ruzov et al. 2008; Shechter, Nicklay et al. 2009). In mice however, only midgestation embryos were examined, but these studies also showed the dynamic nature of H4K20 methylation during development, where H4K20me3 levels increased as those of H4K20me1 decreased, as muscular and neural tissues differentiated (Biron, McManus et al. 2004).

However, the dynamics of H4K20 methylation during zebrafish development have not been studied prior to this investigation. Consequently, in this chapter I report how H4K20 mono-, di- and tri-methylation levels vary during the course of zebrafish development. These marks were investigated using antibodies for H4K20me1, me2 and me3 in a series of whole-embryo immunofluorescence experiments, with concomitant western blots. These studies demonstrated that the levels of H4K20me1 decreased, in concert with a potentially sumoylated form, during the course of zebrafish development. H4K20me2, on the other hand, increased progressively

during embryogenesis, while levels of H4K20me3 decreased rapidly after MBT. Together, these results provide an insight into the potential developmental roles of these modifications during zebrafish embryogenesis.

5.2 Results

5.2.1 Gradual loss of H4K20me1 during zebrafish development

To help elucidate the roles of H4K20me1 during zebrafish development, a combination of immunostaining and western blot techniques were employed to profile its dynamic nature during early embryogenesis, the results of which are shown in Figure 5.1. Once again, to allow direct comparison between the stages, samples were processed simultaneously and subject to identical conditions throughout each procedure. From the earliest stage of development examined (512-cell early blastula stage ≈ 2.75 hpf), it could be seen by immunofluorescence confocal microscopy that there was a strong and specific H4K20me1 signal detected in many of the nuclei present, especially in those containing condensed mitotic chromosomes (Fig. 5.1a). This result was also observed by immunoblottting, where high levels of H4K20me1 were seen at the early blastula stage (Fig. 5.1f). These levels decreased as development progressed, with staining becoming less bright at each successive stage examined by immunofluorescence (these being the early gastrula stage during 50%-epiboly at ≈5.3 hpf; the 3-somite stage at ≈11 hpf; the 18-somite stage at ≈18 hpf; and ≈24 hpf stage) (Figs. 5.1b-e). This was recapitulated in the immunoblots, where a gradual decrease in the levels of H4K20me1 was also observed as development progressed up to 48 hpf, and levels became undetectable by the 18-somite stage (Fig. 5.1f). Once again, the loading was monitored using a modification-insensitive antibody for histone H3 (Fig. 5.1g), and the 48 hpf sample was not examined by immunostaining due to insufficient antibody penetration (data not shown). Western blots were also quantified, and the results are presented in Appendix I. During the course of these experiments, however, it was noted that a higher band at approximately 26 kDa also followed the pattern of the H4K20me1 band that ran at its expected size of 11 kDa (Fig. 5.1f, arrows). Thus, the identity of

this protein would need to be investigated in order to completely validate the findings of this particular experiment.

5.2.2 Confirmation of a mass-shifted H4 isoform

A 512-cell stage protein extract sample was separated by SDS PAGE and blotted on to a PVDF membrane using standard protocols. However, this membrane was left unblocked, and both the 11 kDa and 26 kDa regions of interest were excised for subsequent analysis by MALDI-TOF mass spectrometry, using the protein marker as a guide. Figure 5.2 shows, for each PVDF-eluted protein sample, the MALDI-TOF experimental mass spectrum of the tryptic digests (a, d); the results of subsequent in silico analysis for matches with histone H4 (b, e); and sequence alignment of the identified peptides with zebrafish histone H4 (c, f).

Acting as a positive control, the 11 kDa region of the PVDF was analysed in order to verify the presence of histone H4 in the immunoblot. The masses of all the peptides present within the trypsin digested sample were represented by peaks in the mass spectrometry data (Fig. 5.2a). In order to identify the origins of these peaks, the experimental mass spectrum obtained was compared *in silico* against a library of mass spectra composed of zebrafish histones. This process demonstrated that two peptides from histone H4 were indeed present within the 11 kDa region of the blot, and that the most prominent peak, equating to the most abundant peptide detected, was in fact from an acetylated form of the protein (Fig. 5.2b). Subsequent sequence analysis demonstrated that this peptide formed part of the N-terminal tail of histone H4, while the other peptide formed its C-terminus (Fig. 5.2c).

In contrast, the mass spectrum from the 26 kDa region of interest varied markedly from the previous dataset, indicating that it represented an entirely different population of proteins, as expected from the different size range (Fig. 5.2d). Nevertheless, the *in silico* analysis of the experimental mass spectrum obtained

demonstrated that there were in fact three peptides from histone H4 present within this part of the blot (Fig. 5.2e). Sequence alignment subsequently showed that all three peptides together formed a considerable portion (over 40%) of the protein (Fig. 5.2f), thus confirming that a version of histone H4 was indeed running at an apparent molecular weight of around 26 kDa in the previous experiment. The magnitude of this shift in migration could not be explained by small histone modifications such as acetylation, methylation or phosphorylation, even taking into consideration their charge implications.

5.2.3 Evidence of a sumoylated form of H4K20me1

Histone H4 is a highly conserved histone, and no known variants have been identified that could be responsible for this 16 kDa mass shift (Marino-Ramirez, Kann et al. 2005). However, as discussed in section 1.2, histones are subject to a number of post-translational modifications that could readily affect their overall mass, such as poly-ADP-ribosylation, ubiquitination and sumoylation (Imschenetzky, Morin et al. 1996; Kouzarides 2007). We therefore probed for the presence of these possible histone modifications. The results of this investigation are shown in Figure 5.3, with an immunoblot analysis for poly-ADP-ribose (pADPr) at specific developmental stages (a); infrared detection of possible overlaps between signals for H4K20me1 (red) and ubiquitin (green) at the 512-cell stage (b); immunoblot for SUMO 2/3 at specific developmental stages and a re-probe of the same blot with H4K20me1 (c,d); in silico analysis for matches with zebrafish SUMO proteins and sequence alignment of the identified peptides (e, f).

Previous reports described the electrophoretic heterogeneity of sea urchin histone variants during SDS-PAGE owing to their poly-ADP-ribosylation (Imschenetzky, Morin et al. 1996). Therefore, the levels of poly-ADP-ribose during zebrafish development were assessed by western blot, in order to determine whether this modification was responsible for the phenomenon observed in the earlier experiment. However, upon investigation it could be seen that the banding pattern obtained with

an anti-poly-ADP-ribose antibody did not overlap with that of H4K20me1 (Fig. 5.3a), enabling us to rule out this modification as the cause of our observation.

Histone ubiquitinylation of H2A and H2B has been described previously, but recent studies also revealed that histone H4 can be ubiquitinylated *in vivo* (Wang, Zhai et al. 2006). This modification is known to be approximately 8 kDa in mass, and the band shift observed in this study could indicate that a di-ubiquitinylation event could be taking place. Using western blots with multiple infrared signal detection, it could be seen that there were numerous ubiquitin bands, highlighting the ubiquitous nature of this protein (Fig. 5.3b, green bands). However none of these bands appeared to co-localise with the 26kDa band of H4K20me1, reducing the likelihood of ubiquitin being responsible for this mass shift (Fig. 5.3b).

SUMO is a similarly bulky candidate that has been observed to modify histone H4 *in vivo* (Shiio and Eisenman 2003; Nathan, Ingvarsdottir et al. 2006). In this protein family, there are three paralogs that are observed to be widely expressed in mammals, where SUMO 2 and 3 are 96 % identical, and SUMO 1 and 2 are 45 % identical (Ouyang, Shi et al. 2009). The western blot pattern obtained for SUMO 1 expression in serial protein extracts taken during zebrafish development was unlike that of H4K20me1 (data not shown). However, when using the infrared signal detection system, it could be seen that there were numerous SUMO 2/3 bands present in the lanes sampled during embryogenesis, with one set in particular around 26 kDa decreasing as development progressed (Fig 5.3c, asterisks). This blot was stripped with β-mercaptoethanol under stringent conditions, and re-probed with an antibody for H4K20me1, using a differentially fluorescing secondary antibody to eliminate any potential cross-talk. Once re-scanned, it could be seen that the patterns observed in the 26 kDa regions of both blots were similar, and that the bands appeared to overlap (Fig. 5.3d, asterisks). SUMO 2/3 in its unconjugated form was also observed to run at approximately 17 kDa (Fig. 5.3c), which was reported in numerous other studies (Saitoh and Hinchey 2000; Tatham, Jaffray et al. 2001; Hayashi, Seki et al.

2002; Su and Li 2002), adding yet more weight to the theory that this modification may be responsible for the 16 kDa shift detected in H4K20me1.

Lastly, using the earlier mass spectrometry data, the experimental mass spectrum obtained from the 26 kDa region was this time compared *in silico* against a library of mass spectra composed of zebrafish SUMO proteins. This process demonstrated that there were indeed three peptides from an isoform of SUMO 3 present within this part of the blot (Fig. 5.3e). Subsequent sequence analysis showed that all three peptides contributed to a specific region within the protein (Fig. 5.3f), once again pointing towards the possible sumoylation of H4K20me1 during the course of zebrafish development.

5.2.4 Gradual increase of H4K20me2 levels during zebrafish development

The role of H4K20me2 in the regulation of DNA damage checkpoint control is relatively well defined (Yang and Mizzen 2009). However, it is unclear what part, if any, this modification plays during the embryonic development of various vertebrate organisms. Consequently, the dynamics of this mark were also assessed using both immunostaining and immunoblotting techniques during the development of the zebrafish embryo. Samples were once again processed simultaneously and subject to identical conditions throughout each procedure. Figure 5.4 shows the immunocytochemical detection using confocal microscopy of H4K20me2 (yellow) for a series of developmental stages: namely the 512-cell early blastula stage (a); the early gastrula stage during 50%-epiboly (b); the 3-somite stage (c); the 18-somite stage (d); and the one day old embryo (e). The lower panels show corresponding images of DAPI stained nuclei (blue). Western analysis of the corresponding stages and the 48 hpf embryo are also shown with the C-terminal histone H3 loading control (f), with quantification shown in Appendix I.

During embryogenesis, it was seen by immunoblot that there was initially very little to no H4K20me2 signal detected in the early 512-cell embryo (Fig. 5.4f). After this stage, a gradual increase in the levels of H4K20me2 was observed as development progressed up to 48 hpf (Fig. 5.4f), with loading in the immunoblots monitored using a modification-insensitive H3 antibody (Fig. 5.4f). However, no specific signals corresponding to the DAPI-positive nuclei were detected by immunofluorescence in any of the stages examined (Figs. 5.4a-e), indicating that this antibody may prefer denatured epitopes.

5.2.5 Rapid reduction in the levels of H4K20me3 during the early stages of zebrafish development

The relationship between H4K20me3 and heterochromatin is well documented (Biron, McManus et al. 2004; Kourmouli, Jeppesen et al. 2004; Schotta, Lachner et al. 2004; Sims, Houston et al. 2006). However, the dynamics of H4K20me3 during zebrafish development have not been studied prior to this investigation, thus they were also analysed using a combination of immunofluorescent techniques and western blot. Figure 5.5 shows the immunocytochemical detection using confocal microscopy of H4K20me3 (yellow) at the 512-cell early blastula stage (a); the early gastrula stage during 50%-epiboly (b); the 3-somite stage (c); the 18-somite stage (d); and ≈24 hpf (e). The lower panels show corresponding images of DAPI stained nuclei (blue). Western analysis of the same stages and the 48 hpf embryo are shown with the C-terminal histone H3 loading control (f), with quantification shown in Appendix I.

Similarly to H4K20me2, no specific signals corresponding to DAPI-positive nuclei were detected by immunofluorescence in any of the developmental stages examined (Figs. 5.5a-e). However by western blot, it could be seen that there was a faint signal at the 512-cell stage of development (Fig. 5.5f). Nonetheless, by gastrula, this signal was no longer present, and it remained absent in all subsequent stages studied (Fig. 5.5f). Loading was monitored using a modification-insensitive antibody of histone

H3, which showed that there was indeed some signal coming from each sample (Fig. 5.5g).

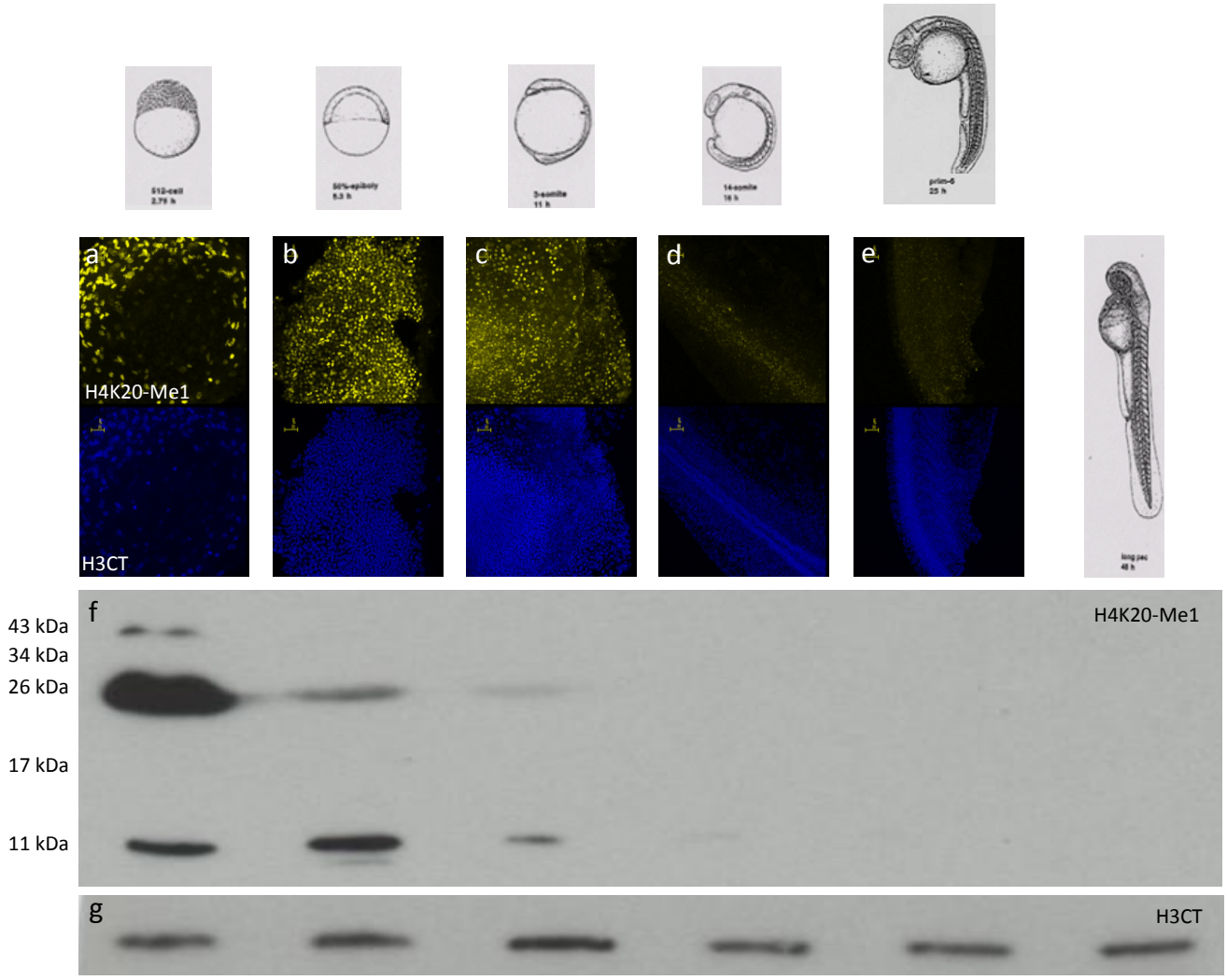

Fig. 5.1: Immunocytochemical detection of mono-methylated lysine 20 of histone H4 (H4K20-Me1) at specific developmental stages (yellow) using confocal microscopy. Shown are full projections of Z-series sections taken every ≤ 5 µm. **(a)** The 512-cell early blastula stage at ≈2.75 hpf. **(b)** The early gastrula stage during 50%-epiboly at ≈5.3 hpf. **(c)** The 3-somite stage at ≈11 hpf. **(d)** The 18-somite stage at ≈18 hpf. **(e)** ≈24 hpf. All stages are accompanied with their corresponding DNA DAPI stain images (blue) and camera lucida sketches from Kimmel *et al*. (1995). Western analysis of the corresponding stages and the 48 hpf embryo are shown below **(f)**, with the C-terminal histone H3 loading control **(g)**. Observe the expected set of H4 bands at 11 kDa, as well as a set of unidentified bands at 26 kDa. Scale bar, 30 µm.

a

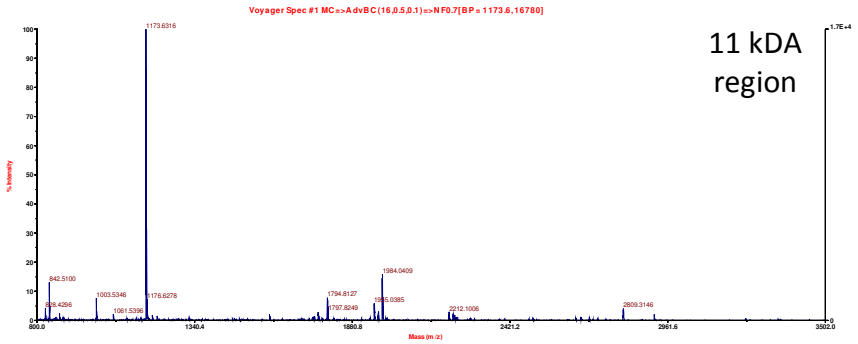

b

1. 2/68 matches (2%). 11397.4 Da, pI = 11.36. Acc. # 4. DANIO. H4 .

m/z submitted	MH+ matched	Delta ppm	start	end	Peptide Sequence (Click for Fragment Ions)	Modifications
1173.6275	1173.6704	-36.5232	1	13	(-)SGRGKGSKGLGK(G)	Acet N
1211.5788	1211.6285	-41.0692	93	103	(K)RQGRTLYGFGG(-)	

c

```
H4              MSGRGKGSKG-LGKGGAKRHR-KVLRDNIQGI-TKPAIRRLAR-RGGVKRISGL-IYEET 55
Unknown         -SGRGKGSKG-LGKG---------------------------------------------- 13
                 ********* ****

H4              RGVLK---VFLENVIRDA-VTYTEHAKRK-TVTAMDVVYA-LKRQGRTLYG-FGG 103
Unknown         ----------------------------------------KRQGRTLYG-FGG 25
                                                        ********* ***
```

d

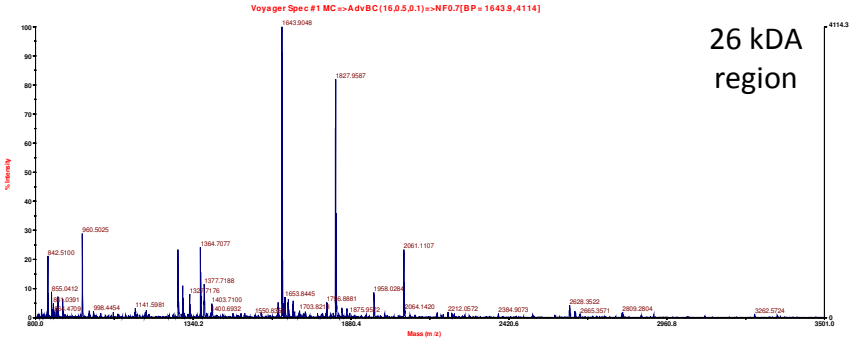

e

1. 3/100 matches (3%). 11397.4 Da, pI = 11.36. Acc. # 4. DANIO. H4 .

m/z submitted	MH+ matched	Delta ppm	start	end	Peptide Sequence (Click for Fragment Ions)	Modifications
1277.6909	1277.8031	-87.7601	14	24	(K)GGAKRHRKVLR(D)	
1325.6586	1325.7541	-72.0300	25	36	(R)DNIQGITKPAIR(R)	
2174.1864	2174.2522	-30.2520	38	56	(R)LARRGGVKRISGLIYEETR(G)	

f

```
H4              --MSGRGKGSKG-LGKGGAKRHR-KVLRDNIQGI-TKPAIRRLAR-RGGVKRISGL-IYE 53
Unknown         ---------------KGGAKRHR-KVLRDNIQGI-TKPAIRRLAR-RGGVKRISGL-IYE 41
                               ******** ********** ********** ********** ***

H4              ETRGVLK---VFLENVIRDA-VTYTEHAKRK-TVTAMDVVYA-LKRQGRTLYG-FGG 103
Unknown         ETRG---------------------------------------------------- 45
                ****
```

Fig. 5.2: MALDI-TOF spectra of tryptic PVDF digests, with subsequent *in silico* analysis. **(a)** MALDI mass spectrum of the 11 kDa region of an immunoblot produced from early blastula embryos (≈2.75 hpf). **(b)** Results from the *in silico* analysis of the experimental mass spectrum from the 11 kDa region showing a match with histone H4. **(c)** Sequence alignment of the identified peptides with zebrafish histone H4. **(d)** MALDI mass spectrum of the 26 kDa region of the same immunoblot as above. **(e)** Results from the *in silico* analysis of the experimental mass spectrum from the 26 kDa region also showing a match with histone H4. **(f)** Sequence alignment of the identified peptides with zebrafish histone H4.

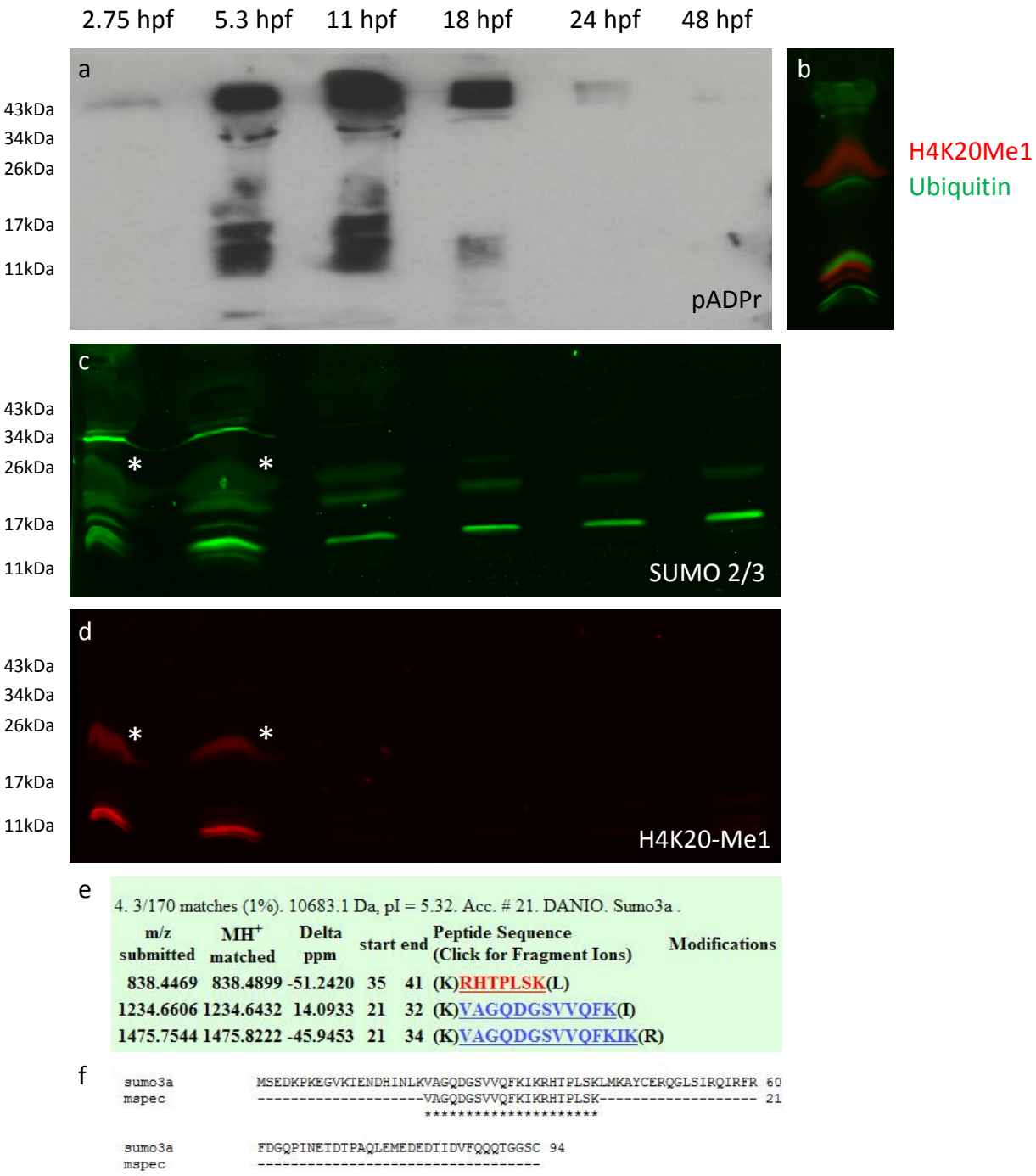

Fig. 5.3: Identification of a potentially sumoylated form of H4K20-Me1. **(a)** Immunoblot analysis of poly-ADP-ribose (pADPr) at specific developmental stages. **(b)** Multiple and non-overlapping infrared signals of H4K20-Me1 (red) and ubiquitin (green) at the 512-cell stage of development (≈2.75 hpf). **(c)** Immunoblot of SUMO 2/3 at specific developmental stages. **(d)** Western analysis of the SUMO 2/3 blot, stripped and re-probed with H4K20-Me1, with asterisks highlighting the diminishing 26 kDa isoforms and the overlapping bands. Mass spectrometry data from the 26 kDa region was consequently compared *in silico* against a library of mass spectra composed of zebrafish SUMO proteins, showing a match with SUMO 3a **(e)**, with a sequence alignment of the identified peptides shown below **(f)**.

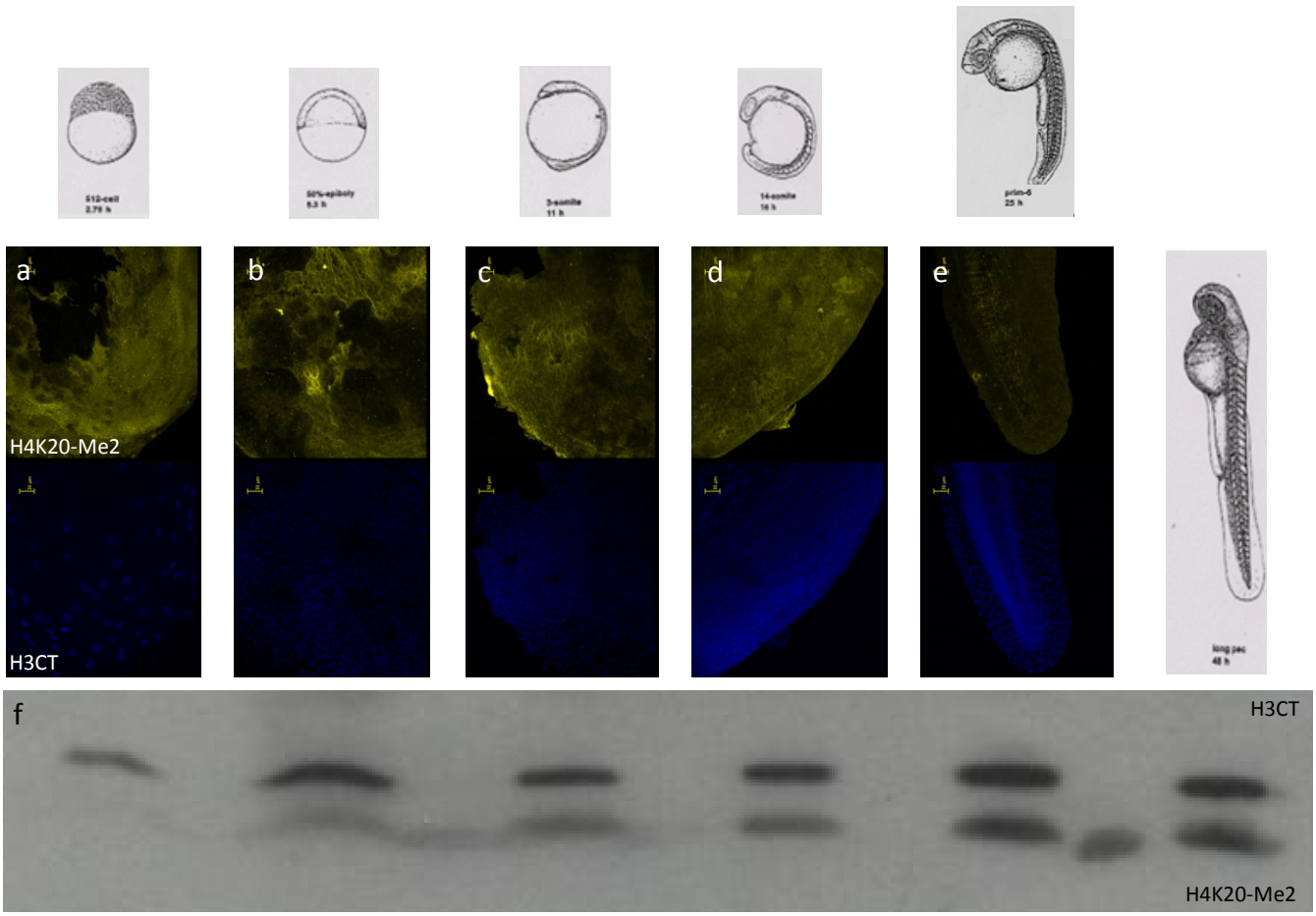

Fig. 5.4: Immunocytochemical detection of di-methylated lysine 20 of histone H4 (H4K20-Me2) at specific developmental stages (yellow) using confocal microscopy. Shown are full projections of Z-series sections taken every ≤ 5 µm. **(a)** The 512-cell early blastula stage at ≈2.75 hpf. **(b)** The early gastrula stage during 50%-epiboly at ≈5.3 hpf. **(c)** The 3-somite stage at ≈11 hpf. **(d)** The 18-somite stage at ≈18 hpf. **(e)** ≈24 hpf. All stages are accompanied with their corresponding DNA DAPI stain images (blue) and camera lucida sketches from Kimmel *et al*. (1995). Western analysis of the corresponding stages and the 48 hpf embryo are shown (lower set of bands), with the C-terminal histone H3 loading control (upper set of bands) **(f)**. Scale bar, 30 µm.

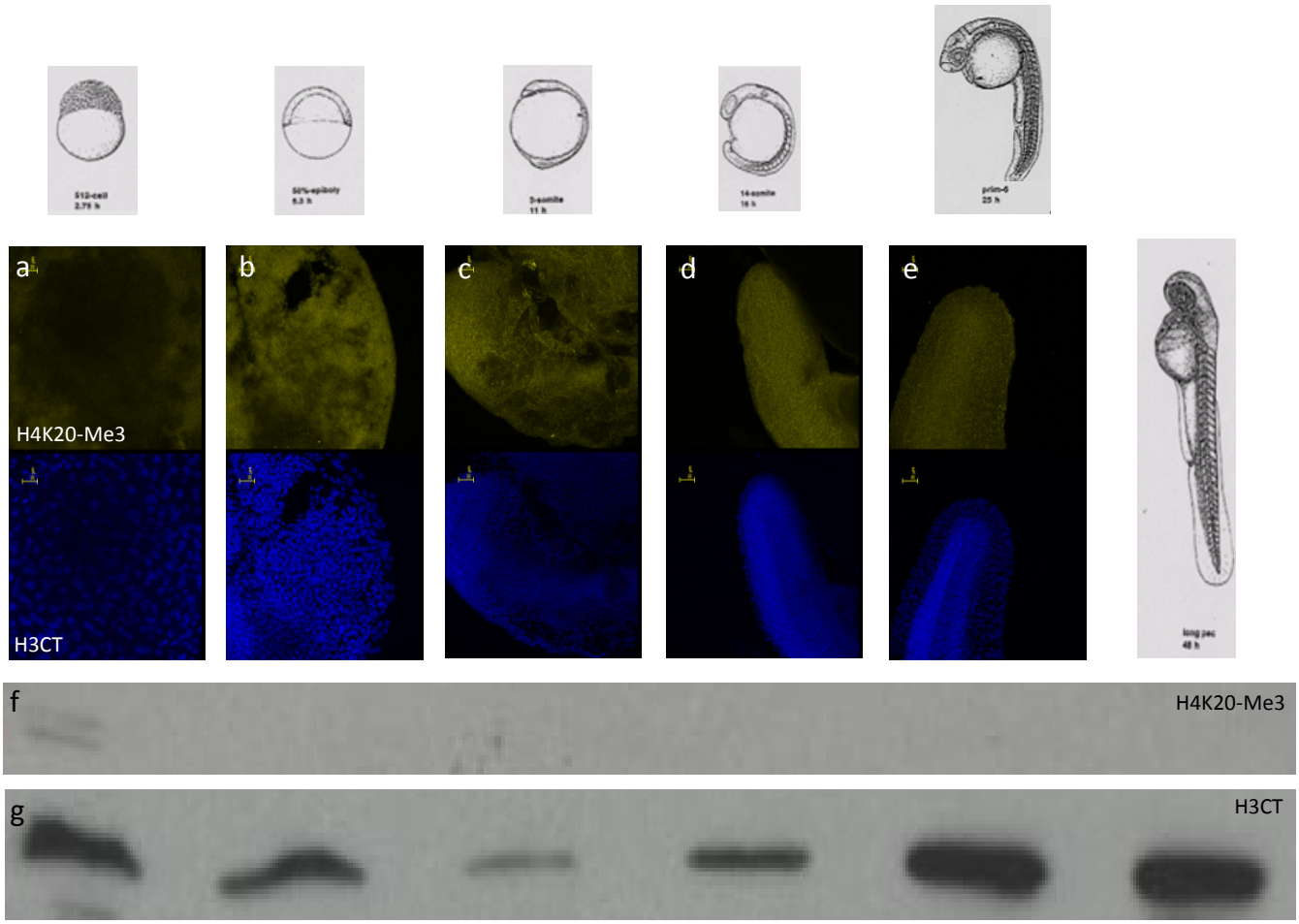

Fig. 5.5: Immunocytochemical detection of tri-methylated lysine 20 of histone H4 (H4K20-Me3) at specific developmental stages (yellow) using confocal microscopy. Shown are full projections of Z-series sections taken every ≤ 5 µm. **(a)** The 512-cell early blastula stage at ≈2.75 hpf. **(b)** The early gastrula stage during 50%-epiboly at ≈5.3 hpf. **(c)** The 3-somite stage at ≈11 hpf. **(d)** The 18-somite stage at ≈18 hpf. **(e)** ≈24 hpf. All stages are accompanied with their corresponding DNA DAPI stain images (blue) and camera lucida sketches from Kimmel *et al*. (1995). Western analysis of the corresponding stages and the 48 hpf embryo are shown below **(f)**, with the C-terminal histone H3 loading control **(g)**. Scale bar, 30 µm.

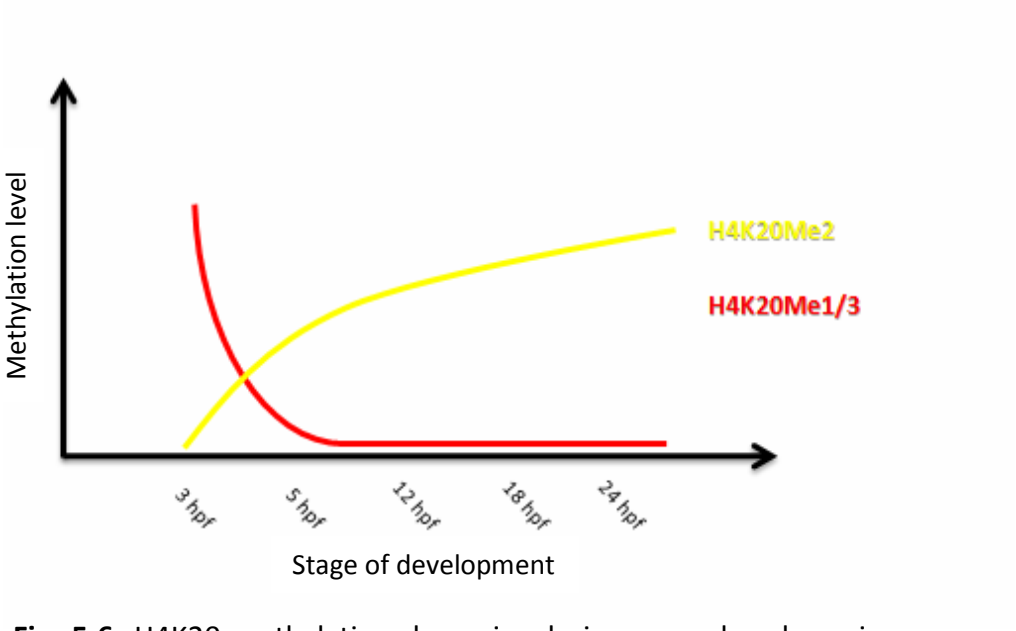

Fig. 5.6: H4K20 methylation dynamics during normal embryonic development in zebrafish. This generalised schematic graph is based on the combined data of Figs. 5.1, 5.4 and 5.5, as well as the data in Appendix I.

5.3 Discussion

The data presented in this chapter and quantified in Appendix I can be summarised as a generalised schematic graph (Fig. 5.6) which illustrates the dynamic and distinct nature of each H4K20 methylation state during the development of the zebrafish embryo. These results highlight the versatile nature of this mark, where each degree of methylation on this residue has been seen to distinctly contribute to the regulation of a diverse range of cellular processes (Yang and Mizzen 2009).

The specificity of various H4K20 KMTs has assisted in the interpretation of these marks. For example, the levels of the H4K20 mono-methyltransferase are dynamically regulated during the cell cycle. They are at their lowest in G_1, and gradually increase to a peak during G_2/M phase (Rice, Nishioka et al. 2002). Consequently, removal of this protein in mice and *Drosophila* results in lethality, which can in part be attributed to defects within the cell cycle (Karachentsev, Sarma et al. 2005; Sakaguchi and Steward 2007; Oda, Okamoto et al. 2009). Furthermore, these mutants also show improper chromosome condensation, indicating an additional role for H4K20me1 in the regulation of chromosome compaction (Sakaguchi and Steward 2007; Oda, Okamoto et al. 2009). This role is also alluded to within our results, where the H4K20me1 mark is preferentially associated with condensed mitotic chromatin, which is especially noticeable during the earlier stages of development (Fig. 5.1a).

Nonetheless, the developmental role of this epigenetic mark during vertebrate embryogenesis is still relatively unclear. A previous study in mice demonstrated that the highest levels of H4K20me1 were associated with proliferating neuroblasts and myoblasts, and that during the course of their differentiation, these levels significantly decreased (Biron, McManus et al. 2004). Within this study, an analogous situation appears to be occurring, where the levels of H4K20me1 are seen to decrease as development proceeds (Fig 5.1). A possible mechanism to explain this phenomenon was recently proposed by Sims and Rice (2008), whereby the

L3MBTL1 repressor protein binds H4K20me1 to repress specific genes, such as *RUNX1*, which is a critical regulator of haematopoietic differentiation. The loss of H4K20me1 and L3MBTL1 at the *RUNX1* promoter was observed to relieve gene repression, as well as being an early differentiation event during megakaryopoiesis (Sims and Rice 2008). Collectively, all these findings suggest that a H4K20me1-mediated repressive mechanism may play a role during development by repressing various lineage-specific genes in order to preserve multipotency.

The association of H4K20me1 with SUMO (Figs. 5.3c-f) is a novel observation, which is particularly interesting as it would further support this repressive role. Sumoylation itself is a relatively new addition to the list of histone modifications, which was first associated with transcriptional repression in mammalian cells on histone H4 (Shiio and Eisenman 2003). In budding yeast, it has also been observed to take place on histones, and is thought to be a key regulatory mechanism for transcriptional repression within this organism (Nathan, Ingvarsdottir et al. 2006). However, more work is necessary to validate this connection with H4K20me1, so that its role within the developing zebrafish embryo can be fully understood. Nevertheless, in previous studies, it has been suggested that sumoylation recruits factors, such as HDACs and HP1, to mediate its repressive effect (Shiio and Eisenman 2003), while others have suggested that it competes with histone acetylation for lysine residues in order to antagonise gene expression (Nathan, Ingvarsdottir et al. 2006). Accordingly, a substantial degree of histone H4 acetylation was detected in the non-sumoylated form of H4K20me1 at the pre-MBT stage of development (Fig. 5.2b). Like in *Xenopus* (Woodland 1979), this suggests that there is a maternal store of acetylated histones present within the zebrafish embryo, which facilitates its rapid rate of cell division before the onset of zygotic transcription. Additionally, in *Drosophila* embryo extracts, a relationship between H4 acetylation and H4K20me1 has been observed, where H4K20me1 recruits a complex containing a HDAC which deacetylates histone H4 during chromatin assembly (Scharf, Meier et al. 2009). Further research into the dynamics of histone acetylation and sumoylation

during zebrafish development will be necessary in order to see whether this myriad of interactions is conserved within vertebrate embryogenesis.

Altogether, these findings suggest that H4K20me1 may very well be associated with transcriptional repression. However, other studies have linked this mark to active gene expression (Talasz, Lindner et al. 2005; Vakoc, Sachdeva et al. 2006; Barski, Cuddapah et al. 2007). Consequently, these discrepancies underline the fact that methyl marks in general can have many functions within cells which are very likely to be context-dependent.

In fission yeast, Set9 is the only KMT necessary for all three degrees of methylation on H4K20 (Sanders, Portoso et al. 2004). Deletion or inactivation of this protein has no discernable effects on transcription or heterochromatin formation, but does result in hypersensitivity to DNA damage (Sanders, Portoso et al. 2004). Subsequent work demonstrated that H4K20 methylation was required for the recruitment of Crb2, a DNA damage checkpoint protein involved in the signalling of DNA double-strand breaks (Sanders, Portoso et al. 2004; Du, Nakamura et al. 2006). The human homolog of Crb2 is known as 53BP1, and both of these proteins were seen to specifically bind H4K20me2 through their tandem Tudor domains (Botuyan, Lee et al. 2006; Greeson, Sengupta et al. 2008). Consequently, depletion of the Suv4-20h enzymes in HeLa cells lead to the reduced recruitment of 53BP1 to damage-associated foci (Yang, Pesavento et al. 2008). It could be due to this vital role in DNA damage signalling, that H4K20me2 is the most abundant form of this modification in a variety of different cells (Pesavento, Bullock et al. 2008; Pesavento, Yang et al. 2008; Phanstiel, Brumbaugh et al. 2008; Yang, Pesavento et al. 2008). Consistent with these observations, during zebrafish embryogenesis, this mark gradually increased as development progressed (Fig. 5.4f), which was also seen during *Drosophila* development (Karachentsev, Druzhinina et al. 2007). This highlights that each degree of methylation does not simply follow the dynamics of the lower methyl state, but little is understood about the general nature of this mark,

and more work will be needed in order to dissect its developmental role. However, the antibody employed in this study did not produce any results by immunofluorescence (Figs. 5.4a-e). Numerous different lots and separate sources of antibody were also tested with no specific nuclear signals obtained (data not shown). The fact that H4K20 is buried within the context of stacked nucleosomes (Dorigo, Schalch et al. 2003) may go some way in explaining why this antibody appears to prefer denatured epitopes, alternatively the nuclear signal may be below the antibody's detection sensitivity.

The antibody for H4K20me3 also failed to detect any specific nuclear signals by immunofluorescence (Fig. 5.5a-e), even after different lots and separate sources were tested (data not shown). Nevertheless, by western blot a faint H4K20me3 signal was detected at the 512-cell stage of development (Fig 5.5f). However, H4K20me3 appears to be a mark of constitutive heterochromatin in mammalian somatic cells (Biron, McManus et al. 2004; Kourmouli, Jeppesen et al. 2004; Schotta, Lachner et al. 2004; Sims, Houston et al. 2006). This is also demonstrated by the interaction of the Suv4-20 enzymes with HP1, which localises them both to heterochromatin (Schotta, Lachner et al. 2004). In *Drosophila*, mutational studies also showed that this methyltransferase was involved with heterochromatin formation (Schotta, Lachner et al. 2004), and detailed analysis in this organism demonstrated that H4K20me3 was present throughout embryogenesis (Karachentsev, Druzhinina et al. 2007). However, in *Xenopus*, preliminary analysis showed that H4K20me3 methylation only became apparent as development progressed (Dunican, Ruzov et al. 2008), and that it was particularly prevalent within their erythrocytes (Nicklay, Shechter et al. 2009). Correspondingly, in midgestation mouse embryos, it was observed that H4K20me3 levels increased as muscular and neural tissues differentiated (Biron, McManus et al. 2004). Thus the presence of this mark during embryonic development appears to reflect a role in stably silencing genes that are no longer necessary for the maintenance and function of various differentiated cell types. However, recent work in our lab has shown that a similar situation to the zebrafish appears to be occurring in preimplantation mouse embryos, where

H4K20me3 rapidly diminishes during the course of their early development, consistent with a prior observation by Kourmouli et al. (2004). The work in our lab also saw that H4K20me3 reappeared only much later during mouse embryogenesis (Tuempong Wongtawan, personal communication). This is conceivable, as H4K20me3 has been shown to be particularly evident within aged tissues and growth-arrested cells when compared to growing cells (Sarg, Koutzamani et al. 2002). It would be of particular interest to see whether this phenomenon also occurs within the tissues of the developing zebrafish embryo, and whether this mark is as tightly associated with heterochromatin as it appears to be in other organisms.

Part II: Technical developments towards cloning zebrafish and isolating pluripotent stem cells

Chapter Six

6 Somatic cell nuclear transfer in zebrafish

6.1 Introduction

Somatic cell nuclear transfer (SCNT) is the process by which a nucleus from a donor adult cell is introduced into the cytoplasm of an enucleated egg. This process has been used successfully in a variety of mammalian species, from domesticated animals to endangered species (Cibelli 2007). However, as described previously in section 1.7, the study of epigenetics in mammalian nuclear transfer is further complicated by genomic imprinting defects. The zebrafish embryo does not seem subject to these, as gynogenetic and androgenetic fish are viable (Westerfield 1995; Corley-Smith, Lim et al. 1996), suggesting that imprinting does not exist in this organism. Combined with the fact that nuclear transfer is also possible in this species (Lee, Huang et al. 2002), this makes the zebrafish a simpler model system with which to investigate the general mechanisms of vertebrate epigenetic reprogramming.

Thus, one of the original goals of this study was to gain insight into the general epigenetic mechanisms that are essential for nuclear reprogramming during SCNT in zebrafish, a model organism which facilitates systematic molecular and genetic approaches, while still maintaining relevance to other vertebrates such as humans. Consequently, in order to be able to monitor the epigenetic reprogramming process, the dynamics of DNA and histone methylation marks were first investigated in naturally fertilised zebrafish embryos. This work is described in Chapters Three to Five, where the novel findings from immunofluorescence and western blot experiments showed that dynamic variations in the levels of a variety of epigenetic modifications took place during embryogenesis, which enabled us to elaborate on some of their potential functions during development. In future studies, these marks could be compared with those of cloned embryos, in order to decipher which

epigenetic signatures are essential for development. Consequently, this chapter describes the preparatory work undertaken to facilitate SCNT in zebrafish, such as the acquisition of recipient unfertilised oocytes, the visualisation of their maternal pro-nuclei and polar bodies, the derivation of differentiated and potentially undifferentiated donor nuclei from cell cultures (Chapter Seven), and the subsequent set-up of the microinjection apparatus.

6.2 Results

6.2.1 Preparation of recipient eggs

In SCNT, an unfertilised recipient oocyte is required for the reprogramming of a donor cell nucleus. Eggs such as these can be obtained by first anaesthetising and then squeezing female fish, as is described previously by Westerfield (1995). However, prior to egg extraction, the fish must first be primed for egg production. In Huang *et al.* (2003), this was achieved by dividing individual pairs of male and female fish in nesting tanks overnight, and then allowing them to briefly interact the following morning. This protocol was augmented using knowledge of zebrafish courtship gained from Darrow & Harris (2004), but was still seen to be inefficient in terms of both time and yield. However, after consulting colleagues within the field, a new three-fold strategy was implemented to try and increase productivity. This involved firstly selecting breeding tanks that had an equal number of male and female fish that were specifically young and fertile. Then secondly, instituting a new feeding regime in which extra food was given to the fish during the day. And finally, much like in Huang *et al.* (2003), pairs of fish were placed in divider tanks overnight, but in this instance, they were immediately squeezed instead of being allowed to interact the following morning. These changes, in combination with the squeezing technique, were seen to greatly increase the efficiency of the egg collection process (data not shown).

6.2.2 Visualisation of cell nuclei and the polar body and maternal pro-nucleus of oocytes

The nuclear visualisation protocol adapted from Huang *et al.* (2003), which involved the enzymatic dechorionation and subsequent fixation and Hoechst staining of embryos, was initially practised on 16-cell to 24 hour old embryos. However, this process caused extensive embryo damage, with a great deal of disintegrative loss of younger embryos and unfertilised oocytes in particular (data not shown). Thus, a complete change of tack was necessary in order to visualise the maternal pro-nuclear DNA, and this came in the form of microinjecting a fixative/dye mix directly into the unfertilised oocyte. Fig. 6.1a shows the fixed and Hoechst 33342-stained maternal pro-nuclear DNA in an unfertilised oocyte. Fig. 6.1b shows the identification of the second polar body, which was seen to co-localise with the maternal pro-nucleus (data not shown). This substantiated the use of the second polar body as a reference point for the enucleation process, as stated by Huang *et al.* (2003), thus mitigating the need for visualising the maternal pro-nuclear DNA directly in future SCNT experiments.

6.2.3 Preparation of donor cells

Primary cells were obtained from 5-15 somite embryos as described in Huang *et al.* (2003), but long-term cultured cells could not be established following their instructions (data not shown). After taking advice, the tissue culture protocol from Westerfield (1995) was initiated, and this was able to produce a healthy heterogeneous population of dividing cells. In order to get a single population of cells, various techniques such as flow cytometry and cell scraping were tried, but to no avail (data not shown). Finally, rbbFGF was added to the culture medium as it was seen to prevent pigment cell growth and reduce expression of neural-specific markers, while simultaneously upregulating the expression of mesodermal genes (Singh, Fischer et al. 2001). Figure 6.2 depicts a tissue culture of H2A.F/Z:GFP cells and shows that this approach, in combination with regular passaging, resulted in the growth of an almost homogenous population of epithelial-like cells for more than three months (Fig. 6.2a), and these cultures were indeed fluorescent (Fig. 6.2b).

Nevertheless, during the many permutations of the long-term tissue culture protocol described above, it could be seen that there were also what looked like ESC clusters growing within the cell population. This was tentatively confirmed using a variety of methods to identify numerous markers of stem cell identity (Chapter Seven). Thus, these cells can also be used as a source of donor nuclei for nuclear transfer, and could be useful in assessing how easily different types of cells can be reprogrammed.

6.2.4 Microinjection set-up

Figure 6.3a shows the microinjection set-up, with manipulations taking place within a Petri dish under the dissecting microscope. The holding pipette was suitable for the chorionated unfertilised oocyte (Fig. 6.3b), and it could be seen that the 0.5% BSA / Hank's saline solution was effective in preventing the premature activation of the egg, as determined by the absence of any cytoplasmic streaming in the yolk towards the animal pole (Fig. 6.3c).

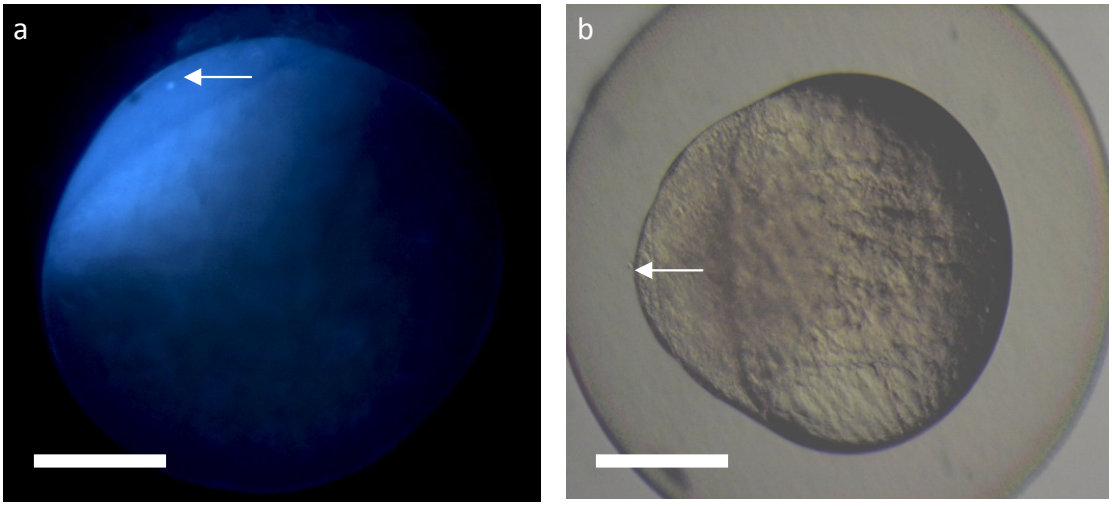

Fig. 6.1: Unfertilised oocytes. **(a)** Fixed and Hoechst 33342-stained egg. Arrow indicating the maternal pro-nuclear DNA. **(b)** Live egg under phase-contrast. Arrow indicating the second polar body. Scale bar, 200 μm.

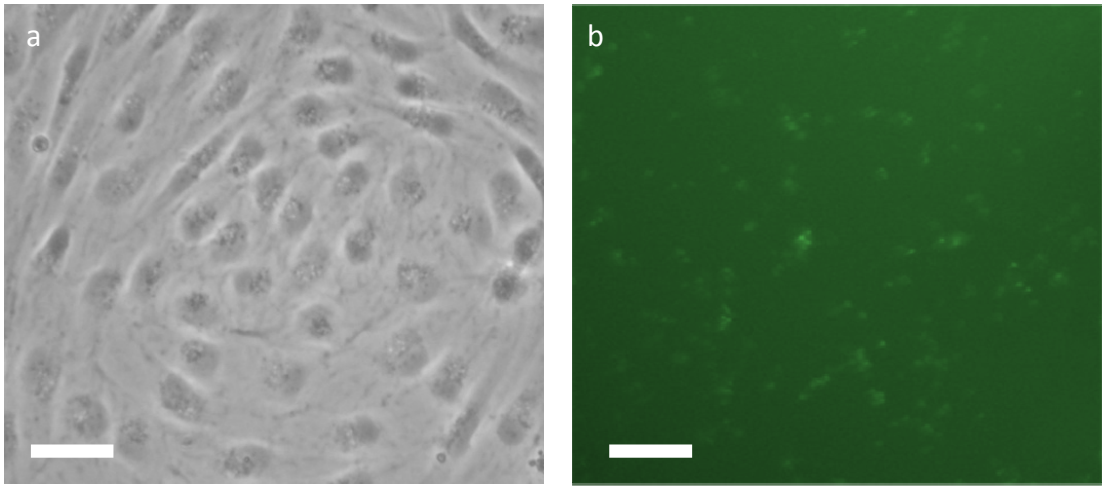

Fig. 6.2: Tissue culture of H2A.F/Z:GFP cells. **(a)** Long-term cultured cells. Scale bar, 50 μm. **(b)** H2A.F/Z:GFP cell fluorescence at low magnification. Scale bar, 200 μm.

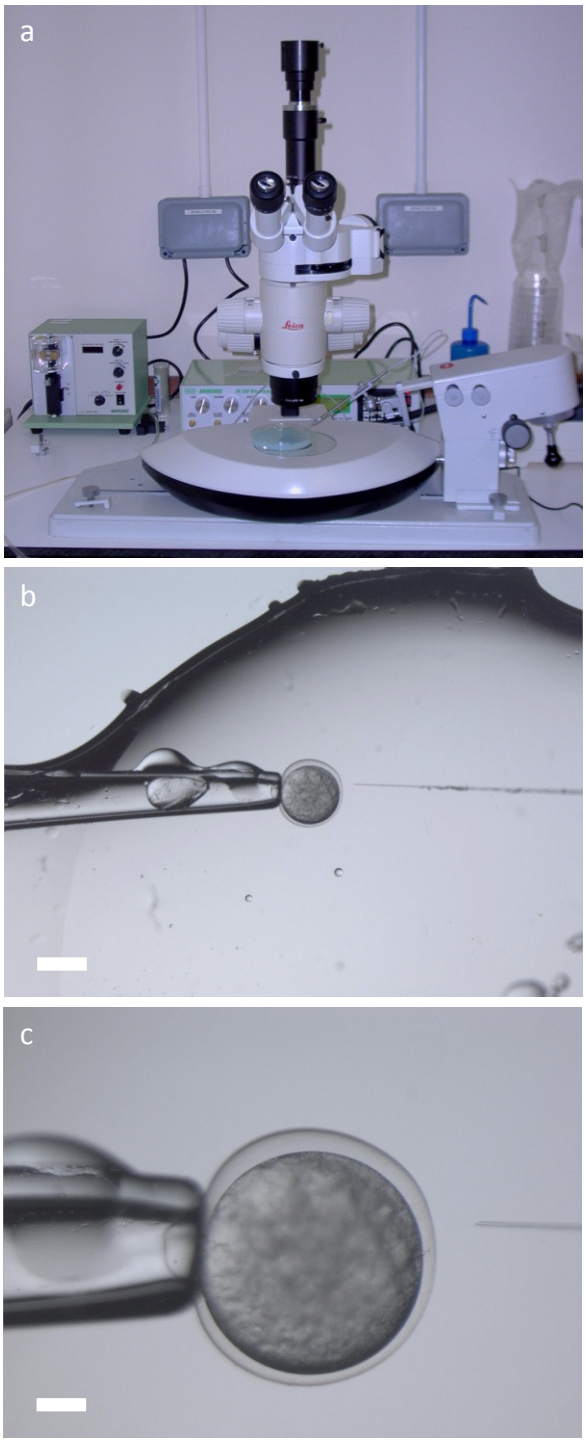

Fig. 6.3: Microinjection set-up. **(a)** Microscope and micromanipulator, with manipulations conducted within a Petri dish. **(b)** Holding pipette and micropipette with an unfertilised oocyte. Scale bar, 0.5 mm. **(c)** Higher magnification image showing the inactivated egg with an intact chorion. Scale bar, 100 μm.

6.3 Discussion

As stated previously, a report in 2002 was the first to demonstrate that SCNT was achievable using zebrafish (Lee, Huang et al. 2002; Huang, Ju et al. 2003). However, as could be seen from our results, the reproducibility of many of the steps within this protocol was extremely poor. We attempted to improve upon this technique by using a number of different strategies.

Firstly, to facilitate phenotypic screening of the potential clones, wild-type long fin recipient eggs were used in combination with H2A.F/Z:GFP transgenic donor nuclei, so that any successful clones at adulthood would possess fluorescent nuclei and no longer express the long fin phenotype. Additionally, unfertilised oocytes were left in an inactivated state to allow time for manipulations to take place, as well as being left within their chorions to prevent any damage during the SCNT procedure.

An encouraging finding was that similar techniques have very recently been employed from another laboratory to once again produce successful clones from zebrafish (Siripattarapravat, Pinmee et al. 2009). Numerous strains of fish were utilised, but a similar phenotypic screening system was implemented, where the H2A.F/Z:GFP transgenic fish was used to supply recipient eggs in one experiment, while the wild-type long fin zebrafish was used to provide donor nuclei in another. Eggs in their chorions were also maintained in an inactivated state, however Chinook salmon ovarian fluid was utilised in this case, rather than 0.5% BSA in Hank's saline.

Several other advances were made in the work by Siripattarapravat *et al.* (2009) which were crucial for the success of this SCNT procedure. One of the most important was that the maternal pro-nucleus was inactivated using a laser; this meant that the technically demanding process of manual enucleation could be completely

avoided. Donor nuclei were also delivered via the micropyle, the route that fish sperm use to enter the egg, and eggs were then finally activated after this procedure.

Thus, the foundation work for the SCNT process within our laboratory has already begun. The next step of the study will be to inactivate the maternal pronucleus within the unfertilised oocyte, and then to inject a donor somatic or ES cell within it. The immunostaining experiments can then be used to assess the epigenetic status of these developing embryos and compare them against normally fertilised eggs, in order to gain more insight into the general epigenetic mechanisms that are essential for nuclear reprogramming in vertebrates. Eventually this process could also help pave the way for future studies involving tissue repair and regeneration, as well as opening up the potential of targeted genetic manipulation in this valuable model organism.

Chapter Seven

7 Epigenetic characterisation of zebrafish embryonic stem cell-like clusters

7.1 Introduction

A pluripotent cell is one that can differentiate into any cell type within an organism, and they exist naturally, albeit briefly, during the course of embryogenesis. This developmental process begins after fertilisation, and in mammals, produces a blastocyst, which consists of the inner cell mass (ICM) and the trophoblast. The ICM itself differentiates into two types of tissues, the epiblast and the hypoblast. The trophoblast and hypoblast together form the extraembryonic lineages, which provide nutrition for the growing embryo, as well as developmental cues (Selwood and Johnson 2006). The pluripotent epiblast, on the other hand, consists of 10-20 cells sandwiched between the trophoblast and hypoblast, and goes on to form the entirety of the foetus (Gardner and Beddington 1988; Nichols and Smith 2009). In mice, it is from this epiblast that embryonic stem cells (ESCs) are derived (Evans and Kaufman 1981; Martin 1981), which under appropriate conditions display the dual properties of unlimited self-renewal and pluripotency. When reintroduced into the embryo, they can still participate in foetal development (Smith 2001), and thus represent an immortalised *in vitro* form of the epiblast.

Despite the progress made in understanding pluripotency in mice, attempts to generate true ESCs in other experimental organisms have been limited. Nonetheless, ESCs have also been isolated and maintained in long-term *in vitro* culture from chickens (Pain, Clark et al. 1996; Petitte, Liu et al. 2004; van de Lavoir, Mather-Love et al. 2006). These cells were derived from pre-primitive streak blastodermal cells and were characterised by the presence of numerous ESC markers, such as SSEA-1 and alkaline phosphatase (AP) activity (Pain, Clark et al. 1996; Petitte, Liu et al. 2004). They have similar growth requirements to mouse ESCs *in vitro*, and like

these pluripotent cells, can give rise to tissues from all three germ layers, both *in vitro* and *in vivo* (Pain, Clark et al. 1996; van de Lavoir, Mather-Love et al. 2006). Recently, it was demonstrated that the maintenance of their pluripotency was also due to the expression of Oct4 and Nanog (Lavial, Acloque et al. 2007). However, in contrast to mouse ESCs, it appears that their germline competence is much more sensitive to culture conditions, and this competency rapidly and dramatically diminishes after long-term tissue culture (Pain, Clark et al. 1996; Petitte, Liu et al. 2004; van de Lavoir, Mather-Love et al. 2006). However recently, rat ESCs capable of chimera production and germline transmission have also been derived (Buehr, Meek et al. 2008). This study utilised a combination of selective small-molecule inhibitors first introduced by Ying *et al.* (2008), and finally opens up the possibility of gene knock-outs being created in rats, much like they are in mice at present.

ESCs have also been derived from zebrafish embryos (Ma, Fan et al. 2001; Fan, Crodian et al. 2004; Fan and Collodi 2006). These cells were cultivated on a rainbow trout spleen cell feeder layer, and after transplantation were shown to contribute to the germ-line (Ma, Fan et al. 2001), even after several culture passages (Fan, Crodian et al. 2004; Fan and Collodi 2006). However, the frequency of germ-line chimera contribution is very low (approximately 2-4%; Ma, Fan et al. 2001; Fan, Crodian et al. 2004; Fan and Collodi, 2006). Advantageously during the course of this project, we were also able to derive zebrafish ESC-like clusters using a novel method. Consequently, in this chapter I describe how these clusters were initially characterised using a variety of methods to identify various markers of stem cell identity. These experiments demonstrated that these clusters were alkaline phosphatase-positive and expressed key ESC factors, as detected by RT-PCR and immunofluorescence. Further studies showed that GFP-expressing ESC-like clusters also contributed to ectodermal tissues when transplanted into wild type zebrafish embryos. Subsequently, these clusters were then epigenetically profiled using immunofluorescence, showing that they had a similar complement of modifications to ESCs derived from mice.

7.2 Results

7.2.1 Morphology and alkaline phosphatase activity consistent with ES-like cell identity

During the course of this project, zebrafish ESC-like clusters were routinely derived from whole dechorionated 18-somite stage embryos, along with a variety of other cell types. These cell clusters were first observed during the development of tissue culture methods for producing donor cells for nuclear transfer, as described in sections 2.4 and 6.2.3. Figure 7.1a shows a bright field image of a single cluster on a feeder layer of cells. These clusters could be maintained for over three weeks in culture. Using an identical protocol, these clusters could also be generated from gastrula stage embryos, however no cells could be derived from blastulas at all (data not shown). Basic FGF (bFGF) was added to the culture medium, as previous work demonstrated that its presence strongly inhibited the emergence of pigment cells (Bradford, Sun et al. 1994). This result was recapitulated in this study, where melanocytes only grew within the clusters when bFGF was omitted from the medium (data not shown). Nevertheless, the clusters that were obtained were morphologically similar to those derived from mice, and in more mature colonies regions of spontaneous contractility were also observed within them (data not shown). This phenomenon is commonly witnessed as ESCs differentiate into embryoid bodies (Doevendans, Kubalak et al. 2000).

Alkaline phosphatase (AP) is also a well established marker of pluripotent stem cell identity (O'Connor, Kardel et al. 2008). Thus to determine whether the clusters derived from the 18-somite embryo were indeed ESC-like, these cultures were stained for AP activity. As demonstrated in Figure 7.1b, cells stained for alkaline phosphatase (AP) activity revealed AP-positive ESC-like clusters (red), which exhibited a strong endogenous AP activity. This positive reaction was used as the first criterion to identify these cells as ESC-like.

7.2.2 Pluripotency markers detected in the cultures by RT-PCR

To detect the presence of ES cell markers in the mixed population of cells, mRNA and cDNA was prepared from the cultures. Figure 7.2 shows a RT-PCR analysis of the cell culture for the expression of mesodermal and neural markers, as well as those for pluripotency. The proto-oncogene *Wnt-1* and the homeodomain gene *engrailed* (*eng3*) are neural markers which are expressed in the developing central nervous system of the zebrafish (Molven, Njolstad et al. 1991; Ekker, Wegner et al. 1992). The homeobox gene *goosecoid* (*gsc*) on the other hand, is required for normal mesoderm development (Stachel, Grunwald et al. 1993), as is *MyoD*, a mesodermal marker involved in the differentiation of muscles (Weinberg, Allende et al. 1996). These markers were used to show that cells of a neural and mesodermal origin were indeed present within the culture (Fig. 7.2). *β-actin* was used as a control, and no PCR products were detected when the reverse transcriptase or DNA was omitted from the reaction (data not shown).

The expression of pluripotency markers within the culture was also investigated. *pou2* and *sox2* are the zebrafish homologues of Oct4 and Sox2 respectively (Takeda, Matsuzaki et al. 1994; Okuda, Yoda et al. 2006), while *vasa* is a primordial germ cell marker (Olsen, Aasland et al. 1997). The RT-PCR results obtained show that these pluripotency markers were also expressed within these cultures (Fig. 7.2).

7.2.3 Markers of pluripotency pinpointed to ESC-like clusters by immunofluorescence

To pinpoint the expression of some of these pluripotency genes, immunostaining experiments were carried out in chamber slides using commercially available antibodies. Figure 7.3 shows the immunofluorescent staining of ES-like clusters for Oct4. However, no specific nuclear signal was obtained in the zebrafish cultures using the antibody against Oct4 (green), since no signal colocalised with the DAPI (blue) stained nuclei (Fig. 7.3a). In marked contrast to this result, the mouse ESC control had a strong and nuclear-specific Oct4 signal (Fig. 7.3b). This result was

unsurprising as the antibody used in this experiment was directed towards the N-terminal of the human version of Oct4, which shares very little homology with its zebrafish homologue, as shown by the sequence alignment of zebrafish and human Oct4 protein sequences (Fig. 7.3c).

Stage-specific mouse embryonic antigen 1 (SSEA-1) is a cell surface marker of pluripotency in mouse ESCs (Solter and Knowles 1978). Figure 7.4 shows the immunofluorescent staining of SSEA-1 (green) in zebrafish cultures, where it could be seen that this marker was specifically expressed by the ESC-like clusters, rather than the surrounding cells (Fig. 7.4a). Zebrafish Sox2, unlike Oct4, is highly homologous to its human counterpart as shown by sequence alignment of zebrafish and human Sox2 protein sequences (Fig. 7.4c). Sox2 could also be seen to be specifically expressed by the zebrafish ESC-like clusters in their nuclei, as the Sox2 signal (red) colocalised with the nuclear DAPI signal (blue) (Fig. 7.4b).

7.2.4 Cell transplantation shows neuroectodermal integration

In order to verify whether these clusters were truly pluripotent, ES-like cells were injected into blastulas to see if they could contribute to each of the three germ layers of the developing zebrafish embryo. For this experiment, clusters were derived from a transgenic zebrafish line expressing a fusion protein of the histone variant, H2A.F/Z, with green fluorescent protein (GFP) (Pauls, Geldmacher-Voss et al. 2001). These H2A.F/Z:GFP cells had fluorescing nuclei which were utilised as a reporter during the transplantation experiments into wild type blastulas. Figure 7.5 shows H2A.F/Z:GFP ES-like cells integrated into the neuroectoderm of wild type zebrafish embryos after transplantation. Fluorescing cells could be clearly seen within wild-type embryos after successful injections into the animal pole of the blastula (Fig. 7.5a), however, these cells were often extruded from acceptor embryos when injected in other locations (data not shown). Nevertheless, blastulas which retained a large number of fluorescing ES-like cells were monitored during

development, and when observed at 24 hpf, often displayed integrations within the neuroectoderm (Figs. 7.5b-d).

Cells from H2A.F/Z:GFP blastula embryos were also directly injected into wild type embryos. This served as a control for the ES-like cell transplantation experiments, to ensure that cells known to be pluripotent could also contribute to tissues within the developing embryo. However, these experiments also showed that injected cells only contributed to the neuroectoderm (data not shown), therefore technical optimisation is needed to control injection bias.

7.2.5 Epigenetic characterisation of the ESC-like clusters

The experiments described above demonstrated that the clusters obtained from the developing zebrafish embryo expressed various markers of stem cell identity. However, it would be valuable to know whether they were also similar epigenetically. Thus, preliminary immunostaining experiments were carried out in chamber slides using antibodies directed towards a variety of histone modifications. Figure 7.6 shows the epigenetic characterisation of zebrafish ESC-like clusters using antibodies against the methylated histone marks H3K4me3 (a); H3K27me3 (b); H4K20me1 (c); H3K9me3 (d), with DAPI nuclear counterstaining (blue). However, as was seen in previous studies, no specific signals from the H4K20me3 antibody were detected by immunofluorescence in the zebrafish samples or a mouse ESC control (data not shown). In contrast, nuclear-specific H3K4me3, H3K27me3 and H4K20me1 were all observed within the cells and clusters of the cultures derived from the zebrafish embryo (Figs. 7.6a-c). The H3K9me3 immunofluorescence result also displayed a specific nuclear staining pattern, however, it was noted that signals from this mark were especially low within the centre of the clusters and particularly evident around their periphery (Fig. 7.6d).

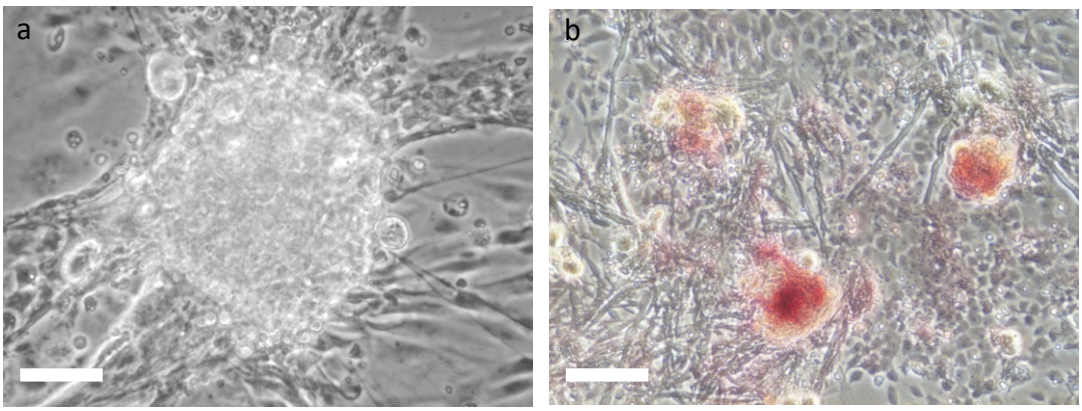

Fig. 7.1: ESC-like clusters derived from the zebrafish embryo at the 18-somite stage of development. **(a)** Bright field image of a single cluster on a feeder layer of cells. Scale bar, 50 μm. **(b)** Cells stained for alkaline phosphatase (AP) activity showing AP-positive ESC-like clusters (red). Scale bar, 100 μm.

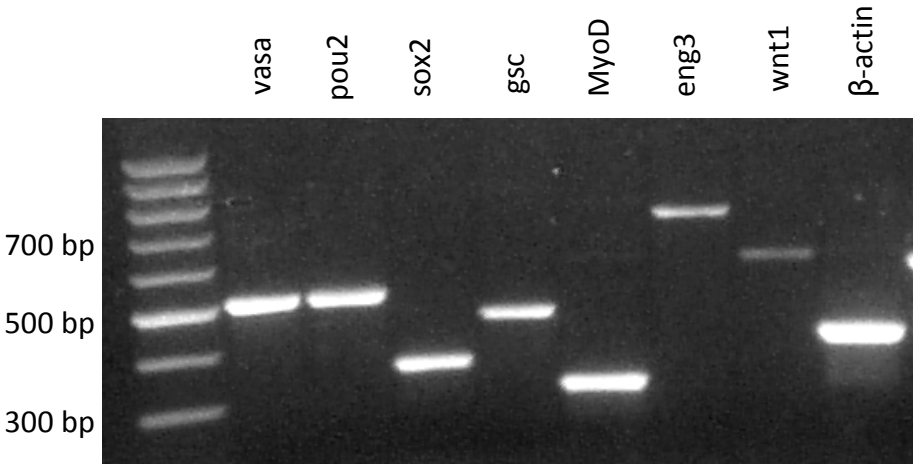

Fig. 7.2: RT-PCR analysis of the cell culture showing the expression of mesodermal and neural markers, as well as those for pluripotency.

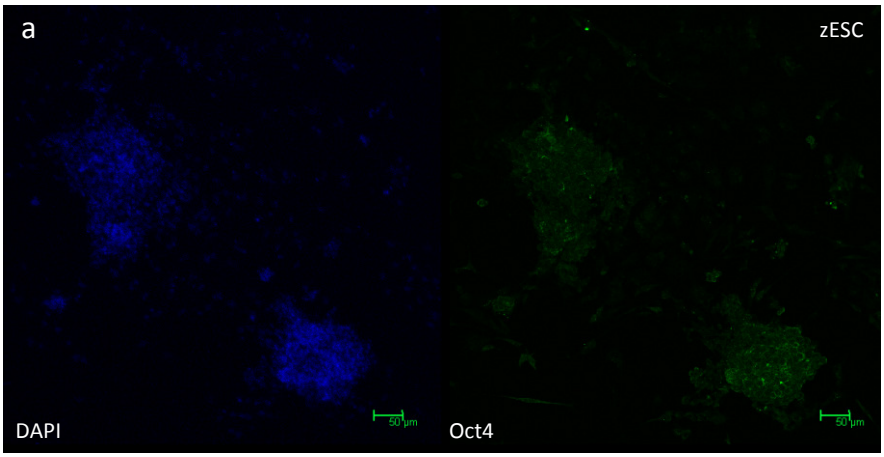

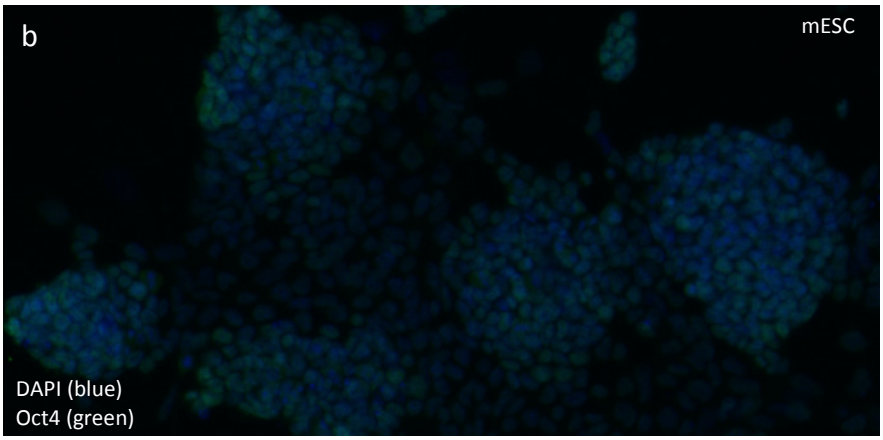

c

```
zOct4           MTERAQSPTAADCRPYEVNRAMYPQAAGLDGLGGASLQFAHGMLQDPSLIFNKAHFNGIT 60
hOct4           MAGHLASDFAFSP----------PPGGGGDGPGGP----------EP------------- 27
                *: :  *  * .           * ..* ** **.          :*

zOct4           PATAQTFFPFSGDFKTNDLQGGDFTQPKHWYPFAAPEFTGQVAGATAATQPANISPPIGE 120
hOct4           ----------------------GWVDPRTWLSFQGPPGG------------PGIGPGVGP 53
                                     .:.:*: * .* .*                ..*.* :*

zOct4           TREQIKMPSEVKTEKDVEEYGNEENKPPSQYHLTAGTSSVPTGVNYYTPWNPNFWPGLSQ 180
hOct4           GSEVWGIP---PCPPPYEFCGGMAYCGP-----QVGVGLVPQGG--LETSQP---EGEAG 100
                  *   :*         *  *.     *      .*.. ** *     . :*    * :

zOct4           ITAQANISQAPPTPSASSPSLSPSPPGNGFGSPGFFSGGTAQNIPSAQAQSAPRSSGSSS 240
hOct4           VGVESNSDGASPEPCTVTP------------------G--AVKLEKEKLEQNPEES---- 136
                : .::* . *.* *.: :*                  *  * :: . : :. *..*

zOct4           GGCSDSEEEETLTTEDLEQFAKELKHKRITLGFTQADVGLALGNLYGKMFSQTTICRFEA 300
hOct4           -------QDIKALQKELEQFAKLLKQKRITLGYTQADVGLTLGVLFGKVFSQTTICRFEA 189
                       :: .   ::****** **:******:*******:** *:**:***********

zOct4           LQLSFKNMCKLKPLLQRWLNEAENSENPQDMYKIERVFVDTRKRKRRTSLEGTVRSALES 360
hOct4           LQLSFKNMCKLRPLLQKWVEEADNNENLQEICKAE-TLVQARKRKR-TSIENRVRGNLEN 247
                **********:****:*::**:*.** *:: * * .:*::***** **:*. **. **.

zOct4           YFVKCPKPNTLEITHISDDLGLERDVVRVWFCNRRQKGKRLALPFDD-ECVEAQ--YYEQ 417
hOct4           LFLQCPKPTLQQISHIAQQLGLEKDVVRVWFCNRRQKGKRSSSDYAQREDFEAAGSPFSG 307
                 *::****.  :*:**:::****:**************** :  : : * .**    :.

zOct4           SPPPPPHMGGTVLPGQGYPGPAHPGGAPALYMPSLHRPDVFKNGLHPGLVGHLTS- 472
hOct4           GPVSFPLAPGPHFGTPGYGSPHFTALYSSVPFP---EGEAFPPVSVTTLGSPMHSN 360
                .* . *   *. :   ** .* ...  .:: :*   . :.*     . * . : *
```

Fig. 7.3: Immunofluorescent staining of Oct4 **(a)** Non-specific Oct4 staining in zebrafish cells (green) with DAPI (blue). **(b)** Merged Oct4 (green) and DAPI (blue) signals in mouse ESC's. **(c)** Sequence alignment of zebrafish and human Oct4 protein sequences. Scale bar, 50 μm.

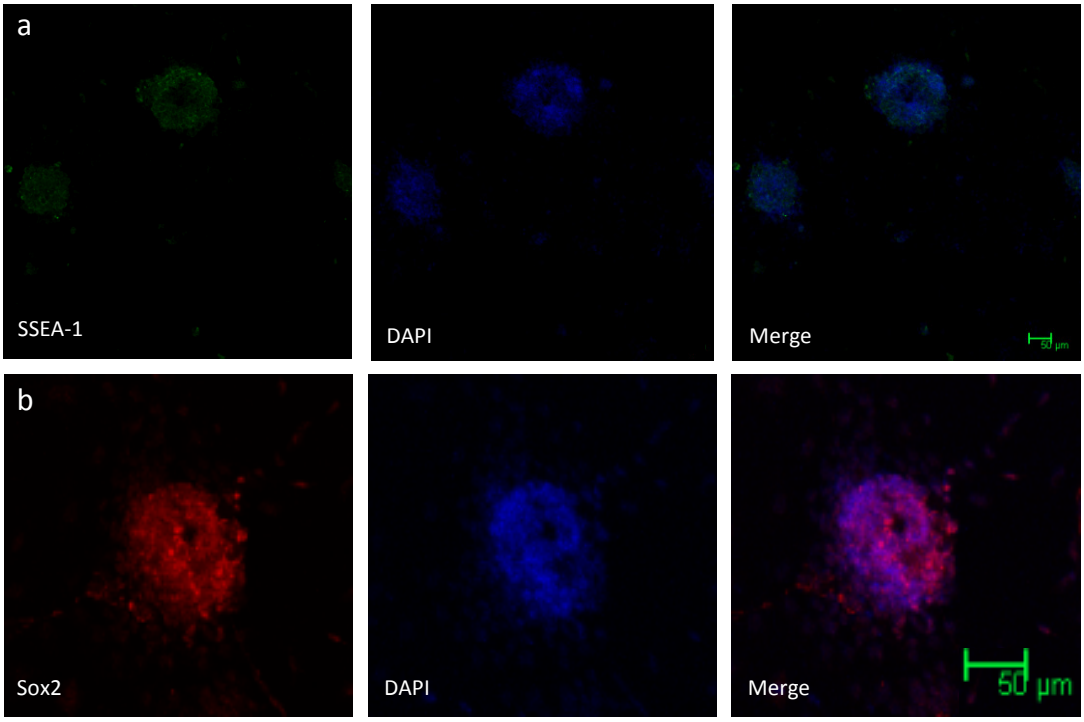

c

```
zSox2   MYNMMETELKPPAPQPNTGGTG---NTNSSGNNQKNSPDRIKRPMNAFMVWSRGQRRKMA 57
hSox2   MYNMMETELKPPGPQQTSGGGGGNSTAAAAGGNQKNSPDRVKRPMNAFMVWSRGQRRKMA 60
        ************.** .:** *   .: ::*.********:******************

zSox2   QENPKMHNSEISKRLGAEWKLLSESEKRPFIDEAKRLRALHMKEHPDYKYRPRRKTKTLM 117
hSox2   QENPKMHNSEISKRLGAEWKLLSETEKRPFIDEAKRLRALHMKEHPDYKYRPRRKTKTLM 120
        ************************:************************************

zSox2   KKDKYTLPGGLLAPGGNGMGAGVGVGAGLGAGVNQRMDSYAHMNGWINGGYGMMQEQLGY 177
hSox2   KKDKYTLPGGLLAPGGNSMASGVGVGAGLGAGVNQRMDSYAHMNGWSNGSYSMMQDQLGY 180
        ****************.*.:*************************:**.*.***:****

zSox2   PQHPSLNAHNTAQMQPMHRYDMSALQYNSMTNSQTYMNGSPTYSMSYSQQSTPGMTLGSM 237
hSox2   PQHPGLNAHGAAQMQPMHRYDVSALQYNSMTSSQTYMNGSPTYSMSYSQQGTPGMALGSM 240
        ****.****.:**********:*********.******************.****:****

zSox2   GSVVKSESSSSPPVVTSSSHSRAGQCQTGDLRDMISMYLPGAEVQDQSAQSRLHMSQHYQ 297
hSox2   GSVVKSEASSSPPVVTSSSHSRA-PCQAGDLRDMISMYLPGAEVPEPAAPSRLHMSQHYQ 299
        *******:***************  **:**************** : :* **********

zSox2   SAPVPGTTINGTIPLSHM 315
hSox2   SGPVPGTAINGTLPLSHM 317
        *.*****:****:*****
```

Fig. 7.4: Immunofluorescent staining of SSEA-1 and Sox2 in zebrafish cell cultures **(a)** Specific SSEA-1 staining in zebrafish ESC-like clusters (green) with DAPI (blue) and merged images alongside. **(b)** Specific nuclear staining of Sox2 in zebrafish ESC-like clusters (red) with DAPI (blue) and merged images. **(c)** Sequence alignment of zebrafish and human Sox2 protein sequences. Scale bar, 50 µm.

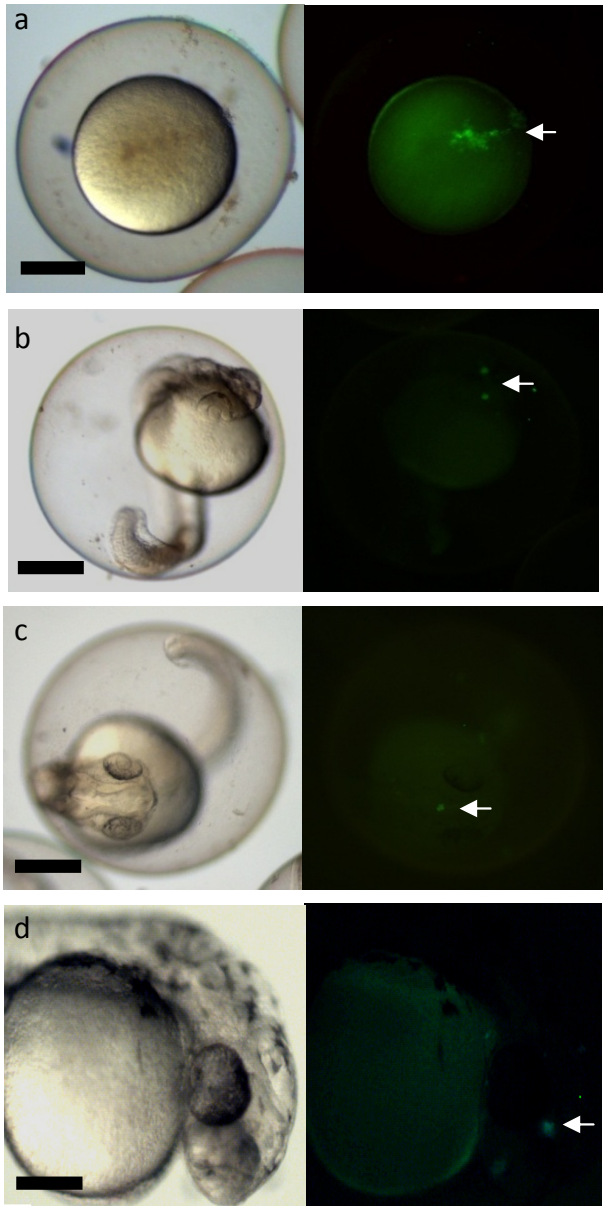

Fig. 7.5: White light and fluorescence images of H2A.F/Z:GFP ES-like cells integrated into the neuroectoderm of wild type zebrafish embryos after transplantation. **(a)** GFP-labelled ES-like cells injected into the animal pole of a wild type blastula embryo. **(b)** Chorionated 24 hpf embryo displaying two sites of neuroectodermal integration. **(c)** 24 hpf embryo in its chorion also showing cephalic integration of ES-like cells. **(d)** Higher magnification of another integration in a 24 hpf embryo. The arrows indicate GFP expression, and the yolk sack shows autofluorescence. Scale bar, 200 μm (a-c) and 100 μm (d).

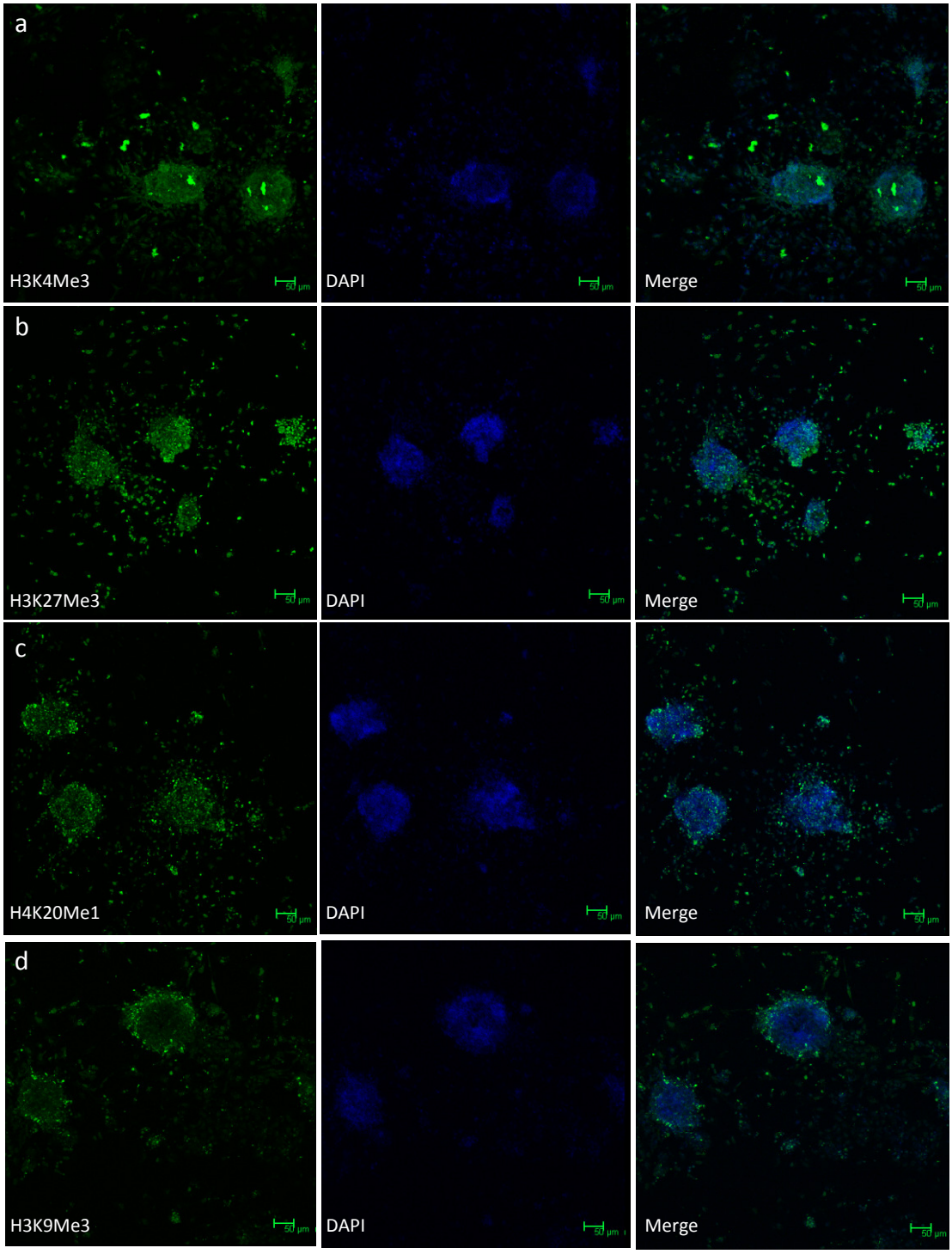

Fig. 7.6: Epigenetic characterisation of zebrafish ESC-like clusters. **(a)** H3K4-Me3 (with fluorescent debris present). **(b)** H3K27-Me3. **(c)** H4K20-Me1. **(d)** H3K9-Me3. The corresponding DAPI (blue) and merged images are shown alongside. Scale bar, 50 μm.

7.3 Discussion

The data presented here demonstrates that these clusters have a degree of ESC-like character, both in terms of their morphology and their expression of various pluripotency markers. However, more work is necessary in order to fully understand the transcriptional network required for pluripotency in zebrafish. Although Sox2 expression has been observed in our ESC-like clusters (Fig. 7.4b), the role of both Oct4 and Nanog within this system is relatively unknown. The existence and equivalent functions of Oct4 in non-mammalian vertebrates was still questioned until data demonstrated that the *Xenopus, Axolotl* and chicken homologues of this factor could rescue Oct4-deficient mouse ESCs (Morrison and Brickman 2006; Lavial, Acloque et al. 2007). However, the zebrafish version of this protein appears to be unable to perform this function (Morrison and Brickman 2006; Lavial, Acloque et al. 2007). Functional assays were used to identify the zebrafish *pou2* gene as the Oct4 homologue (Burgess, Reim et al. 2002), but this gene appears to be mainly involved in endoderm specification (Lunde, Belting et al. 2004; Reim, Mizoguchi et al. 2004). The use of a more appropriate antibody may help define the role of Oct4 within our ESC-like clusters and during zebrafish development in general. Nanog has also been observed to operate within chickens and *axolotl* (Lavial, Acloque et al. 2007; Dixon, Redwood et al. 2009), however, the existence of this factor within the zebrafish genome is still as yet unclear. A group has recently identified a Nanog homologue in medaka, as well as in zebrafish (Camp, Sanchez-Sanchez et al. 2009), but more work will be necessary in order to confirm this finding, as Nanog was thought to be absent from the zebrafish genome (data not shown).

Regardless of the intrinsic factors at play, the true test of an ES cell is its capacity to colonise a host embryo, and to contribute to all the germlayers and the germline of the resulting chimera (Smith 2001). However, the work reported here shows that the ES-like cells derived from a fluorescing transgenic line of zebrafish only appeared to contribute to the neuroectoderm, where integration took place exclusively within the head and the eyes of the embryo (Fig. 7.6). Many of the injections took place within the animal pole of the blastula for ease of transplantation, and it is well known that

the positioning of cells along the animal-vegetal axis influences their contribution to one of the three germ layers (Kimmel and Warga 1988; Kimmel, Warga et al. 1990). It has been seen that cells transplanted close to the margin prior to gastrulation will give rise preferentially to endoderm and mesoderm, while cells transplanted towards the animal pole, as was done in this study, will contribute to ectodermal fates, such as forebrain and eyes (Carmany-Rampey and Moens 2006). Accordingly, the limited differentiation of our ES-like cells could be due to their location of transplantation, rather than their pluripotent potential. This conclusion is supported by the similar results obtained when cells known to be pluripotent from the H2A.F/Z:GFP blastula also gave rise to just neuroectodermal tissues when injected directly into the wild-type acceptors (data not shown). Due to the difficulty in transplanting cells to other locations within the embryo, further experiments will need to be conducted in order to assess the true potential of these ES-like cells, such as the production of teratomas within older embryos or adults.

In addition, it could be seen that the ESC-like clusters grew on a feeder layer composed of numerous cell types from the 18-somite embryo (Fig. 7.1). While every precaution was taken to inject only ES-like cells, the possibility of other cells being injected and potentially contributing to the chimera cannot totally be ruled out. Thus, culture conditions also need to be refined so that these ESC-like clusters can grow in an environment that is feeder free. In mouse this was achieved by the addition of LIF and BMP4 to the culture medium, and now it even seems possible without these factors using a combination of selective small-molecule inhibitors established by Ying *et al.* (2008). Rat ESCs capable of chimera production and germline transmission have now been derived using these inhibitors (Buehr, Meek et al. 2008), and it would be of particular interest to see if these factors could also be used to establish a feeder-free environment within our zebrafish cultures.

As stated earlier, bFGF was added to the culture medium, as previous work demonstrated that its presence strongly inhibited the differentiation of neural-crest-

derived melanocytes (Bradford, Sun et al. 1994). This factor was also observed to inhibit the expression of numerous neural markers during zebrafish cell culture (Singh, Fischer et al. 2001). The fact that bFGF appears to be beneficial for the propagation of our ESC-like clusters echoes the conditions needed for human ESC culture. These cells appear to require exogenous FGF to sustain their self-renewal and pluripotency (Levenstein, Ludwig et al. 2006), and also differ from their mouse counterparts in their morphology, clonogenicity, differentiation behavior and molecular profile, in addition to their culture requirements (Johnson, Shindo et al. 2008). In fact, it is now argued that human ESCs are analogous to a recently derived line of epiblast stem cells (EpiSCs) from mice (Brons, Smithers et al. 2007; Tesar, Chenoweth et al. 2007; Rossant 2008). These EpiSCs are derived from post-implantation mouse epiblasts using conditions without LIF but including FGF and activin (Brons, Smithers et al. 2007; Tesar, Chenoweth et al. 2007). These cells express the core pluripotency-associated transcription factors of Oct4, Sox2 and Nanog, but differ from mouse ESCs in their expression of several other transcripts. EpiSCs are also able to differentiate into various cell types *in vitro*, but appear to lack the ability to contribute to the blastocyst to form chimeras (Tesar, Chenoweth et al. 2007; Guo, Yang et al. 2009). Consequently, it is feasible that the ESC-like clusters observed in this zebrafish study may in fact be equivalent to these EpiSCs, as they are also derived from a relatively late stage in embryonic development. Further work will be necessary in order to fully classify these ESC-like clusters.

Nevertheless, from an epigenetic standpoint, these ESC-like clusters do have a similar complement of modifications to ESCs derived from mice. Both H3K4me3 and H3K27me3 are present within the nuclei of zebrafish ESC-like clusters (Fig. 7.6a-b), opening up the possibility that these cells also possess bivalent domains, although a global nuclear analysis cannot reveal this at domain level. Equally, these markers are not unique to our clusters and are also observed in the background cells to varying degrees. Therefore more work is necessary to evaluate the levels of these modifications at the gene level, possibly using ChIP. Additionally, in order to address the question of how these ES-like cells compare to the pluripotent stages of

early zebrafish embryos, the dynamic patterns of these markers during zebrafish development would also need to be determined.

In contrast, little is known about the function of H4K20me1 in ESCs. In this study it was seen to be present within all cells (Fig. 7.6c) and may be involved with chromatin condensation and the repression of lineage-specific genes (Chapter Five). H4K20me3 on the other hand has previously been observed to be involved with heterochromatin formation at repetitive sequences in mouse ESCs (Martens, O'Sullivan et al. 2005; Mikkelsen, Ku et al. 2007). However, the antibody directed towards this modification has consistently failed in our hands, both in this study and in other experiments (Chapter Five).

Conversely, the H3K9me3 antibody showed an interesting result, as it appeared to be absent from the interior of the ESC-like clusters and noticeably present around their periphery (Fig. 7.6d). Previous work suggested that a low global level of H3K9 methylation was required for the maintenance of ESC potential (Loh, Zhang et al. 2007) and that differentiated cell types exhibited an elevated level of this modification (Meshorer and Misteli 2006). It has been seen in mouse ES cells that spontaneous differentiation occurs around the colony periphery (Johnson, Shindo et al. 2008), and a similar situation could be being occurring within our ESC-like clusters, as indicated by the elevated levels of H3K9me3 around the periphery of the clusters. In agreement with this, at early pluripotent zebrafish embryo stages, levels of this marker are very low but increase as development proceeds (Chapter 4). However, more work needs to be conducted in order to confirm these observations.

Nonetheless, the work presented here demonstrates that ESC-like clusters can be derived from the zebrafish embryo using a novel strategy. More work will be necessary to refine the culture conditions and to classify these cells as bona fide ESCs. However, once this is achieved, these cells could help pave the way for future

studies involving tissue repair and regeneration, as well as opening up the potential of targeted genetic manipulation in this valuable model organism.

Chapter Eight

8 General Discussion and Future Work

8.1 Reprogramming

The term reprogramming has been used to describe many processes, such as the epigenetic changes that occur naturally during fertilisation and during the development of the germ cells. Furthermore, this term has also been used to describe the experimentally induced process by which differentiated cells can revert back into a less differentiated state. This latter form of reprogramming can be achieved in a variety of ways, such as by somatic cell nuclear transfer (SCNT), by the fusion of somatic cells with those that are pluripotent, or by the expression of a defined set of transcription factors in somatic cells. Within this section I shall discuss what may be occurring within the developing zebrafish embryo in regards to reprogramming during natural fertilisation. In addition to this, I shall review the various forms of experimentally induced reprogramming, and discuss how these could be applied to the zebrafish model system.

8.1.1 Epigenetic reprogramming during embryonic development

With the DNA methylation results, it can be seen that both the maternal and paternal contributions to the zebrafish genome undergo a rapid reprogramming event after fertilisation, where in the early cleavage stages of development, the genomic DNA is substantially demethylated. This is followed by a remethylation process, whereby the zygotic DNA becomes remethylated by the early blastula stage and remains so as development proceeds (Fig. 8.1). This is in broad agreement with previous studies in both zebrafish (Martin et al. 1999, Mhanni and McGowan 2004, and MacKay et al. 2007) and mice (Santos, Hendrich et al. 2002). However, DNA demethylation has not been reported to occur in either *Xenopus* or medaka development (Stancheva, El-Maarri et al. 2002; Walter, Li et al. 2002), and the overall significance of this reprogramming process remains unclear, as discussed in Chapter Three.

Unfortunately the levels of H3K9 and H4K20 methylation in the maternal and paternal pronuclei of zebrafish were not directly assessed in this study, due to the extremely short developmental timescales involved and the difficulty in obtaining male and female gametes. However, it is entirely feasible that a reprogramming process may also be occurring with these epigenetic marks, especially those of H3K9 methylation and H4K20me2, which increase during development (Fig. 8.1). In fact, a form of reprogramming may also be occurring with H4K20me1/3, with these marks diminishing as embryogenesis proceeds (Fig. 8.1), only to potentially reappear later on in development. H3K9 methylation levels have also been seen to increase during development in numerous mammalian species (Lepikhov and Walter 2004; Liu, Kim et al. 2004; Santos, Peters et al. 2005; Yeo, Lee et al. 2005; Hou, Liu et al. 2008; Lepikhov, Zakhartchenko et al. 2008), as well as in *Xenopus* (Dunican, Ruzov et al. 2008; Shechter, Nicklay et al. 2009). In addition, similar H4K20me1/3 and H4K20me2 dynamics have been observed in mice (Biron et al., 2004; Tuempong Wongtawan, personal communication) and *Drosophila* (Karachentsev et al., 2007) respectively. However, more work is necessary in order to see whether a form of reprogramming is occurring with any of these marks in zebrafish, and what role these processes may play during its development, as discussed in Chapters Four and Five.

8.1.2 Experimentally induced reprogramming of differentiated cells

It was established that differentiated cells were genetically equivalent to embryonic cells, and that they could be reprogrammed to direct development to term, by seminal SCNT experiments in amphibians in the 1950s and 1960s (Briggs and King 1952; Gurdon 1962), as well as by the first successful cloning of a live mammal in 1996 (Wilmut, Schnieke et al. 1997). These studies indicated that the unfertilised oocyte must contain factors that can mediate the reprogramming process. Since then, SCNT has been used successfully in a variety of mammalian species (Cibelli 2007), as well as in zebrafish (Lee, Huang et al. 2002), and work has been conducted in our laboratory to try and use this process to study nuclear reprogramming within this model organism (Chapter Six).

However, it was seen that this initial protocol for SCNT in zebrafish by Lee *et al.* (2002) was especially difficult to replicate, and further optimisation was undertaken within our laboroatory involving the acquisition of recipient unfertilised oocytes, the visualisation of their maternal pro-nuclei and polar bodies, and the derivation of differentiated and potentially undifferentiated donor nuclei from cell cultures (Chapter Seven). Additionally, the eggs were left in their chorions in an inactivated condition, and a novel phenotypic screen was employed. Encouragingly, this work has been confirmed and extended by another group, where the eggs were also maintained in an inactivated state in their chorions, and a similar phenotypic screen was implemented (Siripattarapravat, Pinmee et al. 2009). Several other advances were made in this study by Siripattarapravat *et al*. (2009), which will hopefully make SCNT in zebrafish a more achievable process in many other labs, as discussed in Chapter Six.

Additionally, differentiated mammalian cells can be reprogrammed by fusion to a variety of pluripotent cells, generating pluripotent tetraploid hybrids (Miller and Ruddle 1976; Tada, Tada et al. 1997; Tada, Takahama et al. 2001; Cowan, Atienza et al. 2005). These experiments indicated that pluripotent cells also contain a reprogramming activity and that the pluripotent state is dominant over the differentiated one. These experiments, in addition to those which demonstrated that transcription factors could induce cell fate changes in somatic cells (Davis, Weintraub et al. 1987; Xie, Ye et al. 2004), laid down the foundations for groundbreaking work conducted by Takahashi and Yamanaka in 2006. These researchers identified four transcription factors, Oct4, Sox2, Klf4 and cMyc, that when expressed retrovirally, could reprogram adult mouse fibroblasts into ES-like induced pluripotent stem (iPS) cells (Takahashi and Yamanaka 2006). These first-generation iPS cells were similar, but not identical, to ESCs, but an explosion of subsequent research has refined techniques, and has even produced iPS cells through a virus-free induction process from mouse and human fibroblasts (Kaji, Norrby et al. 2009). Most recently however, virally-induced iPS cells have been used to produce

viable mice through tetraploid complementation (Boland, Hazen et al. 2009; Kang, Wang et al. 2009; Zhao, Li et al. 2009). Tetraploid complementation is considered the most stringent test for pluripotency and developmental fecundity, as all the adult tissues of the subsequent embryo are derived from the stem cell line, while the extraembryonic tissues are supplied by the tetraploid cells.

It would be of particular interest to see if this system could be adapted to zebrafish somatic cells in order to produce zebrafish iPS cells. Our studies in Chapter Seven described the generation and characterisation of ESC-like clusters from zebrafish embryos, demonstrating that Sox2 was preferentially localised within the nuclei of these cells. Moreover, these clusters were morphologically similar to those from mice and were alkaline phosphatase-positive. However, the true test of their pluripotency would involve the production of a chimeric zebrafish from a feeder-free culture, where the cells are able to contribute to all the germlayers and the germline of the organism. iPS cell experiments could also be useful in finally defining whether Oct4 actually plays a role in the establishment of pluripotency in zebrafish, as well as paving the way for future studies involving tissue repair and regeneration in this valuable model organism.

8.2 Epigenetic cross-talk

Using immunological techniques, we were able to visualise the global patterns of DNA and histone methylation occurring within the cells of the developing zebrafish embryo. Together, these findings can be summarised into a schematic graph (Fig. 8.1) which illustrates the distinct and dynamic nature of each of these epigenetic marks during the course of zebrafish development, grouped into trends. However, it should be noted that these marks do not act independently, but do in fact have the capacity to regulate one another. This cross-talk can occur either *in cis*, on the same histone molecule, or *in trans*, between histone molecules, between histone molecules and DNA methylation, or across nucleosomes. There are many examples of communication occurring between various epigenetic marks; however, in this section

I shall concentrate on the relationships between the modifications investigated in this study and discuss what may be taking place within the zebrafish embryo.

8.2.1 Cross-talk between DNA and H3K9 methylation

As has been alluded to previously, DNA methylation, histone modifications, chromatin structure, and gene silencing all seem to be tightly interconnected. However, the first direct evidence for a link between DNA methylation and H3K9 methylation came from genetic studies involving cytosine hypomethylation mutants in *Neurospora*. Here, mutations in both the cytosine and H3K9 methyltransferase genes appeared to abolish all cytosine methylation within the vegetative cells of this filamentous fungus (Kouzminova and Selker 2001; Tamaru and Selker 2001). Further studies suggested that DNA methylation in *Neurospora* took its cue specifically from H3K9 tri-methylation (Tamaru, Zhang et al. 2003), and that mutations in its homologue of HP1 also lead to the elimination of all detectable DNA methylation within this organism (Freitag, Hickey et al. 2004). A seemingly linear pathway was then elucidated that involved the recognition of H3K9me3 by the adapter HP1, which in turn recruited a cytosine methyltransferase for subsequent DNA methylation (Honda and Selker 2008).

In plants however, a mutation in the DNA methyltransferase of *Arabidopsis* caused a severe reduction in the levels of heterochromatic H3K9me2, as well as a loss of DNA methylation at CpG dinucleotides (Soppe, Jasencakova et al. 2002; Tariq, Saze et al. 2003). Moreover, this H3K9me2 appeared to regulate non-CpG methylation, as was demonstrated by a H3K9 methyltransferase mutant (Jackson, Lindroth et al. 2002). As discussed previously, HP1 is indispensable for DNA methylation in *Neurospora*, however, it does not appear to be required in *Arabidopsis* (Fuks 2005). A chromo domain within the plant DNMT directly interacts with methylated H3K9 (Lindroth, Shultis et al. 2004), however, this situation is potentially unique to plants, as mammalian and *Neurospora* DNA methyltransferases do not contain any chromo domains (Goll and Bestor 2005). Nevertheless, a two-step pathway to transcriptional

silencing appears to be occurring in plants, whereby CpG methylation directs H3K9 methylation, which then goes on to subsequently recruit non-CpG methylation.

In mammals, a more complex system seems to be at play. DNMT1 and DNMT3b mutant mouse cells display altered H3K9 methylation patterns at heterochromatin and specific tumour suppressor loci (Fuks 2005). However, no clear reduction of global H3K9 methylation was observed in DNMT1, DNMT3a and DNMT3b triple knockout mouse ES cells (Tsumura, Hayakawa et al. 2006). Nevertheless, the H3K9 methyltransferase, SETDB1, appears to associate with the methyl-DNA-binding protein, MBD1, and it was suggested that this could be a mechanism by which H3K9 methylation is heritably maintained at sites of DNA methylation during chromatin assembly (Sarraf and Stancheva 2004). On the other hand, there are many examples of H3K9 methylation having an effect on cytosine methylation. For example, it can be seen at pericentromeric heterochromatin that DNMTs are recruited to sites of H3K9 methylation by HP1, which seems capable of binding all mammalian DNMTs (Lehnertz, Ueda et al. 2003; Fuks 2005). In addition, the specific H3K9 methyltransferase involved, known as Suv39, is also reported to interact with DNMT1 and 3a (Fuks 2005). Another H3K9 methyltransferase, G9a/GLP, is also thought to regulate gene silencing through directly recruiting DNMTs, as well as catalysing H3K9 methylation and recruiting DNMTs through HP1 (Esteve, Chin et al. 2006; Smallwood, Esteve et al. 2007; Epsztejn-Litman, Feldman et al. 2008). Thus, it is possible that numerous different mechanisms are in place to stably silence specific regions of the mammalian genome via cross-talk between H3K9 and DNA methylation.

In zebrafish, a significant reduction in the global levels of H3K9me3 was observed in DNMT1 morphants. However, no reduction in DNA methylation levels could be detected when the H3K9 methyltransferase homologue was knocked down (Rai, Nadauld et al. 2006). This work indicates that the activity of DNMT1 appears to lie upstream of H3K9me3. This result is at odds with the established data from

Neurospora, however, the work in our study appears to support these findings, as DNA methylation becomes detectable earlier than that of H3K9, and this may be necessary in order to set up the mark. Also it is entirely conceivable that the two marks are interrelated as their developmental dynamics are similar (Fig. 8.1).

8.2.2 Cross-talk between H4K20 and H3K9 methylation

The H4K20 methylation mark is particularly enigmatic as each degree of methylation on this residue can distinctly contribute to the regulation of a diverse range of cellular processes (Yang and Mizzen 2009). Nevertheless, numerous links with the H3K9 methylation mark have been observed. One of the first was made by Schotta *et al.* (2004), where the H4K20me2/3 methyltransferase was seen to be recruited by various isoforms of HP1 to regions of H3K9 methylation in mammalian cells. This relationship appeared to be evolutionarily conserved as *Drosophila* embryos also exhibited this cross-talk between the H3K9 and H4K20 tri-methylation systems (Schotta, Lachner et al. 2004). Recent work re-confirmed that this sequential mechanism was at work, showing that H4K20 tri-methylation was indeed recruited to regions of pericentric heterochromatin by H3K9me3 and HP1 (Souza, Volkel et al. 2009).

Other studies took this relationship a step further, by demonstrating that mono-, di- and tri-methylated forms of H4K20 and H3K9 specifically co-localised with one another in mammalian cells (Sims, Houston et al. 2006). These findings suggested that the combinatorial presence or absence of various forms of H4K20 and H3K9 methylation could potentially define particular states of silent chromatin. Further analysis of H4K20me1 and H3K9me1 even revealed that both were preferentially and selectively enriched within the same nucleosome particle *in vivo* (Sims, Houston et al. 2006). A mechanism for this interaction was demonstrated whereby H3K9me1 is dependent upon the H4K20 mono-methyltransferase, but independent of its catalytic function, indicating that this enzyme potentially recruits a H3K9 mono-methyltransferase to establish a combinatorial epigenetic mark (Sims and Rice 2008).

However, very little is known about the relationship between these two epigenetic marks in the developing zebrafish embryo. Our study showed that the levels of both mono- and tri-methylated H4K20 decreased as development progressed, in direct opposition to the observed dynamics of H3K9 methylation (Fig. 8.1). Nevertheless, this result does not discount a potential relationship occurring between these marks at particular heterochromatic loci or within the coding regions and regulatory sequences of specific genes. In contrast, the levels of H4K20me2 appeared to follow the patterns of H3K9 methylation during zebrafish development (Fig. 8.1). H4K20me2 has been observed to be the most abundant form of H4K20 methylation present in a variety of cells (Pesavento, Bullock et al. 2008; Pesavento, Yang et al. 2008; Phanstiel, Brumbaugh et al. 2008; Yang, Pesavento et al. 2008), and the recruitment of a zebrafish Suv4-20 homologue by HP1 may be at play to promote the deposition of this mark at sites of H3K9 methylation.

8.2.3 Cross-talk between DNA and H4K20 methylation

Finally, very little is known about the relationship between cytosine methylation and H4K20 methylation. There may in fact be no direct connection, as DNMT null ES cells appear to have no changes in the levels of H4K20me3 in their telomeres (Gonzalo, Jaco et al. 2006). Reciprocally, Suv4-20h knock-outs in MEFs do not show any decreases in telomeric DNA methylation (Benetti, Gonzalo et al. 2007). Nevertheless, in addition to the potential indirect effects of DNA methylation via H3K9 methylation cross-talk, H4K20 tri-methylation appears to be initiated by the activity of DNMT2 at retrotransposon sequences in *Drosophila* (Phalke, Nickel et al. 2009). However, it remains to be studied whether it is DNA methylation or the DNMT itself that recruits the H4K20 methyltransferase enzyme to these retrotransposon sequences. The roles of DNMT2 are still controversial, but appear to be conserved within numerous organisms (Phalke, Nickel et al. 2009), thus the observation that DNMT2 morphants in zebrafish demonstrate no global reduction in DNA methylation (Rai, Chidester et al. 2007) indicates that the enzyme itself may be responsible for the results seen in *Drosophila*. Consequently, very little can be

extrapolated from the results obtained in our study from this limited pool of information, and more work is necessary in order to see whether these two epigenetic marks are in fact connected at all.

8.2.4 Cross-talk between other histone modifications

Nevertheless, our study revealed the novel observation that H4K20me1 can occur in a sumoylated form during the early stages of zebrafish development. This finding offers a new avenue for the investigation of the role of H4K20me1 in the regulation of gene transcription. However, more work is necessary in order to validate and understand this connection between H4K20me1 and SUMO. Previous studies have suggested that sumoylation helps to mediate gene repression by recruiting factors, such as HDACs and HP1 (Shiio and Eisenman 2003), while others have suggested that it competes with histone acetylation for lysine residues in order to antagonise gene expression (Nathan, Ingvarsdottir et al. 2006). The latter hypothesis is of particular interest as a substantial degree of histone H4 acetylation was detected in the non-sumoylated form of H4K20me1 at the pre-MBT stage of development (Fig. 5.2b). However, the levels of histone acetylation in the sumoylated form of H4K20me1 would need to be measured before any conclusions can be made on the possibility of an antagonistic relationship occurring between these two marks in the developing zebrafish embryo. Equally, it would be interesting to see whether this myriad of interactions is conserved within vertebrates as a whole.

8.3 Universality of the histone code

As has been discussed, the role of chromatin structure in gene regulation has been linked to post-translational histone tail modifications, such as acetylation, methylation and phosphorylation, among many others (Kouzarides 2007). These modifications provide an additional layer of information to the genome, and can act combinatorially to specifically alter the transcriptional state of a gene, forming what has been hypothesised to be a “histone code” (Strahl and Allis 2000).

However, this term, although useful in defining the need for a specific set of modifications for a given task, is unlikely to truly reflect the presence of a predictable "code" in the strictest sense of the word (Kouzarides 2007). This idea is supported by work which shows that the patterns of epigenetic modifications on H3 and H4 differ dramatically between various eukaryotes, and that there are in fact many species-specific post-translational modifications in existence (Garcia, Hake et al. 2007). This study by Garcia *et al.* argues against there being a universal histone code, and underscores the need to avoid general conclusions obtained from a single organism. Thus, in summary, the work conducted in our epigenetic study will provide a valuable comparison to the developmental epigenetics of other organisms characterised to date.

8.4 Future work

In addition to the various suggestions made previously, numerous other studies are possible in order to consolidate and extend the work conducted in this thesis. For example, the immunostaining techniques utilised in this study could be used to further dissect the epigenetic patterns occurring during the process of zebrafish development. A closer inspection of the embryo would allow for tissue-specific patterns to be identified, as well as shedding yet more light on the relationship between epigenetic modifications and nuclear architecture. In combination with western blot, the dynamic regulation of other marks and histone variants could be investigated, as well as other important proteins, such as HP1.

Beyond this, embryos treated with chemicals such as Trichostatin A (which inhibits certain HDACs) or 5-azacytidine (which inhibits DNA methylation) could be assessed using the assays developed within this study. Transgenic or N-ethyl-N-nitrosourea (ENU) knock-outs could also be tested to see their epigenetic effects, as could morpholino knock-downs. These studies in particular would help to clarify the links between various epigenetic marks within the zebrafish embryo.

Finally, a closer gene-specific view could be investigated using chromatin immunoprecipitation. This type of study would yield valuable information regarding the genomic localisation of DNA- and chromatin-binding proteins in cells, such as modified histones and specific transcription factors, allowing for the elucidation of their roles during numerous developmental processes.

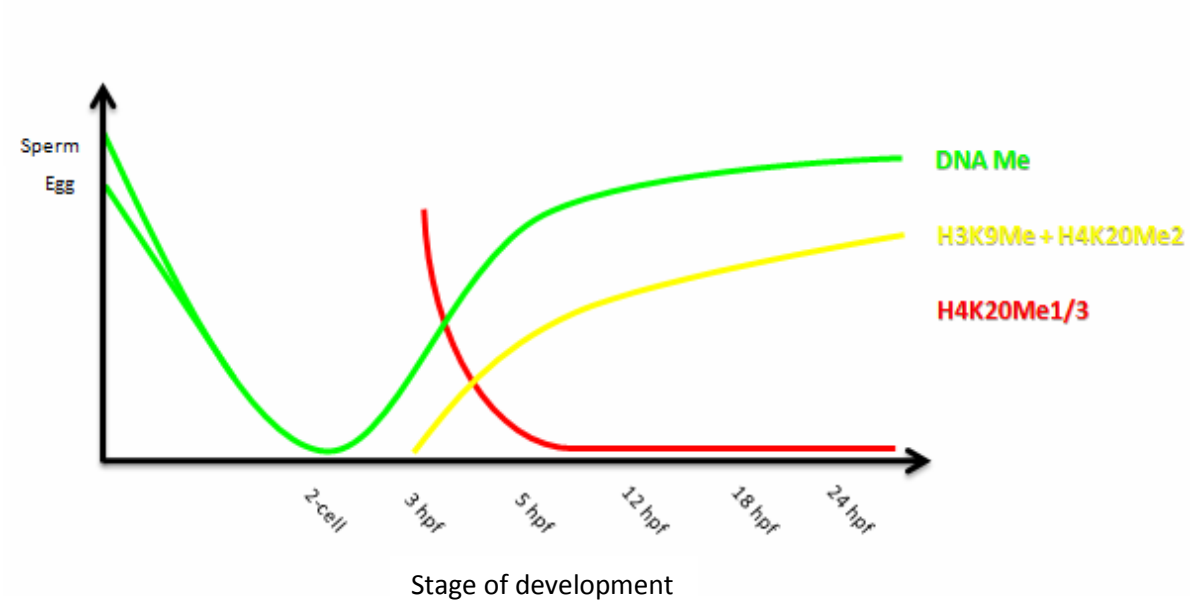

Fig. 8.1: DNA and histone methylation dynamics during normal embryonic development in zebrafish. This generalised schematic graph is based on data from Chapters 3, 4 and 5, as well as Appendix I.

Appendix I

9 Quantative analysis of western blots

Firstly, any results on x-ray film were scanned using a standard flat-bed scanner. Image files were then opened using ImageJ (National Institutes of Health, Maryland, USA) and converted to grayscale. After subtracting the background colouration, the colours on the image were inverted and the intensity of each band measured. This value was then divided by the intensity of the relevant loading control to give the relative intensity of each sample band. Ultimately, the mean of this data was then plotted against the developmental stage for each epigenetic mark, and the error bars calculated using the standard error of the mean. Further information on this process can be found at http://www.lukemiller.org/journal/2007/08/quantifying-western-blots-without.html.

9.1 H3K9me1 (n=3)

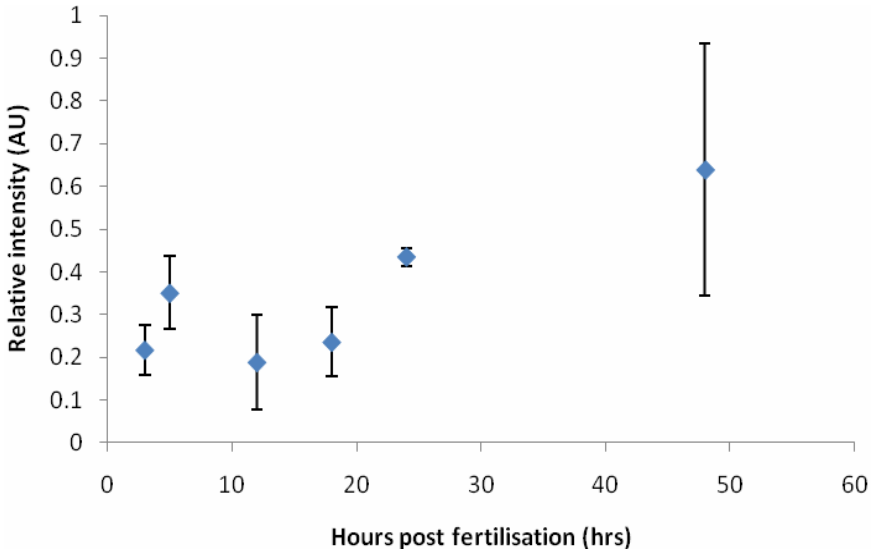

9.2 H3K9me2 (n=3)

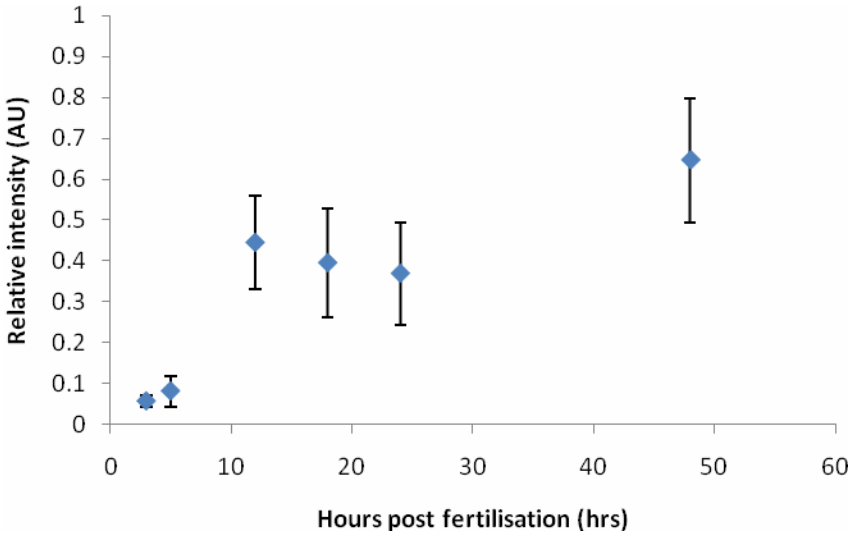

9.3 H3K9me3 (n=3)

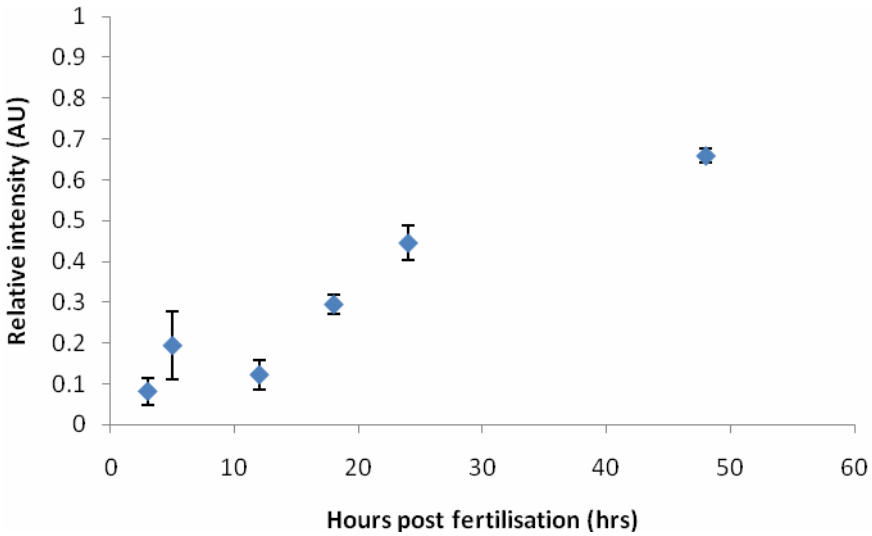

9.4 H4K20me1 (n=4)

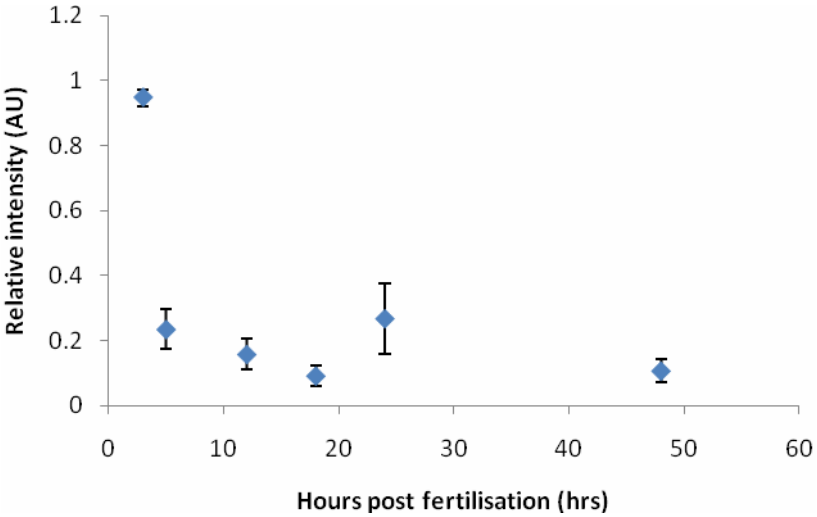

9.5 H4K20me2 (n=5)

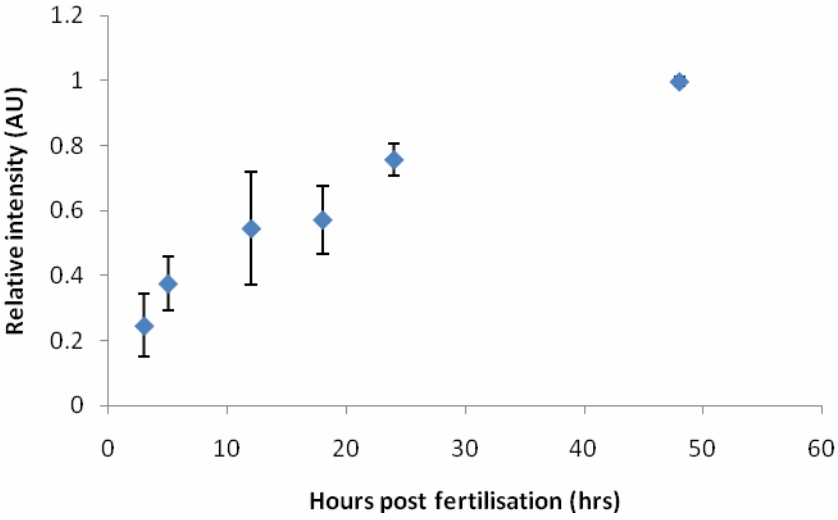

9.6 H4K20me3 (n=3)

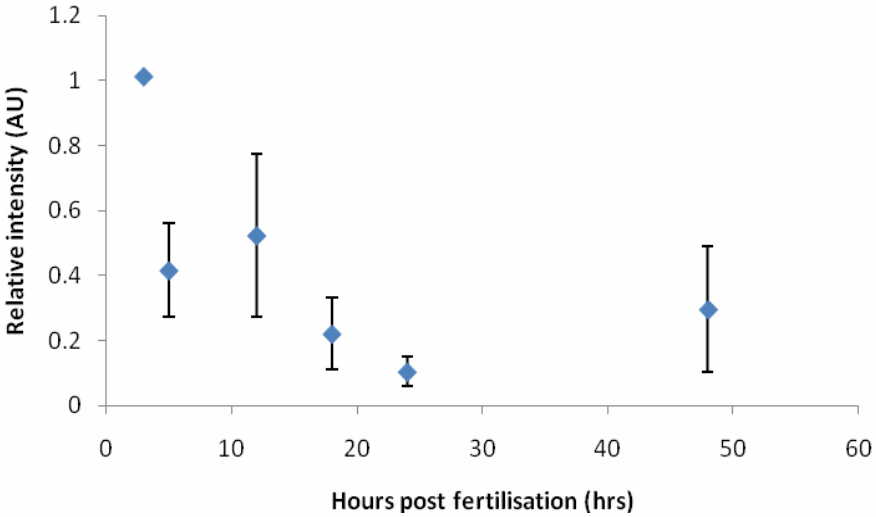

Bibliography

Adamietz, P., and Rudolph, A. (1984). ADP-ribosylation of nuclear proteins in vivo. Identification of histone H2B as a major acceptor for mono- and poly(ADP-ribose) in dimethyl sulfate-treated hepatoma AH 7974 cells. The Journal of biological chemistry 259, 6841-6846.

Adhikary, S., and Eilers, M. (2005). Transcriptional regulation and transformation by Myc proteins. Nat Rev Mol Cell Biol 6, 635-645.

Allfrey, V.G., Faulkner, R., and Mirsky, A.E. (1964). Acetylation and Methylation of Histones and Their Possible Role in the Regulation of Rna Synthesis. Proceedings of the National Academy of Sciences of the United States of America 51, 786-794.

Amano, T., Kato, Y., and Tsunoda, Y. (2001). Full-term development of enucleated mouse oocytes fused with embryonic stem cells from different cell lines. Reproduction (Cambridge, England) 121, 729-733.

Andrews, P.W., Damjanov, I., Simon, D., Banting, G.S., Carlin, C., Dracopoli, N.C., and Fogh, J. (1984). Pluripotent embryonal carcinoma clones derived from the human teratocarcinoma cell line Tera-2. Differentiation in vivo and in vitro. Laboratory investigation; a journal of technical methods and pathology 50, 147-162.

Anest, V., Hanson, J.L., Cogswell, P.C., Steinbrecher, K.A., Strahl, B.D., and Baldwin, A.S. (2003). A nucleosomal function for IkappaB kinase-alpha in NF-kappaB-dependent gene expression. Nature 423, 659-663.

Aoki, A., Suetake, I., Miyagawa, J., Fujio, T., Chijiwa, T., Sasaki, H., and Tajima, S. (2001). Enzymatic properties of de novo-type mouse DNA (cytosine-5) methyltransferases. Nucleic acids research 29, 3506-3512.

Arney, K.L., and Fisher, A.G. (2004). Epigenetic aspects of differentiation. Journal of cell science 117, 4355-4363.

Avilion, A.A., Nicolis, S.K., Pevny, L.H., Perez, L., Vivian, N., and Lovell-Badge, R. (2003). Multipotent cell lineages in early mouse development depend on SOX2 function. Genes & development 17, 126-140.

Azuara, V., Perry, P., Sauer, S., Spivakov, M., Jorgensen, H.F., John, R.M., Gouti, M., Casanova, M., Warnes, G., Merkenschlager, M., et al. (2006). Chromatin signatures of pluripotent cell lines. Nature cell biology 8, 532-538.

Bannister, A.J., Schneider, R., and Kouzarides, T. (2002). Histone methylation: dynamic or static? Cell 109, 801-806.

Barlow, D.P., Stoger, R., Herrmann, B.G., Saito, K., and Schweifer, N. (1991). The mouse insulin-like growth factor type-2 receptor is imprinted and closely linked to the Tme locus. Nature 349, 84-87.

Barr, M.L., and Bertram, E.G. (1949). A morphological distinction between neurones of the male and female, and the behaviour of the nucleolar satellite during accelerated nucleoprotein synthesis. Nature 163, 676.

Barski, A., Cuddapah, S., Cui, K., Roh, T.Y., Schones, D.E., Wang, Z., Wei, G., Chepelev, I., and Zhao, K. (2007). High-resolution profiling of histone methylations in the human genome. Cell 129, 823-837.

Bartolomei, M.S. (2009). Genomic imprinting: employing and avoiding epigenetic processes. Genes & development 23, 2124-2133.

Bartolomei, M.S., and Tilghman, S.M. (1997). Genomic imprinting in mammals. Annual review of genetics 31, 493-525.

Bartolomei, M.S., Zemel, S., and Tilghman, S.M. (1991). Parental imprinting of the mouse H19 gene. Nature 351, 153-155.

Beaujean, N., Hartshorne, G., Cavilla, J., Taylor, J., Gardner, J., Wilmut, I., Meehan, R., and Young, L. (2004). Non-conservation of mammalian preimplantation methylation dynamics. Curr Biol 14, R266-267.

Benetti, R., Gonzalo, S., Jaco, I., Schotta, G., Klatt, P., Jenuwein, T., and Blasco, M.A. (2007). Suv4-20h deficiency results in telomere elongation and derepression of telomere recombination. The Journal of cell biology 178, 925-936.

Ben-Shushan, E., Thompson, J.R., Gudas, L.J., and Bergman, Y. (1998). Rex-1, a gene encoding a transcription factor expressed in the early embryo, is regulated via Oct-3/4 and Oct-6 binding to an octamer site and a novel protein, Rox-1, binding to an adjacent site. Molecular and cellular biology 18, 1866-1878.

Bernstein, B.E., Mikkelsen, T.S., Xie, X., Kamal, M., Huebert, D.J., Cuff, J., Fry, B., Meissner, A., Wernig, M., Plath, K., et al. (2006). A bivalent chromatin structure marks key developmental genes in embryonic stem cells. Cell 125, 315-326.

Bestor, T.H., and Ingram, V.M. (1983). Two DNA methyltransferases from murine erythroleukemia cells: purification, sequence specificity, and mode of interaction with DNA. Proceedings of the National Academy of Sciences of the United States of America 80, 5559-5563.

Bhaumik, S.R., Smith, E., and Shilatifard, A. (2007). Covalent modifications of histones during development and disease pathogenesis. Nature structural & molecular biology 14, 1008-1016.

Bird, A. (2002). DNA methylation patterns and epigenetic memory. Genes & development 16, 6-21.

Bird, A. (2007). Perceptions of epigenetics. Nature 447, 396-398.

Biron, V.L., McManus, K.J., Hu, N., Hendzel, M.J., and Underhill, D.A. (2004). Distinct dynamics and distribution of histone methyl-lysine derivatives in mouse development. Developmental biology 276, 337-351.

Boggs, B.A., Cheung, P., Heard, E., Spector, D.L., Chinault, A.C., and Allis, C.D. (2002). Differentially methylated forms of histone H3 show unique association patterns with inactive human X chromosomes. Nature genetics 30, 73-76.

Boland, M.J., Hazen, J.L., Nazor, K.L., Rodriguez, A.R., Gifford, W., Martin, G., Kupriyanov, S., and Baldwin, K.K. (2009). Adult mice generated from induced pluripotent stem cells. Nature 461, 91-94.

Borsani, G., Tonlorenzi, R., Simmler, M.C., Dandolo, L., Arnaud, D., Capra, V., Grompe, M., Pizzuti, A., Muzny, D., Lawrence, C., et al. (1991). Characterization of a murine gene expressed from the inactive X chromosome. Nature 351, 325-329.

Botquin, V., Hess, H., Fuhrmann, G., Anastassiadis, C., Gross, M.K., Vriend, G., and Scholer, H.R. (1998). New POU dimer configuration mediates antagonistic control of an osteopontin preimplantation enhancer by Oct-4 and Sox-2. Genes & development 12, 2073-2090.

Botuyan, M.V., Lee, J., Ward, I.M., Kim, J.E., Thompson, J.R., Chen, J., and Mer, G. (2006). Structural basis for the methylation state-specific recognition of histone H4-K20 by 53BP1 and Crb2 in DNA repair. Cell 127, 1361-1373.

Boyer, L.A., Lee, T.I., Cole, M.F., Johnstone, S.E., Levine, S.S., Zucker, J.P., Guenther, M.G., Kumar, R.M., Murray, H.L., Jenner, R.G., et al. (2005). Core transcriptional regulatory circuitry in human embryonic stem cells. Cell 122, 947-956.

Boyer, L.A., Plath, K., Zeitlinger, J., Brambrink, T., Medeiros, L.A., Lee, T.I., Levine, S.S., Wernig, M., Tajonar, A., Ray, M.K., et al. (2006). Polycomb complexes repress developmental regulators in murine embryonic stem cells. Nature 441, 349-353.

Bradford, C.S., Sun, L., and Barnes, D.W. (1994). Basic fibroblast growth factor stimulates proliferation and suppresses melanogenesis in cell cultures derived from early zebrafish embryos. Molecular marine biology and biotechnology 3, 78-86.

Briggs, R., and King, T.J. (1952). Transplantation of Living Nuclei From Blastula Cells into Enucleated Frogs' Eggs. Proceedings of the National Academy of Sciences of the United States of America 38, 455-463.

Brinster, R.L. (1974). The effect of cells transferred into the mouse blastocyst on subsequent development. The Journal of experimental medicine 140, 1049-1056.

Brockdorff, N., Ashworth, A., Kay, G.F., Cooper, P., Smith, S., McCabe, V.M., Norris, D.P., Penny, G.D., Patel, D., and Rastan, S. (1991). Conservation of position and exclusive expression of mouse Xist from the inactive X chromosome. Nature 351, 329-331.

Brockdorff, N., Ashworth, A., Kay, G.F., McCabe, V.M., Norris, D.P., Cooper, P.J., Swift, S., and Rastan, S. (1992). The product of the mouse Xist gene is a 15 kb inactive X-specific transcript containing no conserved ORF and located in the nucleus. Cell 71, 515-526.

Brons, I.G., Smithers, L.E., Trotter, M.W., Rugg-Gunn, P., Sun, B., Chuva de Sousa Lopes, S.M., Howlett, S.K., Clarkson, A., Ahrlund-Richter, L., Pedersen, R.A., et al. (2007). Derivation of pluripotent epiblast stem cells from mammalian embryos. Nature 448, 191-195.

Brown, C.J., Ballabio, A., Rupert, J.L., Lafreniere, R.G., Grompe, M., Tonlorenzi, R., and Willard, H.F. (1991). A gene from the region of the human X inactivation centre is expressed exclusively from the inactive X chromosome. Nature 349, 38-44.

Brown, C.J., Hendrich, B.D., Rupert, J.L., Lafreniere, R.G., Xing, Y., Lawrence, J., and Willard, H.F. (1992). The human XIST gene: analysis of a 17 kb inactive X-specific RNA that contains conserved repeats and is highly localized within the nucleus. Cell 71, 527-542.

Buehr, M., Meek, S., Blair, K., Yang, J., Ure, J., Silva, J., McLay, R., Hall, J., Ying, Q.L., and Smith, A. (2008). Capture of authentic embryonic stem cells from rat blastocysts. Cell 135, 1287-1298.

Burgess, S., Reim, G., Chen, W., Hopkins, N., and Brand, M. (2002). The zebrafish spiel-ohne-grenzen (spg) gene encodes the POU domain protein Pou2 related to mammalian Oct4 and is essential for formation of the midbrain and hindbrain, and for pre-gastrula morphogenesis. Development (Cambridge, England) 129, 905-916.

Camp, E.M., Sanchez-Sanchez, A.V., Garcia-Espana, A., Desalle, R., Odqvist, L., O'Connor, J.E., and Mullor, J.L. (2009). Nanog regulates proliferation during early fish development. Stem cells (Dayton, Ohio).

Cao, R., Tsukada, Y., and Zhang, Y. (2005). Role of Bmi-1 and Ring1A in H2A ubiquitylation and Hox gene silencing. Molecular cell 20, 845-854.

Cao, R., Wang, L., Wang, H., Xia, L., Erdjument-Bromage, H., Tempst, P., Jones, R.S., and Zhang, Y. (2002). Role of histone H3 lysine 27 methylation in Polycomb-group silencing. Science (New York, NY 298, 1039-1043.

Carlson, L.L., Page, A.W., and Bestor, T.H. (1992). Properties and localization of DNA methyltransferase in preimplantation mouse embryos: implications for genomic imprinting. Genes & development 6, 2536-2541.

Carmany-Rampey, A., and Moens, C.B. (2006). Modern mosaic analysis in the zebrafish. Methods (San Diego, Calif 39, 228-238.

Catena, R., Tiveron, C., Ronchi, A., Porta, S., Ferri, A., Tatangelo, L., Cavallaro, M., Favaro, R., Ottolenghi, S., Reinbold, R., et al. (2004). Conserved POU binding DNA sites in the Sox2 upstream enhancer regulate gene expression in embryonic and neural stem cells. The Journal of biological chemistry 279, 41846-41857.

Chadwick, B.P., and Willard, H.F. (2003). Chromatin of the Barr body: histone and non-histone proteins associated with or excluded from the inactive X chromosome. Human molecular genetics 12, 2167-2178.

Chadwick, B.P., and Willard, H.F. (2004). Multiple spatially distinct types of facultative heterochromatin on the human inactive X chromosome. Proceedings of the National Academy of Sciences of the United States of America 101, 17450-17455.

Chaillet, J.R., Vogt, T.F., Beier, D.R., and Leder, P. (1991). Parental-specific methylation of an imprinted transgene is established during gametogenesis and progressively changes during embryogenesis. Cell 66, 77-83.

Chamberlain, S.J., Yee, D., and Magnuson, T. (2008). Polycomb repressive complex 2 is dispensable for maintenance of embryonic stem cell pluripotency. Stem cells (Dayton, Ohio) 26, 1496-1505.

Chambers, I., Colby, D., Robertson, M., Nichols, J., Lee, S., Tweedie, S., and Smith, A. (2003). Functional expression cloning of Nanog, a pluripotency sustaining factor in embryonic stem cells. Cell 113, 643-655.

Chambers, I., Silva, J., Colby, D., Nichols, J., Nijmeijer, B., Robertson, M., Vrana, J., Jones, K., Grotewold, L., and Smith, A. (2007). Nanog safeguards pluripotency and mediates germline development. Nature 450, 1230-1234.

Chaumeil, J., Okamoto, I., Guggiari, M., and Heard, E. (2002). Integrated kinetics of X chromosome inactivation in differentiating embryonic stem cells. Cytogenetic and genome research 99, 75-84.

Chen, T., Ueda, Y., Dodge, J.E., Wang, Z., and Li, E. (2003). Establishment and maintenance of genomic methylation patterns in mouse embryonic stem cells by Dnmt3a and Dnmt3b. Molecular and cellular biology 23, 5594-5605.

Cheung, P., Allis, C.D., and Sassone-Corsi, P. (2000). Signaling to chromatin through histone modifications. Cell 103, 263-271.

Chew, J.L., Loh, Y.H., Zhang, W., Chen, X., Tam, W.L., Yeap, L.S., Li, P., Ang, Y.S., Lim, B., Robson, P., et al. (2005). Reciprocal transcriptional regulation of Pou5f1 and Sox2 via the Oct4/Sox2 complex in embryonic stem cells. Molecular and cellular biology 25, 6031-6046.

Cibelli, J. (2007). Developmental biology. A decade of cloning mystique. Science (New York, NY 316, 990-992.

Collas, P. (1998). Modulation of plasmid DNA methylation and expression in zebrafish embryos. Nucleic acids research 26, 4454-4461.

Collins, R.E., Tachibana, M., Tamaru, H., Smith, K.M., Jia, D., Zhang, X., Selker, E.U., Shinkai, Y., and Cheng, X. (2005). In vitro and in vivo analyses of a Phe/Tyr switch controlling product specificity of histone lysine methyltransferases. The Journal of biological chemistry 280, 5563-5570.

Comb, M., and Goodman, H.M. (1990). CpG methylation inhibits proenkephalin gene expression and binding of the transcription factor AP-2. Nucleic acids research 18, 3975-3982.

Corley-Smith, G.E., Lim, C.J., and Brandhorst, B.P. (1996). Production of androgenetic zebrafish (Danio rerio). Genetics 142, 1265-1276.

Costanzi, C., and Pehrson, J.R. (1998). Histone macroH2A1 is concentrated in the inactive X chromosome of female mammals. Nature 393, 599-601.

Costanzi, C., and Pehrson, J.R. (2001). MACROH2A2, a new member of the MARCOH2A core histone family. The Journal of biological chemistry 276, 21776-21784.

Couture, J.F., Collazo, E., Brunzelle, J.S., and Trievel, R.C. (2005). Structural and functional analysis of SET8, a histone H4 Lys-20 methyltransferase. Genes & development 19, 1455-1465.

Cowan, C.A., Atienza, J., Melton, D.A., and Eggan, K. (2005). Nuclear reprogramming of somatic cells after fusion with human embryonic stem cells. Science (New York, NY 309, 1369-1373.

Csankovszki, G., Nagy, A., and Jaenisch, R. (2001). Synergism of Xist RNA, DNA methylation, and histone hypoacetylation in maintaining X chromosome inactivation. The Journal of cell biology 153, 773-784.

Cuthbert, G.L., Daujat, S., Snowden, A.W., Erdjument-Bromage, H., Hagiwara, T., Yamada, M., Schneider, R., Gregory, P.D., Tempst, P., Bannister, A.J., et al. (2004). Histone deimination antagonizes arginine methylation. Cell 118, 545-553.

D'Alessio, A.C., and Szyf, M. (2006). Epigenetic tete-a-tete: the bilateral relationship between chromatin modifications and DNA methylation. Biochemistry and cell biology = Biochimie et biologie cellulaire 84, 463-476.

D'Amours, D., Desnoyers, S., D'Silva, I., and Poirier, G.G. (1999). Poly(ADP-ribosyl)ation reactions in the regulation of nuclear functions. The Biochemical journal 342 (Pt 2), 249-268.

Darr, H., Mayshar, Y., and Benvenisty, N. (2006). Overexpression of NANOG in human ES cells enables feeder-free growth while inducing primitive ectoderm features. Development (Cambridge, England) 133, 1193-1201.

Darrow, K.O., and Harris, W.A. (2004). Characterization and development of courtship in zebrafish, Danio rerio. Zebrafish 1, 40-45.

Daujat, S., Weiss, T., Mohn, F., Lange, U.C., Ziegler-Birling, C., Zeissler, U., Lappe, M., Schubeler, D., Torres-Padilla, M.E., and Schneider, R. (2009). H3K64 trimethylation marks heterochromatin and is dynamically remodeled during developmental reprogramming. Nature structural & molecular biology 16, 777-781.

Davis, R.L., Weintraub, H., and Lassar, A.B. (1987). Expression of a single transfected cDNA converts fibroblasts to myoblasts. Cell 51, 987-1000.

Davis, S., Aldrich, T.H., Stahl, N., Pan, L., Taga, T., Kishimoto, T., Ip, N.Y., and Yancopoulos, G.D. (1993). LIFR beta and gp130 as heterodimerizing signal transducers of the tripartite CNTF receptor. Science (New York, NY 260, 1805-1808.

Dean, W., Santos, F., Stojkovic, M., Zakhartchenko, V., Walter, J., Wolf, E., and Reik, W. (2001). Conservation of methylation reprogramming in mammalian development: aberrant reprogramming in cloned embryos. Proceedings of the National Academy of Sciences of the United States of America 98, 13734-13738.

DeChiara, T.M., Robertson, E.J., and Efstratiadis, A. (1991). Parental imprinting of the mouse insulin-like growth factor II gene. Cell 64, 849-859.

Denslow, S.A., and Wade, P.A. (2007). The human Mi-2/NuRD complex and gene regulation. Oncogene 26, 5433-5438.

Dixon, J.E., Redwood, C., O'Reilly, M.-A., Chatfield, J., Loose, M., Alberio, R., and Johnson, A.D. (2009). Nanog is a master regulator of axolotl development. Mechanisms of development 126, S277-S277.

Dodge, J.E., Kang, Y.K., Beppu, H., Lei, H., and Li, E. (2004). Histone H3-K9 methyltransferase ESET is essential for early development. Molecular and cellular biology 24, 2478-2486.

Doevendans, P.A., Kubalak, S.W., An, R.H., Becker, D.K., Chien, K.R., and Kass, R.S. (2000). Differentiation of cardiomyocytes in floating embryoid bodies is comparable to fetal cardiomyocytes. Journal of molecular and cellular cardiology 32, 839-851.

Dorigo, B., Schalch, T., Bystricky, K., and Richmond, T.J. (2003). Chromatin fiber folding: requirement for the histone H4 N-terminal tail. Journal of molecular biology 327, 85-96.

Du, L.L., Nakamura, T.M., and Russell, P. (2006). Histone modification-dependent and -independent pathways for recruitment of checkpoint protein Crb2 to double-strand breaks. Genes & development 20, 1583-1596.

Dunican, D.S., Ruzov, A., Hackett, J.A., and Meehan, R.R. (2008). xDnmt1 regulates transcriptional silencing in pre-MBT Xenopus embryos independently of its catalytic function. Development (Cambridge, England) 135, 1295-1302.

Eden, S., Hashimshony, T., Keshet, I., Cedar, H., and Thorne, A.W. (1998). DNA methylation models histone acetylation. Nature 394, 842.

Efroni, S., Duttagupta, R., Cheng, J., Dehghani, H., Hoeppner, D.J., Dash, C., Bazett-Jones, D.P., Le Grice, S., McKay, R.D., Buetow, K.H., et al. (2008). Global transcription in pluripotent embryonic stem cells. Cell stem cell 2, 437-447.

Ekker, M., Wegner, J., Akimenko, M.A., and Westerfield, M. (1992). Coordinate embryonic expression of three zebrafish engrailed genes. Development (Cambridge, England) 116, 1001-1010.

Emre, N.C., Ingvarsdottir, K., Wyce, A., Wood, A., Krogan, N.J., Henry, K.W., Li, K., Marmorstein, R., Greenblatt, J.F., Shilatifard, A., et al. (2005). Maintenance of low histone ubiquitylation by Ubp10 correlates with telomere-proximal Sir2 association and gene silencing. Molecular cell 17, 585-594.

Epsztejn-Litman, S., Feldman, N., Abu-Remaileh, M., Shufaro, Y., Gerson, A., Ueda, J., Deplus, R., Fuks, F., Shinkai, Y., Cedar, H., et al. (2008). De novo DNA methylation promoted by G9a prevents reprogramming of embryonically silenced genes. Nature structural & molecular biology 15, 1176-1183.

Esteve, P.O., Chin, H.G., Smallwood, A., Feehery, G.R., Gangisetty, O., Karpf, A.R., Carey, M.F., and Pradhan, S. (2006). Direct interaction between DNMT1 and G9a coordinates DNA and histone methylation during replication. Genes & development 20, 3089-3103.

Evans, M.J., and Kaufman, M.H. (1981). Establishment in culture of pluripotential cells from mouse embryos. Nature 292, 154-156.

Fan, L., and Collodi, P. (2006). Zebrafish embryonic stem cells. Methods in enzymology 418, 64-77.

Fan, L., Crodian, J., Liu, X., Alestrom, A., Alestrom, P., and Collodi, P. (2004). Zebrafish embryo cells remain pluripotent and germ-line competent for multiple passages in culture. Zebrafish 1, 21-26.

Fang, J., Feng, Q., Ketel, C.S., Wang, H., Cao, R., Xia, L., Erdjument-Bromage, H., Tempst, P., Simon, J.A., and Zhang, Y. (2002). Purification and functional characterization of SET8, a nucleosomal histone H4-lysine 20-specific methyltransferase. Curr Biol 12, 1086-1099.

Farthing, C.R., Ficz, G., Ng, R.K., Chan, C.F., Andrews, S., Dean, W., Hemberger, M., and Reik, W. (2008). Global mapping of DNA methylation in mouse promoters reveals epigenetic reprogramming of pluripotency genes. PLoS genetics 4, e1000116.

Feng, Q., Wang, H., Ng, H.H., Erdjument-Bromage, H., Tempst, P., Struhl, K., and Zhang, Y. (2002). Methylation of H3-lysine 79 is mediated by a new family of HMTases without a SET domain. Curr Biol 12, 1052-1058.

Ferguson-Smith, A.C., and Surani, M.A. (2001). Imprinting and the epigenetic asymmetry between parental genomes. Science (New York, NY 293, 1086-1089.

Fernandez, P.C., Frank, S.R., Wang, L., Schroeder, M., Liu, S., Greene, J., Cocito, A., and Amati, B. (2003). Genomic targets of the human c-Myc protein. Genes & development 17, 1115-1129.

Finlan, L.E., Sproul, D., Thomson, I., Boyle, S., Kerr, E., Perry, P., Ylstra, B., Chubb, J.R., and Bickmore, W.A. (2008). Recruitment to the nuclear periphery can alter expression of genes in human cells. PLoS genetics 4, e1000039.

Fischle, W., Tseng, B.S., Dormann, H.L., Ueberheide, B.M., Garcia, B.A., Shabanowitz, J., Hunt, D.F., Funabiki, H., and Allis, C.D. (2005). Regulation of HP1-chromatin binding by histone H3 methylation and phosphorylation. Nature 438, 1116-1122.

Fischle, W., Wang, Y., and Allis, C.D. (2003). Histone and chromatin cross-talk. Current opinion in cell biology 15, 172-183.

Fouse, S.D., Shen, Y., Pellegrini, M., Cole, S., Meissner, A., Van Neste, L., Jaenisch, R., and Fan, G. (2008). Promoter CpG methylation contributes to ES cell gene regulation in parallel with Oct4/Nanog, PcG complex, and histone H3 K4/K27 trimethylation. Cell stem cell 2, 160-169.

Fraga, M.F., Ballestar, E., Villar-Garea, A., Boix-Chornet, M., Espada, J., Schotta, G., Bonaldi, T., Haydon, C., Ropero, S., Petrie, K., et al. (2005). Loss of acetylation at Lys16 and trimethylation at Lys20 of histone H4 is a common hallmark of human cancer. Nature genetics 37, 391-400.

Francastel, C., Schubeler, D., Martin, D.I., and Groudine, M. (2000). Nuclear compartmentalization and gene activity. Nat Rev Mol Cell Biol 1, 137-143.

Freitag, M., Hickey, P.C., Khlafallah, T.K., Read, N.D., and Selker, E.U. (2004). HP1 is essential for DNA methylation in neurospora. Molecular cell 13, 427-434.

Fuks, F. (2005). DNA methylation and histone modifications: teaming up to silence genes. Current opinion in genetics & development 15, 490-495.

Fuks, F., Hurd, P.J., Wolf, D., Nan, X., Bird, A.P., and Kouzarides, T. (2003). The methyl-CpG-binding protein MeCP2 links DNA methylation to histone methylation. The Journal of biological chemistry 278, 4035-4040.

Garcia, B.A., Hake, S.B., Diaz, R.L., Kauer, M., Morris, S.A., Recht, J., Shabanowitz, J., Mishra, N., Strahl, B.D., Allis, C.D., et al. (2007). Organismal differences in post-translational modifications in histones H3 and H4. The Journal of biological chemistry 282, 7641-7655.

Gardner, D.K., Lane, M., and Watson, A.J. (2004). A laboratory guide to the mammalian embryo (Oxford, Oxford University Press).

Gardner, R.G., Nelson, Z.W., and Gottschling, D.E. (2005). Ubp10/Dot4p regulates the persistence of ubiquitinated histone H2B: distinct roles in telomeric silencing and general chromatin. Molecular and cellular biology 25, 6123-6139.

Gardner, R.L., and Beddington, R.S. (1988). Multi-lineage 'stem' cells in the mammalian embryo. J Cell Sci Suppl 10, 11-27.

Gardner, R.L., and Lyon, M.F. (1971). X chromosome inactivation studied by injection of a single cell into the mouse blastocyst. Nature 231, 385-386.

Gaspar-Maia, A., Alajem, A., Polesso, F., Sridharan, R., Mason, M.J., Heidersbach, A., Ramalho-Santos, J., McManus, M.T., Plath, K., Meshorer, E., et al. (2009). Chd1 regulates open chromatin and pluripotency of embryonic stem cells. Nature 460, 863-868.

Gearing, D.P., Thut, C.J., VandeBos, T., Gimpel, S.D., Delaney, P.B., King, J., Price, V., Cosman, D., and Beckmann, M.P. (1991). Leukemia inhibitory factor receptor is structurally related to the IL-6 signal transducer, gp130. The EMBO journal 10, 2839-2848.

Geiss-Friedlander, R., and Melchior, F. (2007). Concepts in sumoylation: a decade on. Nat Rev Mol Cell Biol 8, 947-956.

Goll, M.G., and Bestor, T.H. (2005). Eukaryotic cytosine methyltransferases. Annual review of biochemistry 74, 481-514.

Goll, M.G., Kirpekar, F., Maggert, K.A., Yoder, J.A., Hsieh, C.L., Zhang, X., Golic, K.G., Jacobsen, S.E., and Bestor, T.H. (2006). Methylation of tRNAAsp by the DNA methyltransferase homolog Dnmt2. Science (New York, NY 311, 395-398.

Goncalves Dos Santos Silva, A., Sarkar, R., Harizanova, J., Guffei, A., Mowat, M., Garini, Y., and Mai, S. (2008). Centromeres in cell division, evolution, nuclear organization and disease. Journal of cellular biochemistry 104, 2040-2058.

Gonzalo, S., Jaco, I., Fraga, M.F., Chen, T., Li, E., Esteller, M., and Blasco, M.A. (2006). DNA methyltransferases control telomere length and telomere recombination in mammalian cells. Nature cell biology 8, 416-424.

Gopalakrishnan, S., Sullivan, B.A., Trazzi, S., Della Valle, G., and Robertson, K.D. (2009). DNMT3B interacts with constitutive centromere protein CENP-C to modulate DNA methylation and the histone code at centromeric regions. Human molecular genetics.

Greeson, N.T., Sengupta, R., Arida, A.R., Jenuwein, T., and Sanders, S.L. (2008). Di-methyl H4 lysine 20 targets the checkpoint protein Crb2 to sites of DNA damage. The Journal of biological chemistry 283, 33168-33174.

Grewal, S.I., and Jia, S. (2007). Heterochromatin revisited. Nature reviews 8, 35-46.

Grewal, S.I., and Moazed, D. (2003). Heterochromatin and epigenetic control of gene expression. Science (New York, NY 301, 798-802.

Gruenbaum, Y., Cedar, H., and Razin, A. (1982). Substrate and sequence specificity of a eukaryotic DNA methylase. Nature 295, 620-622.

Grunwald, D.J., and Eisen, J.S. (2002). Headwaters of the zebrafish -- emergence of a new model vertebrate. Nature reviews 3, 717-724.

Guo, G., Yang, J., Nichols, J., Hall, J.S., Eyres, I., Mansfield, W., and Smith, A. (2009). Klf4 reverts developmentally programmed restriction of ground state pluripotency. Development (Cambridge, England) 136, 1063-1069.

Gurdon, J.B. (1962). The developmental capacity of nuclei taken from intestinal epithelium cells of feeding tadpoles. Journal of embryology and experimental morphology 10, 622-640.

Gurdon, J.B., and Byrne, J.A. (2004). The first half-century of nuclear transplantation. Bioscience reports 24, 545-557.

Hart, A.H., Hartley, L., Ibrahim, M., and Robb, L. (2004). Identification, cloning and expression analysis of the pluripotency promoting Nanog genes in mouse and human. Dev Dyn 230, 187-198.

Hay, D.C., Sutherland, L., Clark, J., and Burdon, T. (2004). Oct-4 knockdown induces similar patterns of endoderm and trophoblast differentiation markers in human and mouse embryonic stem cells. Stem cells (Dayton, Ohio) 22, 225-235.

Hayashi, T., Seki, M., Maeda, D., Wang, W., Kawabe, Y., Seki, T., Saitoh, H., Fukagawa, T., Yagi, H., and Enomoto, T. (2002). Ubc9 is essential for viability of higher eukaryotic cells. Experimental cell research 280, 212-221.

Hazzouri, M., Rousseaux, S., Mongelard, F., Usson, Y., Pelletier, R., Faure, A.K., Vourc'h, C., and Sele, B. (2000). Genome organization in the human sperm nucleus studied by FISH and confocal microscopy. Molecular reproduction and development 55, 307-315.

Heard, E., Rougeulle, C., Arnaud, D., Avner, P., Allis, C.D., and Spector, D.L. (2001). Methylation of histone H3 at Lys-9 is an early mark on the X chromosome during X inactivation. Cell 107, 727-738.

Henikoff, S. (2000). Heterochromatin function in complex genomes. Biochimica et biophysica acta 1470, O1-8.

Hill, J.R., Burghardt, R.C., Jones, K., Long, C.R., Looney, C.R., Shin, T., Spencer, T.E., Thompson, J.A., Winger, Q.A., and Westhusin, M.E. (2000). Evidence for placental abnormality as the major cause of mortality in first-trimester somatic cell cloned bovine fetuses. Biology of reproduction 63, 1787-1794.

Hochedlinger, K., and Plath, K. (2009). Epigenetic reprogramming and induced pluripotency. Development (Cambridge, England) 136, 509-523.

Hodges, C.A., and Stice, S.L. (2003). Generation of bovine transgenics using somatic cell nuclear transfer. Reprod Biol Endocrinol 1, 81.

Honda, S., and Selker, E.U. (2008). Direct interaction between DNA methyltransferase DIM-2 and HP1 is required for DNA methylation in Neurospora crassa. Molecular and cellular biology 28, 6044-6055.

Hou, J., Liu, L., Zhang, J., Cui, X.H., Yan, F.X., Guan, H., Chen, Y.F., and An, X.R. (2008). Epigenetic modification of histone 3 at lysine 9 in sheep zygotes and its relationship with DNA methylation. BMC developmental biology 8, 60.

Houston, S.I., McManus, K.J., Adams, M.M., Sims, J.K., Carpenter, P.B., Hendzel, M.J., and Rice, J.C. (2008). Catalytic function of the PR-Set7 histone H4 lysine 20 monomethyltransferase is essential for mitotic entry and genomic stability. The Journal of biological chemistry 283, 19478-19488.

Howlett, S.K., and Reik, W. (1991). Methylation levels of maternal and paternal genomes during preimplantation development. Development (Cambridge, England) 113, 119-127.

Hsieh, C.L. (1999). In vivo activity of murine de novo methyltransferases, Dnmt3a and Dnmt3b. Molecular and cellular biology 19, 8211-8218.

Huang, H., Ju, B., Lee, K.Y., and Lin, S. (2003). Protocol for nuclear transfer in zebrafish. Cloning and stem cells 5, 333-337.

Humphrey, R.K., Beattie, G.M., Lopez, A.D., Bucay, N., King, C.C., Firpo, M.T., Rose-John, S., and Hayek, A. (2004). Maintenance of pluripotency in human embryonic stem cells is STAT3 independent. Stem cells (Dayton, Ohio) 22, 522-530.

Imschenetzky, M., Morin, V., Carvajal, N., Montecino, M., and Puchi, M. (1996). Decreased heterogeneity of CS histone variants after hydrolysis of the ADP-ribose moiety. Journal of cellular biochemistry 61, 109-117.

Jackson, J.P., Lindroth, A.M., Cao, X., and Jacobsen, S.E. (2002). Control of CpNpG DNA methylation by the KRYPTONITE histone H3 methyltransferase. Nature 416, 556-560.

Jackson, M., Krassowska, A., Gilbert, N., Chevassut, T., Forrester, L., Ansell, J., and Ramsahoye, B. (2004). Severe global DNA hypomethylation blocks differentiation and induces histone hyperacetylation in embryonic stem cells. Molecular and cellular biology 24, 8862-8871.

Jahner, D., Stuhlmann, H., Stewart, C.L., Harbers, K., Lohler, J., Simon, I., and Jaenisch, R. (1982). De novo methylation and expression of retroviral genomes during mouse embryogenesis. Nature 298, 623-628.

James, D., Levine, A.J., Besser, D., and Hemmati-Brivanlou, A. (2005). TGFbeta/activin/nodal signaling is necessary for the maintenance of pluripotency in human embryonic stem cells. Development (Cambridge, England) 132, 1273-1282.

Jeong, Y.S., Yeo, S., Park, J.S., Koo, D.B., Chang, W.K., Lee, K.K., and Kang, Y.K. (2007). DNA methylation state is preserved in the sperm-derived pronucleus of the pig zygote. The International journal of developmental biology 51, 707-714.

Jeong, Y.S., Yeo, S., Park, J.S., Lee, K.K., and Kang, Y.K. (2007). Gradual development of a genome-wide H3-K9 trimethylation pattern in paternally derived pig pronucleus. Dev Dyn 236, 1509-1516.

Johnson, B.V., Shindo, N., Rathjen, P.D., Rathjen, J., and Keough, R.A. (2008). Understanding pluripotency--how embryonic stem cells keep their options open. Molecular human reproduction 14, 513-520.

Jones, P.L., Veenstra, G.J., Wade, P.A., Vermaak, D., Kass, S.U., Landsberger, N., Strouboulis, J., and Wolffe, A.P. (1998). Methylated DNA and MeCP2 recruit histone deacetylase to repress transcription. Nature genetics 19, 187-191.

Ju, B.G., Lunyak, V.V., Perissi, V., Garcia-Bassets, I., Rose, D.W., Glass, C.K., and Rosenfeld, M.G. (2006). A topoisomerase IIbeta-mediated dsDNA break required for regulated transcription. Science (New York, NY 312, 1798-1802.

Kaji, K., Norrby, K., Paca, A., Mileikovsky, M., Mohseni, P., and Woltjen, K. (2009). Virus-free induction of pluripotency and subsequent excision of reprogramming factors. Nature 458, 771-775.

Kalakonda, N., Fischle, W., Boccuni, P., Gurvich, N., Hoya-Arias, R., Zhao, X., Miyata, Y., Macgrogan, D., Zhang, J., Sims, J.K., et al. (2008). Histone H4 lysine 20 monomethylation promotes transcriptional repression by L3MBTL1. Oncogene 27, 4293-4304.

Kane, D.A., and Kimmel, C.B. (1993). The zebrafish midblastula transition. Development (Cambridge, England) 119, 447-456.

Kang, L., Wang, J., Zhang, Y., Kou, Z., and Gao, S. (2009). iPS cells can support full-term development of tetraploid blastocyst-complemented embryos. Cell stem cell 5, 135-138.

Kao, C.F., Hillyer, C., Tsukuda, T., Henry, K., Berger, S., and Osley, M.A. (2004). Rad6 plays a role in transcriptional activation through ubiquitylation of histone H2B. Genes & development 18, 184-195.

Karachentsev, D., Druzhinina, M., and Steward, R. (2007). Free and chromatin-associated mono-, di-, and trimethylation of histone H4-lysine 20 during development and cell cycle progression. Developmental biology 304, 46-52.

Karachentsev, D., Sarma, K., Reinberg, D., and Steward, R. (2005). PR-Set7-dependent methylation of histone H4 Lys 20 functions in repression of gene expression and is essential for mitosis. Genes & development 19, 431-435.

Katoh, M., Curk, T., Xu, Q., Zupan, B., Kuspa, A., and Shaulsky, G. (2006). Developmentally regulated DNA methylation in Dictyostelium discoideum. Eukaryotic cell 5, 18-25.

Kazazian, H.H., Jr. (2004). Mobile elements: drivers of genome evolution. Science (New York, NY 303, 1626-1632.

Kim, G.D., Ni, J., Kelesoglu, N., Roberts, R.J., and Pradhan, S. (2002). Co-operation and communication between the human maintenance and de novo DNA (cytosine-5) methyltransferases. The EMBO journal 21, 4183-4195.

Kim, J., Daniel, J., Espejo, A., Lake, A., Krishna, M., Xia, L., Zhang, Y., and Bedford, M.T. (2006). Tudor, MBT and chromo domains gauge the degree of lysine methylation. EMBO reports 7, 397-403.

Kim, S.H., McQueen, P.G., Lichtman, M.K., Shevach, E.M., Parada, L.A., and Misteli, T. (2004). Spatial genome organization during T-cell differentiation. Cytogenetic and genome research 105, 292-301.

Kimmel, C.B., Ballard, W.W., Kimmel, S.R., Ullmann, B., and Schilling, T.F. (1995). Stages of embryonic development of the zebrafish. Dev Dyn 203, 253-310.

Kimmel, C.B., and Warga, R.M. (1988). Cell lineage and developmental potential of cells in the zebrafish embryo. Trends Genet 4, 68-74.

Kimmel, C.B., Warga, R.M., and Schilling, T.F. (1990). Origin and organization of the zebrafish fate map. Development (Cambridge, England) 108, 581-594.

Kimura, H., Hayashi-Takanaka, Y., Goto, Y., Takizawa, N., and Nozaki, N. (2008). The organization of histone H3 modifications as revealed by a panel of specific monoclonal antibodies. Cell structure and function 33, 61-73.

Kleinsmith, L.J., and Pierce, G.B., Jr. (1964). Multipotentiality of Single Embryonal Carcinoma Cells. Cancer research 24, 1544-1551.

Klose, R.J., Yamane, K., Bae, Y., Zhang, D., Erdjument-Bromage, H., Tempst, P., Wong, J., and Zhang, Y. (2006). The transcriptional repressor JHDM3A demethylates trimethyl histone H3 lysine 9 and lysine 36. Nature 442, 312-316.

Klose, R.J., and Zhang, Y. (2007). Regulation of histone methylation by demethylimination and demethylation. Nat Rev Mol Cell Biol 8, 307-318.

Kosak, S.T., and Groudine, M. (2004). Gene order and dynamic domains. Science (New York, NY 306, 644-647.

Kourmouli, N., Jeppesen, P., Mahadevhaiah, S., Burgoyne, P., Wu, R., Gilbert, D.M., Bongiorni, S., Prantera, G., Fanti, L., Pimpinelli, S., et al. (2004). Heterochromatin and tri-methylated lysine 20 of histone H4 in animals. Journal of cell science 117, 2491-2501.

Kouzarides, T. (2007). Chromatin modifications and their function. Cell 128, 693-705.

Kouzminova, E., and Selker, E.U. (2001). dim-2 encodes a DNA methyltransferase responsible for all known cytosine methylation in Neurospora. The EMBO journal 20, 4309-4323.

Kumar, S., Cheng, X., Klimasauskas, S., Mi, S., Posfai, J., Roberts, R.J., and Wilson, G.G. (1994). The DNA (cytosine-5) methyltransferases. Nucleic acids research 22, 1-10.

Kunath, T., Saba-El-Leil, M.K., Almousailleakh, M., Wray, J., Meloche, S., and Smith, A. (2007). FGF stimulation of the Erk1/2 signalling cascade triggers transition of pluripotent embryonic stem cells from self-renewal to lineage commitment. Development (Cambridge, England) 134, 2895-2902.

Kunert, N., Marhold, J., Stanke, J., Stach, D., and Lyko, F. (2003). A Dnmt2-like protein mediates DNA methylation in Drosophila. Development (Cambridge, England) 130, 5083-5090.

Kurita, K., Burgess, S.M., and Sakai, N. (2004). Transgenic zebrafish produced by retroviral infection of in vitro-cultured sperm. Proceedings of the National Academy of Sciences of the United States of America 101, 1263-1267.

Lachner, M., O'Sullivan, R.J., and Jenuwein, T. (2003). An epigenetic road map for histone lysine methylation. Journal of cell science 116, 2117-2124.

Lander, E.S., Linton, L.M., Birren, B., Nusbaum, C., Zody, M.C., Baldwin, J., Devon, K., Dewar, K., Doyle, M., FitzHugh, W., et al. (2001). Initial sequencing and analysis of the human genome. Nature 409, 860-921.

Lane, N., Dean, W., Erhardt, S., Hajkova, P., Surani, A., Walter, J., and Reik, W. (2003). Resistance of IAPs to methylation reprogramming may provide a mechanism for epigenetic inheritance in the mouse. Genesis 35, 88-93.

Lavial, F., Acloque, H., Bertocchini, F., Macleod, D.J., Boast, S., Bachelard, E., Montillet, G., Thenot, S., Sang, H.M., Stern, C.D., et al. (2007). The Oct4 homologue PouV and Nanog regulate pluripotency in chicken embryonic stem cells. Development (Cambridge, England) 134, 3549-3563.

Lee, D.Y., Teyssier, C., Strahl, B.D., and Stallcup, M.R. (2005). Role of protein methylation in regulation of transcription. Endocrine reviews 26, 147-170.

Lee, K.Y., Huang, H., Ju, B., Yang, Z., and Lin, S. (2002). Cloned zebrafish by nuclear transfer from long-term-cultured cells. Nature biotechnology 20, 795-799.

Lee, T.I., Jenner, R.G., Boyer, L.A., Guenther, M.G., Levine, S.S., Kumar, R.M., Chevalier, B., Johnstone, S.E., Cole, M.F., Isono, K., et al. (2006). Control of developmental regulators by Polycomb in human embryonic stem cells. Cell 125, 301-313.

Lehnertz, B., Ueda, Y., Derijck, A.A., Braunschweig, U., Perez-Burgos, L., Kubicek, S., Chen, T., Li, E., Jenuwein, T., and Peters, A.H. (2003). Suv39h-mediated histone H3 lysine 9 methylation directs DNA methylation to major satellite repeats at pericentric heterochromatin. Curr Biol 13, 1192-1200.

Lei, H., Oh, S.P., Okano, M., Juttermann, R., Goss, K.A., Jaenisch, R., and Li, E. (1996). De novo DNA cytosine methyltransferase activities in mouse embryonic stem cells. Development (Cambridge, England) 122, 3195-3205.

Leonhardt, H., Page, A.W., Weier, H.U., and Bestor, T.H. (1992). A targeting sequence directs DNA methyltransferase to sites of DNA replication in mammalian nuclei. Cell 71, 865-873.

Lepikhov, K., and Walter, J. (2004). Differential dynamics of histone H3 methylation at positions K4 and K9 in the mouse zygote. BMC developmental biology 4, 12.

Lepikhov, K., Zakhartchenko, V., Hao, R., Yang, F., Wrenzycki, C., Niemann, H., Wolf, E., and Walter, J. (2008). Evidence for conserved DNA and histone H3 methylation reprogramming in mouse, bovine and rabbit zygotes. Epigenetics & chromatin 1, 8.

Levenstein, M.E., Ludwig, T.E., Xu, R.H., Llanas, R.A., VanDenHeuvel-Kramer, K., Manning, D., and Thomson, J.A. (2006). Basic fibroblast growth factor support of human embryonic stem cell self-renewal. Stem cells (Dayton, Ohio) 24, 568-574.

Li, E. (2002). Chromatin modification and epigenetic reprogramming in mammalian development. Nature reviews 3, 662-673.

Li, E., Beard, C., and Jaenisch, R. (1993). Role for DNA methylation in genomic imprinting. Nature 366, 362-365.

Li, E., Bestor, T.H., and Jaenisch, R. (1992). Targeted mutation of the DNA methyltransferase gene results in embryonic lethality. Cell 69, 915-926.

Li, Y., McClintick, J., Zhong, L., Edenberg, H.J., Yoder, M.C., and Chan, R.J. (2005). Murine embryonic stem cell differentiation is promoted by SOCS-3 and inhibited by the zinc finger transcription factor Klf4. Blood 105, 635-637.

Liang, G., Chan, M.F., Tomigahara, Y., Tsai, Y.C., Gonzales, F.A., Li, E., Laird, P.W., and Jones, P.A. (2002). Cooperativity between DNA methyltransferases in the maintenance methylation of repetitive elements. Molecular and cellular biology 22, 480-491.

Lin, W., and Dent, S.Y. (2006). Functions of histone-modifying enzymes in development. Current opinion in genetics & development 16, 137-142.

Lindroth, A.M., Shultis, D., Jasencakova, Z., Fuchs, J., Johnson, L., Schubert, D., Patnaik, D., Pradhan, S., Goodrich, J., Schubert, I., et al. (2004). Dual histone H3 methylation marks at lysines 9 and 27 required for interaction with CHROMOMETHYLASE3. The EMBO journal 23, 4286-4296.

Liu, H., Kim, J.M., and Aoki, F. (2004). Regulation of histone H3 lysine 9 methylation in oocytes and early pre-implantation embryos. Development (Cambridge, England) 131, 2269-2280.

Lodish, H. (2000). Molecular cell biology, 4th edn (New York, W.H. Freeman).

Loh, Y.H., Wu, Q., Chew, J.L., Vega, V.B., Zhang, W., Chen, X., Bourque, G., George, J., Leong, B., Liu, J., et al. (2006). The Oct4 and Nanog transcription network regulates pluripotency in mouse embryonic stem cells. Nature genetics 38, 431-440.

Loh, Y.H., Zhang, W., Chen, X., George, J., and Ng, H.H. (2007). Jmjd1a and Jmjd2c histone H3 Lys 9 demethylases regulate self-renewal in embryonic stem cells. Genes & development 21, 2545-2557.

Loyola, A., Tagami, H., Bonaldi, T., Roche, D., Quivy, J.P., Imhof, A., Nakatani, Y., Dent, S.Y., and Almouzni, G. (2009). The HP1alpha-CAF1-SetDB1-containing complex provides H3K9me1 for Suv39-mediated K9me3 in pericentric heterochromatin. EMBO reports 10, 769-775.

Lu, B.Y., Emtage, P.C., Duyf, B.J., Hilliker, A.J., and Eissenberg, J.C. (2000). Heterochromatin protein 1 is required for the normal expression of two heterochromatin genes in Drosophila. Genetics 155, 699-708.

Luger, K., Mader, A.W., Richmond, R.K., Sargent, D.F., and Richmond, T.J. (1997). Crystal structure of the nucleosome core particle at 2.8 A resolution. Nature 389, 251-260.

Lunde, K., Belting, H.G., and Driever, W. (2004). Zebrafish pou5f1/pou2, homolog of mammalian Oct4, functions in the endoderm specification cascade. Curr Biol 14, 48-55.

Lyon, M.F. (1961). Gene action in the X-chromosome of the mouse (Mus musculus L.). Nature 190, 372-373.

Ma, C., Fan, L., Ganassin, R., Bols, N., and Collodi, P. (2001). Production of zebrafish germ-line chimeras from embryo cell cultures. Proceedings of the National Academy of Sciences of the United States of America 98, 2461-2466.

Maatouk, D.M., Kellam, L.D., Mann, M.R., Lei, H., Li, E., Bartolomei, M.S., and Resnick, J.L. (2006). DNA methylation is a primary mechanism for silencing postmigratory primordial germ cell genes in both germ cell and somatic cell lineages. Development (Cambridge, England) 133, 3411-3418.

MacKay, A.B., Mhanni, A.A., McGowan, R.A., and Krone, P.H. (2007). Immunological detection of changes in genomic DNA methylation during early zebrafish development. Genome / National Research Council Canada = Genome / Conseil national de recherches Canada 50, 778-785.

Macleod, D., Clark, V.H., and Bird, A. (1999). Absence of genome-wide changes in DNA methylation during development of the zebrafish. Nature genetics 23, 139-140.

Mahadevan, L.C., Willis, A.C., and Barratt, M.J. (1991). Rapid histone H3 phosphorylation in response to growth factors, phorbol esters, okadaic acid, and protein synthesis inhibitors. Cell 65, 775-783.

Maherali, N., Sridharan, R., Xie, W., Utikal, J., Eminli, S., Arnold, K., Stadtfeld, M., Yachechko, R., Tchieu, J., Jaenisch, R., et al. (2007). Directly reprogrammed fibroblasts show global epigenetic remodeling and widespread tissue contribution. Cell stem cell 1, 55-70.

Margueron, R., Trojer, P., and Reinberg, D. (2005). The key to development: interpreting the histone code? Current opinion in genetics & development 15, 163-176.

Marino-Ramirez, L., Kann, M.G., Shoemaker, B.A., and Landsman, D. (2005). Histone structure and nucleosome stability. Expert review of proteomics 2, 719-729.

Martens, J.H., O'Sullivan, R.J., Braunschweig, U., Opravil, S., Radolf, M., Steinlein, P., and Jenuwein, T. (2005). The profile of repeat-associated histone lysine methylation states in the mouse epigenome. The EMBO journal 24, 800-812.

Martin, C.C., Laforest, L., Akimenko, M.A., and Ekker, M. (1999). A role for DNA methylation in gastrulation and somite patterning. Developmental biology 206, 189-205.

Martin, G.R. (1981). Isolation of a pluripotent cell line from early mouse embryos cultured in medium conditioned by teratocarcinoma stem cells. Proceedings of the National Academy of Sciences of the United States of America 78, 7634-7638.

Masui, S., Nakatake, Y., Toyooka, Y., Shimosato, D., Yagi, R., Takahashi, K., Okochi, H., Okuda, A., Matoba, R., Sharov, A.A., et al. (2007). Pluripotency governed by Sox2 via regulation of Oct3/4 expression in mouse embryonic stem cells. Nature cell biology 9, 625-635.

Matsui, Y., Zsebo, K., and Hogan, B.L. (1992). Derivation of pluripotential embryonic stem cells from murine primordial germ cells in culture. Cell 70, 841-847.

Mayer, W., Niveleau, A., Walter, J., Fundele, R., and Haaf, T. (2000). Demethylation of the zygotic paternal genome. Nature 403, 501-502.

McGowan, R.A., and Martin, C.C. (1997). DNA methylation and genome imprinting in the zebrafish, Danio rerio: some evolutionary ramifications. Biochemistry and cell biology = Biochimie et biologie cellulaire 75, 499-506.

McGrath, J., and Solter, D. (1984). Completion of mouse embryogenesis requires both the maternal and paternal genomes. Cell 37, 179-183.

McLaren, A., and Durcova-Hills, G. (2001). Germ cells and pluripotent stem cells in the mouse. Reproduction, fertility, and development 13, 661-664.

McMahon, A., and Monk, M. (1983). X-chromosome activity in female mouse embryos heterozygous for Pgk-1 and Searle's translocation, T(X; 16) 16H. Genetical research 41, 69-83.

McMahon, S.B., Wood, M.A., and Cole, M.D. (2000). The essential cofactor TRRAP recruits the histone acetyltransferase hGCN5 to c-Myc. Molecular and cellular biology 20, 556-562.

Meehan, R.R. (2003). DNA methylation in animal development. Seminars in cell & developmental biology 14, 53-65.

Meehan, R.R., Dunican, D.S., Ruzov, A., and Pennings, S. (2005). Epigenetic silencing in embryogenesis. Experimental cell research 309, 241-249.

Meissner, A., Mikkelsen, T.S., Gu, H., Wernig, M., Hanna, J., Sivachenko, A., Zhang, X., Bernstein, B.E., Nusbaum, C., Jaffe, D.B., et al. (2008). Genome-scale DNA methylation maps of pluripotent and differentiated cells. Nature 454, 766-770.

Meshorer, E., and Misteli, T. (2006). Chromatin in pluripotent embryonic stem cells and differentiation. Nat Rev Mol Cell Biol 7, 540-546.

Meshorer, E., Yellajoshula, D., George, E., Scambler, P.J., Brown, D.T., and Misteli, T. (2006). Hyperdynamic plasticity of chromatin proteins in pluripotent embryonic stem cells. Developmental cell 10, 105-116.

Metzger, E., Wissmann, M., Yin, N., Muller, J.M., Schneider, R., Peters, A.H., Gunther, T., Buettner, R., and Schule, R. (2005). LSD1 demethylates repressive histone marks to promote androgen-receptor-dependent transcription. Nature 437, 436-439.

Mhanni, A.A., and McGowan, R.A. (2004). Global changes in genomic methylation levels during early development of the zebrafish embryo. Development genes and evolution 214, 412-417.

Mhanni, A.A., Yoder, J.A., Dubesky, C., and McGowan, R.A. (2001). Cloning and sequence analysis of a zebrafish cDNA encoding DNA (cytosine-5)-methyltransferase-1. Genesis 30, 213-219.

Miao, F., and Natarajan, R. (2005). Mapping global histone methylation patterns in the coding regions of human genes. Molecular and cellular biology 25, 4650-4661.

Migeon, B.R. (1994). X-chromosome inactivation: molecular mechanisms and genetic consequences. Trends Genet 10, 230-235.

Mikkelsen, T.S., Hanna, J., Zhang, X., Ku, M., Wernig, M., Schorderet, P., Bernstein, B.E., Jaenisch, R., Lander, E.S., and Meissner, A. (2008). Dissecting direct reprogramming through integrative genomic analysis. Nature 454, 49-55.

Mikkelsen, T.S., Ku, M., Jaffe, D.B., Issac, B., Lieberman, E., Giannoukos, G., Alvarez, P., Brockman, W., Kim, T.K., Koche, R.P., et al. (2007). Genome-wide maps of chromatin state in pluripotent and lineage-committed cells. Nature 448, 553-560.

Miller, R.A., and Ruddle, F.H. (1976). Pluripotent teratocarcinoma-thymus somatic cell hybrids. Cell 9, 45-55.

Mitsui, K., Tokuzawa, Y., Itoh, H., Segawa, K., Murakami, M., Takahashi, K., Maruyama, M., Maeda, M., and Yamanaka, S. (2003). The homeoprotein Nanog is required for maintenance of pluripotency in mouse epiblast and ES cells. Cell 113, 631-642.

Mohandas, T., Sparkes, R.S., and Shapiro, L.J. (1981). Reactivation of an inactive human X chromosome: evidence for X inactivation by DNA methylation. Science (New York, NY 211, 393-396.

Mohd-Sarip, A., and Verrijzer, C.P. (2004). Molecular biology. A higher order of silence. Science (New York, NY 306, 1484-1485.

Molven, A., Njolstad, P.R., and Fjose, A. (1991). Genomic structure and restricted neural expression of the zebrafish wnt-1 (int-1) gene. The EMBO journal 10, 799-807.

Monk, M., Adams, R.L., and Rinaldi, A. (1991). Decrease in DNA methylase activity during preimplantation development in the mouse. Development (Cambridge, England) 112, 189-192.

Monk, M., Boubelik, M., and Lehnert, S. (1987). Temporal and regional changes in DNA methylation in the embryonic, extraembryonic and germ cell lineages during mouse embryo development. Development (Cambridge, England) 99, 371-382.

Moore, T., and Haig, D. (1991). Genomic imprinting in mammalian development: a parental tug-of-war. Trends Genet 7, 45-49.

Morgan, H.D., Santos, F., Green, K., Dean, W., and Reik, W. (2005). Epigenetic reprogramming in mammals. Human molecular genetics 14 Spec No 1, R47-58.

Morrison, G.M., and Brickman, J.M. (2006). Conserved roles for Oct4 homologues in maintaining multipotency during early vertebrate development. Development (Cambridge, England) 133, 2011-2022.

Mullins, L.J., Wilmut, I., and Mullins, J.J. (2004). Nuclear transfer in rodents. The Journal of physiology 554, 4-12.

Mutskov, V., and Felsenfeld, G. (2004). Silencing of transgene transcription precedes methylation of promoter DNA and histone H3 lysine 9. The EMBO journal 23, 138-149.

Nakatake, Y., Fukui, N., Iwamatsu, Y., Masui, S., Takahashi, K., Yagi, R., Yagi, K., Miyazaki, J., Matoba, R., Ko, M.S., et al. (2006). Klf4 cooperates with Oct3/4 and Sox2 to activate the Lefty1 core promoter in embryonic stem cells. Molecular and cellular biology 26, 7772-7782.

Nan, X., Cross, S., and Bird, A. (1998). Gene silencing by methyl-CpG-binding proteins. Novartis Foundation symposium 214, 6-16; discussion 16-21, 46-50.

Nan, X., Ng, H.H., Johnson, C.A., Laherty, C.D., Turner, B.M., Eisenman, R.N., and Bird, A. (1998). Transcriptional repression by the methyl-CpG-binding protein MeCP2 involves a histone deacetylase complex. Nature 393, 386-389.

Nathan, D., Ingvarsdottir, K., Sterner, D.E., Bylebyl, G.R., Dokmanovic, M., Dorsey, J.A., Whelan, K.A., Krsmanovic, M., Lane, W.S., Meluh, P.B., et al. (2006). Histone sumoylation is a negative regulator in Saccharomyces cerevisiae and shows dynamic interplay with positive-acting histone modifications. Genes & development 20, 966-976.

Nelson, C.J., Santos-Rosa, H., and Kouzarides, T. (2006). Proline isomerization of histone H3 regulates lysine methylation and gene expression. Cell 126, 905-916.

Newport, J., and Kirschner, M. (1982). A major developmental transition in early Xenopus embryos: I. characterization and timing of cellular changes at the midblastula stage. Cell 30, 675-686.

Ng, H.H., Feng, Q., Wang, H., Erdjument-Bromage, H., Tempst, P., Zhang, Y., and Struhl, K. (2002). Lysine methylation within the globular domain of histone H3 by Dot1 is important for telomeric silencing and Sir protein association. Genes & development 16, 1518-1527.

Nichols, J., Evans, E.P., and Smith, A.G. (1990). Establishment of germ-line-competent embryonic stem (ES) cells using differentiation inhibiting activity. Development (Cambridge, England) 110, 1341-1348.

Nichols, J., and Smith, A. (2009). Naive and primed pluripotent states. Cell stem cell 4, 487-492.

Nichols, J., Zevnik, B., Anastassiadis, K., Niwa, H., Klewe-Nebenius, D., Chambers, I., Scholer, H., and Smith, A. (1998). Formation of pluripotent stem cells in the mammalian embryo depends on the POU transcription factor Oct4. Cell 95, 379-391.

Nicklay, J.J., Shechter, D., Chitta, R.K., Garcia, B.A., Shabanowitz, J., Allis, C.D., and Hunt, D.F. (2009). Analysis of histones in Xenopus laevis. II. mass spectrometry reveals an index of cell type-specific modifications on H3 and H4. The Journal of biological chemistry 284, 1075-1085.

Nishimoto, M., Fukushima, A., Okuda, A., and Muramatsu, M. (1999). The gene for the embryonic stem cell coactivator UTF1 carries a regulatory element which selectively interacts with a complex composed of Oct-3/4 and Sox-2. Molecular and cellular biology 19, 5453-5465.

Nishioka, K., Rice, J.C., Sarma, K., Erdjument-Bromage, H., Werner, J., Wang, Y., Chuikov, S., Valenzuela, P., Tempst, P., Steward, R., et al. (2002). PR-Set7 is a nucleosome-specific methyltransferase that modifies lysine 20 of histone H4 and is associated with silent chromatin. Molecular cell 9, 1201-1213.

Niwa, H. (2007). How is pluripotency determined and maintained? Development (Cambridge, England) 134, 635-646.

Niwa, H., Burdon, T., Chambers, I., and Smith, A. (1998). Self-renewal of pluripotent embryonic stem cells is mediated via activation of STAT3. Genes & development 12, 2048-2060.

Niwa, H., Miyazaki, J., and Smith, A.G. (2000). Quantitative expression of Oct-3/4 defines differentiation, dedifferentiation or self-renewal of ES cells. Nature genetics 24, 372-376.

Nothias, J.Y., Majumder, S., Kaneko, K.J., and DePamphilis, M.L. (1995). Regulation of gene expression at the beginning of mammalian development. The Journal of biological chemistry 270, 22077-22080.

Nottke, A., Colaiacovo, M.P., and Shi, Y. (2009). Developmental roles of the histone lysine demethylases. Development (Cambridge, England) 136, 879-889.

Nusslein-Volhard, C., and Dahm, R. (2002). Zebrafish : a practical approach (Oxford, Oxford University Press).

O'Connor, M.D., Kardel, M.D., Iosfina, I., Youssef, D., Lu, M., Li, M.M., Vercauteren, S., Nagy, A., and Eaves, C.J. (2008). Alkaline phosphatase-positive colony formation is a sensitive, specific, and quantitative indicator of undifferentiated human embryonic stem cells. Stem cells (Dayton, Ohio) 26, 1109-1116.

Oda, H., Okamoto, I., Murphy, N., Chu, J., Price, S.M., Shen, M.M., Torres-Padilla, M.E., Heard, E., and Reinberg, D. (2009). Monomethylation of histone H4-lysine 20 is involved in chromosome structure and stability and is essential for mouse development. Molecular and cellular biology 29, 2278-2295.

Okano, M., Bell, D.W., Haber, D.A., and Li, E. (1999). DNA methyltransferases Dnmt3a and Dnmt3b are essential for de novo methylation and mammalian development. Cell 99, 247-257.

Okano, M., Xie, S., and Li, E. (1998). Cloning and characterization of a family of novel mammalian DNA (cytosine-5) methyltransferases. Nature genetics 19, 219-220.

Okita, K., Ichisaka, T., and Yamanaka, S. (2007). Generation of germline-competent induced pluripotent stem cells. Nature 448, 313-317.

Okuda, Y., Yoda, H., Uchikawa, M., Furutani-Seiki, M., Takeda, H., Kondoh, H., and Kamachi, Y. (2006). Comparative genomic and expression analysis of group B1 sox genes in zebrafish indicates their diversification during vertebrate evolution. Dev Dyn 235, 811-825.

Okumura-Nakanishi, S., Saito, M., Niwa, H., and Ishikawa, F. (2005). Oct-3/4 and Sox2 regulate Oct-3/4 gene in embryonic stem cells. The Journal of biological chemistry 280, 5307-5317.

Olek, A., and Walter, J. (1997). The pre-implantation ontogeny of the H19 methylation imprint. Nature genetics 17, 275-276.

Olsen, L.C., Aasland, R., and Fjose, A. (1997). A vasa-like gene in zebrafish identifies putative primordial germ cells. Mechanisms of development 66, 95-105.

O'Neill, L.P., Randall, T.E., Lavender, J., Spotswood, H.T., Lee, J.T., and Turner, B.M. (2003). X-linked genes in female embryonic stem cells carry an epigenetic mark prior to the onset of X inactivation. Human molecular genetics 12, 1783-1790.

Oswald, J., Engemann, S., Lane, N., Mayer, W., Olek, A., Fundele, R., Dean, W., Reik, W., and Walter, J. (2000). Active demethylation of the paternal genome in the mouse zygote. Curr Biol 10, 475-478.

Ouyang, J., Shi, Y., Valin, A., Xuan, Y., and Gill, G. (2009). Direct binding of CoREST1 to SUMO-2/3 contributes to gene-specific repression by the LSD1/CoREST1/HDAC complex. Molecular cell 34, 145-154.

Pain, B., Clark, M.E., Shen, M., Nakazawa, H., Sakurai, M., Samarut, J., and Etches, R.J. (1996). Long-term in vitro culture and characterisation of avian embryonic stem cells with multiple morphogenetic potentialities. Development (Cambridge, England) 122, 2339-2348.

Palmieri, S.L., Peter, W., Hess, H., and Scholer, H.R. (1994). Oct-4 transcription factor is differentially expressed in the mouse embryo during establishment of the first two extraembryonic cell lineages involved in implantation. Developmental biology 166, 259-267.

Papp, B., and Muller, J. (2006). Histone trimethylation and the maintenance of transcriptional ON and OFF states by trxG and PcG proteins. Genes & development 20, 2041-2054.

Park, S.H., Park, S.H., Kook, M.C., Kim, E.Y., Park, S., and Lim, J.H. (2004). Ultrastructure of human embryonic stem cells and spontaneous and retinoic acid-induced differentiating cells. Ultrastructural pathology 28, 229-238.

Pasini, D., Bracken, A.P., Hansen, J.B., Capillo, M., and Helin, K. (2007). The polycomb group protein Suz12 is required for embryonic stem cell differentiation. Molecular and cellular biology 27, 3769-3779.

Passarge, E. (1979). Emil Heitz and the concept of heterochromatin: longitudinal chromosome differentiation was recognized fifty years ago. American journal of human genetics 31, 106-115.

Pauls, S., Geldmacher-Voss, B., and Campos-Ortega, J.A. (2001). A zebrafish histone variant H2A.F/Z and a transgenic H2A.F/Z:GFP fusion protein for in vivo studies of embryonic development. Development genes and evolution 211, 603-610.

Paulsen, M., and Ferguson-Smith, A.C. (2001). DNA methylation in genomic imprinting, development, and disease. The Journal of pathology 195, 97-110.

Pazin, M.J., and Kadonaga, J.T. (1997). What's up and down with histone deacetylation and transcription? Cell 89, 325-328.

Pera, M.F., Andrade, J., Houssami, S., Reubinoff, B., Trounson, A., Stanley, E.G., Ward-van Oostwaard, D., and Mummery, C. (2004). Regulation of human embryonic stem cell differentiation by BMP-2 and its antagonist noggin. Journal of cell science 117, 1269-1280.

Pesavento, J.J., Bullock, C.R., LeDuc, R.D., Mizzen, C.A., and Kelleher, N.L. (2008). Combinatorial modification of human histone H4 quantitated by two-dimensional liquid chromatography coupled with top down mass spectrometry. The Journal of biological chemistry 283, 14927-14937.

Pesavento, J.J., Yang, H., Kelleher, N.L., and Mizzen, C.A. (2008). Certain and progressive methylation of histone H4 at lysine 20 during the cell cycle. Molecular and cellular biology 28, 468-486.

Pesce, M., and Scholer, H.R. (2001). Oct-4: gatekeeper in the beginnings of mammalian development. Stem cells (Dayton, Ohio) 19, 271-278.

Peters, A.H., Kubicek, S., Mechtler, K., O'Sullivan, R.J., Derijck, A.A., Perez-Burgos, L., Kohlmaier, A., Opravil, S., Tachibana, M., Shinkai, Y., et al. (2003). Partitioning and plasticity of repressive histone methylation states in mammalian chromatin. Molecular cell 12, 1577-1589.

Peters, A.H., O'Carroll, D., Scherthan, H., Mechtler, K., Sauer, S., Schofer, C., Weipoltshammer, K., Pagani, M., Lachner, M., Kohlmaier, A., et al. (2001). Loss of the Suv39h histone methyltransferases impairs mammalian heterochromatin and genome stability. Cell 107, 323-337.

Petitte, J.N., Liu, G., and Yang, Z. (2004). Avian pluripotent stem cells. Mechanisms of development 121, 1159-1168.

Pfeifer, G.P., Tanguay, R.L., Steigerwald, S.D., and Riggs, A.D. (1990). In vivo footprint and methylation analysis by PCR-aided genomic sequencing: comparison of active and inactive X chromosomal DNA at the CpG island and promoter of human PGK-1. Genes & development 4, 1277-1287.

Phalke, S., Nickel, O., Walluscheck, D., Hortig, F., Onorati, M.C., and Reuter, G. (2009). Retrotransposon silencing and telomere integrity in somatic cells of Drosophila depends on the cytosine-5 methyltransferase DNMT2. Nature genetics 41, 696-702.

Phanstiel, D., Brumbaugh, J., Berggren, W.T., Conard, K., Feng, X., Levenstein, M.E., McAlister, G.C., Thomson, J.A., and Coon, J.J. (2008). Mass spectrometry identifies and quantifies 74 unique histone H4 isoforms in differentiating human embryonic stem cells. Proceedings of the National Academy of Sciences of the United States of America 105, 4093-4098.

Plath, K., Fang, J., Mlynarczyk-Evans, S.K., Cao, R., Worringer, K.A., Wang, H., de la Cruz, C.C., Otte, A.P., Panning, B., and Zhang, Y. (2003). Role of histone H3 lysine 27 methylation in X inactivation. Science (New York, NY 300, 131-135.

Pogo, B.G., Allfrey, V.G., and Mirsky, A.E. (1966). RNA synthesis and histone acetylation during the course of gene activation in lymphocytes. Proceedings of the National Academy of Sciences of the United States of America 55, 805-812.

Pokholok, D.K., Harbison, C.T., Levine, S., Cole, M., Hannett, N.M., Lee, T.I., Bell, G.W., Walker, K., Rolfe, P.A., Herbolsheimer, E., et al. (2005). Genome-wide map of nucleosome acetylation and methylation in yeast. Cell 122, 517-527.

Pokholok, D.K., Zeitlinger, J., Hannett, N.M., Reynolds, D.B., and Young, R.A. (2006). Activated signal transduction kinases frequently occupy target genes. Science (New York, NY 313, 533-536.

Prokhortchouk, E., and Defossez, P.A. (2008). The cell biology of DNA methylation in mammals. Biochimica et biophysica acta 1783, 2167-2173.

Rai, K., Chidester, S., Zavala, C.V., Manos, E.J., James, S.R., Karpf, A.R., Jones, D.A., and Cairns, B.R. (2007). Dnmt2 functions in the cytoplasm to promote liver, brain, and retina development in zebrafish. Genes & development 21, 261-266.

Rai, K., Huggins, I.J., James, S.R., Karpf, A.R., Jones, D.A., and Cairns, B.R. (2008). DNA demethylation in zebrafish involves the coupling of a deaminase, a glycosylase, and gadd45. Cell 135, 1201-1212.

Rai, K., Nadauld, L.D., Chidester, S., Manos, E.J., James, S.R., Karpf, A.R., Cairns, B.R., and Jones, D.A. (2006). Zebra fish Dnmt1 and Suv39h1 regulate organ-specific terminal differentiation during development. Molecular and cellular biology 26, 7077-7085.

Rando, O.J., and Ahmad, K. (2007). Rules and regulation in the primary structure of chromatin. Current opinion in cell biology 19, 250-256.

Razin, A., and Cedar, H. (1977). Distribution of 5-methylcytosine in chromatin. Proceedings of the National Academy of Sciences of the United States of America 74, 2725-2728.

Reddien, P.W., and Sanchez Alvarado, A. (2004). Fundamentals of planarian regeneration. Annual review of cell and developmental biology 20, 725-757.

Regha, K., Sloane, M.A., Huang, R., Pauler, F.M., Warczok, K.E., Melikant, B., Radolf, M., Martens, J.H., Schotta, G., Jenuwein, T., et al. (2007). Active and repressive chromatin are interspersed without spreading in an imprinted gene cluster in the mammalian genome. Molecular cell 27, 353-366.

Reik, W. (1989). Genomic imprinting and genetic disorders in man. Trends Genet 5, 331-336.

Reik, W., Dean, W., and Walter, J. (2001). Epigenetic reprogramming in mammalian development. Science (New York, NY 293, 1089-1093.

Reik, W., Santos, F., Mitsuya, K., Morgan, H., and Dean, W. (2003). Epigenetic asymmetry in the mammalian zygote and early embryo: relationship to lineage commitment? Philosophical transactions of the Royal Society of London 358, 1403-1409; discussion 1409.

Reik, W., and Walter, J. (2001). Evolution of imprinting mechanisms: the battle of the sexes begins in the zygote. Nature genetics 27, 255-256.

Reik, W., and Walter, J. (2001). Genomic imprinting: parental influence on the genome. Nature reviews 2, 21-32.

Reim, G., Mizoguchi, T., Stainier, D.Y., Kikuchi, Y., and Brand, M. (2004). The POU domain protein spg (pou2/Oct4) is essential for endoderm formation in cooperation with the HMG domain protein casanova. Developmental cell 6, 91-101.

Rein, T., DePamphilis, M.L., and Zorbas, H. (1998). Identifying 5-methylcytosine and related modifications in DNA genomes. Nucleic acids research 26, 2255-2264.

Resnick, J.L., Bixler, L.S., Cheng, L., and Donovan, P.J. (1992). Long-term proliferation of mouse primordial germ cells in culture. Nature 359, 550-551.

Reuter, G., and Spierer, P. (1992). Position effect variegation and chromatin proteins. Bioessays 14, 605-612.

Rice, J.C., Briggs, S.D., Ueberheide, B., Barber, C.M., Shabanowitz, J., Hunt, D.F., Shinkai, Y., and Allis, C.D. (2003). Histone methyltransferases direct different degrees of methylation to define distinct chromatin domains. Molecular cell 12, 1591-1598.

Rice, J.C., Nishioka, K., Sarma, K., Steward, R., Reinberg, D., and Allis, C.D. (2002). Mitotic-specific methylation of histone H4 Lys 20 follows increased PR-Set7 expression and its localization to mitotic chromosomes. Genes & development 16, 2225-2230.

Richards, E.J., and Elgin, S.C. (2002). Epigenetic codes for heterochromatin formation and silencing: rounding up the usual suspects. Cell 108, 489-500.

Rideout, W.M., 3rd, Wakayama, T., Wutz, A., Eggan, K., Jackson-Grusby, L., Dausman, J., Yanagimachi, R., and Jaenisch, R. (2000). Generation of mice from wild-type and targeted ES cells by nuclear cloning. Nature genetics 24, 109-110.

Riggs, A.D., and Pfeifer, G.P. (1992). X-chromosome inactivation and cell memory. Trends Genet 8, 169-174.

Ringrose, L., and Paro, R. (2004). Epigenetic regulation of cellular memory by the Polycomb and Trithorax group proteins. Annual review of genetics 38, 413-443.

Rodda, D.J., Chew, J.L., Lim, L.H., Loh, Y.H., Wang, B., Ng, H.H., and Robson, P. (2005). Transcriptional regulation of nanog by OCT4 and SOX2. The Journal of biological chemistry 280, 24731-24737.

Rossant, J. (2008). Stem cells and early lineage development. Cell 132, 527-531.

Rougeulle, C., Chaumeil, J., Sarma, K., Allis, C.D., Reinberg, D., Avner, P., and Heard, E. (2004). Differential histone H3 Lys-9 and Lys-27 methylation profiles on the X chromosome. Molecular and cellular biology 24, 5475-5484.

Rougier, N., Bourc'his, D., Gomes, D.M., Niveleau, A., Plachot, M., Paldi, A., and Viegas-Pequignot, E. (1998). Chromosome methylation patterns during mammalian preimplantation development. Genes & development 12, 2108-2113.

Rountree, M.R., Bachman, K.E., and Baylin, S.B. (2000). DNMT1 binds HDAC2 and a new co-repressor, DMAP1, to form a complex at replication foci. Nature genetics 25, 269-277.

Russo, V.E.A., Riggs, A.D., and Martienssen, R.A. (1996). Epigenetic mechanisms of gene regulation (Plainview, N.Y., Cold Spring Harbor Laboratory Press).

Sagerstrom, C.G., Grinbalt, Y., and Sive, H. (1996). Anteroposterior patterning in the zebrafish, Danio rerio: an explant assay reveals inductive and suppressive cell interactions. Development (Cambridge, England) 122, 1873-1883.

Saito, S., Liu, B., and Yokoyama, K. (2004). Animal embryonic stem (ES) cells: self-renewal, pluripotency, transgenesis and nuclear transfer. Hum Cell 17, 107-115.

Saitoh, H., and Hinchey, J. (2000). Functional heterogeneity of small ubiquitin-related protein modifiers SUMO-1 versus SUMO-2/3. The Journal of biological chemistry 275, 6252-6258.

Sakaguchi, A., Karachentsev, D., Seth-Pasricha, M., Druzhinina, M., and Steward, R. (2008). Functional characterization of the Drosophila Hmt4-20/Suv4-20 histone methyltransferase. Genetics 179, 317-322.

Sakaguchi, A., and Steward, R. (2007). Aberrant monomethylation of histone H4 lysine 20 activates the DNA damage checkpoint in Drosophila melanogaster. The Journal of cell biology 176, 155-162.

Sakai, R.R., Tamashiro, K.L., Yamazaki, Y., and Yanagimachi, R. (2005). Cloning and assisted reproductive techniques: influence on early development and adult phenotype. Birth Defects Res C Embryo Today 75, 151-162.

Sanders, S.L., Portoso, M., Mata, J., Bahler, J., Allshire, R.C., and Kouzarides, T. (2004). Methylation of histone H4 lysine 20 controls recruitment of Crb2 to sites of DNA damage. Cell 119, 603-614.

Santos, F., and Dean, W. (2004). Epigenetic reprogramming during early development in mammals. Reproduction (Cambridge, England) 127, 643-651.

Santos, F., Hendrich, B., Reik, W., and Dean, W. (2002). Dynamic reprogramming of DNA methylation in the early mouse embryo. Developmental biology 241, 172-182.

Santos, F., Peters, A.H., Otte, A.P., Reik, W., and Dean, W. (2005). Dynamic chromatin modifications characterise the first cell cycle in mouse embryos. Developmental biology 280, 225-236.

Sarg, B., Koutzamani, E., Helliger, W., Rundquist, I., and Lindner, H.H. (2002). Postsynthetic trimethylation of histone H4 at lysine 20 in mammalian tissues is associated with aging. The Journal of biological chemistry 277, 39195-39201.

Sarraf, S.A., and Stancheva, I. (2004). Methyl-CpG binding protein MBD1 couples histone H3 methylation at lysine 9 by SETDB1 to DNA replication and chromatin assembly. Molecular cell 15, 595-605.

Scharf, A.N., Meier, K., Seitz, V., Kremmer, E., Brehm, A., and Imhof, A. (2009). Monomethylation of lysine 20 on histone H4 facilitates chromatin maturation. Molecular and cellular biology 29, 57-67.

Schotta, G., Lachner, M., Sarma, K., Ebert, A., Sengupta, R., Reuter, G., Reinberg, D., and Jenuwein, T. (2004). A silencing pathway to induce H3-K9 and H4-K20 trimethylation at constitutive heterochromatin. Genes & development 18, 1251-1262.

Schotta, G., Sengupta, R., Kubicek, S., Malin, S., Kauer, M., Callen, E., Celeste, A., Pagani, M., Opravil, S., De La Rosa-Velazquez, I.A., et al. (2008). A chromatin-wide transition to H4K20 monomethylation impairs genome integrity and programmed DNA rearrangements in the mouse. Genes & development 22, 2048-2061.

Segal, E., Fondufe-Mittendorf, Y., Chen, L., Thastrom, A., Field, Y., Moore, I.K., Wang, J.P., and Widom, J. (2006). A genomic code for nucleosome positioning. Nature 442, 772-778.

Selwood, L., and Johnson, M.H. (2006). Trophoblast and hypoblast in the monotreme, marsupial and eutherian mammal: evolution and origins. Bioessays 28, 128-145.

Shahbazian, M.D., and Grunstein, M. (2007). Functions of site-specific histone acetylation and deacetylation. Annual review of biochemistry 76, 75-100.

Shaklai, S., Amariglio, N., Rechavi, G., and Simon, A.J. (2007). Gene silencing at the nuclear periphery. The FEBS journal 274, 1383-1392.

Shamblott, M.J., Axelman, J., Wang, S., Bugg, E.M., Littlefield, J.W., Donovan, P.J., Blumenthal, P.D., Huggins, G.R., and Gearhart, J.D. (1998). Derivation of pluripotent stem cells from cultured human primordial germ cells. Proceedings of the National Academy of Sciences of the United States of America 95, 13726-13731.

Shechter, D., Nicklay, J.J., Chitta, R.K., Shabanowitz, J., Hunt, D.F., and Allis, C.D. (2009). Analysis of histones in Xenopus laevis. I. A distinct index of enriched variants and modifications exists in each cell type and is remodeled during developmental transitions. The Journal of biological chemistry 284, 1064-1074.

Shen, Y., Matsuno, Y., Fouse, S.D., Rao, N., Root, S., Xu, R., Pellegrini, M., Riggs, A.D., and Fan, G. (2008). X-inactivation in female human embryonic stem cells is in a nonrandom pattern and prone to epigenetic alterations. Proceedings of the National Academy of Sciences of the United States of America 105, 4709-4714.

Shi, W., Dirim, F., Wolf, E., Zakhartchenko, V., and Haaf, T. (2004). Methylation reprogramming and chromosomal aneuploidy in in vivo fertilized and cloned rabbit preimplantation embryos. Biology of reproduction 71, 340-347.

Shi, W., Wang, H., Pan, G., Geng, Y., Guo, Y., and Pei, D. (2006). Regulation of the pluripotency marker Rex-1 by Nanog and Sox2. The Journal of biological chemistry 281, 23319-23325.

Shi, W., Zakhartchenko, V., and Wolf, E. (2003). Epigenetic reprogramming in mammalian nuclear transfer. Differentiation; research in biological diversity 71, 91-113.

Shi, Y. (2007). Histone lysine demethylases: emerging roles in development, physiology and disease. Nature reviews 8, 829-833.

Shiio, Y., and Eisenman, R.N. (2003). Histone sumoylation is associated with transcriptional repression. Proceedings of the National Academy of Sciences of the United States of America 100, 13225-13230.

Shilatifard, A. (2006). Chromatin modifications by methylation and ubiquitination: implications in the regulation of gene expression. Annual review of biochemistry 75, 243-269.

Shimoda, N., Yamakoshi, K., Miyake, A., and Takeda, H. (2005). Identification of a gene required for de novo DNA methylation of the zebrafish no tail gene. Dev Dyn 233, 1509-1516.

Silva, J., Mak, W., Zvetkova, I., Appanah, R., Nesterova, T.B., Webster, Z., Peters, A.H., Jenuwein, T., Otte, A.P., and Brockdorff, N. (2003). Establishment of histone h3 methylation on the inactive X chromosome requires transient recruitment of Eed-Enx1 polycomb group complexes. Developmental cell 4, 481-495.

Silva, J., Nichols, J., Theunissen, T.W., Guo, G., van Oosten, A.L., Barrandon, O., Wray, J., Yamanaka, S., Chambers, I., and Smith, A. (2009). Nanog is the gateway to the pluripotent ground state. Cell 138, 722-737.

Simonsson, S., and Gurdon, J. (2004). DNA demethylation is necessary for the epigenetic reprogramming of somatic cell nuclei. Nature cell biology 6, 984-990.

Sims, J.K., Houston, S.I., Magazinnik, T., and Rice, J.C. (2006). A trans-tail histone code defined by monomethylated H4 Lys-20 and H3 Lys-9 demarcates distinct regions of silent chromatin. The Journal of biological chemistry 281, 12760-12766.

Sims, J.K., and Rice, J.C. (2008). PR-Set7 establishes a repressive trans-tail histone code that regulates differentiation. Molecular and cellular biology 28, 4459-4468.

Singh, N.N., Fischer, K., Hedstrom, O., and Barnes, D.W. (2001). Fibroblast growth factor inhibits expression of neural markers in cultures of zebrafish early embryo cells. Marine biotechnology (New York, NY 3, 27-35.

Siripattarapravat, K., Pinmee, B., Venta, P.J., Chang, C.C., and Cibelli, J.B. (2009). Somatic cell nuclear transfer in zebrafish. Nature methods.

Skromne, I., and Prince, V.E. (2008). Current perspectives in zebrafish reverse genetics: moving forward. Dev Dyn 237, 861-882.

Smallwood, A., Esteve, P.O., Pradhan, S., and Carey, M. (2007). Functional cooperation between HP1 and DNMT1 mediates gene silencing. Genes & development 21, 1169-1178.

Smith, A.G. (2001). Embryo-derived stem cells: of mice and men. Annual review of cell and developmental biology 17, 435-462.

Smith, T.H., Dueck, C.C., Mhanni, A.A., and McGowan, R.A. (2005). Novel splice variants associated with one of the zebrafish dnmt3 genes. BMC developmental biology 5, 23.

Solter, D., and Knowles, B.B. (1978). Monoclonal antibody defining a stage-specific mouse embryonic antigen (SSEA-1). Proceedings of the National Academy of Sciences of the United States of America 75, 5565-5569.

Soppe, W.J., Jasencakova, Z., Houben, A., Kakutani, T., Meister, A., Huang, M.S., Jacobsen, S.E., Schubert, I., and Fransz, P.F. (2002). DNA methylation controls histone H3 lysine 9 methylation and heterochromatin assembly in Arabidopsis. The EMBO journal 21, 6549-6559.

Souza, P.P., Volkel, P., Trinel, D., Vandamme, J., Rosnoblet, C., Heliot, L., and Angrand, P.O. (2009). The histone methyltransferase SUV420H2 and Heterochromatin Proteins HP1 interact but show different dynamic behaviours. BMC cell biology 10, 41.

Spangrude, G.J., Heimfeld, S., and Weissman, I.L. (1988). Purification and characterization of mouse hematopoietic stem cells. Science (New York, NY 241, 58-62.

Spence, R., Gerlach, G., Lawrence, C., and Smith, C. (2008). The behaviour and ecology of the zebrafish, Danio rerio. Biological reviews of the Cambridge Philosophical Society 83, 13-34.

Stachel, S.E., Grunwald, D.J., and Myers, P.Z. (1993). Lithium perturbation and goosecoid expression identify a dorsal specification pathway in the pregastrula zebrafish. Development (Cambridge, England) 117, 1261-1274.

Stancheva, I., El-Maarri, O., Walter, J., Niveleau, A., and Meehan, R.R. (2002). DNA methylation at promoter regions regulates the timing of gene activation in Xenopus laevis embryos. Developmental biology 243, 155-165.

Stancheva, I., Hensey, C., and Meehan, R.R. (2001). Loss of the maintenance methyltransferase, xDnmt1, induces apoptosis in Xenopus embryos. The EMBO journal 20, 1963-1973.

Stancheva, I., and Meehan, R.R. (2000). Transient depletion of xDnmt1 leads to premature gene activation in Xenopus embryos. Genes & development 14, 313-327.

Stavridis, M.P., Lunn, J.S., Collins, B.J., and Storey, K.G. (2007). A discrete period of FGF-induced Erk1/2 signalling is required for vertebrate neural specification. Development (Cambridge, England) 134, 2889-2894.

Stephens, C., Reisenauer, A., Wright, R., and Shapiro, L. (1996). A cell cycle-regulated bacterial DNA methyltransferase is essential for viability. Proceedings of the National Academy of Sciences of the United States of America 93, 1210-1214.

Stoger, R., Kubicka, P., Liu, C.G., Kafri, T., Razin, A., Cedar, H., and Barlow, D.P. (1993). Maternal-specific methylation of the imprinted mouse Igf2r locus identifies the expressed locus as carrying the imprinting signal. Cell 73, 61-71.

Strahl, B.D., and Allis, C.D. (2000). The language of covalent histone modifications. Nature 403, 41-45.

Strunnikova, M., Schagdarsurengin, U., Kehlen, A., Garbe, J.C., Stampfer, M.R., and Dammann, R. (2005). Chromatin inactivation precedes de novo DNA methylation during the progressive epigenetic silencing of the RASSF1A promoter. Molecular and cellular biology 25, 3923-3933.

Su, H.L., and Li, S.S. (2002). Molecular features of human ubiquitin-like SUMO genes and their encoded proteins. Gene 296, 65-73.

Sun, X.J., Xu, P.F., Zhou, T., Hu, M., Fu, C.T., Zhang, Y., Jin, Y., Chen, Y., Chen, S.J., Huang, Q.H., et al. (2008). Genome-wide survey and developmental expression mapping of zebrafish SET domain-containing genes. PloS one 3, e1499.

Surani, M.A., Barton, S.C., and Norris, M.L. (1984). Development of reconstituted mouse eggs suggests imprinting of the genome during gametogenesis. Nature 308, 548-550.

Suzuki, M.M., and Bird, A. (2008). DNA methylation landscapes: provocative insights from epigenomics. Nature reviews 9, 465-476.

Tachibana, M., Nozaki, M., Takeda, N., and Shinkai, Y. (2007). Functional dynamics of H3K9 methylation during meiotic prophase progression. The EMBO journal 26, 3346-3359.

Tachibana, M., Sugimoto, K., Nozaki, M., Ueda, J., Ohta, T., Ohki, M., Fukuda, M., Takeda, N., Niida, H., Kato, H., et al. (2002). G9a histone methyltransferase plays a dominant role in euchromatic histone H3 lysine 9 methylation and is essential for early embryogenesis. Genes & development 16, 1779-1791.

Tachibana, M., Ueda, J., Fukuda, M., Takeda, N., Ohta, T., Iwanari, H., Sakihama, T., Kodama, T., Hamakubo, T., and Shinkai, Y. (2005). Histone methyltransferases G9a and GLP form heteromeric complexes and are both crucial for methylation of euchromatin at H3-K9. Genes & development 19, 815-826.

Tada, M., Tada, T., Lefebvre, L., Barton, S.C., and Surani, M.A. (1997). Embryonic germ cells induce epigenetic reprogramming of somatic nucleus in hybrid cells. The EMBO journal 16, 6510-6520.

Tada, M., Takahama, Y., Abe, K., Nakatsuji, N., and Tada, T. (2001). Nuclear reprogramming of somatic cells by in vitro hybridization with ES cells. Curr Biol 11, 1553-1558.

Takagi, N., Wake, N., and Sasaki, M. (1978). Cytologic evidence for preferential inactivation of the paternally derived X chromosome in XX mouse blastocysts. Cytogenetics and cell genetics 20, 240-248.

Takahashi, K., and Yamanaka, S. (2006). Induction of pluripotent stem cells from mouse embryonic and adult fibroblast cultures by defined factors. Cell 126, 663-676.

Takeda, H., Matsuzaki, T., Oki, T., Miyagawa, T., and Amanuma, H. (1994). A novel POU domain gene, zebrafish pou2: expression and roles of two alternatively spliced twin products in early development. Genes & development 8, 45-59.

Takizawa, T., Nakashima, K., Namihira, M., Ochiai, W., Uemura, A., Yanagisawa, M., Fujita, N., Nakao, M., and Taga, T. (2001). DNA methylation is a critical cell-intrinsic determinant of astrocyte differentiation in the fetal brain. Developmental cell 1, 749-758.

Talasz, H., Lindner, H.H., Sarg, B., and Helliger, W. (2005). Histone H4-lysine 20 monomethylation is increased in promoter and coding regions of active genes and correlates with hyperacetylation. The Journal of biological chemistry 280, 38814-38822.

Tamaru, H., and Selker, E.U. (2001). A histone H3 methyltransferase controls DNA methylation in Neurospora crassa. Nature 414, 277-283.

Tamaru, H., Zhang, X., McMillen, D., Singh, P.B., Nakayama, J., Grewal, S.I., Allis, C.D., Cheng, X., and Selker, E.U. (2003). Trimethylated lysine 9 of histone H3 is a mark for DNA methylation in Neurospora crassa. Nature genetics 34, 75-79.

Tariq, M., Saze, H., Probst, A.V., Lichota, J., Habu, Y., and Paszkowski, J. (2003). Erasure of CpG methylation in Arabidopsis alters patterns of histone H3 methylation in heterochromatin. Proceedings of the National Academy of Sciences of the United States of America 100, 8823-8827.

Tatham, M.H., Jaffray, E., Vaughan, O.A., Desterro, J.M., Botting, C.H., Naismith, J.H., and Hay, R.T. (2001). Polymeric chains of SUMO-2 and SUMO-3 are conjugated to protein substrates by SAE1/SAE2 and Ubc9. The Journal of biological chemistry 276, 35368-35374.

Terstappen, L.W., Huang, S., Safford, M., Lansdorp, P.M., and Loken, M.R. (1991). Sequential generations of hematopoietic colonies derived from single nonlineage-committed CD34+CD38- progenitor cells. Blood 77, 1218-1227.

Tesar, P.J., Chenoweth, J.G., Brook, F.A., Davies, T.J., Evans, E.P., Mack, D.L., Gardner, R.L., and McKay, R.D. (2007). New cell lines from mouse epiblast share defining features with human embryonic stem cells. Nature 448, 196-199.

Thomson, J.A., Itskovitz-Eldor, J., Shapiro, S.S., Waknitz, M.A., Swiergiel, J.J., Marshall, V.S., and Jones, J.M. (1998). Embryonic stem cell lines derived from human blastocysts. Science (New York, NY 282, 1145-1147.

Thraves, P.J., Kasid, U., and Smulson, M.E. (1985). Selective isolation of domains of chromatin proximal to both carcinogen-induced DNA damage and poly-adenosine diphosphate-ribosylation. Cancer research 45, 386-391.

Tian, X.C. (2004). Reprogramming of epigenetic inheritance by somatic cell nuclear transfer. Reproductive biomedicine online 8, 501-508.

Tokuzawa, Y., Kaiho, E., Maruyama, M., Takahashi, K., Mitsui, K., Maeda, M., Niwa, H., and Yamanaka, S. (2003). Fbx15 is a novel target of Oct3/4 but is dispensable for embryonic stem cell self-renewal and mouse development. Molecular and cellular biology 23, 2699-2708.

Tomioka, M., Nishimoto, M., Miyagi, S., Katayanagi, T., Fukui, N., Niwa, H., Muramatsu, M., and Okuda, A. (2002). Identification of Sox-2 regulatory region which is under the control of Oct-3/4-Sox-2 complex. Nucleic acids research 30, 3202-3213.

Torres-Padilla, M.E., Parfitt, D.E., Kouzarides, T., and Zernicka-Goetz, M. (2007). Histone arginine methylation regulates pluripotency in the early mouse embryo. Nature 445, 214-218.

Tremblay, K.D., Saam, J.R., Ingram, R.S., Tilghman, S.M., and Bartolomei, M.S. (1995). A paternal-specific methylation imprint marks the alleles of the mouse H19 gene. Nature genetics 9, 407-413.

Trojer, P., Li, G., Sims, R.J., 3rd, Vaquero, A., Kalakonda, N., Boccuni, P., Lee, D., Erdjument-Bromage, H., Tempst, P., Nimer, S.D., et al. (2007). L3MBTL1, a histone-methylation-dependent chromatin lock. Cell 129, 915-928.

Tsumura, A., Hayakawa, T., Kumaki, Y., Takebayashi, S., Sakaue, M., Matsuoka, C., Shimotohno, K., Ishikawa, F., Li, E., Ueda, H.R., et al. (2006). Maintenance of self-renewal ability of mouse embryonic stem cells in the absence of DNA methyltransferases Dnmt1, Dnmt3a and Dnmt3b. Genes Cells 11, 805-814.

Vaissiere, T., Sawan, C., and Herceg, Z. (2008). Epigenetic interplay between histone modifications and DNA methylation in gene silencing. Mutation research 659, 40-48.

Vakoc, C.R., Mandat, S.A., Olenchock, B.A., and Blobel, G.A. (2005). Histone H3 lysine 9 methylation and HP1gamma are associated with transcription elongation through mammalian chromatin. Molecular cell 19, 381-391.

Vakoc, C.R., Sachdeva, M.M., Wang, H., and Blobel, G.A. (2006). Profile of histone lysine methylation across transcribed mammalian chromatin. Molecular and cellular biology 26, 9185-9195.

Vallier, L., Alexander, M., and Pedersen, R.A. (2005). Activin/Nodal and FGF pathways cooperate to maintain pluripotency of human embryonic stem cells. Journal of cell science 118, 4495-4509.

van de Lavoir, M.C., Mather-Love, C., Leighton, P., Diamond, J.H., Heyer, B.S., Roberts, R., Zhu, L., Winters-Digiacinto, P., Kerchner, A., Gessaro, T., et al. (2006). High-grade transgenic somatic chimeras from chicken embryonic stem cells. Mechanisms of development 123, 31-41.

van Leeuwen, F., Gafken, P.R., and Gottschling, D.E. (2002). Dot1p modulates silencing in yeast by methylation of the nucleosome core. Cell 109, 745-756.

VandeBerg, J.L., Johnston, P.G., Cooper, D.W., and Robinson, E.S. (1983). X-chromosome inactivation and evolution in marsupials and other mammals. Isozymes 9, 201-218.

von Hofsten, J., and Olsson, P.E. (2005). Zebrafish sex determination and differentiation: involvement of FTZ-F1 genes. Reprod Biol Endocrinol 3, 63.

Waddington, C.H. (1957). The Strategy of the Genes. A discussion of some aspects of theoretical biology ... With an appendix by H. Kacser (pp. ix. 262. George Allen & Unwin: London).

Walsh, C.P., Chaillet, J.R., and Bestor, T.H. (1998). Transcription of IAP endogenous retroviruses is constrained by cytosine methylation. Nature genetics 20, 116-117.

Walter, R.B., Li, H.Y., Intano, G.W., Kazianis, S., and Walter, C.A. (2002). Absence of global genomic cytosine methylation pattern erasure during medaka (Oryzias latipes) early embryo development. Comparative biochemistry and physiology 133, 597-607.

Wang, H., Wang, L., Erdjument-Bromage, H., Vidal, M., Tempst, P., Jones, R.S., and Zhang, Y. (2004). Role of histone H2A ubiquitination in Polycomb silencing. Nature 431, 873-878.

Wang, H., Zhai, L., Xu, J., Joo, H.Y., Jackson, S., Erdjument-Bromage, H., Tempst, P., Xiong, Y., and Zhang, Y. (2006). Histone H3 and H4 ubiquitylation by the CUL4-DDB-ROC1 ubiquitin ligase facilitates cellular response to DNA damage. Molecular cell 22, 383-394.

Wang, Y., and Jia, S. (2009). Degrees make all the difference: The multifunctionality of histone H4 lysine 20 methylation. Epigenetics 4.

Wang, Y., Reddy, B., Thompson, J., Wang, H., Noma, K., Yates, J.R., 3rd, and Jia, S. (2009). Regulation of Set9-mediated H4K20 methylation by a PWWP domain protein. Molecular cell 33, 428-437.

Wang, Y., Wysocka, J., Sayegh, J., Lee, Y.H., Perlin, J.R., Leonelli, L., Sonbuchner, L.S., McDonald, C.H., Cook, R.G., Dou, Y., et al. (2004). Human PAD4 regulates histone arginine methylation levels via demethylimination. Science (New York, NY 306, 279-283.

Watanabe, D., Suetake, I., Tada, T., and Tajima, S. (2002). Stage- and cell-specific expression of Dnmt3a and Dnmt3b during embryogenesis. Mechanisms of development 118, 187-190.

Waterston, R.H., Lindblad-Toh, K., Birney, E., Rogers, J., Abril, J.F., Agarwal, P., Agarwala, R., Ainscough, R., Alexandersson, M., An, P., et al. (2002). Initial sequencing and comparative analysis of the mouse genome. Nature 420, 520-562.

Weiler, K.S., and Wakimoto, B.T. (1995). Heterochromatin and gene expression in Drosophila. Annual review of genetics 29, 577-605.

Weinberg, E.S., Allende, M.L., Kelly, C.S., Abdelhamid, A., Murakami, T., Andermann, P., Doerre, O.G., Grunwald, D.J., and Riggleman, B. (1996). Developmental regulation of zebrafish MyoD in wild-type, no tail and spadetail embryos. Development (Cambridge, England) 122, 271-280.

Wernig, M., Meissner, A., Foreman, R., Brambrink, T., Ku, M., Hochedlinger, K., Bernstein, B.E., and Jaenisch, R. (2007). In vitro reprogramming of fibroblasts into a pluripotent ES-cell-like state. Nature 448, 318-324.

West, J.D., Frels, W.I., Chapman, V.M., and Papaioannou, V.E. (1977). Preferential expression of the maternally derived X chromosome in the mouse yolk sac. Cell 12, 873-882.

Westerfield, M. (1995). The zebrafish book : a guide for the laboratory use of zebrafish (danio rerio) (Eugene, Or., [M. Westerfield?]).

Whetstine, J.R., Nottke, A., Lan, F., Huarte, M., Smolikov, S., Chen, Z., Spooner, E., Li, E., Zhang, G., Colaiacovo, M., et al. (2006). Reversal of histone lysine trimethylation by the JMJD2 family of histone demethylases. Cell 125, 467-481.

Wiblin, A.E., Cui, W., Clark, A.J., and Bickmore, W.A. (2005). Distinctive nuclear organisation of centromeres and regions involved in pluripotency in human embryonic stem cells. Journal of cell science 118, 3861-3868.

Williams, R.R., Azuara, V., Perry, P., Sauer, S., Dvorkina, M., Jorgensen, H., Roix, J., McQueen, P., Misteli, T., Merkenschlager, M., et al. (2006). Neural induction promotes large-scale chromatin reorganisation of the Mash1 locus. Journal of cell science 119, 132-140.

Wilmut, I., Schnieke, A.E., McWhir, J., Kind, A.J., and Campbell, K.H. (1997). Viable offspring derived from fetal and adult mammalian cells. Nature 385, 810-813.

Wood, H.B., and Episkopou, V. (1999). Comparative expression of the mouse Sox1, Sox2 and Sox3 genes from pre-gastrulation to early somite stages. Mechanisms of development 86, 197-201.

Woodcock, C.L. (2006). Chromatin architecture. Current opinion in structural biology 16, 213-220.

Woodcock, C.L., Skoultchi, A.I., and Fan, Y. (2006). Role of linker histone in chromatin structure and function: H1 stoichiometry and nucleosome repeat length. Chromosome Res 14, 17-25.

Woodland, H.R. (1979). The modification of stored histones H3 and H4 during the oogenesis and early development of Xenopus laevis. Developmental biology 68, 360-370.

Workman, J.L., and Kingston, R.E. (1998). Alteration of nucleosome structure as a mechanism of transcriptional regulation. Annual review of biochemistry 67, 545-579.

Wutz, A., and Gribnau, J. (2007). X inactivation Xplained. Current opinion in genetics & development 17, 387-393.

Wyce, A., Xiao, T., Whelan, K.A., Kosman, C., Walter, W., Eick, D., Hughes, T.R., Krogan, N.J., Strahl, B.D., and Berger, S.L. (2007). H2B ubiquitylation acts as a barrier to Ctk1 nucleosomal recruitment prior to removal by Ubp8 within a SAGA-related complex. Molecular cell 27, 275-288.

Xiao, B., Jing, C., Kelly, G., Walker, P.A., Muskett, F.W., Frenkiel, T.A., Martin, S.R., Sarma, K., Reinberg, D., Gamblin, S.J., et al. (2005). Specificity and mechanism of the histone methyltransferase Pr-Set7. Genes & development 19, 1444-1454.

Xie, H., Ye, M., Feng, R., and Graf, T. (2004). Stepwise reprogramming of B cells into macrophages. Cell 117, 663-676.

Xu, W., Edmondson, D.G., Evrard, Y.A., Wakamiya, M., Behringer, R.R., and Roth, S.Y. (2000). Loss of Gcn5l2 leads to increased apoptosis and mesodermal defects during mouse development. Nature genetics 26, 229-232.

Yamaguchi, S., Kimura, H., Tada, M., Nakatsuji, N., and Tada, T. (2005). Nanog expression in mouse germ cell development. Gene Expr Patterns 5, 639-646.

Yamamoto, Y., Verma, U.N., Prajapati, S., Kwak, Y.T., and Gaynor, R.B. (2003). Histone H3 phosphorylation by IKK-alpha is critical for cytokine-induced gene expression. Nature 423, 655-659.

Yamane, K., Toumazou, C., Tsukada, Y., Erdjument-Bromage, H., Tempst, P., Wong, J., and Zhang, Y. (2006). JHDM2A, a JmjC-containing H3K9 demethylase, facilitates transcription activation by androgen receptor. Cell 125, 483-495.

Yang, H., and Mizzen, C.A. (2009). The multiple facets of histone H4-lysine 20 methylation. Biochemistry and cell biology = Biochimie et biologie cellulaire 87, 151-161.

Yang, H., Pesavento, J.J., Starnes, T.W., Cryderman, D.E., Wallrath, L.L., Kelleher, N.L., and Mizzen, C.A. (2008). Preferential dimethylation of histone H4 lysine 20 by Suv4-20. The Journal of biological chemistry 283, 12085-12092.

Yang, L., Xia, L., Wu, D.Y., Wang, H., Chansky, H.A., Schubach, W.H., Hickstein, D.D., and Zhang, Y. (2002). Molecular cloning of ESET, a novel histone H3-specific methyltransferase that interacts with ERG transcription factor. Oncogene 21, 148-152.

Yang, X., Smith, S.L., Tian, X.C., Lewin, H.A., Renard, J.P., and Wakayama, T. (2007). Nuclear reprogramming of cloned embryos and its implications for therapeutic cloning. Nature genetics 39, 295-302.

Yao, T.P., Oh, S.P., Fuchs, M., Zhou, N.D., Ch'ng, L.E., Newsome, D., Bronson, R.T., Li, E., Livingston, D.M., and Eckner, R. (1998). Gene dosage-dependent embryonic development and proliferation defects in mice lacking the transcriptional integrator p300. Cell 93, 361-372.

Yasuhara, J.C., and Wakimoto, B.T. (2006). Oxymoron no more: the expanding world of heterochromatic genes. Trends Genet 22, 330-338.

Yeo, S., Lee, K.K., Han, Y.M., and Kang, Y.K. (2005). Methylation changes of lysine 9 of histone H3 during preimplantation mouse development. Molecules and cells 20, 423-428.

Yin, Y., Liu, C., Tsai, S.N., Zhou, B., Ngai, S.M., and Zhu, G. (2005). SET8 recognizes the sequence RHRK20VLRDN within the N terminus of histone H4 and mono-methylates lysine 20. The Journal of biological chemistry 280, 30025-30031.

Ying, Q.L., Nichols, J., Chambers, I., and Smith, A. (2003). BMP induction of Id proteins suppresses differentiation and sustains embryonic stem cell self-renewal in collaboration with STAT3. Cell 115, 281-292.

Ying, Q.L., Wray, J., Nichols, J., Batlle-Morera, L., Doble, B., Woodgett, J., Cohen, P., and Smith, A. (2008). The ground state of embryonic stem cell self-renewal. Nature 453, 519-523.

Yoder, J.A., Walsh, C.P., and Bestor, T.H. (1997). Cytosine methylation and the ecology of intragenomic parasites. Trends Genet 13, 335-340.

Young, L.E., and Beaujean, N. (2004). DNA methylation in the preimplantation embryo: the differing stories of the mouse and sheep. Animal reproduction science 82-83, 61-78.

Zemel, S., Bartolomei, M.S., and Tilghman, S.M. (1992). Physical linkage of two mammalian imprinted genes, H19 and insulin-like growth factor 2. Nature genetics 2, 61-65.

Zhang, Y. (2003). Transcriptional regulation by histone ubiquitination and deubiquitination. Genes & development 17, 2733-2740.

Zhao, X.Y., Li, W., Lv, Z., Liu, L., Tong, M., Hai, T., Hao, J., Guo, C.L., Ma, Q.W., Wang, L., et al. (2009). iPS cells produce viable mice through tetraploid complementation. Nature 461, 86-90.

Zhu, B., Zheng, Y., Pham, A.D., Mandal, S.S., Erdjument-Bromage, H., Tempst, P., and Reinberg, D. (2005). Monoubiquitination of human histone H2B: the factors involved and their roles in HOX gene regulation. Molecular cell 20, 601-611.

Zink, D., Amaral, M.D., Englmann, A., Lang, S., Clarke, L.A., Rudolph, C., Alt, F., Luther, K., Braz, C., Sadoni, N., et al. (2004). Transcription-dependent spatial arrangements of CFTR and adjacent genes in human cell nuclei. The Journal of cell biology 166, 815-825.

Website links

Abcam website: http://www.abcam.com/

Clustal W sequence alignment website: http://www.ebi.ac.uk/clustalw

Harwell imprinting website: http://www.har.mrc.ac.uk/research/genomic_imprinting

ImageJ website: http://rsb.info.nih.gov/ij/index.html

Western blot quantification website:
http://www.lukemiller.org/journal/2007/08/quantifying-western-blots-without.html

ZFIN zebrafish resource website: http://www.zfin.org